Title
Vehicle To Roadside Communications Study

Authors
Polydoros, Andreas
Dessouky, Khaled
Pereira, Jorge M. N.
et al.

Publication Date
1993

CALIFORNIA PATH PROGRAM
INSTITUTE OF TRANSPORTATION STUDIES
UNIVERSITY OF CALIFORNIA, BERKELEY

Vehicle to Roadside Communications Study

Andreas Polydoros

Contributors: **Khaled Dessouky, Jorge M.N. Pereira, Chung-ming Sun, Kuo-chun Lee, Thomas D. Papavassiliou, Victor O.K. Li**

University of Southern California

PATH Research Report
UCB-ITS-PRR-93-4

This work was performed as part of the California PATH Program of the University of California, in cooperation with the State of California Business, Transportation, and Housing Agency, Department of Transportation; and the United States Department of Transportation, Federal Highway Administration.

June **1993**

ISSN 1055-1425

Vehicle to Roadside Communications Study

Prof. Andreas Polydoros
Principal Investigator

Communication Science Institute
Department of Electrical Engineering-Systems
University of Southern California
Los Angeles, CA 90089-2565

Contributors

Dr. Khaled Dessouky
Jorge M.N. Pereira
Chung-ming Sun
Kuo-chun Lee
Thomas D. Papauassiliou
Prof. Victor O.K. Li

Working Group/AP, CSI/USC

Jorge M.N. Pereira, Ed.

Preface

The present final report is in response to the contractual requirements of the Memorandum Of Understanding MOU#67, provided to the University of Southern California (USC) by the Partners for Advanced Transit and Highways (PATH) administered at the University of California, Berkeley, covering the period March 1, 1992 to November 30, 1992. This reports represents solely the conclusions and opinions of the Principal Investigator, Prof. A. Polydoros, the consultant, Dr. K. Dessouky, and of the other contributing authors and researchers and should not be construed as representing the opinions of the University of Southern California or any other organization.

Acknowledgments

The Principal Investigator wishes to acknowledge the help and support provided throughout this project by Mr. Ramez Gerges, Staff Engineer for the California Department of Transportation, Office of Advanced Transportation, who acted as the Technical Officer on behalf of Caltrans, and Dr. Randolph Hall, Program Manager of PATH for the California Advanced Driver Information Systems (CADIS). He also wishes to thank deeply the project consultant and the other contributors for a job done with great competence, dedication and professionalism.

Executive Summary

The present final report is in response to the contractual requirements of the Memorandum Of Understanding MOU#67, provided to the University of Southern California (USC) by the Partners for Advanced Transit and Highways (PATH) of the University of California, Berkeley, covering the period March 1, 1992 to November 30, 1992.

The scope of the contract has been twofold : (a) the study of the vehicle-to-roadside radio communications problem as it applies to California Advanced Driver Information Systems (CADIS) designs, and (b) to provide general educational and consulting support to Caltrans, in particular with respect to Advanced Vehicle Identification (AVI) specifications and their upward compatibility with general Intelligent Vehicle and Highway Systems (IVHS) communications requirements. In particular, regarding the first category, some of the detailed deliverables have included:

- Identifying vehicle-to-roadside communication design options;
- Establishing tradeoffs between Frequency Division Multiple Access (FDMA), Time Division Multiple Access (TDMA), and Code Division Multiple Access (CDMA), as they pertain to the particular radio communications system at hand;
- Identifying and quantifying important parameters such as: signal-to-noise ratio (SNR), multiple-access capability in terms of number of simultaneously supportable users, frequency demand and allocation, throughput/delay characteristics, etc.

It was understood from the beginning that this short-term contract was in response to Caltrans' immediate needs, and that a complete treatment of the fundamental problem of vehicle-to-roadside and vehicle-to-vehicle communications will be addressed in a subsequent multi-phase study which will include, among other issues, a feasibility component

regarding the simultaneous servicing of ADIS and Advanced Vehicle Control Systems (AVCS) requirements.

The overall activity has been organized around eight topics, each of which occupies a separate chapter in this report. These are: Review of AVI proposals (Chapter 2); a survey of IVHS worldwide efforts, proposed standards and associated functional requirements (Chapter 3); a first study of the fading nature of the communication channels likely to be encountered in such a system (Chapter 4); a fairly detailed analysis of the multiple-access capabilities of TDMA and CDMA (under rather idealized conditions, such as perfect power control for CDMA), including the impact of modulation and coding on the bit- and packet-error rate performance of the corresponding systems (Chapter 5); a description of an initial simulation package developed internally for modeling the salient aspects of such a system, which has been employed to verify the analytical conclusions regarding AVI (Chapter 6); initial architectural tradeoff analyses on the system layout level with two case studies, one TDMA- and another CDMA-based, which briefly examine the feasibility, efficiency, and implications of each option (Chapter 7); a tentative throughput/delay analysis and simulation verification for each such option in a limited (single, short transaction as in AVI) topological environment (Chapter 8); and, finally, a list of conclusions, recommendations and open problems to be addressed in the future (Chapter 9).

In the briefest and most general of terms (the interested reader can find a more detailed list of conclusions in Chapter 9), the study has concluded thus far that a **short-range, packetized, either random- or reservation-access based radio system** is indeed a feasible, viable and (most likely, although this aspect has not been addressed at length herein) cost-effective solution for addressing the currently perceived (and rapidly evolving) requirements for a vehicle-to-roadside, two-way communication system for IVHS. Although the worldwide efforts in this development arena in terms of establishing functional requirements, design specifications and standards are currently in great flux, it can be said with sufficient degree of confidence that there exist architectural options which will satisfy most (if not all) of such requirements, and that there also exist many degrees of design freedom for achieving these goals. **In** particular, we have found through the preliminary architectural tradeoff study of Chapter 7 that a

well-designed and deployed, TDMA- or CDMA-based structure will be able to support significant aggregate data throughput under worst-case traffic conditions. Such a conclusion has been reached under fairly pessimistic channel and highway traffic conditions and under the assumptions of (a) a reasonable infrastructure deployment of highway cells (of the order of one mile diameter), (b) properly selected operating frequency (either 900 MHz or 1800 MHz) (c) proper transmitted power levels (fractions of a Watt) and (d) proper modulation and coding formats. We should emphasize that this conclusion is based strictly on capacity computations and has, out of necessity, incorporated a number of simplifying modeling assumptions; thus, it is ripe for significant substantiation and more detailed evaluation, in particular in the direction of incorporating actual channel characteristics, data traffic fluctuations, and signaling/protocol refinements, especially for longer messages and multiple simultaneous transactions. Nonetheless, the main flavor of the conclusion is expected to remain intact: short-range packet radio technology, currently existing and under development, can and should be considered a primary means for performing many communication tasks so vital in a successful IVHS environment.

Regarding radio systems for AVI applications, as currently proposed by various industrial concerns and administrative laws, it is expected that they will, in general, be able to fulfill their designated mission (the ease by which this will be accomplished does vary from one proposal to the other). However, it is the opinion of the present study group that these systems have been tailored to a very restricted and restrictive application, namely, the exchange of limited information over very short ranges. This has impacted the choice of architecture and thus limited the potential of upward compatibility, since they have not been configured or designed to carry any other significant data traffic for unrelated IVHS tasks. As such, they constitute a parallel, independent system whose task (AVI) could easily be embedded in a single overall radio architecture, thus providing enhanced value to the end user.

The study has unveiled many interesting facts regarding the behavior of the system components in such an environment (channel characteristics, modulation/coding/spreading performance in fading environments, etc.), which will be submitted for broader publication in due time. The interested reader can find them either at the end of each chapter or, in condensed form, in the final conclusions and recommendations chapter.

Contents

List of Figures

List of Tables

Chapter 1

Introduction

Intelligent Vehicle and Highway Systems (IVHS) are an emerging application area that exemplifies the transition between the challenges of the second half of the twentieth century and those at the start of the third millennium. It aims to utilize the vast telecommunication knowledge base developed over the last forty years, both in theory and practice, to enhance the efficiency and quality of a fundamental activity integral to daily life which is the use of highways and streets.

Predictably, IVHS comprises a large set of specific applications, with disparate anticipated requirements and configuration alternatives. These applications include, among others :

1. Advanced Traffic Management and Information Systems (ATMIS);
2. Advanced Driver Information Systems (ADIS);
3. Automatic Vehicle Control Systems (AVCS);
4. Commercial Vehicle Operation (CVO) Systems;
5. Advanced Public Transportation Systems (APTS).

All these application categories require substantial communication system capabilities, the details of which could be quite different in response to widely varying requirements.

The objective of this study, performed at CSI/USC under the sponsorship of the California Department of Transportation (Caltrans) and the PATH program office, is to address the communication system design issues of IVHS. The focus of Phase I of this research, which has spanned the period of March 1 through November 30, 1992, is CADIS design (the 'C' stands for California). The emphasis is on the architecture and topology aspects of the physical link and access layers connecting the moving vehicles with the fixed infrastructure. The longer term goal of Phase II, which starts in December 1992, is the joint design of a communication system architecture that simultaneously addresses the needs of both ADIS and AVCS.

An important milestone in the introduction of ADIS to California, and consequently a milestone in Caltrans' and CSI/USC's involvement in ADIS, has been Automatic Vehicle Identification (AVI). It is the application wherein toll collection is performed electronically, in a manner far safer and far more efficient than the mechanical means familiar to all. The first of CSI/USC's tasks was the analysis of the prominent proposals for systems or architectural specifications for performing AVI. This served as a valuable introduction to highway communications through which the critical components of the ADIS design problem were identified. This report thus starts with a treatment of the AVI systems in Chapter 2 immediately following this introduction.

In Chapter 2 two AVI proposals are analyzed and critiqued in some detail. First, the so-called "Vehicle to Roadside Communication" (VRC) system proposed by Hughes Aircraft is analyzed. It proposes to accomplish the AVI function while allowing for growth to other IVHS applications. The analysis in Chapter 2 permits the introduction of the physical link parameters, such as thermal and urban noises and multipath, as well as access-layer parameters like request and data message slots and the concepts of data congestion as a function of vehicular traffic. This analysis is accompanied by a critique from both the AVI and IVHS perspectives. This is followed by a critique of the formal AVI interface specification proposed by Caltrans/Lawrence Livermore National Laboratory (LLNL). Conclusions are drawn on the implied communication system architecture and its predicted performance for both AVI and ADIS.

An ADIS system that goes beyond simple vehicle identification poses a rich set of unique design problems, in that it combines: "short" range packet data communications, through propagation in a fairly confined yet highly dynamic highway or street environment, with signals susceptible to fading due to multipath and shadowing, in significant urban and background or receiver thermal noise, to meet requirements that are still not well defined; in a frequency band that can only be guessed at, using an infrastructure of reasonable cost, and accommodating a possibly very large number of users with inexpensive equipment.

In order to bound the design problem and ensure that it treats practical and realistic scenarios, an extensive review of proposed IVHS communication systems had to be performed. This survey is presented in the first part of Chapter 3 and summarizes North American, European and Japanese programs and systems. Mention is also made of standardization proposals and product innovations. One of the primary goals of such a survey is to deduce or extract a likely set of functional requirements to be placed on the ADIS under consideration. The formulation of a broad system functional requirements is treated in the second half of Chapter 3.

After such requirements have been identified, the design process proceeds with a multitude of architectural options and associated tradeoffs. These attempt to optimize the matching of the physical and access layers subject to the constraints of a practical, cost effective system. Before embarking on such an involved architectural tradeoff task, it is necessary to develop an in depth understanding of the models that govern the impact of the various parameters to be traded. Those are the models of the physical channel and of the multiple access schemes to be overlaid onto the candidate channel configurations and conditions.

Channel modeling is addressed in detail in Chapter 4. The effects of the geometry of the highway (e.g., walled, depressed, open/elevated), the position of the base station (BS) (e.g., middle-of-the-road versus side-of-the-road), BS antenna patterns and configuration, mobility and interaction of the vehicles, mobile (M) antenna placement, polarization choice, and system frequency band are all discussed in this chapter. An original, comprehensive model tailored to the IVHS environment with multiple signal

reflections, scattering and shadowing is developed. The effects of the various parameters above are manifested in the model which makes it an essential ingredient to be used later in system layout studies.

The pertinent models for the access layer are the subject of Chapter 5. Available results for bit and packet error rate performance of time-division multiple-access (TDMA) and code-division multiple-access (CDMA) for the non-fading, additive white Gaussian noise (AWGN) channel are compiled and/or derived. These are then extended to the multipath channel encountered in the ADIS mobile environment. Original and heretofore unpublished results are proven to be essential to characterizing the performance of the access scheme configurations over the channels described in the previous chapter.

None but the simplest of tradeoffs between the physical and access layers could be performed analytically, and the analysis would be under significant simplifying assumptions. It is therefore imperative to arrive at a powerful simulation capability to enable the design process which starts in this phase of the project and is to undergo extensive refinement and expansion in Phase II. The effort in simulation has taken a two-track approach. The first is investigating the feasibility of adapting and extending existing commercial packages to the IVHS environment, and the other is that of developing a custom simulation program tailored to the requirements of the ADIS design problem. Both approaches have their substantial challenges and the efforts in both areas are described in Chapter 6. The advantages and disadvantages of packages like OPNET and MODSIM are highlighted, and the level of effort required to adapt them to serve as ADIS design tools are identified. This is followed by a detailed description of the in-house simulation package that has been written in C. This includes the models and assumptions used, the structure and operation of the program, its capabilities and limitations at present, and the extensions that are required for a full-blown IVHS communication system simulation. Finally some results obtained from the simulation are presented, primarily to demonstrate its capability at the present stage of development.

Various system layout options are discussed in Chapter 7. The possibilities that can be considered are in theory numerous. Various selections of access techniques and their hybrids are possible, and all can be applied to disparate physical channel configurations

or highway geometries. To stay within the bounds of available resources, and make the size of this report manageable, focus is placed on certain access scheme choices. Those not only appear to be promising from a first cut analysis, but also serve to set up the architecture design problem, highlighting its steps and ingredients. Of particular importance is the identification of the factors that are critical to performance in a realistic environment and which need considerably more refined evaluation through simulation.

Among the design options considered in Chapter 7 are the combinations of TDMA with frequency or time division multiplexing (FDM or TDM), and CDMA with or without FDM[1]. The FDM or TDM is used to reduce the interference from adjacent cells which is typically the limiting factor to TDMA or CDMA performance for short-range, spatially distributed multi-user systems. In the case of FDM, as an example, the extent to which one assigns different frequency sub-bands to adjacent cells (frequency reuse) is a tradeoff parameter that is integral to the layout/architecture problem. Using several frequency bands for adjacent cells may reduce interference, and consequently improve the delay/throughput performance of TDMA, but it does so at the substantial cost of an increased spectrum requirement. That, however, may not be unacceptable if the required volume of ADIS transactions is not too large. This brings into the tradeoff the projected service requirements and their cost in terms of resources. The treatment in Chapter 7 aims to express these apparently qualitative characteristics in quantitative terms.

Frequency or time multiplexing are by no means the only approaches to controlling interference and improving system performance or capacity (in supportable number of transactions). Another approach that can mitigate the inter-cell interference relies on using BS antenna configurations that result in a sharper drop in signal level beyond a selected cell boundary. Unfortunately, this is generally achieved at the cost of smaller cells, or mobile receivers with a larger dynamic range requirement. This brings into the tradeoff the issues of infrastructure cost and user equipment complexity. Again, these issues are introduced and discussed in Chapter 7. Other issues that have substantial impact on performance are identified. These include power control for CDMA, with its impact on acquisition and intra-/intercell interference, protocol constructs and retransmission

[1] **The TDMA schemes addressed in Chapter 7 are general and unrelated to the specific Hughes VRC system proposed.**

schemes for both TDMA and CDMA, frame size for TDMA, etc.

Obviously, the system layout problem is a multi-dimensional one, and not all of its aspects could be analyzed in detail within the scope of Phase I. Thus, our goal here will be modest: to provide the reader and the sponsor with an understanding of the ADIS communication design issues, and to lay the groundwork for the more thorough and in depth treatment of Phase II.

After the system-oriented treatment of Chapter 7 analytical results for selected layouts under some simplifying assumptions are presented in Chapter 8. The delay/throughput analysis assumes transaction profiles and system attributes that lead to mathematically tractable solutions. The results aim to illustrate the utility of mathematical analysis as a validation tool for more elaborate simulation. Analytical performance results are derived for simple IVHS scenarios for both TDMA and CDMA, and are compared with the results obtained from simulation.

In the course of Phase I of the study it became apparent that recommendations fall into two broad categories: those that can be drawn from a good understanding of the problem at a system level coupled with preliminary analysis, and those that can only be arrived at after thorough analysis aided by extensive simulation. The conclusions of this phase generally belong to the first category. In Chapter 9 the conclusions, recommendations and open issues requiring further effort are summarized.

Finally, the appendices contain either detailed, self-contained analytical developments, or engineering evaluations that pertain to IVHS communications in general but do not fit readily into the flow of the report (e.g., FM subcarrier systems). A comprehensive glossary of IVHS terms, trying to cover not only the North American but also the European and Japanese experiments and ongoing work, completes the report.

Chapter 2

Automatic Vehicle Identification (AVI)

2.1 Introduction

Automatic Vehicle Identification (AVI) is the application wherein vehicle identification, primarily for the purpose of toll collection, is performed electronically. It is an important first step in the introduction of IVHS to California. AVI system analysis has therefore been the first of CSI/USC's tasks in this phase of the project. It is addressed in this chapter also because it offers a good introduction to highway communications principles, and serves as a vehicle through which the critical components of the ADIS design problem can be identified.

In the following sections two AVI proposals are analyzed. First, the so-called Vehicle to Roadside Communication (VRC) system proposed by Hughes Aircraft is addressed. The analysis introduces the physical link parameters, such as thermal and urban noise and multipath. It also introduces the access layer parameters like request and data message slots and relates them to traffic and congestion. The analysis is accompanied by a critique from both the AVI and IVHS perspectives. This is followed by a brief analysis and critique of the AVI interface specification proposed by Caltrans/Lawrence Livermore National Laboratory (LLNL). Conclusions are drawn on its implied communication system architecture and predicted performance for both AVI and ADIS.

The ADIS design problem extends far beyond the confines of AVI. Nevertheless, in the balance of this report, various more general analyses and simulations will utilize AVI as a convenient case study for the demonstration of concepts and results.

2.2 The VRC System Proposed by Hughes

2.2.1 Background

The Vehicle to. Roadside- Communication (VRC) system proposed by Hughes is a short-range two-way communication system between vehicle and infrastructure. It is intended to fulfill the requirements of an AVI system, primarily for toll collection, and is also claimed to include significant expansion potential to support future IVHS applications. It differs from the system, or rather specification, proposed by Caltrans/LLNL for AVI in that it goes beyond the simplified, extremely narrow coverage (5 m) scenario intended for no more than the toll collection function. It uses an active transponder as well as a multiple access scheme, both necessary in the ADIS application. The VRC system is analyzed, and then preliminary conclusions are drawn about it from the perspectives of AVI as well as IVHS.

In the VRC system the vehicle transponders are activated by a wake-up trigger pulse emitted from the reader. The system's centerpiece is a TDMA system architecture. The architecture/multiple-access scheme addresses some critical issues that were a source of criticism for the original AVI specification. The following analyses aim to characterize the system and its performance under worst case AVI conditions. Regardless of its exact performance this system is worthy of analysis as it provides a good example to illustrate and give insight into the vehicle to roadside communication problem. In the process, the merits and potential drawbacks of Hughes' VRC system are identified.

2.2.2 VRC System Overview

One of the weakest points in the original AVI specification proposal was the lack of an inherent contention or a collision resolution scheme. These collisions could result

from multipath or simply multiple vehicles responding to the reader's trigger in near unison. The Hughes system proposes to use TDMA with a reservation slotted-ALOHA [1] type of access protocol to resolve the collisions that would result from multiple vehicles responding to the trigger of the reader. To further regulate the transmissions on the channel the reader controls the actions of all of the transponders. The TDMA system has the fairly high composite rate (including overhead) of 500 kbps. The modulation is Manchester-coded ASK in both directions and the total bandwidth is approximately 1.5 MHz.

The TDMA protocol has a basic frame length of 9.58 ms (including guard and dead times) during which both the reader and transponders communicate. Because of the short range the propagation delay is insignificant, on the order of 0.2 μs. The frame can be viewed as consisting of three primary active segments. The first is the segment where the reader sends a control message to activate the transponders and/or give them instructions. The second segment is the data message exchange segment. It contains four slots and is the largest of the three segments. The third active segment is the one in which the transponders respond to the reader's trigger with their respective IDs, randomly placed among 16 slots. In the control segment the transponders that have responded in the previous frame with their IDs are assigned message slots and are given the type of transaction to take place. In basic toll collection one slot of one frame is used. In more advanced applications more than one slot in a frame or more than one frame (at one or more slots per frame) can be assigned to a given transceiver. The basic capacity of the message slot is 512 bits-256 for read only and 256 for read/write fro-m or to the transponder's erasable memory.

The length of the frame, the number and size of the data message slots (4), and the number of random access slots (16) all play a key role in how the protocol functions, and are strongly related to the physical parameters of the radio link, particularly its range. The larger the range, the more vehicles the reader will reach simultaneously, the more the potential for interference, but also the longer the time in which the transfer of information can be performed while the vehicle traverses the coverage area of the reader.

The key link parameters on the forward (reader to vehicle) link that define the cov-

erage area are : the reader effective isotropic radiated power (EIRP), the transponder antenna gain and noise figure, the background noise in the environment, and finally the minimum electrical field strength to which the transponder can respond. As will be seen, not all of these parameters carry equal weight in the given application.

The reader EIRP in the Hughes proposal is specified to be up to 4 W. The minimum field strength to which the vehicle receiver is sensitive is set to be 200 mV/m. The actual range will be either a function of the received signal to noise plus interference ratio or of the minimum field strength. The computations given in next subsection will reveal that this maximum range (based on 4 W) is approximately 77 m for an assumed 0 dB gain vehicle antenna. Specifying a higher transponder antenna gain, as in the case of an antenna with hemispherical coverage (front of vehicle field of view only) increases this range as the transponder is sensitive to the received signal power (collected from the medium) rather than the field strength existing in the medium. The Hughes proposal adopts the original AVI specification of 160“ half-power conical angle. Assuming then a roughly 3 dB antenna gain, the maximum range increases to about 110 m. This antenna pattern alters the coverage from a 77 m-radius circle, as shown in Figure 2.1, to a roughly 110 m segment of the highway in a direction heading toward the reader which is assumed to be located in the median (Figure 2.2).

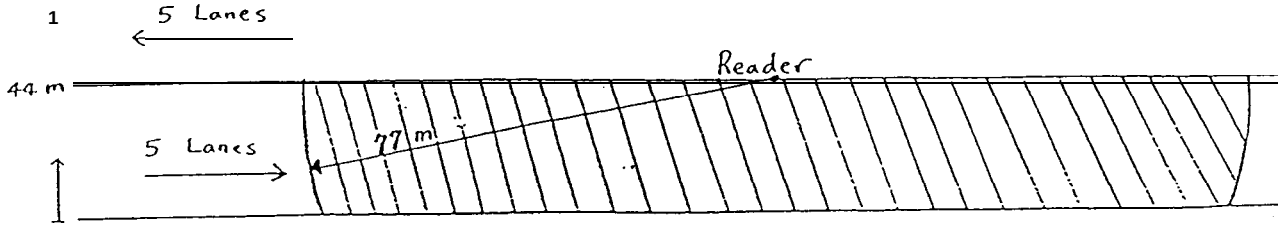

Figure 2.1: Reader Coverage Area for one Freeway Direction for Omni (0 dB) Vehicle Transponders (maximum reader EIRP = 4 W)

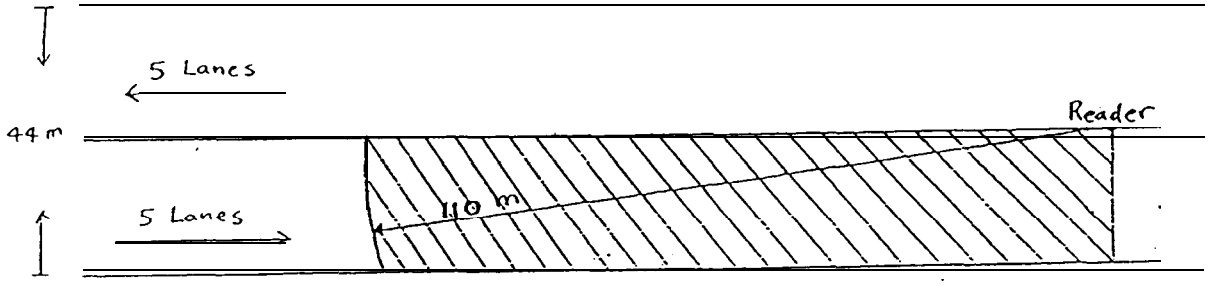

Figure 2.2: Reader Coverage Area for one Freeway Direction for Hemispherical (3 dB) Vehicle Transponders (maximum reader EIRP = 4 W)

2.2.3 Computation of Communication Range in an Urban Enviroment

The transponder will be capable of responding to the reader when it enters the reader communication zone. This zone is defined by the area in which the received field strength exceeds the specified transponder threshold (i.e., the minimum peak field strength). Given this threshold, the received power at the transponder receiver front end is [2]

$$P_r = \text{EIRP}\left(\frac{1}{4\pi d^2}\right) A_e = \frac{|\vec{E}_r|^2}{2Z_0} A_e \ , \tag{2.1}$$

where A_e is the equivalent antenna aperture, $|\vec{E}_r|$ is the minimum transponder receiver peak field strength which is set to be 200 mV/m, and Z_0 is the spatial characteristic impedance (377 Ω). Therefore, the maximum range (d_{max}) of the communication zone from the reader is given by

$$d_{max} = \sqrt{\frac{2Z_0}{|\vec{E}_r|^2}\frac{\text{EIRP}}{4\pi}} = 77 \text{ m} \ . \tag{2.2}$$

In addition to being based on the minimum field strength, d_{max} can also be achieved by using the maximum bit error rate (BER) requirement. Assume the receiver front-end noise figure, F_e, is 9 dB (which is common in mobile radio equipment) and the urban noise,

which includes thermal noise, local industry environmental noise, and vehicle ignition noise, etc, is 20 dB [3] higher than kT_0B, where k is the Boltzman constant, T_0 is 295°K and B is the equivalent noise bandwidth. Then, the system effective noise temperature, T_e, can be expressed as

$$T_e = F_u T_0 + (F_e - 1) T_0 = (100 + 6.94) T_0 = 31547.3 \ ^\circ\mathrm{K}, \tag{2.3}$$

and the one-sided noise power spectral density, N_e, is

$$N_e = k T_e . \tag{2.4}$$

For coherent ASK modulation (an ON/OFF modulation), the BER is a function of signal-to-noise ratio (SNR)

$$P_e = \mathrm{Q}\left(\sqrt{\frac{E_b}{N_e}} \right) , \tag{2.5}$$

where $E_b = P_r/R_b$ is the signal bit energy, R_b is the data rate, and $\mathrm{Q}(x)$ is the complementary error function defined as

$$\mathrm{Q}(x) \triangleq \int_x^\infty \frac{1}{\sqrt{2\pi}} e^{-\frac{y^2}{2}} dy .$$

If BER is 10^{-6}, then the required E_b/N_e is 14.5 dB (which includes 1 dB system implementation/processing loss). The signal power, P_r, at the receiver front end is given by

$$\begin{aligned} P_r &= 10\log(N_e) + 10\log(R_b) + 10\log\left(\frac{E_b}{N_e}\right) \\ P_r(\mathrm{dBW}) &= -183.6 + 57.0 + 14.5 = -112.11 \ \mathrm{dBW} , \end{aligned} \tag{2.6}$$

for R_b = 500 kbps as per Hughes' VRC proposal.

On the other hand, in the absence of multipath, P_r can be obtained by

$$P_r = \mathrm{EIRP}\left(\frac{c}{4\pi d f_c}\right)^2 g_r , \tag{2.7}$$

where c = 3 x 10^8 m/s is the speed of light, f_c = 915 MHz is the carrier frequency, the receiver antenna gain, g_r, equals 3 dB, and square law propagation loss is assumed. Thus, P_r can be computed from

$$\begin{aligned} P_r(\mathrm{dBW}) &= \mathrm{EIRP(dB)} + 20\log\left(\frac{3}{40\pi}\right) - 20\log(D) - 20\log(F_c) + 3 \\ &= -82.67 - 20\log(D) \ \mathrm{dBW} , \end{aligned} \tag{2.8}$$

where F_c is f_c in MHz and D is d in km. Comparing equations (2.6) and (2.8), the d_{max} is found to be 29.65 km in a fading and multipath free enviroment. A distance of the above magnitude is similar to that encountered in conventional (macro) cellular systems. It is therefore reasonable to assume that the channel suffers from Rayleigh fading. A more realistic communication range can, then, be obtained. In this case, the amplitude-conditional BER should be modified as

$$P_e(\beta) = Q\left(\sqrt{\frac{E_b}{N_e}}\,\beta\right) , \tag{2.9}$$

where β, the transmitted signal amplitude attenuation, is a Rayleigh distributed random variable with $E(\beta^2) = 1$. In this case, the average BER is [4]

$$\overline{P}_e = \int_0^\infty Q\left(\sqrt{\frac{E_b}{N_e}}\beta\right) 2\beta\exp(-\beta^2)\, d\beta = \frac{1}{2}\left[1 - \frac{1}{\sqrt{1+\frac{N_e}{E_b}}}\right] . \tag{2.10}$$

Knowing $\overline{P}_e$, we can compute E_b/N_e by

$$\frac{E_b}{N_e} = \frac{2}{\left(\frac{1}{1-2P_e}\right)^2 - 1} . \tag{2.11}$$

If the required $\overline{P}_e$ is still 10^{-6}, d_{max} reduces to 198 m. For the case of maximum reader EIRP (4 W), this worst case analysis including fading indicates that the maximum range of the reader is determined by the proposed sensitivity of the receiver (200 mV/m). The maximum range is accordingly 110 m as shown in Figure 2.2.

2.2.4 Preliminary Throughput Analysis

According to the reservation ALOHA-like multiple access protocol used in the Hughes' VRC system, some preliminary throughput analysis can be easily performed to test whether it is appropriate for the AVI application. The following assumptions are used in this analysis:

1. The average length (L_v) of vehicles is 4 meters.

2. Three traffic conditions will be analyzed (1) Normal : velocity of vehicles (V_h) = 60 mph (2) Light : V_h = 100 mph (3) Congested : V_h = 10 mph.

3. V_h in the expressway is constant throughout the reader coverage area. The separation (L_s) between two moving vehicles is determined by $L_v V_h / L_c$, where L_c is a factor. It is suggested by the DMV that the L_c for safe separation distance is 10 (for V_h in mph). In this analysis, $L_c = 20$ for normal city traffic whereas 15 is used for light and congested traffic to correspond to typical condition. If V_h = 60 mph, then $L_s = 460/20$ = 12 m.

4. The range of the communication zone, d_C, is 100 m, basically from about 10 m from the reader out to 110 m as shown in Figure 2.2.

5. The frame interval is 9.58 ms. There are 16 request time slots (RTS) and 4 message slots in each frames.

6. For the AVI application, one slot message for each transponder is enough.

7. There are five lanes ($L_a = 5$) in each direction of the expressway. (We consider communicating with only one direction.)

Under normal traffic conditions, $V_h = 60$ mph = 26.7 m/s. Each vehicle will remain for $T_h = 100/26.7$ = 3.75 s in the communication zone. There are m = $L_a \lceil d_C/(L_v + L_s) \rceil$ vehicles in the zone, where $\lceil x \rceil$ is the smallest integer which is larger than x. Thus, m = $5\lceil 100/(12 + 4) \rceil$ = 35. In this 3.75 s interval, the reader can transmit N_{OFFER} = (3.75 s/9.58 ms) = 391 frames. Among these 35 vehicles, some may have finished their transactions with the reader and are waiting their sleep time out while others are still trying to communicate with the reader. The worst case is when none of them has successfully transmitted their message to the reader and all have to compete for the RTS.

Let P_c be the probability that one particular transponder among m successfully transmits its request without collision. Then P_c is given by

$$P_c = \left(\frac{15}{16} \right)^{m-1} , \tag{2.12}$$

where we assume that the time slots are equally likely.

Assume that the probability that one particular transponder transmits it request without collision **in** each frame is a constant (equal to P_c, for worst case consideration). Let the random variable X denote the number of failures (transmit request with collision) before the first success in a sequence of frames, then

$$P[X = k] = (1 - P_c)^k P_c \ , \tag{2.13}$$

where we assume that the interference caused by urban noise and multipath can be ignored as justified by the analysis in Section 2.2.3.

Clearly, X is geometrically distributed with parameter P_c. Therefore, the average number of frames (N_{ave}) for that transponder to successfully transmit its request is

$$N_{ave} = E\ (\ X\ ) = \frac{1}{P_c} \ , \tag{2.14}$$

where E (X) is the expected value of X.

For the normal traffic condition, m = 35 and P_c = 0.11, thus N_{ave} = 9 frames. Again, this is the worst case result because m in each frame may be less than 35. Under this worst case condition, the upper bound of frames (N_{UB}) needed for these 35 transponders to finish contact with the reader are 9 x 35 = 315 frames. Using the same procedure, the other two traffic conditions can also be evaluated and the results are shown in Table 2.1.

	Traffic Conditions		
	Normal	Congested	Light
V_h(mph)	60	10	I 100
L_s	12.0	2.7	26.7
T_h(s)	3.75	22.52	2.25
m	35	75	20
P_c	0.11	0.0084	0.29
N_{ave}	9.0	118.6	3.41
N_{OFFER}	391	2351	235
N_{UB}	315	8895	69

Table 2.1: Upper Bound of Number of Frames Needed for Three Traffic Conditions

It should be cautioned that the upper bound tends to give an inflated number of frames because it does not take into account that the transponder times out for 30 **s**

after the AVI transaction. If it were instead a more complex transaction a bottle neck could conceivably occur under congested traffic conditions. It should be kept in mind, however, that the above analysis assumes the maximum EIRP of 4 W which corresponds to the maximum coverage area.

Accurate performance figures under more generalized data traffic conditions would require simulation of the actual operation of the protocol and assumptions about the data transactions.

2.2.5 Conclusion

From the above analyses it can be concluded that the Hughes' VRC system easily meets the requirements of the AVI application. An area of possible concern is using 4 W of reader EIRP to achieve a communication range of only about 100 m. The system can and should perform the AVI function with considerably less power. But then its coverage range per reader, and potential for supporting anticipated IVHS requirements, could be severely curtailed. Although the potential for supporting IVHS applications is hard to ascertain without detailed simulations, it is apparent that the system is optimized for applications with occasional, short range, very short data transactions. For example, the protocol adopted with only 4 message slots per frame is ill suited to longer data transactions and would lead to huge overhead penalties. Later, in Chapter 7, more general TDMA architectures, unrelated to the Hughes' VRC system, will be introduced and analyzed.

2.3 The AVI Specification Proposed by Caltrans

2.3.1 Background

The AVI Compatibility Specification proposed by Caltrans has undergone a few review, comment and revision cycles. In the process, many elements in the proposed specification have been modified. Certain RF specifications, data record formats and transaction attributes have been changed to alleviate a number of well founded con-

cerns that were raised in the numerous comments received by Caltrans. Nevertheless, the fundamental approach to performing the AVI function as well as the implied system architecture to do so remain intact. The objective here is not to duplicate the previous comments submitted by many, nor is it to trace the evolution of the specification, but rather, it is to summarize the technical opinion that we have formed of the specification with an emphasis on presenting an evaluation of the underlying communication system architecture. This will be approached from various angles: "protocol", propagation, hardware requirements, implementation approach and growth potential.

In what follows we present a very concise summary of the AVI specification to highlight its critical elements, and then provide a brief analysis of its key attributes.

2.3.2 Summary of the Proposed AVI Specification

The equipment required for the AVI application essentially consists of two types: the vehicle-mounted transponder and the fixed-position reader. Modulated backscatter technology is used to effect two way communication between the reader and the transponder [5],[6]. Although conceivably the reader could be either at the roadside or overhead (directly above the lanes of traffic), the overhead configuration is the only viable one as will be pointed out later. (Note that the in-pavement configuration has been deleted.)

When the transponder enters the small (few meter) read zone as will be discussed subsequently, the communication sequence between the reader and the transponder is as follows [6]:

1. The reader sends a 33 μs wake-up signal to trigger the transponder and then follows that with a 100 μs delay during which no power is transmitted.

2. The reader sends a polling message to the transponder of 200 μs duration containing 60 bits.

3. The transponder then sends a data message to the reader if the reader's polling message is correctly received. This consists of 76 bits and contains the transaction record type and the transponder ID number and an error detection code.

4. If the transponder's message is correctly received, the reader sends an acknowledgment back to the transponder. This contains 124 bits.

5. The transponder will not respond to an identical polling message for 10 s if the reader's acknowledgment is correctly received. If, on the other hand, the transponder detects an error in the polling message it waits for a new wake-up signal and polling message. Similarly, if the reader detects an error in the transponder-to-reader message or the transponder detects an error in the acknowledgment message the communication sequence starts anew from the wake-up signal.

The communication zone is an important parameter that determines how the system functions for AVI, and determines as well its potential for supporting more sophisticated or demanding transactions as envisioned in IVHS. The length and position of the communication zone is very dependent on several parameters, namely, antenna position and beam shape, transmit power, vehicle transponder antenna gain and positioning, transceiver sensitivity, among other factors. The choice of communication zone length is a delicate balance between permissible transaction data volume and mitigation of interference from unintended vehicles, either in the same lane or in adjacent lanes. This is a consequence of the lack of a multiple access protocol that permits resource sharing in the proposed specification as will be addressed in the next section. It is worth noting that several of the revisions to the AVI specification have aimed, directly or indirectly, at limiting the communication range to ensure a higher degree of communication reliability through minimizing the likelihood of packet collisions. For example, increasing the minimum transponder sensitivity from 100 mV/m to 450 mV/m shortens the range for a given transmit EIRP by a factor of 4.5.

To solve the problems of collision of the transmitted data packets, a conceptualized solution has been proposed as follows. One antenna per lane is used. The antennas are beam shaped to reduce potential interference caused by reflections off vehicles in adjacent lanes. Horizontal polarization is adopted for the same reason (unlike cellular telephone and mobile radio systems which use vertical polarization). The reader antennas are time multiplexed as transmitters but when a particular antenna transmits, all nearby antennas listen. Finally, valid records are reported by each reader after each poll. This

solution approach is coupled with a certain flexibility in RF parameters to allow for sight dependent variations. Such variations would be critically important due to the reliance on RF isolation and the lack of a multiple access protocol.

Turning again to the communication or reader zone, some reasonable estimate of this zone is necessary to enable a critique of the communication attributes and potential of the underlying system architecture. With this in mind we proceed to extract such an estimate from the available information.

In [7] the selection of the data rate of 300 kbps after the initial comments period is explained. This choice corresponds, based on some assumptions, to a 2 m reader zone for in-pavement antennas and vehicles traveling at 100 mph. Unfortunately, in-pavement antennas have been deleted as a requirement. As mentioned earlier, the lack of a multiple access protocol precludes using a single antenna for all lanes, and the only option available is one antenna per lane- overhead. Now assuming a 90" conical beam for the transponder as given in the updated specification [6], and assuming the same for the reader (although it is not specified but appears to be reasonable) we find that the maximum communication range about 7.7 m (slant) for the specified 450 mV/m minimum transponder sensitivity and a 50 mW reader power. This would imply a 5.3 m longitudinal distance (along the lane) from the antenna if the antenna height is 5.5 m. Considering the 35" from horizontal inclination of the axis of the transponder antenna, and the 45" half-conical angle, the actual communication range would be less than 5.3 m, roughly 5 m. It should be noted that a different choice of parameters can lead to a smaller distance with respectively less potential for interference from adjacent cars but also less communication duration.

It is now instructive to compute the maximum number of bits that can be transferred by this type of system, assuming of course that the appropriate data structures that are defined. Starting from the 300 kbps rate, and an assumed 100 mph maximum speed, the 5 m zone is found to support 6750 bits total. This would include transmissions in both directions, triggers, preambles, acknowledgments, message data, and any repetitions of failed attempts. In [7] it is mentioned that 5 copies of the transaction were considered in the 300 kbps AVI data rate computation to ensure a completed transaction with no

corruption due to packet collisions. If the same rationale is followed, the data volume should be reduced to 1350 bits. If the transaction is less critical than identification and toll collection, and correspondingly less repetitions are deemed necessary, the data volume that could be handled would then be somewhere between 1350 and 6750 bits.

2.3.3 Critique of the Proposed Specification

Multipath Interference Protection

Very careful (and potentially costly) engineering of the toll sites or reader stations would be required because of the modulation formats adopted and the lack of a multiple access protocol. The proposed Amplitude Shift Keying (ASK) modulation from the reader to the vehicle transponder is simple and easy to implement, but is very vulnerable to multipath interference caused by reflections from other vehicles and objects in the proximity of the intended vehicle. Very careful toll site antenna placement and antenna beam shaping would be required to significantly mitigate multipath interference. Site by site analysis, field testing and iteration would be necessary for implementation. Furthermore, in an environment with variations in vehicle shapes, vehicle antenna mounting positions, and road conditions, this toll site design process would be complicated by the lack of an inherent protection to multipath. System setup costs could be high.

Multiple Access and Packet Collisions

An important issue is the potential presence of multiple packets from different vehicles responding to a single reader's trigger pulse and the resulting collisions among them. The responding vehicles could be in adjacent lanes or conceivably the same lane. Repetition of requests from the reader may not be a dependable solution since, as vehicles pass by the reader station (particularly those in adjacent lanes at some speed), their relative geometry may not change sufficiently to alter the number of vehicles that simultaneously receive the trigger. Repeated response collisions could take place. Again, very careful toll site antenna placement and design would be essential to attempt to reduce the number of vehicles that simultaneously communicate with the reader. We note that this issue has been mentioned in Section 1704.7 entitled "Closely-Spaced Transponders in the Same

Lane", but it is not clear how the proposed system would cope with this.

Use of Data Rate

The high data rate transmission of initially 500 kbps and more recently 300 kbps is a centerpieceof system design as it permits repetition of messages in the case of corruption– which is likely due to the lack of inherent resistance to multipath. However, this is a very inefficient utilization of the data rate that dramatically reduces the transaction data volume that can be handled in a non-AVI application. A true channel access protocol would permit a far better utilization of the radio resources of the channel.

Horizontal Polarization

Horizontal polarization is adopted to mitigate reflections from the vertical sides of vehicles in adjacent lanes. In general, the received signal in the mobile environment is significantly more stable if vertical polarization is used. This is the principal reason for the use of vertical polarization in cellular and now microcellular applications. It could be argued that for the very short ranges dealt with in AVI (8 m slant range) this is not a critical issue. Yet what causes the strong variation in the received wave with horizontal polarization is reflection on horizontal surfaces, namely, the ground, which is always present, and the hood of the vehicle (if applicable). In both cases the differential path length is generally small. That is, such reflections could prove to be problematic even for very short ranges. Again, careful toll site analysis, engineering and testing is necessary to assure that reflections from the ground are not a problem.

Reader Transmit Power

Because of the doubled range, backscatter technology in general requires four times the transmit power required when the transponder is an active one. This could be offset somewhat by requiring the reader to have lower sensitivity than the transponder. The same could be done too if the transponder were active. If reducing or limiting the range were not an objective, as would be the case in a general IVHS system with a multiple access protocol, then the increase in reader transmit power to offset a doubled range or an increased minimum transponder sensitivity would be a significant drawback.

Data Volume, Coverage and Potential for Expansion

Due to the very short communication zone of the AVI system, the data transaction volume could be as low as 1350 bits including all overheads of the two transmission directions. It is anticipated [8] that the IVHS application of route guidance would require 5 - 10 kbits. It is not likely that the system architecture implied by the present specification would support that important application. Vehicle guidance is anticipated [8] to require transactions on the order of 10 kbits. These transaction would not be supportable either. Finally, digital map transmission can require as much as 64 kbits. This would obviously be well outside the realm of the architecture at hand.

The very short range also implies that whatever the supportable transactions may be, they are only available in the immediate vicinity of the toll collection facility and no where else. Such discontinuity is either unacceptable or simply undesirable in many IVHS functions. Examples of such functions include in-vehicle signing, traffic information updates, driver alerting and mayday.

The present specification is quite inadequate in meeting even the basic requirements of an IVHS system. The claimed potential for expansion is simply inconsistent with the extremely short range required to enable the system based on the specification to function properly.

2.3.4 Conclusion

The AVI specification proposed by Caltrans has launched a debate about the use of advanced technologies to enhance the highways of the State of California. Perhaps due to the time pressures created by the legislative action to quickly start implementing AVI/toll collection systems, a specification narrowly focused on that application arose. Unfortunately, the system architecture implied in the specification does not take advantage of the well established concepts and techniques in use in today's mobile or multi-user systems, e.g., multiple access protocols, signals resistant to multipath, low cost active user transceivers. The specification as initially conceived suffered from serious flaws that cast doubt on its viability even for the simple AVI application. The period of comments

mandated by the State of California resulted in modifications that will remedy some of these flaws. The system as presently envisioned will probably work for AVI if, as pointed out above, special care is exercised in deploying it. Yet, because the underlying architecture has not changed, significant inefficiencies and weaknesses still exist even for the AVI application. Those are in the areas of system setup, fielding, cost, and physical channel resources usage. In essence, the rapid development of the specification has burdened the implementors with challenges that the system architects should have resolved.

From an IVHS perspective that goes beyond mere vehicle identification, the proposed specification implies a system that is inherently and essentially very limited in scope. Further, it is incapable of expansion to meet the demands of the most basic functions of IVHS functions. It is extremely unlikely that such a system could serve as a nucleus for IVHS in California.

2.4 References

[1] W. Crowther, et.al., " A System for Broadcast Communication : Reservation–ALOHA," *Proc.* 6th *HICSS*, Univ. Hawaii, Honolulu, Jan 73

[2] E. Skomal, ***Man-Made Radio*** Noise, Chap. 6, Van Nostrand Reinhold, 1978

[3] William ***C. Y.*** Lee, Mobile ***Cellular Telecommunications*** Systems, Chap 1, McGraw–Hill, 1989

[4] E. Geraniotis, M. B. Pursely, "Performance of Coherent Direct-Sequence Spread–Spectrum Communications Over Specular Multipath Fading Channels," IEEE *Trans. Comm.,* Vol. COM-33, pp.502–508, Jun 85.

[5] "Notice of Proposed Regulatory Action Concerning the California Code of Regulations, Title 21, Chapter 16, Articles l-7, Compatibility Specification for Automatic Vehicle Identification Equipment", Caltrans, Aug 91

[6] "Notice of Modifications to Text of Proposed Regulations," Caltrans, Feb 92

[7] "Rationale- California AVI Compatibility Specification," prepared by Lawrence Livermore National Laboratory, in Caltrans' "Final Statement of Reasons", re: Proposed Additions to Title 21, Chapter 16, Articles l-4 of the California Code of Regulations, Mar 92

[8] *TRB's* ***"Communicating with Vehicles" Workshop,*** Chicago, Jul 92; To appear in Workshop's Circular to be published, Fall 92.

Chapter 3

IVHS Survey and Functional Requirements

3.1 IVHS Survey

Most of the information provided below is from the viewpoint of the communication link and communication system design, within the general area of IVHS research.

For further information, the interested reader is referred to the publications listed in the References (Section 3.3).

3.1.1 US Programs

SMART Corridor -- It is a cooperative venture for integrating traffic sensors, computers, and various communication links to coordinate traffic and disseminate traffic information for the Santa Monica Freeway (110) and five major arterials between downtown Los Angeles and the San Diego Freeway 14 miles to the west. Participating agencies include the Federal Highway Administration (FHWA), the California Department of Transportation (Caltrans), the California Highway Patrol (CHP), the Los Angeles County Transportation Commission, the Los Angeles Department of Transportation, and the Los Angeles Police Department.

The $50-million project started with a conceptual design study in 1989; full imple-

mentation is scheduled for 1993. A major focus of the SMART Corridor project is the implementation and evaluation of a broad range of methods for communicating information to drivers on traffic conditions and alternate routes, as well as receiving information from drivers. Use of changeable message signs (CMSs) will be extended to include surface streets, and low-power highway advisory radio will be installed along both the highway and surface streets. The SMART Corridor is also the site for the Pathfinder project.

Pathfinder – an ATIS/ATMS project ($2.5 million) sponsored by Caltrans, the FHWA, and GM, intended for *testing in Los Angeles's SMART Corridor. It is a system that informs drivers of existing traffic congestion. The hardware in the vehicle includes a processor, voice synthesis equipment, a modem radio, and a Travelpilot system (a navigation system from ETAK, Inc. that displays electronic road maps). At the central station, traffic information collected from various sources, is processed. This information is broadcast to all vehicles once every minute. Each vehicle is assigned a timeslot within the minute for making a return transmission. When the vehicle's timeslot arrives, data on position, heading and speed are transmitted by radio back to the traffic operations center.

PATH – Partners for Advanced Transit and Highways – a $56 million project, which began in 1986, is sponsored by Caltrans, the FHWA and the National Highway Traffic Safety Administration. PATH is administered by the University of California's Institute of Transportation Studies (ITS) at Berkeley. PATH is investigating a national automated highway system, starting with the gradual automation of driver functions and ultimately moving to completely automated vehicle operations.

One of the projects PATH examined was the transfer of energy inductively from a conductor embedded in the roadway – a transformer primary – to a transformer secondary mounted below the automated vehicle. Vehicles could be controlled longitudinally with minimum spacing between vehicles. The roadway electrification project is a continuation of the Santa Barbara Electric Bus System, which, through 1985, expended $5 million in funds from the Urban Mass Transportation and Caltrans.

PATH research includes studies of the performance, impacts and benefits of route guidance. One study modeled portions of Los Angeles's SMART Corridor to predict benefits from in-vehicle information systems in recurring and incident-induced congestion. Other studies of driver information systems focus on driver behavior and safety aspects.

TravTek – Travel Technology – an over $ 8 million project being developed for the Orlando, FL, area. It is a cooperative partnership of GM Corp., the FHWA, the AAA, the Florida DoT and the city of Orlando. TravTek uses in-vehicle information equipment to provide motorists with up-to-date traffic information and directions to destinations. It will also provide useful information about Orlando-area attractions, accommodations and services.

The in-vehicle equipment consists of a video screen, two microcomputers, a voice synthesizer, and a radio for data communications. When drivers select a destination, the TravTek processor uses travel times to determine the best routes and uses both graphics displays and synthesized voice to guide the drivers. The traffic management center will combine and sort the traffic-related information received from a variety of sources throughout the Orlando metropolitan area. From all the data, information on accidents is estimated and transmitted to the vehicles. The in-vehicle processor then determines if the driver's selected route is affected, calculates new routing if necessary and informs the driver that a revised routing is available.

HELP – Heavy Vehicle Electronic License Plate – an ATIS and CVO project involving 14 U.S. states, the Port Authority of New York-New Jersey, the Canadian Province of British Columbia, U.S. National Transportation agencies and U.S. and Canadian trucking industries. Among several technologies, the focus is to use satellite communication data links.

ADVANCE – A large ATIS project has been proposed for the Chicago area. It is sponsored by the Illinois DoT, Northwestern University, the University of Illinois (Chicago), Motorola Inc., and the FHWA. Unlike Los Angeles's Pathfinder project and Orlando's

TravTek project, the Chicago experiment focuses on arterials rather than expressways because much of the commuting in the area does not involve freeways. The objectives are to test alternative approaches for driver information systems, dynamic traffic information acquisition, incident detection, and analysis and forecasting as steps towards determining the best IVHS approach for relieving traffic congestion in Illinois. About 4000 business, government and private vehicles would be linked to a traffic management center by a two-way mobile radio network. In addition to dead-reckoning equipment with map-matching, vehicles would contain a GPS satellite receiver for position calibration. Routing software will be included, and traffic-dependent route guidance will be presented by synthesized voice, as well as displayed:on a color screen. Operations are scheduled to begin in late 1992, assuming a favorable decision by Illinois DOT in early 1991.

GuideStar – it is a cooperative effort between the Minnesota DoT (MN/DoT) and the University of Minnesota's Center for Transportation Studies, with partnership with other public and private organizations. The initial focus is on testing and evaluating **Autoscope,** a patented machine-vision device that collects and analyzes traffic information. Autoscope was developed over a six-year period of research at the University of Minnesota. It is being tested in 1394 using $1.4 million granted by the FHWA and MN/DoT, and is expected to become the centerpiece of a traffic communication for monitoring 300 miles of freeways and major arterials in the Minneapolis/Saint Paul area by 1995. This GuideStar network will provide passenger vehicles and trucks with a variety of traffic information services.

3.1.2 European Programs

Whereas most of the North American projects have, to date, been pursued on a stand-alone basis with only a small amount of coordination from Mobility 2000 and IVHS America, most of the numerous European IVHS projects are fully coordinated elements of major programs that transcend the borders of individual countries. Most are under the auspices of the Commission of the European Community (CEC), or of **EUREKA,** an industrial research coordination initiative of 19 European countries, including some from EFTA besides some from EEC, a group of 12 member countries working towards

the economic unification of Europe.

DRIVE

The principal objective of DRIVE (Dedicated Road Infrastructure for Vehicle Safety in Europe) is development of functional specifications and standards for a coherent Integrated Road Transport Environment (IRTE), to support communications, route guidance and driver information, advanced traffic management and control, collision avoidance and other IVHS applications; DRIVE is a public-sector oriented initiative of the European Commission that started with pilot studies in 1985; it led to the definition and approval in 1988 of the work plan for a three-year, $140-million program of pre-competitive IVHS research that is jointly funded by government and industry.

The DRIVE work plan is organized in separate modules dealing with management and systems approach, evaluation tasks, road transport management systems, road safety systems and implementation aspects. It is being implemented through some 70 projects, each carried out by a consortium representing at least two countries and including a minimum of one industrial partner. The projects fall under seven categories:

1. **Evaluation and modeling –** eleven projects are devoted to the application of modeling approaches to evaluate the performance and impact of IVHS.

2. **Behavior aspects and traffic safety –** thirteen projects deal with topics ranging from accident data analysis to collision avoidance systems.

3. **Traffic control –** seven projects cover a wide range of topics including demand management, traffic signal control, parking management, incident detection and tunnel control systems.

4. **Route guidance, vehicle location, digital maps and in-vehicle information systems –** specific projects in this group include Vehicle Location Systems using Satellites, PANDORA (Prototyping a Navigation Database of Road Attributes), Integration of Dynamic Route Guidance and Traffic Control, European Digital Road Map Task Force, Driver Information Systems, Standards for RDS-TMC (Radio

Data System-Traffic Message Channel) throughout Europe, and Road Information and Management AURO-System.

5. **Public transport and freight management** – four projects are included that investigate how commercial vehicles and public transportation may take advantage of vehicle location, communications, and real-time traffic information.

6. **Telecommunications** – this group of projects seeks to define the communications and information processing required for and integrated IVHS infrastructure to support dynamic route guidance and driver information systems, AVI and account debiting, collision avoidance, and freight and commercial vehicle management systems. Candidate technologies include inductive loops, microwave transmissions, infrared transmissions, radiating cables, cellular radio, and satellites. Two major DRIVE projects in this area are:

   - **SOCRATES** – System for Cellular Radio for Traffic Efficiency and Safety – a program investigating using dedicated channels from the Pan-European GSM system to broadcast information to vehicles [3]. The same data set is broadcast to all equipped vehicles in a particular cell. To provide transmission from vehicles to the control center, a multiple-access protocol is used. Initial tests in Gothenburg are scheduled to be completed by the end of 1991.
   - **TARDIS** – Traffic and Roads-Drive Integrated Systems – project aiming at establishing common functional specifications for systems that are not wholly vehicle-based and that depend on communication between vehicles and roadside infrastructures. It includes investigating the possibility of combining communication for route guidance with that for automatic toll-collection.

7. **Consensus formation** – The Systems Engineering and Consensus Formation Office (SECFO), co-located with the DRIVE central office at the CEC's Brussels Headquarters, is a project responsible for reviewing deliverables of all DRIVE projects to synthesize systems engineering approaches for iteration with both the central office and other projects to seek consensus.

The first phase of the DRIVE program, DRIVE I, was concluded at the end of 1991. DRIVE II is scheduled for 1992-1994. With funding of $280 million – twice that of

DRIVE I – it will focus on field trials and demonstrating projects investigated in DRIVE I.

PROMETHEUS

PROMETHEUS – Programme for European Traffic with Higher Efficiency and Unprecedented Safety – is the largest ($700 million over an eight-year period) and best known IVHS-research project of EUREKA, a $5-billion, 19-country European program founded in 1985 to stimulate cooperative R&D among Europe's industries and government. Whereas DRIVE is infrastructure-oriented, PROMETHEUS is a vehicle-oriented project started in 1986 by a consortium of European carmakers, which now includes numerous electronic firms, research institutions, and public-sector organizations as well. An important PROMETHEUS concept is that of the ***intelligent co-pilot,*** an integrated set of vehicular systems linked by communication networks with the infrastructure and with other vehicles to aid and enhance the capability of the driver for safe and more efficient road traffic. Thus PROMETHEUS and DRIVE are highly complementary.

PROMETHEUS, which originated with a one-year definition study, was restructured based on the results of earlier experience as it entered a new six-year phase of R&D in 1989. The overall objectives of PROMETHEUS are now interpreted in terms of 23 functions grouped in four industrial research application areas: improved driver information, active driver support, cooperative driving, and traffic and fleet management.

The applied research performed by the motor industry groups is supported by basic research performed by universities, scientific institutes and government laboratories.

In 1989 a six-year R&D phase consisting of seven subprograms began. The motor industry subprograms are:

- **Pro-Net –** a program developing a communications network between vehicles:

  * system engineering (Volkswagen);
  * communications (Renault);
  * emergency warnings (Saab, Volkswagen, Daimler-Benz);

- **Pro-Road –** a program developing communication systems between the vehicle and roadside infrastructure and traffic control systems:

  * information processing and data acquisition (Volvo);
  * infrastructure-based systems (Daimler-Benz);
  * on- board elements (Renault).

The basic research projects are:

- **Pro-Corn –** a program defining the structure, standards, and architecture of communication systems;
- **Pro-Chip –** a program developing microelectronics for information systems;
- **Pro-Art** – a program that clarifies the exact requirements for artificial intelligence within PROMETHEUS;
- **Pro-Gen –** a program for analyzing traffic scenarios.

The results of this research will be integrated in what are called Common European Demonstrators (CED), that will involve collaboration of different automotive companies on components, systems, and functions, as well as tests and evaluations. The main goals are preparation of standards and establishment of general architecture for future systems. Among the CEDs planned is a ***post accident system*** to alert oncoming vehicles to prevent secondary accidents. It will also call rescue services automatically via a cellular telephone.

Other Navigation and Route Guidance Systems

Radio Data System (RDS) is a system for transmitting data by means of a data channel on the sidebands of existing FM radio broadcasts. Initially, RDS is being used to enable broadcasting stations to transmit a unique identification code, allowing self-tuning radios and current station name displays.

The Traffic Message Channel (TMC) is one of several other applications proposed for RDS. TMC is planned to enable the provision of low-cost, digital data traffic to the motorists.

RDS provides a silent data system, superimposed on normal FM radio broadcasts. The data rate used is 1187.5 baud, divided into groups of 14 bits. Each group is further subdivided into four blocks of 26 bits, with each block containing 16 data and one error-correction bits. Messages can be specific instructions for negotiating a hazard or diversion, or other details such as prevailing speed, weight and width restrictions.

Philips and Bosch have been involved in the initial development of RDS, with further development taking place within the DRIVE project RDS-ALERT. Work is underway to set standards for the TMC. The RDS-ALERT project seeks to establish a consensus among European broadcasters, industry and government for a protocol covering traffic messages for European road traffic. RDS is also under investigation in the U.S. under the NCHRP project 3-38, Assessment of Advanced Technologies for Relieving Urban Traffic Congestion.

ALI-SCOUT (now renamed Euro-Scout) is a dynamic route guidance system utilizing a network of roadside beacons to provide two-way communications between vehicle and control center. Infrared is used as the communication medium. ALI-SCOUT is the basis of both the Autoguide and ULLISSE systems, adopted in the U.K. and France, respectively. It has been developed by Siemens Automotive and is the system installed in the current LISB field trial in Berlin.

Trafficmaster – a real-time traffic information system (by General Logistics PLC, England) that provides motorists with up-to-the-minute information on the speed, direction and length of any traffic backup. It enables drivers to assess the situation and take avoiding action, if desired, but does not suggest what evasive action to take.

The system uses infrared sensors mounted on highway bridges at approximately 3-km intervals that log the speed of traffic passing below them. Each unit illuminates two detection zones with encoded streams of infrared light. If the speed drops below a preset threshold of 25 mph, the sensors relay that information over a radio link to the control center. From there the information is transmitted by means of a radio paging network to a receiver mounted on the dashboard, of the vehicle. The display unit is portable and therefore can be used to make travel assessments prior to starting a journey. The cost of Trafficmaster to the subscriber is $580 for the receiver plus a monthly subscription charge of $35.

Autoguide – a dynamic route guidance system based on a network of short-range beacons connected to a control center based on the ALI-SCOUT concept. A consortium headed by GEC Marconi will build and operate Autoguide. All equipped vehicles passing a particular beacon at a particular time receive a set of data via a communication link based on infrared pulses at a high data rate (currently 500 kbps). The data set includes location, map and route data, which were calculated during the last 5 minutes at the control center, based on actual traffic conditions. Communication with the beacons is two-way. Travel time data from fitted vehicles are transmitted to the beacons and hence to the control center.

A demonstration system in London consists of five independent beacons covering part of central London and the route to Heathrow Airport and 15 vehicles equipped with Autoguide units. A large-scale pilot installation with 200-300 beacons and 1000 vehicles is planned soon. If that is successful, the system will be expanded to 1000 beacons.

LISB – *Leit und Information System Berlin* – is the main project using the ALI-SCOUT concept. It is funded by the German government and the Senate of Berlin.

Infrared communications beacons at 250 intersections in and around Berlin transmit traffic-dependent routing information to 700 equipped vehicles as they pass the beacons.

CARIN – CAR Information and Navigation System – is an in-car information and navigation system utilizing CD-ROM for data storage[5]. Developed by Philips, in the Netherlands, CARIN is a true route guidance system, which calculates shortest routes based on the on-board map data. Prototypes featured a map display similar to ETAK and TRAVELPILOT. However, further development has resulted in a man-machine interface approach closed to that used in. ALI-SCOUT and Autoguide. The driver is guided with spoken directions from a speech synthesizer during the journey, supplemented by a picture display.

CARMINAT – is a collaborative project, involving Philips and Renault, investigating the use of RDS to provide a limited amount of dynamic traffic information to an on-board CARIN unit.

Standardization of the Road-Vehicle Communication Link

Nearly half of the DRIVE I projects work has been done on specification and some will contribute to formal standardization development. However, what is most representative of the state of the standardization progress to date is the following quote from [2]: "It is important to note that much of this work is at an early stage and some time will elapse before any formal standards evolve". DRIVE I has delivered Common Specifications which will be taken up by standardization bodies such as CEN, CENELEC and ETSI for further refinement towards European standards.

In March 1991, CEN decided to set up a new technical committee, TC278 with the title Road Transport and Traffic Telematics. Parallel to the CEN TC278 activities, CENELEC prepared to start work on its TC114, Surface Transport Electrotechnical System Equipment, with a tentative scope clearly overlapping that of CEN TC2788. In ETSI no new activity was started in the field of RTI but several work items of great

potential interest in **RTI** are well in the process of standardization or even completed.

In October 1991, a tripartite coordination group (CEN/CENELEC/ETSI) convened, which had the task of appointing a team of experts (TET – Transport Experts Team) in order to list the standardization needs in the RTI area with an indication of the ongoing work and the priorities and proposals as to the allocation of the work among CEN, CENELEC and ETSI. The final report from the TET team, produced the first quarter of 1992, lists 65 work items grouped under the main headings: application, databases, interfaces and basic concepts and will be an important work instrument for the projects in DRIVE II. The following is a list of contributions of various DRIVE I projects towards standards. The work has been classified into: recommendations, codes of practice, functional specifications, common functional specifications and pre-standards.

- Project V1005 (PREDICT) produced recommendations for pollution level control.
- Project V1049 produced a manual of ***recommendations*** and specifications. concerning field trials.
- Project V1051 produced proposals for a ***pre-standard*** on procedures for the development of safe software and hardware for safety critical electronic RTI systems.
- Project V1037 (STAMMI) produced ***recommendations*** for in-vehicle man-machine interface (MMI), together with appropriate performance criteria and values.
- Project V1041 (GIDS) produced requirements and ***recommendations*** concerning intelligent co-driver systems.
- Project V1042 produced ***recommendations*** for in-depth accident data collection.
- Project V1050 (DRACO) developed a ***functional specification*** for an in-vehicle "black box" accident recorder.
- Project V1003 (VAMOS) provided ***recommendations*** for standards in the field of VMS (variable message signs).
- Project V1024 provided ***recommendations*** on a uniform and comprehensive driven information system for all European countries.

- Project V1026 (INVAID) p*re*pared ***a junctional specification*** for an incident and congestion detection system integrating computer vision and image processing techniques with conventional detection methods.

- Agreement has been reached between several projects for a basic frame structure for OSI layer 2, based on HDLC (High-level Data Link Control) frame for infra-red, microwave and millimetric wave vehicle-beacon systems.

- Projects V1018 (TARDIS) and VITA have arrived at ***junctional specifications*** for automatic debiting systems.

- Project V1029 (RDS-ALERT) has obtained a real consensus among broadcasters, national traffic authorities and manufacturers and has developed a Traffic Message Coding ***pre-standard*** known as the "ALERT-C" protocol, for RDS-TMC. This protocol defines the message catalogue, its structure and contents, as well as its presentation to the driver.

- In the DRIVE framework, a working group has been set up for standardization of smart cards.

- Projects V1001 (BARTOC) and V1019 (CASSIOPE) made ***recommendations*** for the architecture of of a future integrated Pulic Transport vehicle scheduling and control system.

- Projects V1010 and V1021 produced what is currently a ***code ojpractide*** among those concerned with electronic navigation, for a common European digital road map.

- The objective of Project V1044 (FLEET) was to develop a framework for a pan-European fleet management system. Specifications have been drawn up for the data content and exchange between the different modules. Regarding the exchange of data, ***recommendations*** have been put forward for ED1 messages using the EDIFACT standard.

- The project EUROTRIP investigated the exchange of information between existing systems to provide a Europe-wide trip planning system. ***Recommendations*** were

made to allow existing services such as Minitel(F), Prestel(U.K.), and Videotext(D) to be linked to provide wider coverage of data.

A multinational working group set up by the German, British, and French Governments has produced a draft standard [7] for the road-vehicle communication link based on the infrared system in use in London and Berlin.

The draft standard is currently being considered by CENELEC, the European standardization body for electrotechnical developments. A number of TARDIS partners have participated in drawing- up this draft standard and have ensured that the requirements of a wide range of RTI applications can be accommodated within the standard without duplication of transmission equipment.

Microwave is the major candidate for adoption as a carrier technology for communication for transport services and other purposes. Its use on a large scale would be dependent, however, on the allocation of suitable frequencies, on a Europe-wide basis.

As a result of meetings between DRIVE and PROMETHEUS, the CEPT Working Group proposed the following frequency bands which have been formally approved by the European Radio Communications Committee (ERCC) in February 1991. For initial systems like toll collection, vehicle-to-road communication, road pricing, parking control and route guidance:

- 5.795 - 5.805 GHz for pan-European applications
- 5.795 - 5.815 GHz to meet specific local requirements

For future systems to supersede the initial systems, vehicle-to-vehicle communications, co-operative driving, lane changing, "instant" advance incident warning the frequency range is 63-64 GHz. For radar systems, such as on-vehicle anti-collision radar and cruise control, the frequency range is 76-81 GHz

The Commission is in the process of preparing a Directive on this topic taking into account the CEPT recommendations which will be communicated to the Council and European Parliament in the second quarter of 1992.

In DRIVE II, topic groups are set up with the objective of contributing to the standarisation in the following fields: automatic fee collection and access control, smart cards, traffic data dictionary, traffic data exchange, geographical location referencing, travel and traffic information, man-machine interfaces, hazardous goods monitoring, public transport, automatic ticketing, communication architectures, freight and fleet management systems, extension of the RDS-TMC protocol to urban areas, individual route guidance and parking management. The results coming out of the topic groups will be coordinated by the CORD project which will transfer them to the corresponding working groups of the standarisation bodies.

3.1.3 Japanese Programs

Most of the information presented here is taken from [4]. That document provides a broad overview of the development and applications of IVHS in Japan. It is derived largely form a Study Mission to Japan conducted in March of 1991 and reflects one American's (the Team Director of the IVHS Program at the University of Michigan) perspective on what was shown in Japan, presented in Japanese publications, and learned through various personal interviews. It should be noted that Japan has not used the term IVHS per se in characterizing its programs – although R&D in Japan has certainly dealt with most of the elements of what is understood as IVHS in the western world.

The JSK Organization

The Ministry of International Trade and Industry (MITI) started the first major IVHS-type project in Japan called the Comprehensive Automobile Traffic Control System (CACS). The system design in CACS involved two-way digital communications between vehicles and the roadside for obtaining cooperative route guidance. Begun in 1973, the CACS program was funded by MITI and supervised by its Agency of Industrial Science and Technology.

At the close of this project in 1979, MITI created the Association of Electronic Technology for Automotive Traffic and Driving (known by the initials of its Japanese trans-

lation, Jidosha Soko denshi gijutsu Kyokai, or JSK) as a continuous facilitator of IVHS technology including interest in autonomous vehicle control. The mission of JSK is premised upon the concern that electronics technology must help to address "the needs and pressures imposed on (society) by the ever-increasing use of the automobile." This association counts 57 companies among its members (including Bosch, General Motors, Mercedes-Benz, Philips, and Volvo from outside of Japan). Perhaps a good summary of the MITI/JSK dynamic is that various IVHS technologies are *incubated* with a nearly seamless interface between MITI's own projects which are typically rather advanced, and the near-application programs (like AMTICS and RACS) headed by other agencies.

The AACS Project

At least from 1981 through 1987, JSK has conducted a variety of studies under its "Automobile-Automobile Communication System" (AACS) project. The project has not sought to produce a single system per se, but rather has explored the broad area of autonomous digital communications between vehicles in relatively near proximity to one another (at least partially analogous to the ***hand-shake*** communication between vehicles that is being explored in the European PROMETHEUS program). Communications using inductive radio, low-power UHF, and packet radio schemes have been reported [6]. Some twenty-one functions for automobile-to-automobile communications have been considered in this work, ranging from simple relay of traffic information beyond the range of spot communications at intersections, to accident-site warnings, emergency messaging, and even warnings to avoid head-on collision.

The RACS and AMTICS Projects

Several phases of Japan's two major in-vehicle information systems programs, **RACS** (for expressways) and **AMTICS** (for surface streets), have been completed and are now being evaluated. The results of that evaluation will determine the direction of the future program.

RACS (Road Aut omobile Communication System) – a 4 billion yen (US $ 30.3 million) project which involves a beacon-based communication architecture providing spot-coverage of the road system through thousands of strategically-placed communication zones, each of which covers a 60 m long piece of roadway. Two candidate communication systems were selected for evaluation, an inductive radio system and a microwave system [8]. After experimental study, it was decided that RACS is going to adopt the microwave system which has the following characteristics: the frequency band is 2-3 GHz with a choice of frequency around 2.5 GHz; the modulation is PSK/Reverse Amplitude Modulation; the data rate is 512 kbps; the beacon antenna is a two-element antenna; the automobile antenna is an upward beam antenna; the communication area is 5 lanes x 60 m; almost error-free (< 10^{-7} bit-error rate) with a few burst errors; the maximum data volume attainable at a beacon is 370 kbits; the accuracy of position determination is ± 1 m; and the detection of automobile moving direction is very good.

The transmissions, in the 2.5 GHz microwave band provides for highly localized functionality such as location-specific traffic messages and routing as well as toll-collection. The high level of data capacity provides for FAX transmission as well.

In the RACS design, the vehicle incorporates on-board navigation and the optimal route selection is made by means of an on-board computation. The road map database is kept on-board the vehicle stored on a CD-ROM. The RACS experiment was initiated in 1984. From 1986 to 1988 the Ministry of Construction formed a joint R&D project with 25 private companies. In 1987 and 1988 field tests were conducted using a digital road map database and inductive radio and microwave beacons.

It should be mentioned that recently the Ministry of Posts & Telecommunications has ruled that the use of a microwave uplink from vehicle-to-beacon, as was intended in the original RACS design, will not be permitted [1].

AMTICS – About 50 corporations participate in AMTICS (Advanced Mobile Traffic Information and Communication System), for which total expenses have not been released. This project employs in-vehicle equipment which is similar in many respects to that of RACS except for the communication interface. The AMTICS data link is

by means of a one-way broadcast of traffic data from a cellular system of teleterminals operating at 900 MHz. The data rate from this transmission system is 9.6 kbps. An uplink capability is also available through the teleterminal system, but no vehicle-to-central communication was required in the basic AMTICS design.

A traffic control center transmits traffic congestion information by using the downlink part of the teleterminal system, a cellular digital packet system with 3 km radius area. For accurate information, additional 13 GHz microwave radio units called sign posts are used. Like RACS, AMTICS uses maps stored in CD-ROMs and CRT display terminals. The Teleterminal System providesreal-time information on traffic conditions, weather, and available parking spaces. In addition to showing maps, the CRTs display local traffic regulations, locations of gas stations, and tourist information.

An AMTICS experiment was conducted in central Tokyo in 1988 with about 12 different versions of in-vehicle equipment. In 1990 a second demonstration involving 34 vehicles took place at the Osaka Flower and Greenery Exposition. Each demonstration reportedly cost about 300 million yen (US $ 23 million).

While it was expedient for the AMTICS project to employ the digital cellular teleterminal system, this approach may well yield to an alternate broadcast method in the next generation. The primary candidate is "FM multiplex" which offers a high data-rate downlink that, if incorporated in FM broadcast stations across Japan, would provide low-cost nationwide coverage. Both RACS and AMTICS are seen as exploratory "vehicles" through which a host of collaborating players can examine system-level and in-vehicle issues. Both projects are viewed as having been very successful even though neither will probably ever be built quite as prototyped during the 1988 to 1990 time frame.

The VICS Program

It is yet another collaborative program involving virtually all the players in Japan's IVHS development, but it is shaping up differently from the others. Namely, the "Vehicle Information and Communication System" **(VICS)** program was formed under the combined direction of the MC (Ministry of Construction), NPA (National Police Agency)

and MPT (Ministry of Posts and Telecommunications) agencies to establish a consensus on the architecture and operational practices for a cooperative driver information and routing system. Thus, it is not developing as another system demonstration project. Rather, it appears that VICS seeks to determine an architecture and associated protocols so that an infrastructure supporting this system can be implemented throughout Japan well within this decade. VICS is committed to a cooperative effort to unite the AMTICS and RACS approaches into one harmonious system. The formal launching of VICS began with one-day conferences in Tokyo and Osaka in March 1991. From the events in these conferences, it is virtually guaranteed that the needed cooperation will, in fact, occur.

For communication media, VICS will consider the possible future use of the 900 MHz teleterminal system, FM multiplex, microwave beacons, and signposts. Nevertheless, the candid view is that the teleterminal is all but eliminated as an option because of its relative cost, where it is currently installed, and because of the impracticality of gaining complete nationwide coverage using such a cellular grid.

Joint development of an IVHS technology by industry and government has proceeded with characteristic speed in Japan. On the order of fifty large Japanese corporations have collaborated in these developments, many of whom have designed and built their own in-vehicle packages for communication with prototype infrastuctures. These experiences have advanced the need for certain standards, two of which have already been accomplished – namely, that for the map database and the format for coding data and application programs on CD-ROMs.

Communication Media for IVHS

A broad variety of radio data links are under consideration for application to IVHS in Japan and elsewhere. Japanese demonstration experiments have employed two-way inductive radio in the CACS program, two-way microwave transmission in the RACS program, and a 900 MHz one-way data broadcast in the AMTICS program (which could also have supported full-duplex communications if needed). While there has been a con-

sortium of companies gathered to build a network of 900 MHz teleterminals to serve a broad variety of applications, there seems to be little expectation in Japan that this system will be adopted by VICS. On the other hand the Ministry of Construction maintains a strong interest in deploying the microwave beacon. There is also an expectation that a large number of the estimated 40,000 traffic detectors to be added to the existing network throughout Japan in the next few years will be microwave devices capable of giving absolute location data and an increasing set of dynamic information to a passing vehicle. The beacons can also employ a speed-sensing function which is to enable a more careful assessment of travel times. The fact that such devices will provide data communication obviously requires microwave receivers in vehicles (a version of which were supposed to be sold to the public on some new Nissan models beginning in the summer of 1991). As a relatively new development, there is a strong emerging interest in FM multiplex which can provide a nationwide system using the virtually unused sideband capacity on the nationally-owned FM stations throughout Japan. The cognizant entity, the Japanese broadcasting organization known by its Japanese acronym, NHK (for Nippon Hoso Kyokai), operates the stations and is eager to see fuller utilization of their sideband capacity through IVHS and other applications.

NHK has developed special schemes for digital modulation and error correction to gain a high delivery rate through FM multiplex for the mobile environment. Currently a data rate of 9.6 kbps is assured and rates of 12 to 15 kbps are being studied. The data throughput is said to reflect the net rate accounting for loss factors in mobile reception which reduce the 45 kHz bandwidth of the FM subcarrier to an effective value of 35 kHz or so. If the primary function of an IVHS data broadcast is to transmit link-times covering a metropolitan road network, the 9.6 kbps capability would appear to be more than adequate. This is especially apparent if link-times are to be updated only every minute or so and if the transmitted data include only those link-times which have changed substantially over the last minute.

Interestingly, NHK currently offers round-the-clock television programming which is paid for through a directly-collected *tax* from all television owners. This rather unique taxing authority is noted by some as a possible means of financing the costs of a communications infrastructure serving IVHS. While the FM sideband modulation is inexpensive

to install as an enhancement on an existing entertainment station, the implicit cost will rise in the future as increased demand for all communication capacity causes the value of the FM sideband resource to rise.

Recognizing the possibility **that** both a broadcast data link and localized communication beacons,could be deployed, it should not be surprising that some auto manufacturers in Japan are already making contingency plans for dual receivers as the basic in-car communication device. **A** few of the veterans of Japanese IVHS programs have indicated that they fully expect such dual-mode communications to be implemented for the long term.

Product Innovations

It is an implicit part of the IVHS vision that, while cooperative infrastructures may be rationalized on the basis of specific in-vehicle devices and specific functionalities, the prospect of real-time data communications with motor vehicles will open the door to a variety of unexpected and perhaps profound innovations. While it is still early in the Japanese IVHS process to confirm this expectation, a couple of examples suggest that many levels of opportunity are likely to materialize.

At the Toshiba Research and Development Center in Kawasaki, a newly-created unit called the Automobile Systems Division has been formed to reposition the company for marketing systems-level IVHS products, and thus emerge from the role of providing only components to automotive assemblers. One early example of this unit's activities is the AMTICS Radio. It is essentially an alternative to the complete navigator package seen in the AMTICS-equipped vehicles. The device involves a lap-top computer which is outfitted with a teleterminal receiver to accept the AMTICS link-time broadcast. The road network of interest, for example in metropolitan Tokyo, is represented by a map database stored within the device. After the user enters current location and destination, both a graphical display of congested streets and text information are presented on the LCD screen. The device can be used for trip planning by individuals, or could alternatively be carried within a moving vehicle.

3.2 IVHS Functional Requirements

It is expected that various types of applications/services will be provided to meet the goal of IVHS and satisfy customer needs. Naturally, it would be desirable to have a single communications infrastructure to support all the applications envisioned within IVHS. However, it is conceivable that more than one communications interface be in a vehicle because of the differing requirements of different applications.

A partial list of IVHS user services/applications that are envisioned is as follows:

- Traveler Information – such as traveler advisory, traveler information services (value-added), trip planning, position location systems, navigation, route guidance (including collision avoidance) weather, visitor attractions, restaurants, events, hotels, gas.
- Traffic Management – such as incident detection and management, demand management, traffic network monitoring, traffic control, parking management, workzone management and automatic toll collection.
- Freight and Fleet Management – such as intermodal transport planning, route planning and scheduling, hazardous material monitoring and tracking, vehicle and cargo monitoring. law enforcement and regulatory support.
- Public Transportation and Emergency Vehicle Management – such as planning and scheduling systems, signal pre-emption traffic control, automatic payment, dynamic ride sharing, prediction of arrivals and emergency services systems management.
- Additional Services – examples are traveler safety and security, MAYDAY transmissions and hazard warning.

These diverse IVHS application areas and services are summarized in Figure 3.1.

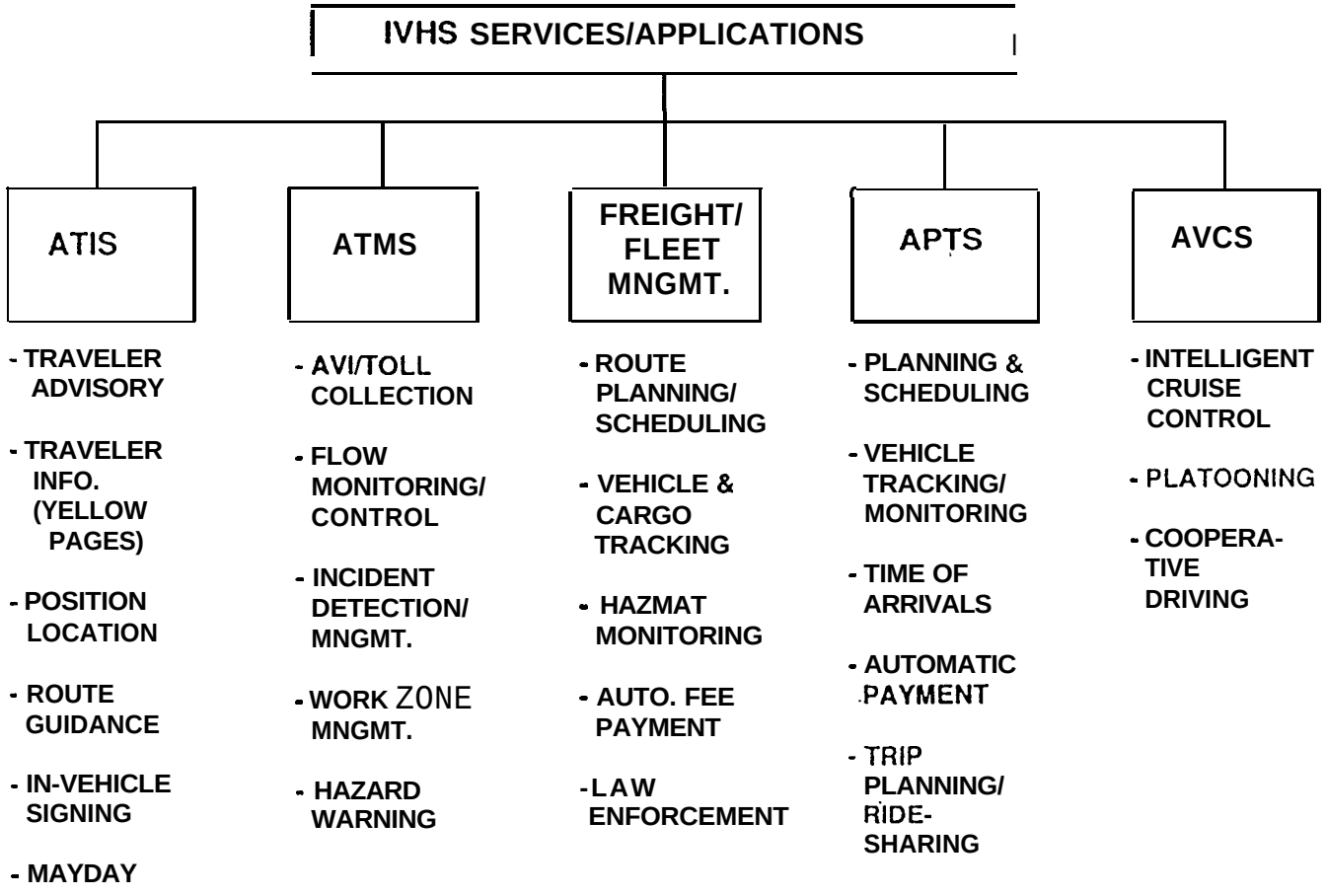

Figure 3.1: IVHS Applications and Services

Each of the above services has its detailed requirements such as volume of data to be communicated, the size of the communication zone, the quality of the communication in terms of maximum tolerable bit error rate, the priority of the communication, the need for one-way or two-way, voice or data communication. Clearly, a wide range of requirements are possible.

An example of a difference in requirement is demonstrated by that between route guidance and automatic debiting. For route guidance, there is no need for true dialogue between beacon and vehicle – a bidirectional ***monologue*** ensures that the vehicle receives a substantial amount of data and in turn transmits its own message, neither directly dependent on the contents of the other. For automatic debiting, however, there must be a true dialogue in which messages are exchanged between individual vehicles and the roadside controller.

Several technologies have been suggested as candidates in order to provide communications for the above mentioned services. They include subcarrier FM TV, SAP signals, Highway Advisory Radio (HAR) at 530 kHz and 1610 kHz, leaky cable, satellites (LEO, GEO), beacons (IR and microwave), 2-way wide area radio, cellular systems, inductive loops, HF, Personal Communication Services (PCS), microcellular, and even meteor burst. Some technologies are more suitable for certain services than others. Table 3.1 shows the applicability of communication technologies to different types of services.

Communication requirements are also dependent upon overall IVHS system architecture. For example, a centralized architecture requires ***more*** communications than a decentralized or distributed one. The task of setting IVHS communications requirements and proposing standards is particularly difficult because of the great variety of IVHS systems under consideration, and because these systems are expected to evolve with time. The system architecture may have to be defined before specifications or standards can be considered meaningfully. The specification of the communication protocols will depend partly on how spatial and temporal aspects of traffic networks are implemented, and how intelligence is distributed between the infrastructure and the vehicles.

Services Technologies	ATIS ATMS	Public Transport	Fleet Management	Truck Monitoring	Vehicle/Hwy Automation	Rural Systems
Subcarrier FM RDS, SAP, SCA	Some Voice, Data	Some	Niche	No	No	Some
HAR 530/1610 kHz	Some V	No	No	No	No	Some
Leaky cable	Some V	No	No	No	No	Some
LEO Satellites GEO	Yes V, D Cost	Wide area	Yes V, D	Yes	No	Yes V,D
Beacons IR, Microwave	Yes D	Yes D	Some D	Some	Some (Veh/Veh)	Some
2-way wide area radio	Yes V, D	Yes V, D	Yes V, D	Some	Some	Yes V, D
Cellular Voice,data	Yes? V, D	Yes V, D	Yes V, D	Some	Some	Yes V, D
Inductive loops	Very few D	No rail Y	No	No	Maybe	Very few
HF	?	No	No	No	No	?
PCS Microcellular	Yes? V, D	Yes V, D	Yes V, D	No	Maybe	No
Meteor burst	No	No	No	?	NO	No

Table 3.1: Applicability of different Technologies to different Types of Service

In this Report we focus on a microwave beacon. The following generic requirements can be placed on such a system :

- The beacons are to be mounted on posts (on the side of the road or in the center divider) at a distance of approximately 1 mile (possibly to take advantage of the highway infrastructure [RG private communication]). Therefore the communication zone is 4 or 5 lanes by 1 mile (one half mile to the left and one half mile to the right of each beacon).

- The carrier frequency is to be either in the 1800 MHz or 900 MHz band[1].

- The system is not required to provide real-time two-way voice communication. If voice needs to be transmitted it will be packetized and combined with the data (canned voice). The system is to be used either one-way data communication or two-way links organized in a half-duplex mode.

- The maximum tolerable bit error rate is to be 10^{-4}–10^{-5}, similar to data communication.

- The data transmission rate, although not specified as of yet, should be at least 80 kbps, depending on the access protocol and the specific amount of data to be communicated. (In the Japanese project RACS a transmission rate of 64 kbps is proposed for a maximum data transaction size of 80 kbits.

- The required transmission power of the beacon should be as low as possible, below 1 W, with 100 mW or even lower as a target.

- The required received power will depend on such receiver parameters as receiver dynamic range, sensitivity, and antenna design. These parameters must lead to inexpensive vehicle equipment. The dynamic range should not exceed 40 dB, and the receiver noise figure should be about 6 dB.

- The beacon antenna height should be 5-8 m, and the antenna heights for the mobiles are 1.3 m for cars, 2 m for vans and 34 m for trucks, with an average value of 1.6 m for all kinds of vehicles.

[1] Recently, **WARC 92 and the FCC have allocated 230 MHz in the 1800 to 2200 MHz band for emerging mobile and personal technologies. On the other hand, the 900 MHz band contains bands that could accommodate ADIS-type communications.**

An important issue in the system specification, which greatly impacts the design of the physical and access layers, is the volume of information to be communicated and the data transmission rate. Some of the services listed above, such as route guidance, may require either large or moderate amounts of data to be communicated between vehicle and roadside, depending on implementation. For example, route guidance could be done in two ways. One approach could be to send the entire map of a requested area together with the traffic congestion information for it. Another approach could be to have the maps stored in memory in each vehicle (in CD-ROMs like in the RACS project in Japan) and communicate only the traffic information for a particular area. Other applications, like toll collection, may require small amounts of. data and communication that is more interactive in nature. Table 3.2 summarizes some of the data transaction requirements for ATIS and ATMS, which generally overlap ADIS.

	FUNCTIONS/ USER SERVICES	INFO. DIRECTION	MESSAGE TYPE	REAL-TIME	DATA VOLUME	MESSAGE PRIORITY	SECURITY	COVERAGE
A T I S	TRAVELER ADVISORY	1 WAY IN/ 2 WAY	D/V	Y	< 100 CHAR.	HIGH	N	LOCAL/WIDE/ REGIONAL
	TRAVELER INFO (YELLOW PAGES)	2 WAY	D/V	N	LARGE	LOW	Y	LOCAL/WIDE/ REGIONAL
	TRIP PLANNING (RIDE SHARING)	2 WAY	D	N		L O W	N/Y	WIDE/ REGIONAL
	ROUTE SELECTION ROUTE GUIDANCE	2 WAY	D	Y	5-10 KBIT	MED	Y	LOCAL/WIDE
	IN-VEHICLE SIGNING	1 WAY IN	D	Y	5 KBIT	HIGH	Y	LOCAL
	DIGITAL MAP TRANSMISSION	1 WAY IN	D		64 KBIT	MED	Y	LOCAL
A T M S	INCIDENT' DETECT. & MANAGEMENT	1 WAY IN	D/V	Y	c 100 CHAR.	HIGH	Y	LOCAL/WIDE REGIONAL
	CONGESTION MONITORING		D	Y		MED		
	PARKING MANAGEMENT	2 WAY	D/V	N	1 KBIT	MED	N	LOCAL/WIDE
	TOLL COLLECTION (ELECTRONIC)	2 WAY	D	Y	1 KBIT	HIGH	Y	LOCAL
	TRAVELER SAFETY ROAD ASSISTANCE	1 WAY OUT 2 WAY	D/V	N	< 100 CHAR.	HIGH	Y	WIDE/ REGIONAL

IN = TO VEHICLE; LOCAL < 1 MILE; WIDE AREA 1-10 MILES; REGIONAL > 10 MILES

Table 3.2: ATIS / ATMS Communication Requirements

For the purpose of the ADIS communication system architecture study, and the associated system layout tradeoffs in Chapter 7, it is advantageous to express the ADIS transaction requirements in a more focused form. This will enable a straight-forward derivation of the transmission data rate requirements for the candidate multiple access architectures. It is convenient to think of the transactions as belonging to three distinct categories, each category having a distinct size. This generic classification is summarized in Table 3.3.

Transaction	Size	Priority	Examples
Small	< 1 kbit	High, Medium	AVI, Road Pricing, MAYDAY, Traveler Advisory, Vehicle Location, Vehicle Status
Medium	5-10 kbit	Medium	Route Guidance, In-Vehicle Signing, Value Added Services, Dispatch
Large	~ 64 kbit	Low	Digital Map, Trip Planning

Table 3.3: Generic ADIS Transaction Requirements

The generic data transaction requirements identified in Table 3.3 will be used to derive the transmission data rate requirements for the different layout options considered in Chapter 7.

3.3 References

[1] Oral Presentation to the IVHS Study Team at the MEX Center in Tokyo, Public Works Research Institute, Mar 91

[2] DRIVE 1992, Research and Technology Development in Advanced Road Transport Telematics, Commission of the European Communities, Apr 92

[3] I. Catling, Op be Beek, "SOCRATES: System for Cellular Radio for Traffic Efficiency and Safety", *NAV '90 Conj. Proc.*, vol. 42, Sep 90

[4] R. D. Ervin, "An American Observation of IVHS in Japan", Technical Report, Univ. Michigan, 1991

[5] M. L. G. Thoone et al, "The Car Information and Navigation System CARIN and the Use of Compact Disc Interactive", SAE Tech. Paper 870139, 1987

[6] Association of Electronic Technology for Automobile Traffic and Driving (JSK), ***International Survey of Automobile Information and Communication Systems,*** Tokyo, Japan, Mar 91

[7] U.K. Dep. Transp., "Draft Standard for the Road-Vehicle Communication Link", Dept. Transp. TCC Div., 1989

[8] Y. Shibano, T. Norikane, T. Iwai, M. Yamada, S. Tsurul, "Development of Mobile Communication System for RACS", *IEEE Veh. Tech. Conf. Proc.*, pp 376-383, 1989

Chapter 4

Modeling of IVHS Fading Channels

4.1 Introduction

In this chapter, the Mobile Channel for Intelligent Vehicle and Highway Systems (IVHS) scenarios of interest, namely surface streets and highways, is characterized in detail. Due to its economic interest, and geometrical similarities (man-made structures confining signal propagation), emphasis is placed, without much loss of generality, on the analysis of Highway IVHS.

In Section 4.2 the envisioned IVHS scenarios are studied within the context of Mobile Radio. The IVHS channel is characterized by a particular set of propagation conditions which are initially analyzed in light of the recently proposed two-ray model (2RM). This 2RM is found to be lacking in detail for IVHS applications, thus pointing to the necessity of a more elaborate model.

Multiple access (MA) techniques allow for coverage of a section of highway (cell) with a single base station (BS) antenna instead of one antenna per lane. In Section 4.3 an original and detailed multi-ray model (MRM), tailored for IVHS applications and single BS per cell, is proposed. The MRM is used to compute the mean of the, usually Rician (due to the presence of line-of-sight [LOS]) fading, characteristic of this kind of short range communications. This applies to most IVHS situations of interest. The diffuse component, however, still requires an extensive measurement campaign for all IVHS environments.

In Section **4.3** the effects of polarization on the observable fading are studied taking into account the extant propagation conditions. The effects of operating frequency and of BS antenna height on cell size are analyzed, with the MRM supplying a natural way of defining the cell size.

All geometries of interest, in terms both of infrastructure profile (elevated, depressed or walled highway) and BS placement (middle-of-the-road or side-of-the-road), are also analyzed making use of this extended MRM. Furthermore, the effect of BS antenna beam shaping through the use of inexpensive passive or active configurations is also analyzed.

Section 4.4 combines all the previous theory in order to construct a detailed description of the IVHS Mobile Channel as a mobile unit moves through the cell, under given traffic conditions, facing the occurrence of blockage of some of the rays, including possibly the LOS.

Finally, in Section **4.5** the package used to implement the detailed MRM presented here in first hand, is briefly described. The package includes the simulation of highway traffic (parameterized by traffic intensity), displaying the actual Multi-Ray structure for all actively communicating mobiles. Moreover, by building upon the blockage status of each ray for every active mobile plus surrounding traffic, the package is able to precisely characterize the slowly time-varying fading channel “seen” by the mobile as it traverses a given cell. This is performed for any lane, selected speed, and a randomly generated traffic of given characteristics.

4.2 Fading in Land Mobile Communication Systems

In this Section the envisioned Intelligent Vehicle and Highway Systems (IVHS) are analyzed in the context of Mobile Radio, namely of what Korn [1] called Land Mobile Communication (LMC) systems, corresponding to the conventional cellular, and macro-/micro-/picocellular environments [2],[3]. The particular propagation conditions in the variety of environments intended for coverage are studied in light of the recently proposed 2RM which is thoroughly analyzed.

4.2.1 Cell Classification

LMC Systems are based upon cellular structures whose classification varies significantly from author to author. Cell classification is usually based upon cell size, although it may also be based on dimensionality (e.g., 1-D for highway micro-/picocells, 2-D for urban macro-/microcells, 3-D for certain building picocells [4]). We propose to adapt and extend the comprehensive radio cell definitions for urban environments of COST 231's Working Group 2's Subgroup on Propagation Models [5] which not only take into account the cell size but also the BS antenna positioning :

- Large/Small Cells - the BS antenna is installed above roof tops, usually atop a high rise building, the path loss being determined mainly by diffraction and scattering at roof tops in the vicinity of the mobile (M), i.e., the main rays propagate above the roof tops [5]. Large/Small cells differ in maximum range which is 3-10/1-3 km, respectively. These cell sizes correspond to the conventional/macro cellular scenario [2].

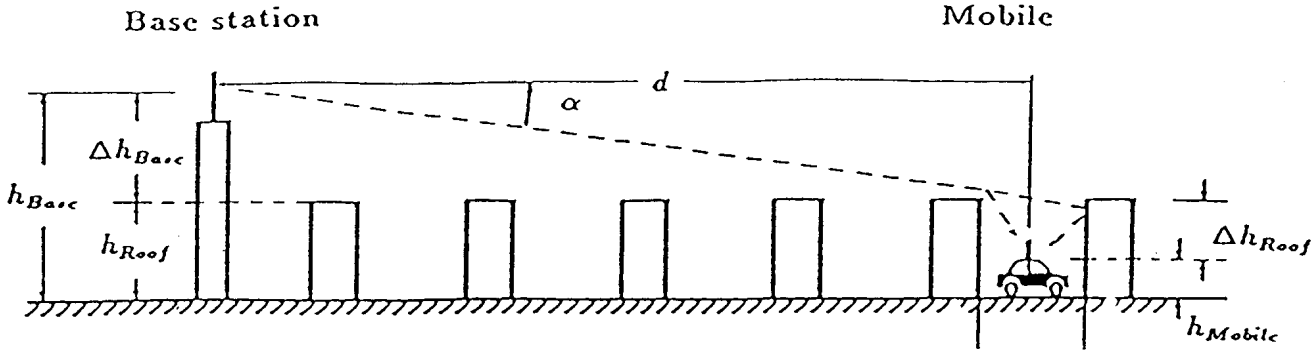

Figure 4.1: Conventional/Macro Cellular Scenario [5, Figure 1]

- Microcells - the BS antenna is mounted generally below building roof top level, and wave propagation is determined by diffraction and scattering around buildings, i.e., the main rays propagate in street "canyons" somehow like in grooved waveguides [5]. The maximum range is 0.2-1 km, corresponding to the microcellular scenario [2].

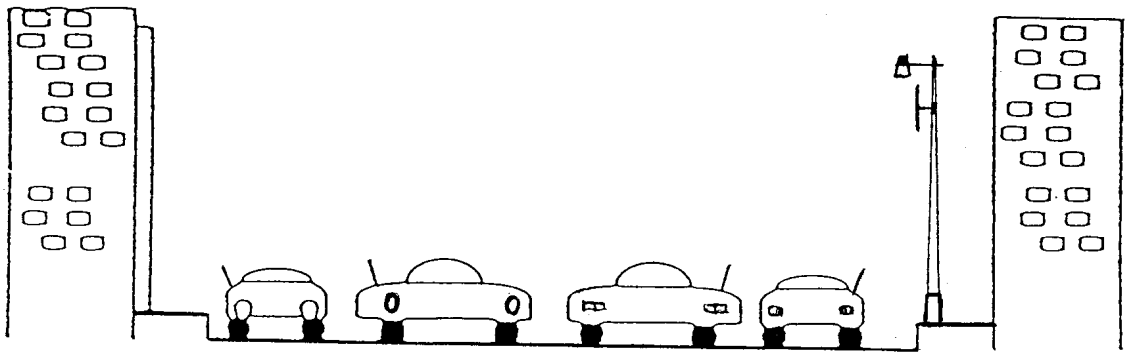

Figure 4.2: Micro-/Picocellular Scenario – adapted from [6, Figure 1]

- Picocells - the BS antenna is mounted below roof tops in small high traffic density cells in the downtown, highrise building areas of big cities, or inside buildings (e.g., wireless PABX), and at/below lamp post height in roadway structures. In this scenario, wave propagation is definitely guided by man-made structures. The maximum range for picocells is typically 0.2 km.

In the last two cases, except for indoor communications, due to the short range nature of the communication, LOS is in general present, especially if care is taken to position

the BS antenna at such a height that it virtually insures no shadowing effects due to the traffic, vehicular or otherwise (e.g., of persons or objects), in presence.

4.2.2 IVHS in the Cellular Context

The two main IVHS environments of interest are surface streets (Figure 4.3.a) and highways (Figure 4.3.b). In terms of cell size, the microcellular scenario adequately describes the IVHS surface streets environment. For highways one may be either at the microcellular level or possibly at the transition between the micro- and the picocellular, depending on the desired granularity of the coverage.

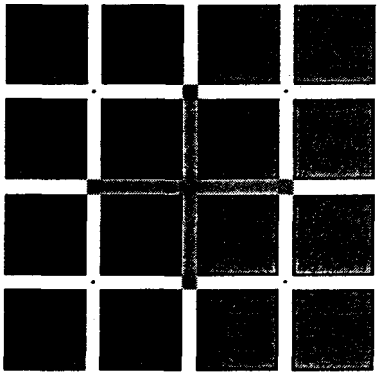

(a) Section of Surface Street Blocks

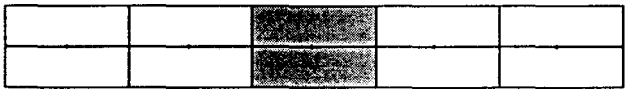

(b) Highway Section

Figure 4.3: Examples with centrally located Base Station Antennas showing schematically the Region of Coverage for a given Cell

The characterization of fading in microcellular systems, which typically correspond to the IVHS environment, has attracted little attention until very recently (e.g., [6], Proceed***ings of the Vehicular Technology Society Conference '92***), since it was erroneously thought that Conventional/Macro Cellular characteristics could be extrapolated for small-celled systems [6].

The available models for microcellular systems, and those for the conventional/macro cellular case, are herein presented. In fact, it is important to understand the similarities, and especially the differences, between the two types of environment in order to arrive at the appropriate model for **the IVHS applications. At the same time, it is very likely** for overlaying of the above cellular structures to take place in the IVHS scenario[1]. A new, comprehensive MRM specialized for the IVHS environment was deemed necessary, and is introduced. Its main characteristic is the presence of a LOS component in most circumstances, leading to a Rician, slowly time-varying channel model.

Microcellular Systems

In microcellular systems, usually operating at low power levels, typically in the range of a few tens of mW [7],[4], th**e cell radii vary** from 200 m to 1 km [2],[4], a situation where multipath propagation conditions are significantly less severe than in the conventional/macro cellular case [2],[7]:

- the average rms delay spread (see Section 4.3.2) is smaller by a factor of 3.7 [2];
- microcellular-type channels have Rician ($K \simeq 7$ dB for surface streets), rather than mostly Rayleigh, envelope fading characteristics [2], due to the presence of LOS, and correspondingly different spaced-frequency correlation[2] statistics [8]. The area bounded by the spaced frequency correlation envelope[3] is larger, approximately by a 1.5 factor [2], for these Rician channels, thus representing a flatter (i.e., less frequency-sellective) fading channel (Figure 4.4).

[1] **For instance, the traffic information of interest to drivers concerns not only the highways and their micro-/picocells, but also at least the neighboring surface streets (see the Los Angeles Pathfinder Smart Corridor experiment). In that scenario, the conventional/macro cells can act as umbrella cells, i.e., as a safety net to even teletraffic [4].**

[2] **The spaced-frequency correlation function of a channel is the Fourier transform of the multipath intensity profile (a.k.a. delay power spectrum) of the channel.**

[3] **This area is a more convenient measure of** the **frequency coherence of the channel [2] than the often employed practice of assigning as the correlation bandwidth the bandwidth at which the spaced-frequency correlation function envelope decreases to a -3dB relative level.**

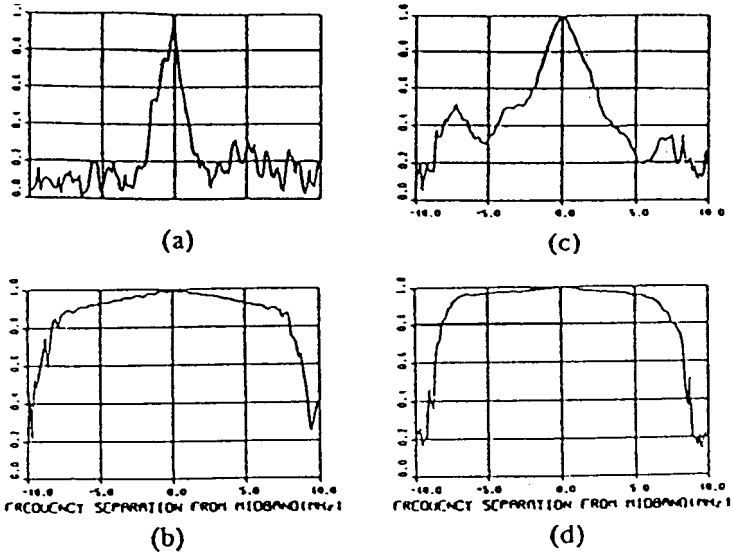

Figure 4.4: Spaced Frequency Correlation Function Envelopes for (a) **the poorest** (Bayleigh), and (b) **the best** (Rician) Conventional Channels; and (c) the poorest, and (d) the **best (both** Rician) **Microcellular Channels – from** [2, **Figure** 8]

In fact, extrapolation of Okumura's Model results for the conventional cellular environment [9] to the attenuation rate at a distance of 1 km, resulted in predictions of 30-35 dB per decade against the measured 20-25 dB per decade [6]. This is attributed to the strong LOS component present at short distances, and not considered by Okumura.

In order to achieve signal confinement to the size of the cell [6], the antenna height must be reduced to below that of the surrounding buildings/structures/barriers but still above that of the vehicular traffic. Alternately, one would require the addition, at an extra cost, of appropriate reflectors. Besides providing for LOS, the positioning of the antennas above the vehicular traffic virtually eliminates the shadow induced fading due to local traffic [7]. On the other hand, the positioning of the antennas below roof level minimizes excess delay spread, since the distant reflectors are blocked [10].

Conventional/Macro Cellular Systems

Conventional/macro cellular BS antennas usually radiate large powers, 0.6-10 W, from the top of tall buildings [4]. The effects of shadowing and multipath are modeled as multiplicative [11],[12]. It is widely accepted that the LMC channel associated with

conventional/macro cellular systems [2],[13], can be modeled as being affected by a compound fading process consisting of a Rician fading process which has a constant mean square value (which can be zero, leading to Rayleigh fading) over a distance range of some tens of wavelengths, and a log-normal shadowing process which affects the mean square value of the Rician process at larger distance ranges. The median value of the log-normal density function is, in turn, subject to an inverse power law distance dependence the exponent of which varies according to the specific location.

4.2.3 Propagation Models for Microcellular Systems with Near and Far Regions

Piecewise Linear Models

Let us analyze the microcellular environment, following mostly [7] which corrects and complements the initial analysis in [6]. Harley's original contribution [6] for the understanding of the propagation conditions in small-celled, guided propagation environments should not be forgotten.

A propagation model for microcellular systems is defined by

$$S = -10 \log_{,,} \left[d^{a} \left(1 + \frac{d}{g} \right)^{b} \right] + c \qquad (4.1)$$

where

- S is the signal level in dBm;
- ***d*** is the distance from the transmitting antenna;
- a is the basic attenuation rate for short distances;
- *b* is the additional attenuation rate coefficient for distances greater than g,
- g is the turning point of the attenuation curve;
- c is an offset in dBm.

The model simplifies to

$$s = \begin{cases} -10 \log_{,,} \left(d^{a}\right) + c & d \ll g \\ -10 \log_{10}\left(d^{a} + b\right) + c' & d \gg g \end{cases} \quad (4.2)$$

For all LOS measurements [7], even in different environments, the variation of signal strength with distance was found to show distinct near and far regions separated by a break point [6], the turning point of equation (4.2) above. The measured slope is less than two indicating a ducting effect[4] before the break point, and much greater then two after the break point.

It was found that the location of the break point could be calculated based on the first Fresnel zone clearance [7]. The first Fresnel zone is defined as an ellipsoid whose foci are the transmitting and receiving antennas, the distance from either antenna to a point on the ellipsoid and back to the other antenna being $\lambda/2$ greater than the direct path distance between antennas. According to [7], the break point is defined as the distance between antennas for which the first Fresnel zone touches the ground (see Figure 4.5).

When the signal propagation has first Fresnel zone clearance, the signal attenuation is essentially due to the spreading of the waveform [7], which is limited by the ground plane, leading to a slope which is less than two. Due to the small incremental path (and the value of the reflection coefficient), the wave reflected by the ground reinforces the direct wave, i.e., a ducting effect is present. When the first Fresnel zone starts to become blocked, a slope much greater than two results from the obstruction of the ellipsoid where most of the energy is concentrated[5], this in addition to the wavefront spreading [7] and increased refraction effects.

The radius of the family of ellipsoids corresponding to the successive Fresnel zones

[4] **Ducting** occurs whenever a natural (or, in the present case, man-made) structure traps, even if partially, the wave inside [14], thus guiding the wave. Some rays which normally would not reach the receiving antenna in this case do, and a stronger-than-normal signal will be received. Instead of the usual inverse square law typical of free space propagation (i.e., a = 2), ducting produces a smaller attenuation rate (i.e., a < 2).

[5] Propagation is assumed to be pure LOS, i.e., without diffraction attenuation occurring, if there is no obstacle within the first. **Fresnel** zone [14].

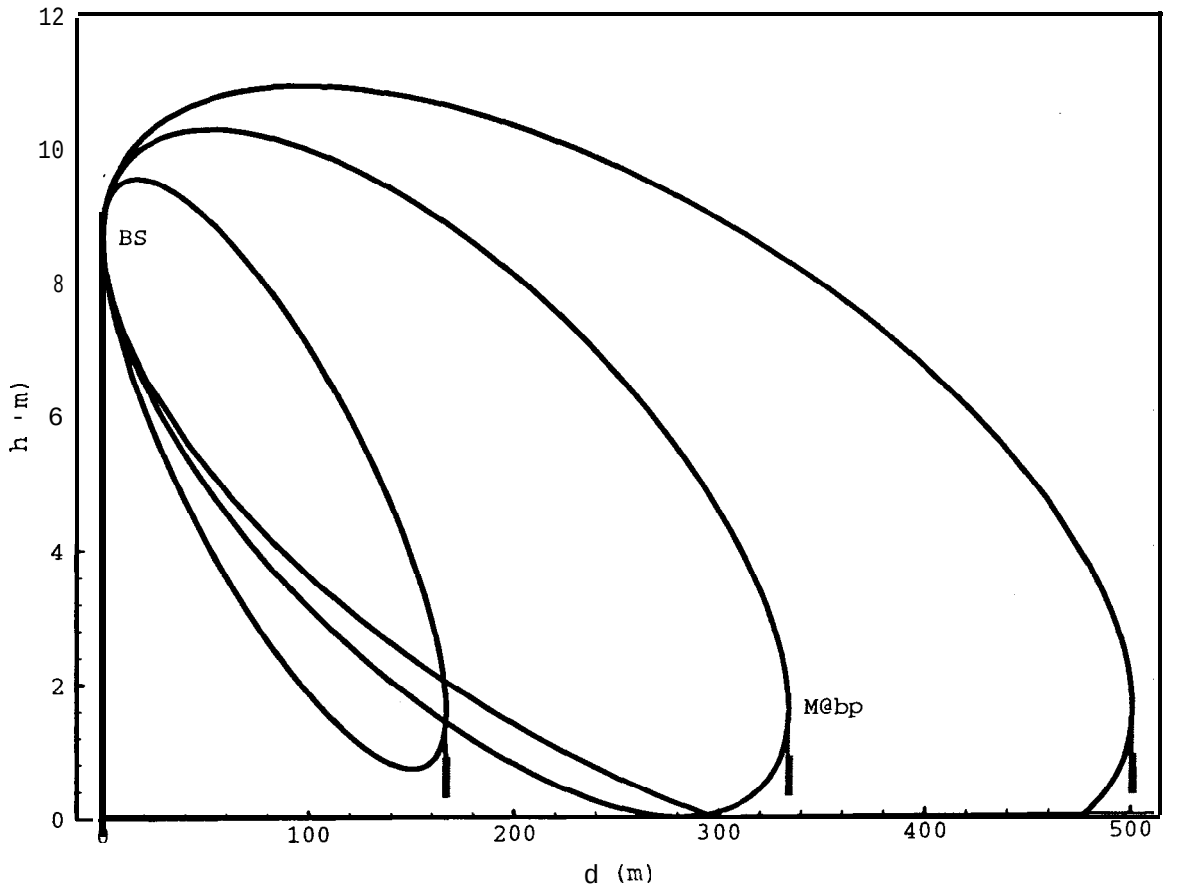

(a)

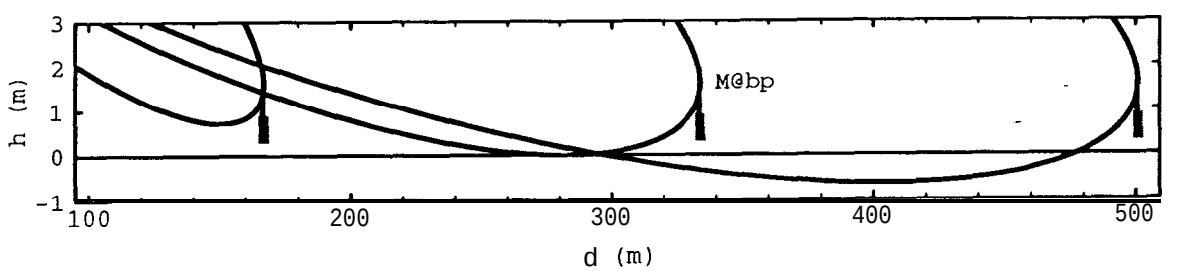

(b)

Figure 4.5: (a) First Fresnel Zone Clearance and Attenuation Curve Break Point; (b) Detail showing Clearance for distances smaller than d_{bp}, Street Surface Osculation for distances equal to d_{bp}, and Partial Blockage for distances greater than d_{bp}

about the direct path (LOS) varies along the propagation path according to

$$F_n \triangleq \sqrt{n\lambda \frac{d_1 d_2}{d}} \quad , \tag{4.3}$$

where

- n is the Fresnel zone index;
- $d_{1,2}$ are the distances from the terminals to the point where the Fresnel zone radius is being calculated;
- $d \triangleq d_1 + d_2$ is the distance between transmitter and receiver.

The distance at which the first Fresnel zone just touches the ground, herein defined as the break point, is given, under flat Earth and specular reflection hypothesis, by [7]

$$d_{bp} = \frac{1}{\lambda}\sqrt{(\Sigma^2 - \Delta^2)^2 - 2(\Sigma^2 + \Delta^2)\left(\frac{\lambda}{2}\right)^2 + \left(\frac{\lambda}{2}\right)^4} = \sqrt{\left(\frac{4h_t h_r}{\lambda}\right)^2 - (h_t^2 + h_r^2) + \left(\frac{\lambda}{4}\right)^2} \quad , \tag{4.4}$$

where

- λ is the signal wavelength;
- $\Sigma \triangleq h_t + h_r$;
- $\Delta = h_t - h_r$;
- h_t is the transmitter's antenna height;
- h_r is the receiver's antenna height.

For high frequencies, i.e., $\frac{h_t}{\lambda} >> 1$, d_{bp} can be approximated by

$$d_{bp} \simeq \frac{4h_t h_r}{\lambda} = \frac{4}{c}(h_t \; f \; h_r) \quad , \tag{4.5}$$

a linear function of the carrier frequency, f, and the transmitter and receiver antenna heights.

Piecewise Linear versus Linear Models

A question that needs to be answered **now is** the following : Is it necessary to use such a Piecewise Linear Model as presented above? Wouldn't a Linear Model be enough?

In [6], the piecewise linear model of equation (4.2) was compared to a simplified linear model defined by

$$S = -10 \log_{10}\left(d^{A}\right) + C \,. \tag{4.6}$$

A slightly better fit (Table 4.1) was achieved by this simplified model for antenna heights up to about 9 m. A much better fit, however, was obtained for the piecewise-linear mode for greater antenna heights (up to 15-20 m). We can therefore conclude that the piecewise-linear model provides for a good description of propagation in a microcellular environment.

h_t(m)	a	b	g(m)	c	Squared Error	A	c	Squared Error
5	2.30	-.28	148.6	189.0	309	2.10	183.8	268
9	1.48	0.54	151.8	179.6	246	1.68	164.2	242
15	0.40	2.10	143.9	111.0	577	1.58	147.4	946
19	-.96	4.72	158.3	74.6	296	0.90	111.4	946

Table 4.1: Results of Least Square Regression using the Piecewise-Linear and the Linear Models [6]

Basic Two-Ray Model

For a 2RM, the one most frequently used to predict the trend of the Path Loss, L_p (see Section 4.3.3), and for the general geometry of Figure 4.6, where

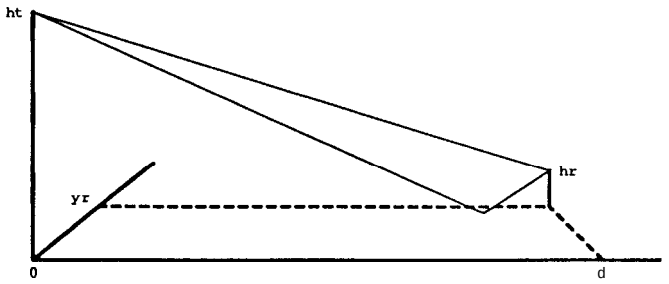

Figure 4.6: General Geometry showing Line-of-Sight and Ground Reflection

- h_t is the BS antenna height;
- h_r is the M antenna height;
- y_r is the transversal distance (across the highway) from the M antenna to the BS antenna;
- d is the longitudinal distance (along the highway) between M and BS,

the associated "path loss", L_p, is defined, for isotropic antennas, as

$$L_p \triangleq \frac{P_r}{P_t} = \left(\frac{\lambda}{4\pi}\right)^2 \left| \frac{\exp(-jkr_1)}{r_1} + \Gamma(\alpha_2)\frac{\exp(-jkr_2)}{r_2} \right|^2 , \tag{4.7}$$

or, more precisely,

$$L_p = \left(\frac{\lambda}{4\pi r_1}\right)^2 \left| 1 + \Gamma(\alpha_2)\frac{r_1}{r_2}\exp[-jk(r_2-r_1)] \right|^2 , \tag{4.8}$$

where

- P_t is the transmitted power;
- P_r is the received power;
- $k \triangleq \frac{2\pi}{\lambda}$ is the wave number;
- r_1 is the length of the direct path;
- r_2 is the length of the path including the reflection;
- $(r_2 - r_1)$ is, thus, the incremental path associated with the reflected ray;
- α_2 is the grazing angle;
- $\Gamma(\cdot)$ is the reflection coefficient.

This model is approximated in that it neglects the so called "surface wave", which is reasonable since both antennas are elevated more than λ above the ground [15]. Moreover, the model ignores diffraction effects, a correction term to apply to geomectrical optics (i.e., ray-tracing – RT), to obtain a more accurate wave optics model (i.e., geometrical theory of diffraction – GTD).

4.2.4 Effects of Frequency and Antenna Characteristics

In general, the received power is obtained from the link budget expression

$$P_r = P_t L_t G_t L_p G_r L_r \quad , \tag{4.9}$$

where ,

- L_t, L_r are the implementation losses at the transmitter and receiver, respectively;
- G_t, G_r are the antenna gains.

This expression remains valid for the present multipath case if and only if the gain associated with each of the rays is almost the same. The path loss expression will hereafter contain the whole geometrical information of interest, i.e., it will thoroughly characterize the guided propagation conditions.

At this point it is appropriate to analyze the antennas that are likely to be used in the IVHS environment. These are, due to their simplicity and low cost, simple X/2 dipoles and grounded $\lambda/4$ monopoles.

Figure 4.7: Simple Antennas

The gain associated with the (optimum) X/2 dipole is G = 1.64 = 2.15 dB [16]. The grounded X/4 monopole, i.e., a monopole located preferably at the center of a ground (preferably good conductor) plane has an azimuthal gain that increases with the size of the plane (Figure 4.8), the same happening to the number of lobes appearing in its radiation pattern and to the gain near the horizontal plane [17] (which is particularly important when the receiving grounded monopole is far from the transmitter). If the ground plane were infinite, the grounded monopole would have a gain G = 3.28 = 5.15 dB. For a worst-case monopole mounting on the border of the plate one can expect a gain of only 3 dB.

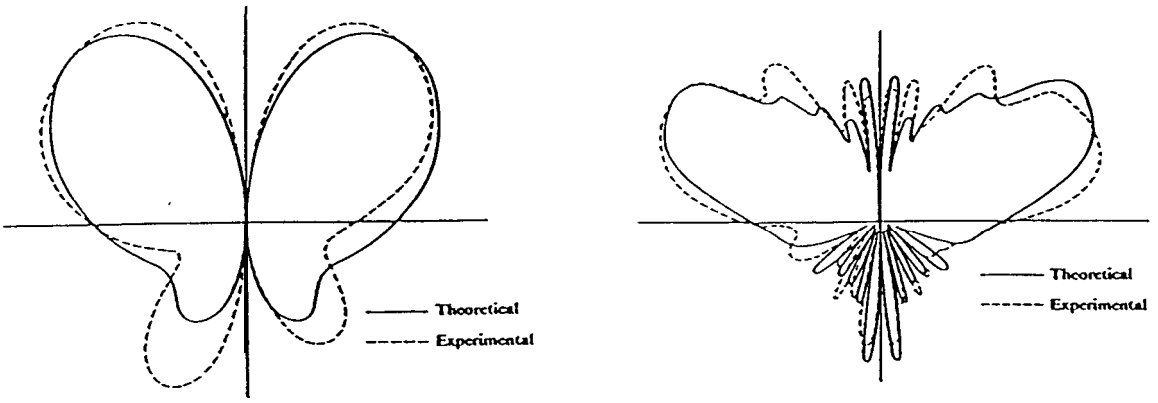

(a) X/4 **Monopole** on a $1.2\lambda \oslash$ Plate (b) $.224\lambda$ **Monopole** on a 6X $\oslash$ Plate

Figure 4.8: Grounded **Monopole** Radiation Patterns in the Vertical Plane (from [17])

Getting back to equation (4.8), one readily identifies the first term as corresponding to free-space losses, the second therefore being the extra gain (which can be negative) associated with the guided propagation effects. We will call the second term the multipath-gain factor, G_M, similar to the path-gain factor of [18, Chapt.6]. Figure 4.9 shows the path loss for the 2RM for the two bands of immediate interest for IVHS (1 and 2 GHz). In the plot we have signalled the break points as per equation (4.4); they basically coincide with the turning/break points of the two curves.

For small distances from the BS antenna, the path loss practically coincides with that determined by free-space propagation, therefore increasing with frequency. However, as the distance increases, the trend (in terms of local spatial average) becomes at first slightly better than that of free-space (i.e., the channel promotes an effective average gain), and at large distance it becomes much worse (i.e., confinement causes additional losses). Another important aspect deserving notice is that fluctuations are more frequent and accentuated for the higher frequency.

At the same time, the path loss will be practically the same for large distances for both frequencies. More importantly, the two curves have the same slope in the "far" region which is of special interest in terms of the interaction with neighboring cells. In

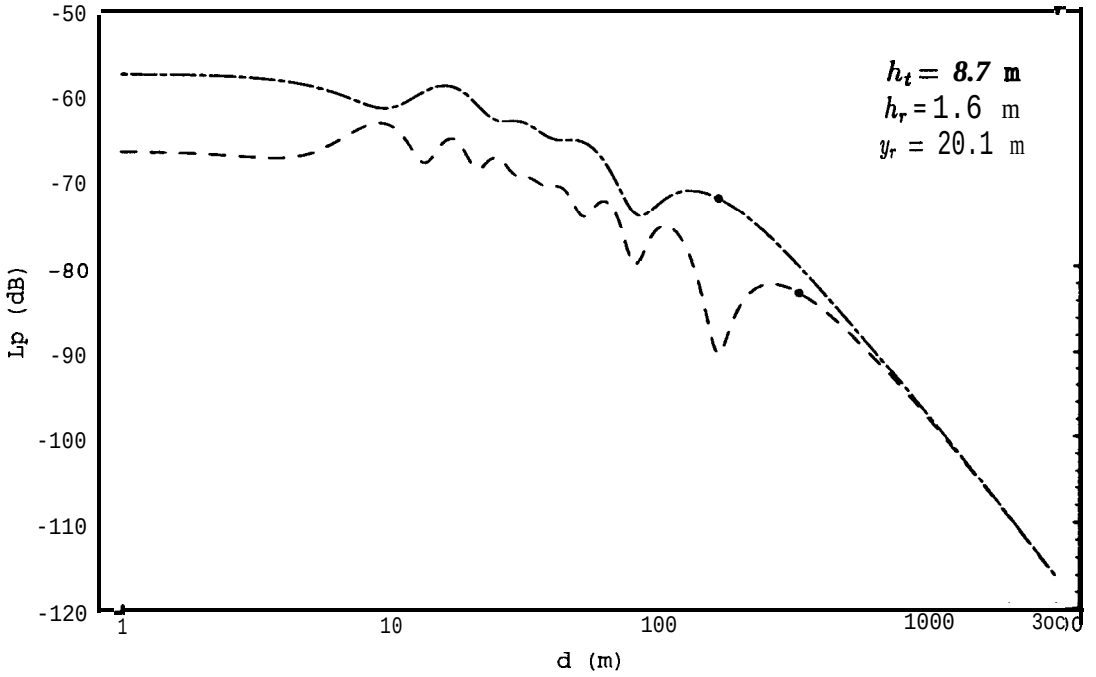

Figure 4.9: Two-Ray Model Path Loss as a Function of Distance for Vertical Polarization for (- • –) 900 MHz and (- –) 1800 MHz

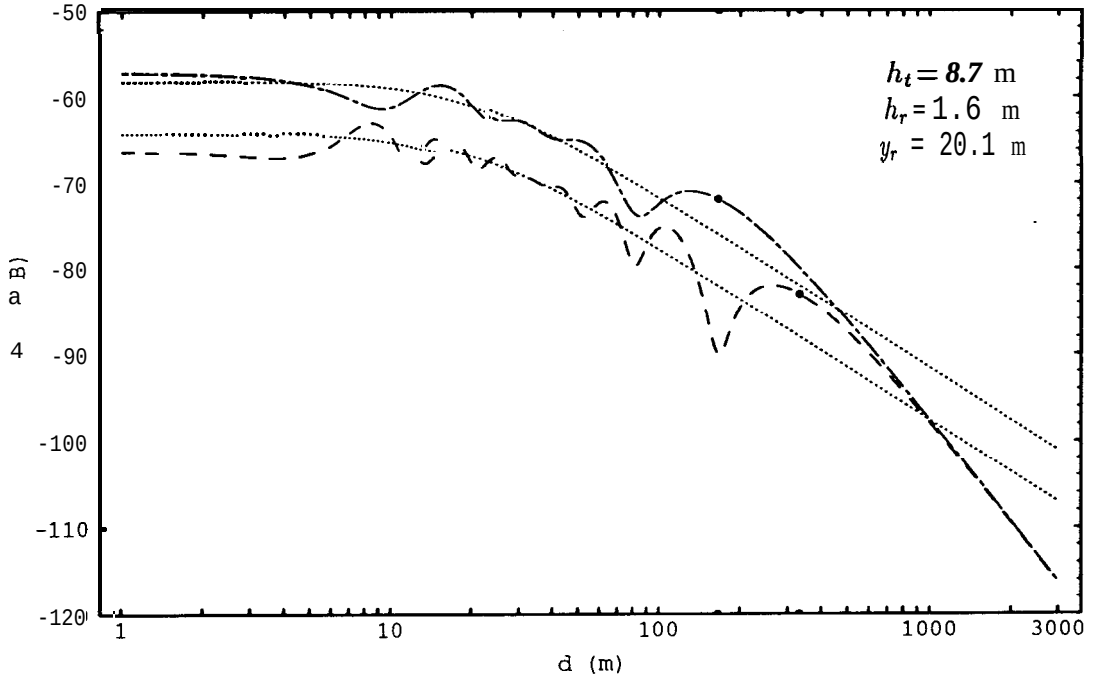

Figure 4.10: Two-Ray Model versus Free-Space Path Loss as a Function of Distance for Vertical Polarization for (- - –) 900 MHz and (- –) 1800 MHz

fact, for large distances, the multipath-gain factor is (approximately) given by [19]

$$G_M = \left|1 + \Gamma(\alpha_2)\frac{r_1}{r_2}\exp[-jk(r_2 - r_1)]\right|^2$$
$$\approx \left|1 - \exp\left[-jk\frac{2h_t h_r}{d}\right]\right|^2 \approx [\sin\left(2k\frac{h_t h_r}{d}\right)]^2 \approx \left(2k\frac{h_t h_r}{d}\right)^2 \qquad (4.10)$$

since for large distances $(d \approx r_1 \approx r_2 >> h_t, h,)$ the grazing angle α_2 is very small which makes $\Gamma(\alpha_2) \approx$ -1, and, for small angles, $|1 - \exp(-j\alpha)| \approx |\sin\alpha| \approx |\alpha|$. Thus,

$$L_p = \left(\frac{\lambda}{4\pi r_1}\right)^2 G_M \approx \left(\frac{\lambda}{4\pi d}\right)^2 \left(2\frac{2\pi}{\lambda}\frac{h_t h_r}{d}\right)^2 = \left(\frac{h_t h_r}{d^2}\right)^2 , \qquad (4.11)$$

which is known as the plane-Earth propagation equation. Here it is obvious the (approximate) path loss independence with frequency, and more importantly, the inverse fourth-power law with distance, which is visible in Figure 4.9 for large distances.

From the above analysis, one can conclude that, by doubling the frequency, the dynamic range is reduced, yielding a clear gain in terms of range. This can be seen in either of two ways. For approximately the same near distance gain, which implies about 6 dB (4 times) more power for the 1800 MHz case (Figure 4.11), it is obvious the gain in range for the same received power. Alternatively, for the same transmitted power, the same dynamic range defines a bigger cell range (Figure 4.9).

In [7], Xia et al. suggested using the break point, the "boundary" between the "near" and "far" regions, as the range of the microcell. From the path loss curves, however, and from the previous elaboration, it seems more natural to define as the χ **dB difference-range** of the microcell the distance at which the 2RM is χ dB better than the one-ray model (1RM) corresponding to free-space propagation before becoming definitively worse. The effective range of the cell, as we shall see in Chapter 7, will depend not only on propagation, but also on several radio link parameters, most notably the receiver dynamic range, as already hinted at.

It is also of interest to analyze the effect of the base station antenna height. From equation (4.5), the distance to the break point is expected to increase with increasing antenna height. Figure 4.12 shows that the depth and "frequency" of the fades also increases with the height of the BS antenna. Furthermore, as expected from equation (4.11), the path 1oss "increases" with BS antenna height, something that a free-space

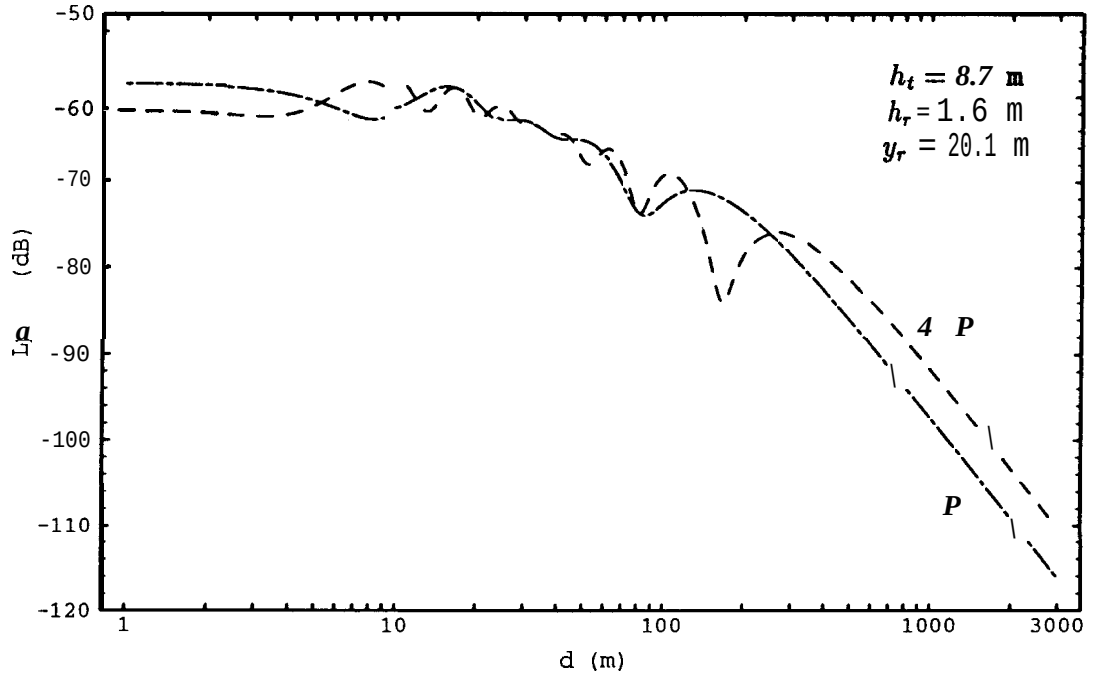

Figure 4.11: Received Power as a Function of Distance (assuming Isotropic Antennas) for (- · -) 900 MHz @ P and (- –) 1800 MHz @ $4P$

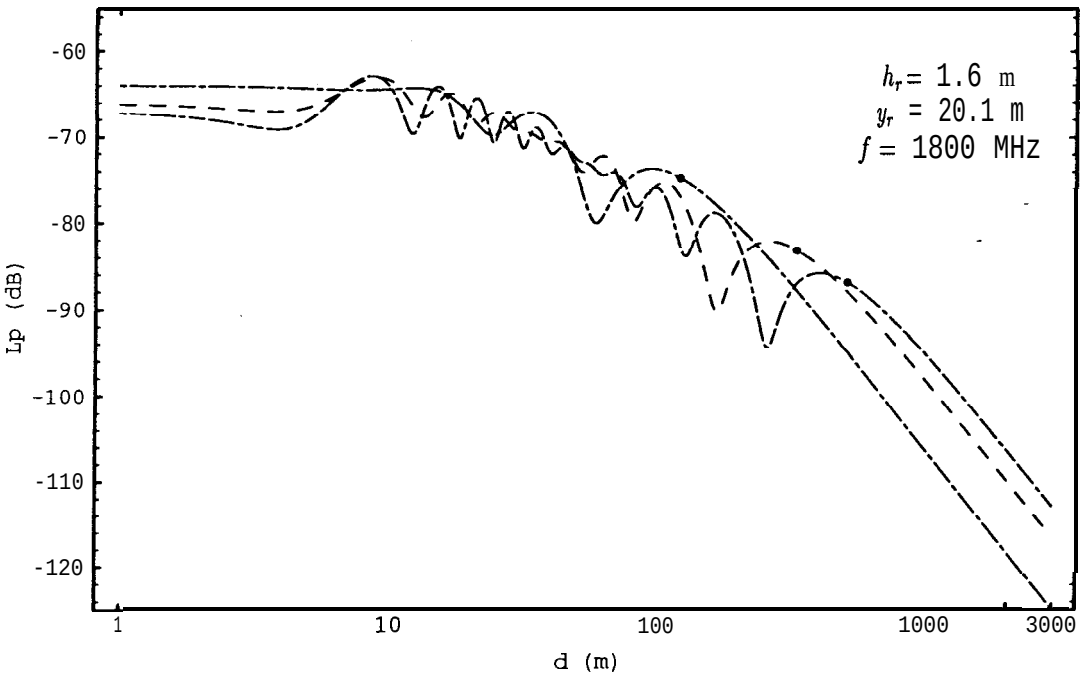

Figure 4.12: Two-Ray Model Path Loss for Vertical Polarization and different Base Station Antenna Heights : h_t = (- · –) 3.2, (- -) 8.7, (- – —) 13.4 m

model can not account for, since for large distances r_1 is approximately independent of h_t :

$$r_1 = d\sqrt{1 + \frac{h_t - h_r}{d^2}} \approx d \quad . \tag{4.12}$$

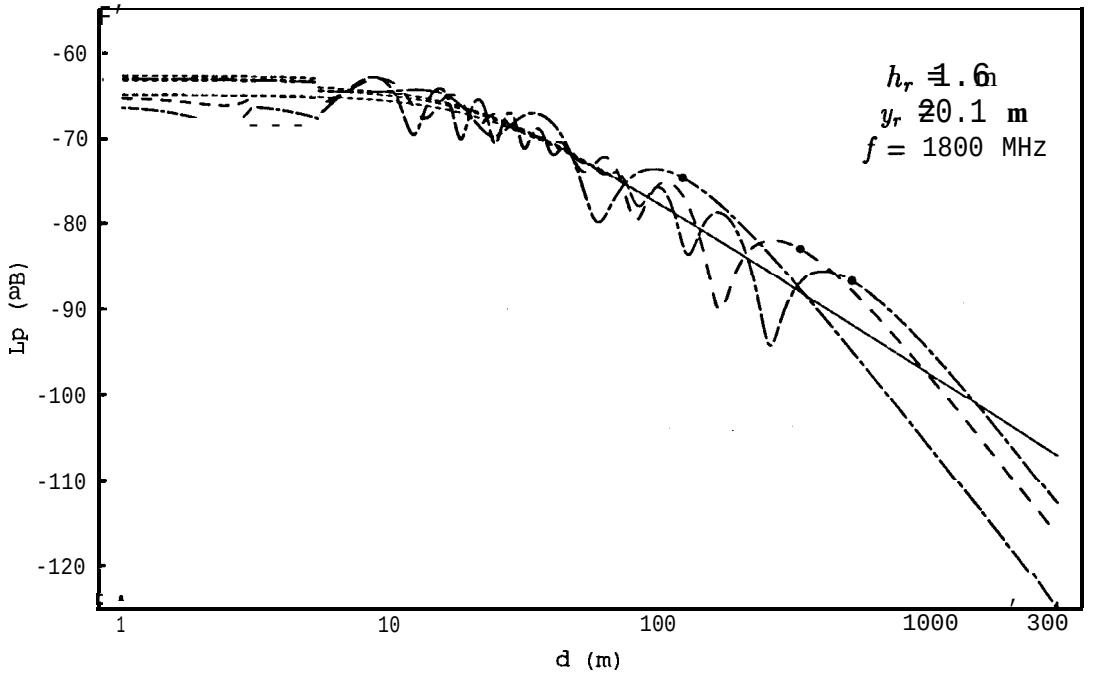

Figure 4.13: Two-Ray Model versus Free-space Path Loss for Vertical Polarization and different Base Station Antenna Heights : h_t = *(- · –) 3.2, (- –) 8.7, (- – -)* 13.4 m

In summary, according to the 2RM, fading pattern "quickens" in the near region, for fixed receiving (M) antenna height, with increasing transmitting (BS) antenna height and/or transmitting frequency. At this point, one comes to the first **design tradeoff :** cell size versus fading. In our case, the height of the M antenna will be a function of the type of vehicle (car, van or truck/bus), thus it tends to be fixed. In order to adjust the cell size one has to control the BS antenna height, within reasonable limits. A reasonable objective is to attain a cell diameter of around one mile to provide for convenient granularity without requiring too high an infrastructure investment. Since cars correspond to the smallest receiving antenna heights, and since they are the predominant type of vehicle, system design should be geared for them. The behavior of other mobile types will need however to be checked, particularly at cell boundaries.

If one were to use the break point as the cell boundary (as suggested in [7]), i.e., setting $d_{bp} \approx 800$ m, for a M antenna height of $h_r = 1.6$ m, corresponding to cars, and frequencies in the 2 GHz band, one would need, as per equation (4.4), BS antenna heights in the order of 18.6 m, a totally impractical value. In Chapter 7, dealing with system architectural design tradeoffs, we shall see that the range of a cell is in fact determined by the receiver dynamic range, and will typically be larger than just the distance to the break point as per equation (4.4), thus leading to more reasonable numbers. Furthermore, by playing with the directivity of the BS antenna (see Section 4.3.5), one can further reduce the required BS antenna height.

4.2.5 Shadowing Effects in the Microcellular Environment

In microcellular systems, scattered multipath gives rise to a Rician channel due to the presence of the LOS path and of specular components. In fact, over a relatively short propagation path, it is generally possible to arrange for a LOS path between transmitter and receiver by properly locating the BS antenna [7]. Traffic, however, can block, possibly even most of the time, some of the specular components.

The shadowing effects encountered in microcellular systems are expected to be different from those that normally cause log-normal envelope mean variations in conventional/macro cellular systems [20], and need to be modeled if system performance is to be predicted. In fact, the log-normal distribution of the local mean for conventional/macro cellular scenario results from many, and independent, reflection losses suffered by the rays arriving at the M from the BS. In the IVHS scenario, however, there will be a reduced number of specular components, added to the LOS, which appear above the diffuse multipath, and which result from a reduced number of reflections, usually only one or two. Specular components suffering several reflections will be buried in the difuse multipath background.

Bultitude and Bedal [2] assume that shadowing and multipath are multiplicative in the conventional/macro cellular scenario. However, this will not be the case for the micro-/picocellular scenario if a MRM is indeed appropriate. In fact, shadowing will af-

fect differently each of the specular components and even the LOS[6]. At the same time, the myriad of scattered components will be by definition independently attenuated. Thus, the sum of all rays (LOS, specularly reflected, and scattered) will not reflect any multiplicative character. In fact, an interesting observation [21] is that the strength of paths with small delays beyond the LOS delay, corresponding to Quasi-LOS (QLOS) paths, are well modeled by Nakagami distributions.

In Section 4.4, and as a first approach, we will consider the effect of surrounding traffic on each of the specularly reflected rays that could possibly reach the M antenna but only in terms of ON/OFF, i.e., ignoring all intermediate stages where the ray itself may be blocked, but the First Fresnel Zone is not entirely obstructed, and all refractions effects that might partially compensate for the obstruction, even if total.

4.3 The IVHS Environment

IVHS, the Intelligent Vehicle and Highway System, is a major initiative of Government, Industry and Academia to apply advanced technology to the operation of our surface transportation systems in order to improve mobility and transportation efficiency, enhance safety, maximize the use of existing transportation facilities, conserve energy resources, and reduce adverse environment al effects [22].

IVHS is based upon information exchange between the highway/surface streets infrastructure and the vehicles, and, at a later stage, between the vehicles themselves. The system will have to accommodate speeds up to 160 km/h, with platoon spacing that goes from 1 m at 100 km/h to 3 m at 160 km/h, with transversal spacing as low as 1 m [23],[24].

Similar to what happens in a Mobile-Satellite link [25], the signal arriving at a mobile has two components : a specular component which can experience shadowing (in our case due mostly to vehicle shadowing[7], and independently affecting each of the rays), and a

[6] **LOS will generally exist, yet due to eventual partial blockage of its first Fresnel zone, it can still suffer attenuation.**

[7] **Blockage from man-made structures, like that from bridge pillars, is an obviously serious short term blockage, but is not statistically significant. Thus, it can be ignored in the model.**

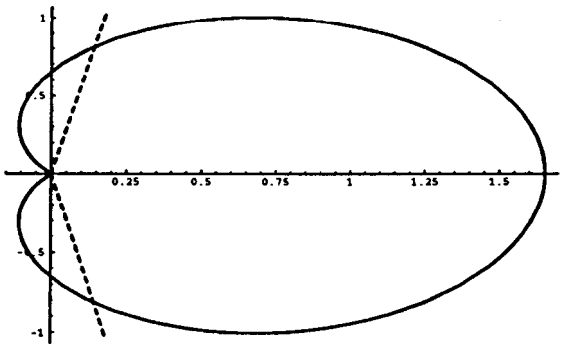

Figure 4.14: Proposed Antenna Pattern – adapted from Hughes' VRC Proposal [24]

diffuse component which is the sum of signals scattered by nearby objects (especially from nearby tops of trees/bushes, utility poles, and in our specific case, from Changeable Message Signs (CMS) and the like, and all neighboring vehicles).

The extent of fading due to multipath, is dependent on the receiving antenna pattern, which can assume either the doughnut shape characteristic of conventional/macro cellular, or approximately hemispherical (for instance, in Hughes' VRC proposal [24], a 3 dB beamwidth of 160" looking at the front of the vehicle – see Figure 4.14).

For roof mounted antennas, negligible contributions should arise due to scattering from nearby vehicles and from reflections from the ground, since the corresponding ray paths are incident at the antenna at angles near the horizontal, where the gain should be at least a few dB down (see Figure 4.8). It is also very likely that, for that configuration, those ray paths become effectively blocked by the mobile itself, especially near the BS.

On the other hand, multipath variations are independent of the elevation angle, with short fades and long nonfades, although no model has been settled upon for their fade durations.

4.3.1 Proposed Propagation Models

The recently proposed North American and Japanese Digital Cellular systems, NADC [26] and JDC [27], respectively, provide a system capacity increase over their current analog counterparts, AMPS and TACS, through the use of digital modulation and speech coding techniques [28]. Both standards use TDMA as multiple access technique. The

NADC standard specifies a 3% Bit Error Rate (BER), corresponding to good voice quality.

The NADC standards committee has recommended a propagation model to include time dispersion of the received signal. This standardized channel model is a two-ray, equal power model with up to 41.2 μs excess delay. As we will see later, this 2RM assumption does not reflect many real world situations of interest. The equal power assumption, on the other hand, does not seem appropriate with such huge excess delays, which, moreover, are not to be expected in the majority of IVHS environments.

The NADC time dispersion profile significantly departs from the JDC system design assumptions and published delay spread profiles for typical urban, suburban, and bad urban propagation environments [29],[30],[31], including the European COST 207 specification for GSM [32] which has a worst case root-mean-square (rms) delay spread of 5 μs. Although there is no JDC delay spread specification, a design criterion of 5 μs rms delay spread was also used.

Quoting [28], it is crucial that a propagation model be representative of real world propagation conditions. A model which is too stringent will burden the system with hardware that is not required by the actual channel. Thus, we need to accurately characterize the radio channel for the IVHS environments.

4.3.2 Multi-Ray Channel Impulse Response Model

Turin proposed [33] a band-limited complex impulse response, h(t), given by

$$h(t) = \sum_{i} \alpha_i \exp[j\phi_i]\delta(t - \tau_i) \quad , \tag{4.13}$$

where the received signal is formed by the addition of attenuated and time delayed versions of the transmitted signal.

We propose a slightly modified version of the above, namely

$$\begin{aligned} h(t) &= \delta[t - t_0(t)] + \sum_{i=1}^{M} \alpha_i(t) \exp[j\phi_i(t)]\delta[t - \tau_i(t)] + \int_S \alpha_s(t) \exp[j\phi_s(t)]\delta[t - \tau_s(t)]ds \\ &= h_{\mathrm{LOS}}(t) + h_{\mathbf{specular}}(t) + h_{\mathbf{scattered(t)}} \end{aligned} \quad , \tag{4.14}$$

where

- $h_{\text{LOS}}(t)$ corresponds to the LOS path;
- $h_{\text{specular}}(t)$ corresponds to the M rays suffering specular reflection;
- $h_{\text{scattered}}(t)$ corresponds to the myriad of scattered rays that arrive at the receiving antenna.

The scattered component, by itself, has an envelope that may be described by the Rayleigh probability density function (pdf)

$$\text{p(R)} = \frac{R}{\sigma^2}\exp\left(-\frac{R^2}{2\sigma^2}\right) \quad , \quad R \geq 0 \quad . \tag{4.15}$$

The overall received signal, on the other hand, for a given received specular envelope, S, will have an envelope with Rician distribution [34]

$$p(R|S) = 2K\frac{R}{S^2}\exp\left\{-\left[\left(\frac{R}{S}\right)^2 + 1\right]\right\} I_0\left(2K\frac{R}{S}\right) \quad , \quad R \geq 0 \quad , \tag{4.16}$$

where

- $I_0(\cdot)$ is the zeroth-order modified Bessel function of the first kind;
- K denotes the received power ratio between specular and scattered components, which needs to be measured in situ.

A detailed analysis will initially focus on the specular components, since the scattered components are more difficult to predict analytically and generally require field measurements (that should cover all IVHS environments of interest) in order to accurately characterize the attendant Rician channels.

RMS Delay Spread for the Two-Ray Model

After Bello's initial work [35] on the characterization of fading channels, Cox [29] arrived at the expression for the power-weighted rms delay spread, τ_{rms}, for a two-ray

channel model (2RM) :

$$\tau_{\text{rms}} \triangleq \frac{\sqrt{P_d}}{1+P_d}\, t_d \quad , \tag{4.17}$$

where [28]

- t_d is the relative delay of the second ray;
- P_d is its relative power.

Kazecki and Baker [28] used the above definitions to compare the measured detector delay spread profiles, defined as the amount of delay spread that the detector can tolerate while maintaining a specified BER (with and without diversity – see Figure 4.15), with the theoretical 2RM rms delay spread curves.

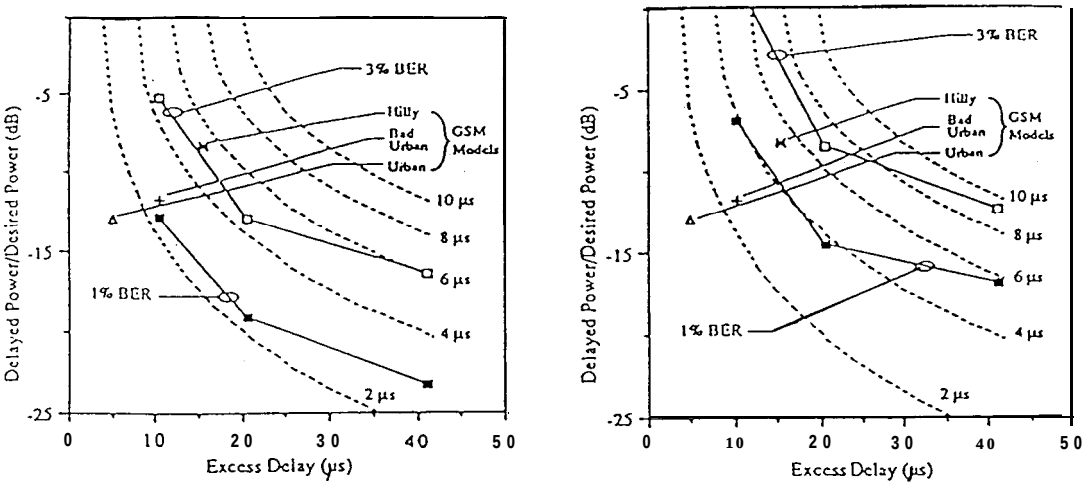

(a) Without Diversity (b) With Diversity

Figure 4.15: Coherent Detector 1% and 3% BER Delay Spread Profiles at 50 km/h without and with Diversity – from [28]

We observe that the points corresponding to the equivalent GSM two-ray delay spread models are almost within the 3% BER specification even without diversity. With diversity the detector can achieve the desired BER with much higher rms delay spread. Thus,we can a priori relax our model from the NADC 41.2 μs maximum excess delay standard to a worst case rms delay spread of 5 μs in the absence of actual measurements in the IVHS environment. In any event, a low number M of contributing rays with small excess delays is to be expected in both the highway and the surface streets environment. One therefore should expect even lower worst case values.

For the 2RM, P_d of equation (4.17), is

$$P_d = |\Gamma(\alpha)|^2 \left(\frac{r_1}{r_2}\right)^2 \quad , \tag{4.18}$$

reflecting the power loss in the incremental path, i.e., $r_2 - r_1$, and that due to the reflection coefficient $\Gamma(\alpha)$. The incremental path also leads to the relative delay of the reflected ray

$$t_d = \frac{r_2 - r_1}{c} \quad . \tag{4.19}$$

Then, the rms delay spread, τ_{rms}, becomes

$$\tau_{\text{rms}} = \frac{|\Gamma(\alpha)|\frac{r_1}{r_2}}{1 + |\Gamma(\alpha)|^2 \left(\frac{r_1}{r_2}\right)^2} \left(\frac{r_2 - r_1}{c}\right) \quad . \tag{4.20}$$

From Figure 4.16 one observes that the maximum rms delay spread is negligible (approximately 1 ns), and, furthermore, that, except for a deep null, it decreases, as expected, with distance (the relative incremental path decreases).

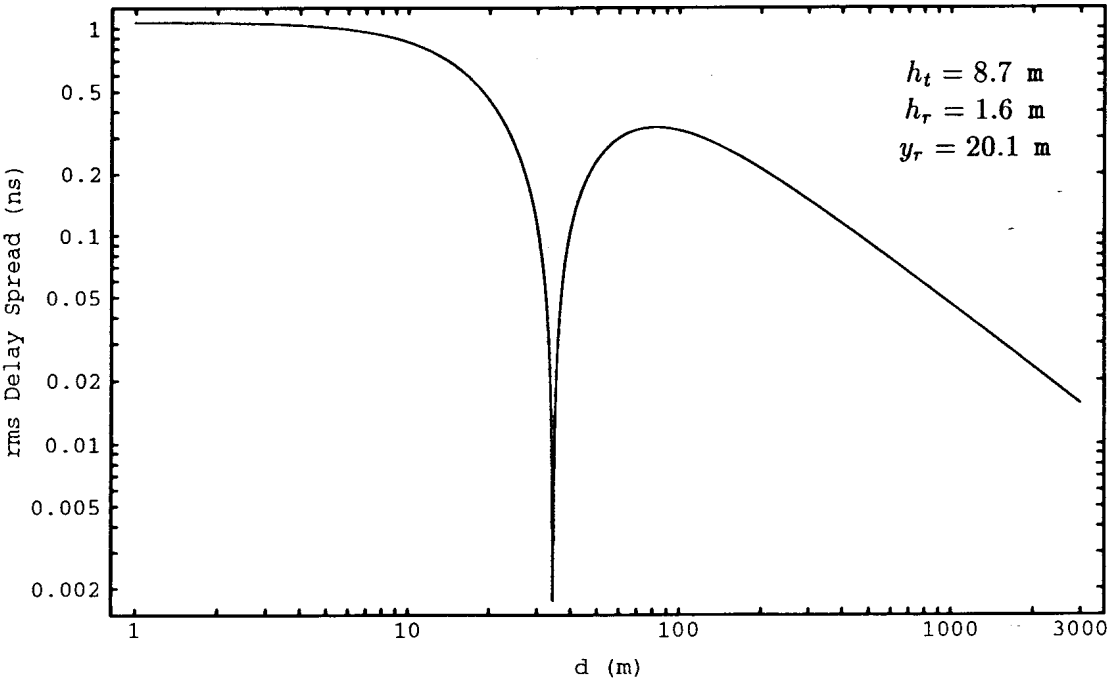

Figure 4.16: RMS Delay Spread for the Two-Ray Model at 1800 MHz

The Reflection Coefficient and its Relation to Polarization

The reflection coefficient deserves a separate section, specially due to its dependence on the chosen polarization, In fact, $\Gamma(\alpha)$ depends explicitly on the grazing angle α, but implicitly on the type of polarization :

$$\Gamma(\alpha) \triangleq \frac{a \sin\alpha - \sqrt{\epsilon_c - \cos^2\alpha}}{a \sin\alpha + \sqrt{\epsilon_c - \cos^2\alpha}} \quad , \tag{4.21}$$

where

- $\epsilon_c \overset{A}{=} \epsilon_r - 60\,\sigma\lambda$ is the relative dielectric constant (ϵ_r is the permittivity, and σ the conductivity of the reflecting material);
- a = ϵ_c or 1 for Vertical or Horizontal polarization, respectively.

Note that Vertical and Horizontal are necessarily referred to the reflecting surface.

The typical values of ϵ_r and σ are obtained from the following Table :

Reflector	ϵ_r	σ (S/m)
Urban Ground	3	3×10^{-5} to 3×10^{-4}
Rural Ground	14	3×10^{-3} to 3×10^{-2}
Metal Alloys	1	10^{6} to 10^{8}

Table 4.2: Relative Dielectric Constant for different Reflectors

A plot of the path loss, $L_,$, for the basic geometry of Figure 4.6, as a function of distance and of the reflection coefficient, I'(Q), in the horizontal plane, is shown in Figure 4.17, adapted from [7]. We observe that before the break point the approximation $\Gamma(\alpha)$ = -1, valid for large distances (α << 1) and/or reflection on metallic surfaces (e.g., hood/trunck or side panels of nearby vehicles), overestimates the peaks as well as the depth of the fades. Moreover, as $|\Gamma(\alpha)|$ is larger for Horizontal polarization than for Vertical polarization, the signal fluctuates much less severely for Vertical polarization than for Horizontal polarization as the M moves away from the BS.

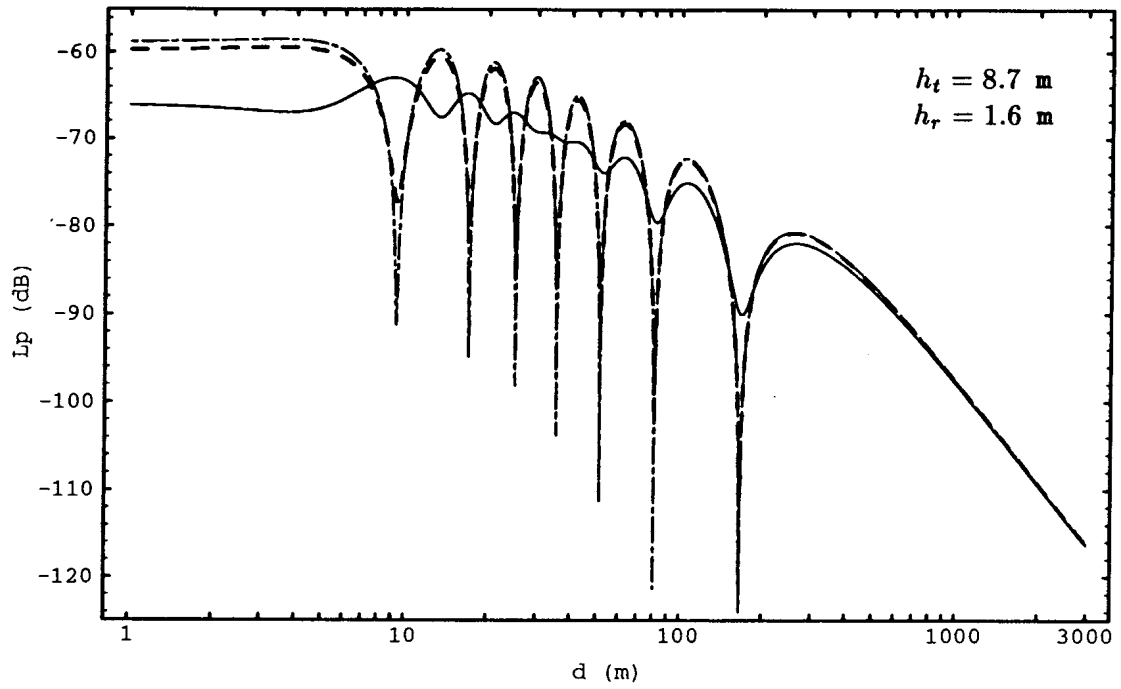

(a) Reflection on the Ground

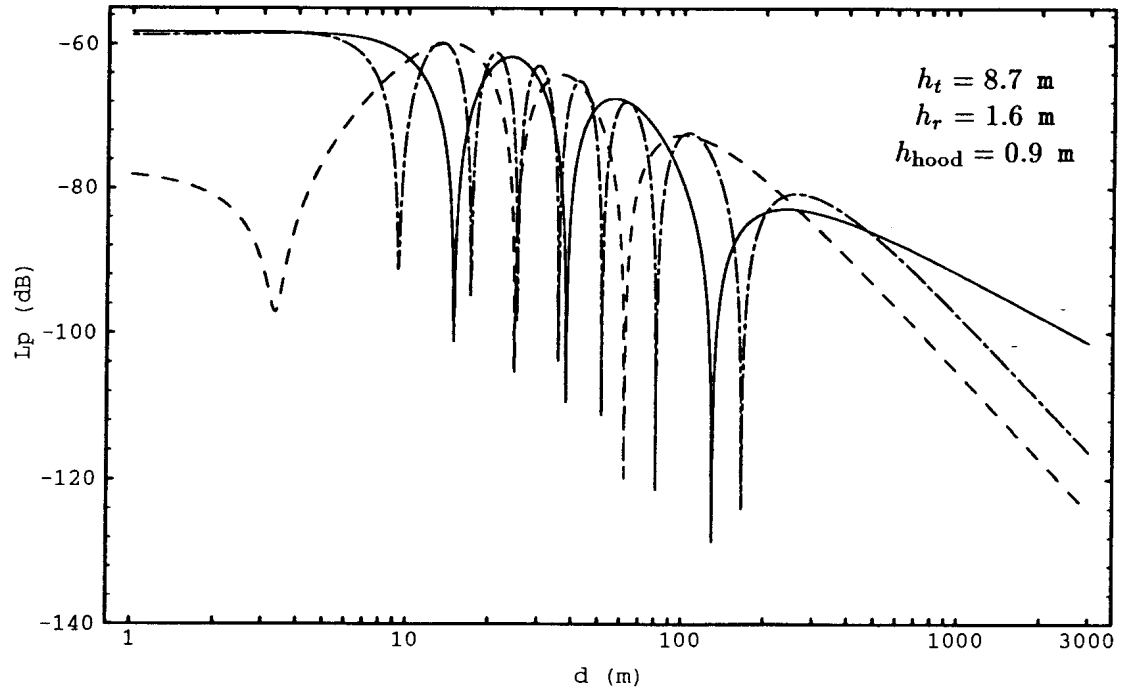

(b) Reflection on the Hood/Trunck of a nearby Car

Figure 4.17: Path Loss at 1800 MHz as a function of $\Gamma(\alpha)$ for (——) Vertical and (– –) Horizontal Polarization, and for (– · –) $\Gamma(\alpha) = -1$

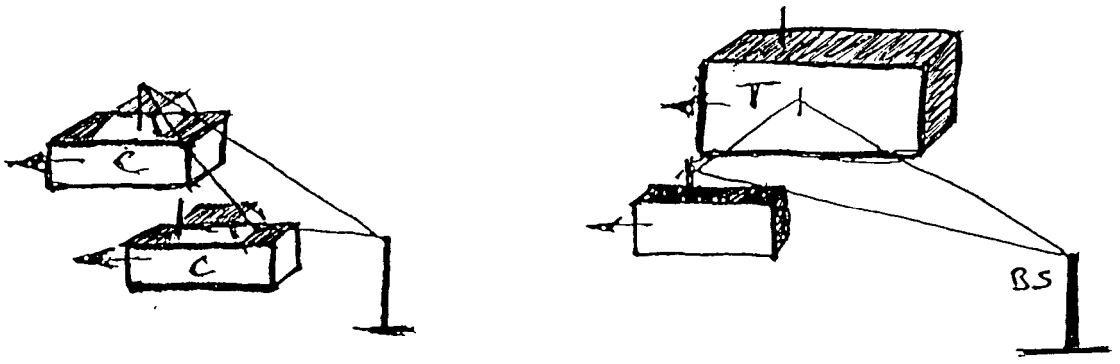

(a) On the Hood/Trunck of a nearby Car (b) On the Side of a nearby Truck/Bus

Figure 4.18: Examples of Reflection on neighboring Vehicles

The occurrence of reflections on trucks/buses', corresponding to $\Gamma(o) \approx -1$ for Vertical polarization, which is in this case horizontal referring to the reflective metallic surface (see Figure 4.18.b), will only be a very localized effect, given the speed differential between lanes. From the foregoing, the issue of Vertical versus Horizontal polarization seems to be settled, for the IVHS case, in favor of Vertical polarization.

In Caltrans' AVI compatibility specifications [45], horizontal polarization was advocated due to the choice of one Reader (BS antenna) per lane. Then, the worst reflections come from the side of cars in neighboring lanes. Horizontal polarization is seen as vertical by those reflector planes, thus being the proper choice. In a more general IVHS setting, and making use of Multiple Access techniques, only a single Base Station antenna for the cell would be needed. It can be placed either in the middle of the road, in the center divider (middle-of-the-road (MoR) BS) or in the side of the road (side-of-the-road (SoR) BS). In fact, single BS antennas support both single-lane and multi-lane configurations through Multiple Access techniques (CDMA, TDMA or FDMA).

In general, any lane-oriented BS antenna, be it in-pavement or overhead, leads to the choice of horizontal polarization with the corresponding imposition of M antenna, which must be of the aperture or planar type. Any single BS antenna, due to the appropriateness of the vertical polarization, is usually a dipole or array of dipoles, leading to the choice of the usual monopoles mounted on a metallic surface for the vehicle-mounted transponders.

'Reflections on other types of vehicles are not significant, except in case of congestion of the surface streets/highways.

The metallic surface can be the roof, the hood or the trunk. However, in order to reduce the variability of the system, i.e., its dependence on the exact geometry involved (MoR versus SoR BS antennas), it should be put in the middle of the car, preferentially in the middle of the roof (since it is higher). An immediate advantage of that positioning is that the monopole will work (see Figure 4.8) as a dipole with a relative gain of approximately 3 dB, except for low incidence angles. This, however, means that the ground reflected ray will be substantially attenuated, reducing its importance in terms of multipath.

In order to evaluate the system performance in the IVHS environment one will have to consider for the single BS antenna the range of heights at which antennas might be installed on highway fixtures or street-lamp posts, ranging from 3.7 m to 8.7 m [2],[7].

4.3.3 Side-Of-The-Road Base Station Antennas

The first example of single BS antenna to be considered is the SoR, the one corresponding a priori to smaller installation costs. The objective is to be able to decide between SoR and MoR BS antennas at the system design stage.

Two-Ray Model

In the 2RM, commonly used for predicting radio signal propagation over flat Earth (i.e., negligible effect of the Earth curvature, which is consistent with micro- and picocell ranges), and smooth terrain as defined below [11], the first ray travels directly from the transmitting antenna, of height h_t, to the receiving antenna, of height h_r, at distance d, and the second ray suffers specular reflection on the ground (Figure 4.19).

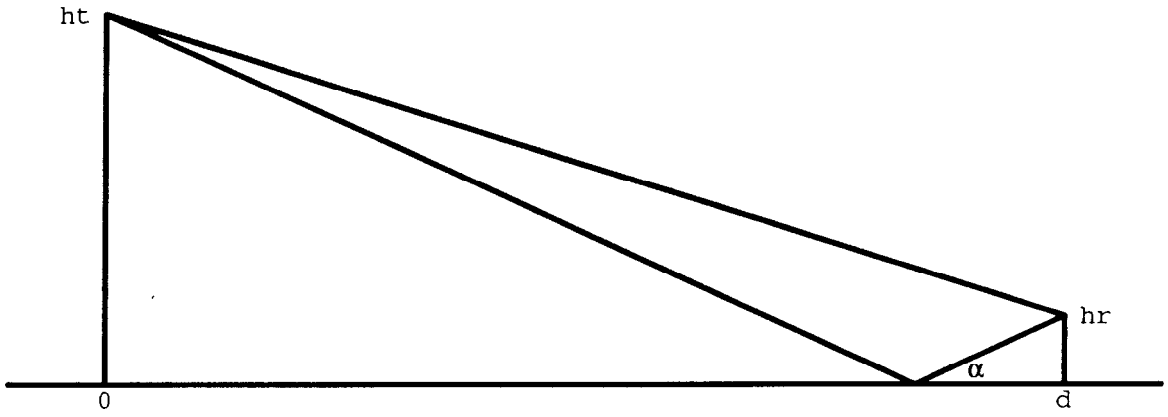

Figure 4.19: Two-Ray Model over Flat Earth and Smooth Terrain

The Rayleigh roughness criterion **is** used to define "smooth terrain". The terrain will be defined as smooth [36] if s < 0.3, where

$$s = 4\pi \frac{S_h}{\lambda} \sin\alpha \ , \qquad \textit{(4.22)}$$

and

- S_h is the rms surface height about the local mean value within the first Fresnel zone;
- λ is the wave length;
- α is the grazing angle.

Then, smooth terrain corresponds to a normalized (by λ) rms surface height of

$$\frac{S_h}{\lambda} = \frac{s}{4\pi \sin\alpha} < 0.3 \frac{1}{4\pi \sin\alpha} \approx \frac{1}{40\pi \sin\alpha} \ . \qquad \textit{(4.23)}$$

Under the above conditions, specular reflection will occur, and the theoretical value of $\Gamma(\alpha)$ applies.

Six-Ray Model

Under certain conditions, namely the existence of reflectors bordering the highway (depressed or walled highway), there will exist more than one specular component leading to a MRM.

In order to obtain a six-ray model (6RM) the geometry of the highway needs to satisfy certain requisites. More specifically in the case of depressed highways,

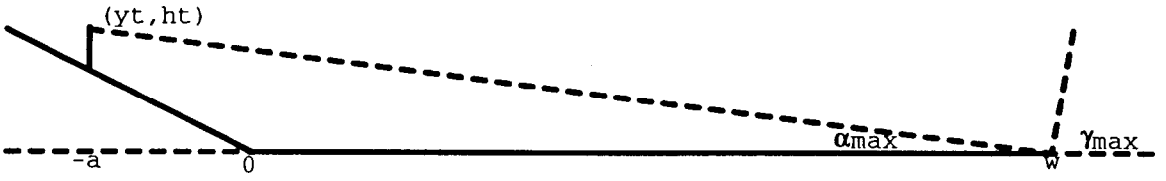

Figure 4.20: Six-Ray Model Constraints

the slope of the man-made "canyon", namely γ_{far}, must at least be

$$\gamma_{far} > \frac{\pi}{2} - \alpha_{max} \ , \tag{4.24}$$

where

$$\alpha_{max} = \arctan\left(\frac{h_t}{a+w}\right) \ . \tag{4.25}$$

Thus, for most of the inclined "canyons" there will be no contributing reflection on the far side of the highway, leading to a four-ray model (4RM).

For vertical walls/barriers bordering the highway, the 6RM exhibited in Figures 4.21a, 4.22 and 4.23a is obtained. The 4RM for inclined confinement is depicted in Figures 4.21b and 4.23b.

The highway geometry can be described by the following parameters :

- w is the highway width;
- l is the highway lane width;
- p is the highway pullout lane width;
- c is the highway central division width;
- b is the boardwalk width;
- y_t is the transversal distance from the BS antenna to the nearest wall (reference) in the case of SoR BS antennas;

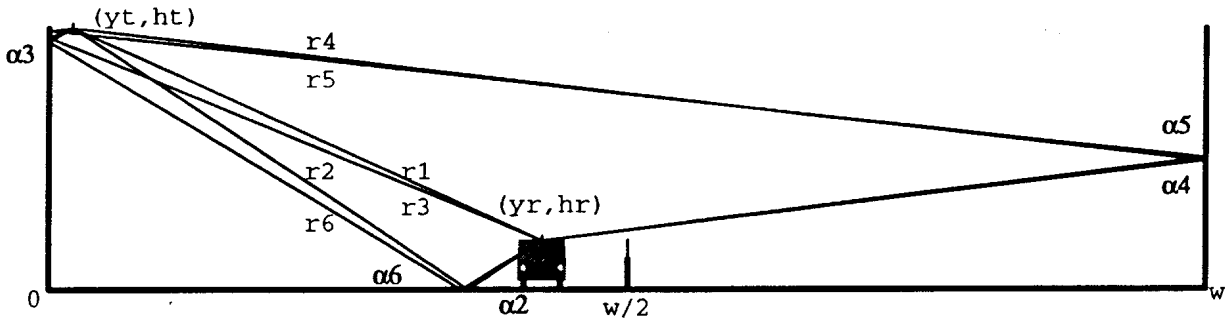

(a) Vertical Confinement

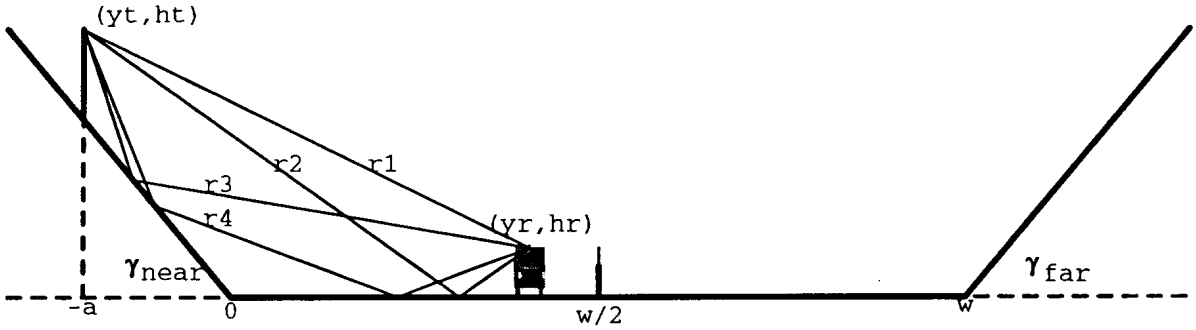

(b) Inclined Confinement

Figure 4.21: Confined Highways

- y_r is the transversal distance from the M antenna to the reference wall (SoR BS antennas);
- $\alpha_2, \alpha_3, \alpha_4$ are the reflection angles on the ground, the nearest wall, and the far wall, for the rays r_2, r_3, r_4, respectively;
- α_5 is the reflection angle on the two walls for the ray r_5 that suffers double reflection;
- α_6 is the reflection angle on the ground for the ray r_6 that also suffers double reflection, the first one on the near wall.

In the case of MoR BS antennas, the definitions of y_t and y_r would be changed to reflect a different reference

- $y_t = 0$ – the transversal distance to the central division, presumably the location of the BS antenna;
- y_r – the transversal distance from the M antenna to the central division.

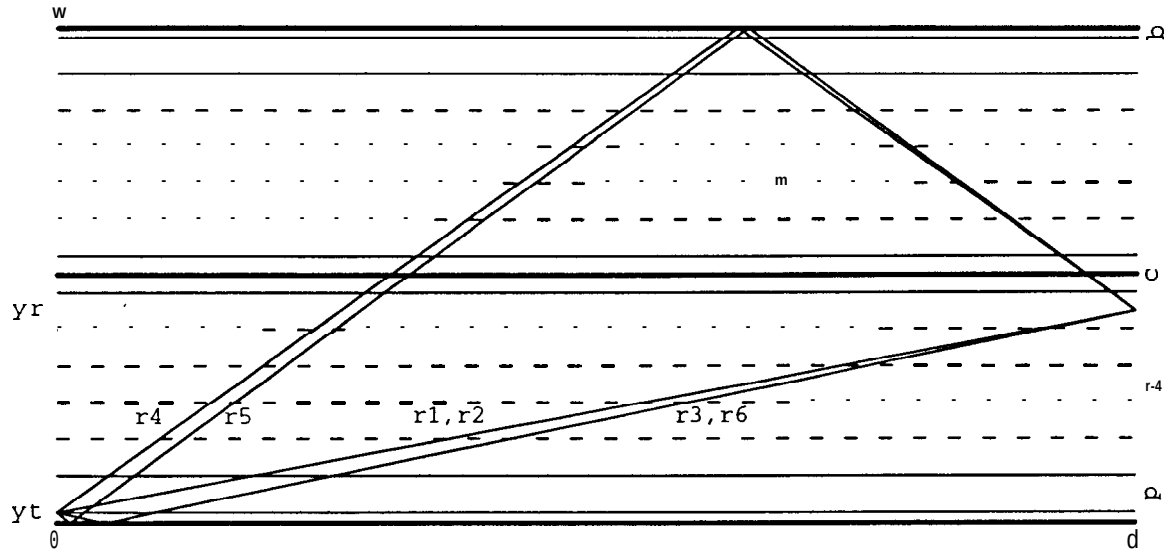

Figure 4.22: Six-Ray Model : Walled Highway (or Surface Street Block)

One must note here that, unless the first reflection on the near wall occurs on a metallic surface $(\Gamma \approx -1)$, the rays r_5 and r_6 will contribute little to the received signal due to the attenuation losses involved. Thus, it is as if the MRM is, for all other cases, just a 4RM. The analysis that follows, starts with the most general case, and moves to narrow down the number of rays for the different specific IVHS scenarios.

In the general case the Path Loss, L_p, is given by

$$L_p = \left(\frac{\lambda}{4\pi r_1}\right)^2 \left| 1 + \sum_{i=2}^{M} \Gamma(\alpha_i) \frac{r_1}{r_i} \exp[-jk(r_i - r_1)] \right|^2 , \qquad (4.26)$$

where M is the number of non-scattered (i.e., specularly reflected) rays present.

The resulting path loss plot, as a function of the distance to the BS antenna, follows (Figure 4.24) for a walled highway with p = c = l = 12 foot (the standard freeway lane width in California), $b = y_t$ = 1 m, and 5 lanes in each direction, at f = 1800 MHz. Shown is the path loss curves for vehicles moving in the fast lane nearest to the reference wall and for Vertical polarization, assuming that the second-ray reflection occurs on the ground (i.e., asphalt), when it does occur.

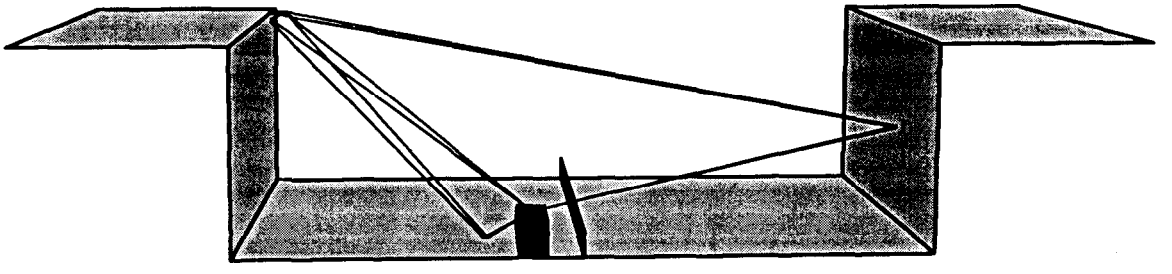

(a) Six-Ray Model for Vertical Confinement

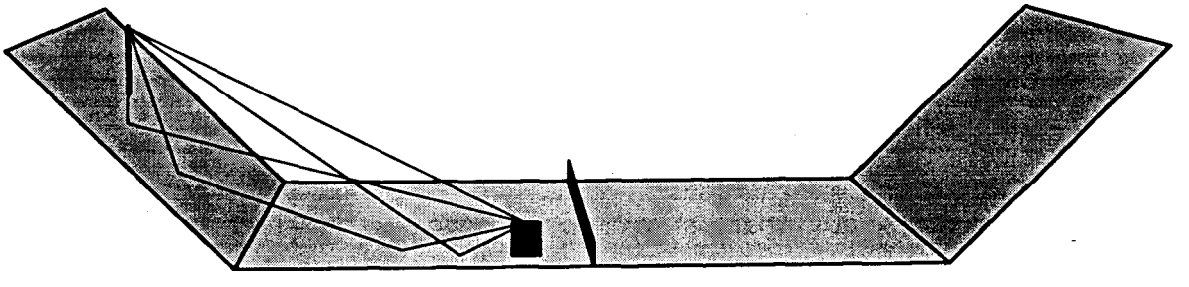

(b) Four-Ray Model for Inclined Confinement

Figure 4.23: Multi-Ray Model for Side-Of-The-Road Base Station Antennas

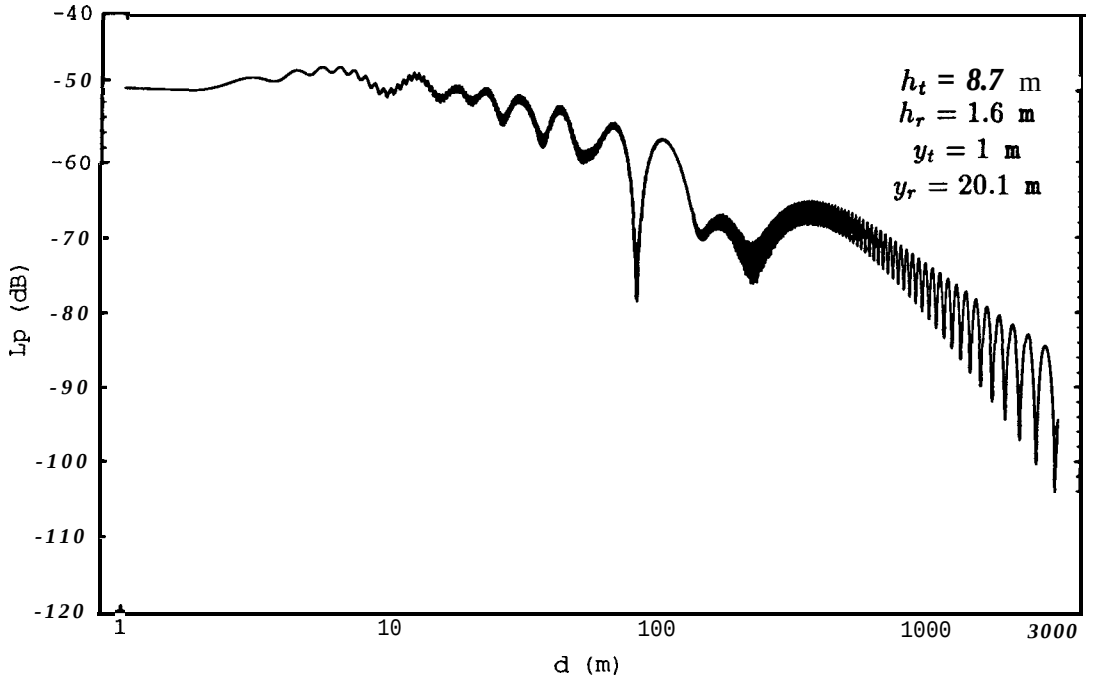

Figure 4.24: Path Loss in presence of Reflection on the Ground

Although we intuitively expect the delay spread to be negligible, even for the six ray model case, we proceed to give the corresponding rms delay spread result in order to determine the worst possible value. At the same time, we try to gain insight into the effects of double reflections through a comparative plot (Figure 4.25b).

For the general case of a M-ray model, we will have

$$\tau_{\text{rms}} \triangleq \sqrt{\frac{\sum_{i=1}^{M} P_{d_i} (t_i - t_{\text{avg}})^2}{\sum_{i=1}^{M} P_{d_i}}}, \qquad \textit{(4.27)}$$

where

- t_i is the delay of the ith ray;
- P_{d_i} ⌧ ⌧♦ ❒ℳ●♋♦⌧❖ℳ ◻◻▪ℳ❒▭

- t_{avg} is the average (power-weighted) delay defined as

$$t_{avg} \triangleq \frac{\sum_{i=1}^{M} P_{d_i} t_i}{\sum_{i=1}^{M} P_{d_i}} \qquad \textbf{(4.28)}$$

The corresponding rms delay spread curves (Figure 4.25) show the negligible contribution of the rays r_5 and r_6, and the effect of the reflections on the walls, especially the increase in delay due to reflection on the far wall (ray r_4). The maximum delay, however, is quite small (circa **20** ns) and still not significant for the ranges of data or chip rates of interest. In fact, only if $\tau_{rms} > T/10$, where T is the symbol or chip time, respectively, will intersymbol interference (ISI) become significant, i.e, only if $R \triangleq \frac{1}{T} > \frac{1}{10\tau_{rms}}$. That is, only if the symbol/chip rate is in excess of 5 Mcps would the delay spread have to be taken into account.

If the reflection would occur on the hood/trunk of a nearby car as opposed to on the ground (possible in all but the slowest lane near the SoR BS), the curves would be different (Figure 4.26), presenting much more pronounced fades. It must be noticed, however, that, due to the expected speed differentials between lanes, it is not very likely that the second-ray will result, for a long time, from reflection on the hood of a vehicle in a neighboring lane. In fact, the M will face, as it moves along, different multi-ray "channels" : the second-ray will alternate from resulting from reflection on the ground, or on the hood/trunk of a nearby car, or will be temporarily obstructed by neighboring vehicles (see Section 4.4). Figure 4.26 gives just an idea of what would be the worst case fading, and would warrant addressing fading mitigation methods, if it were not the case that the multiple-access protocol will "lead" the M through those deep fades until successful transmition is achieved.

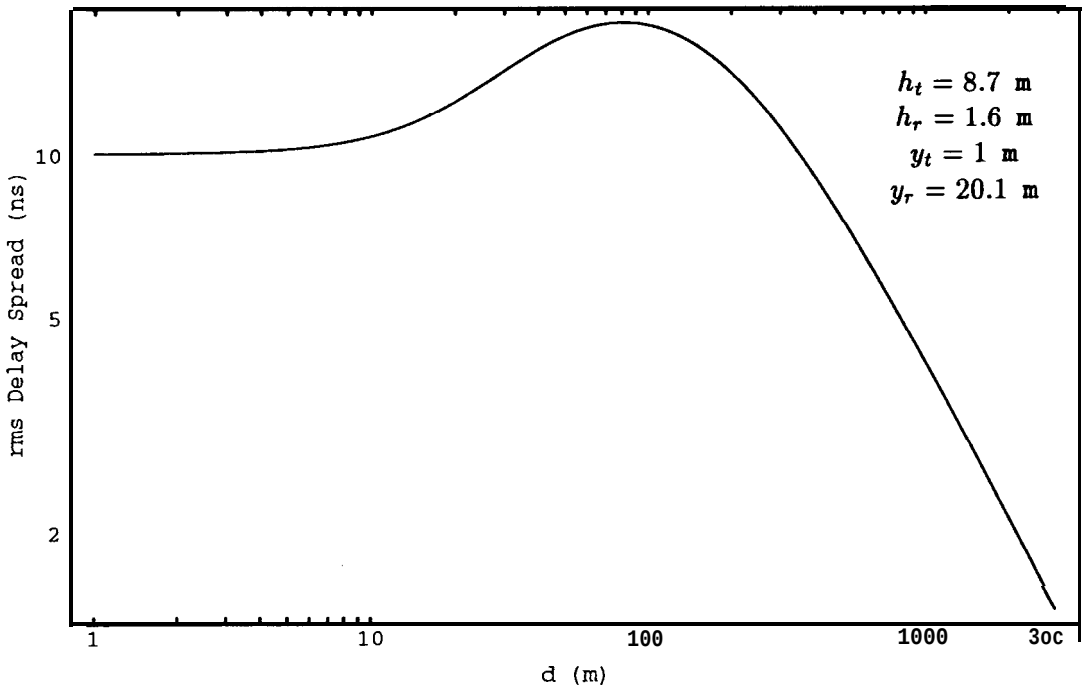

(a) Six-Ray Model

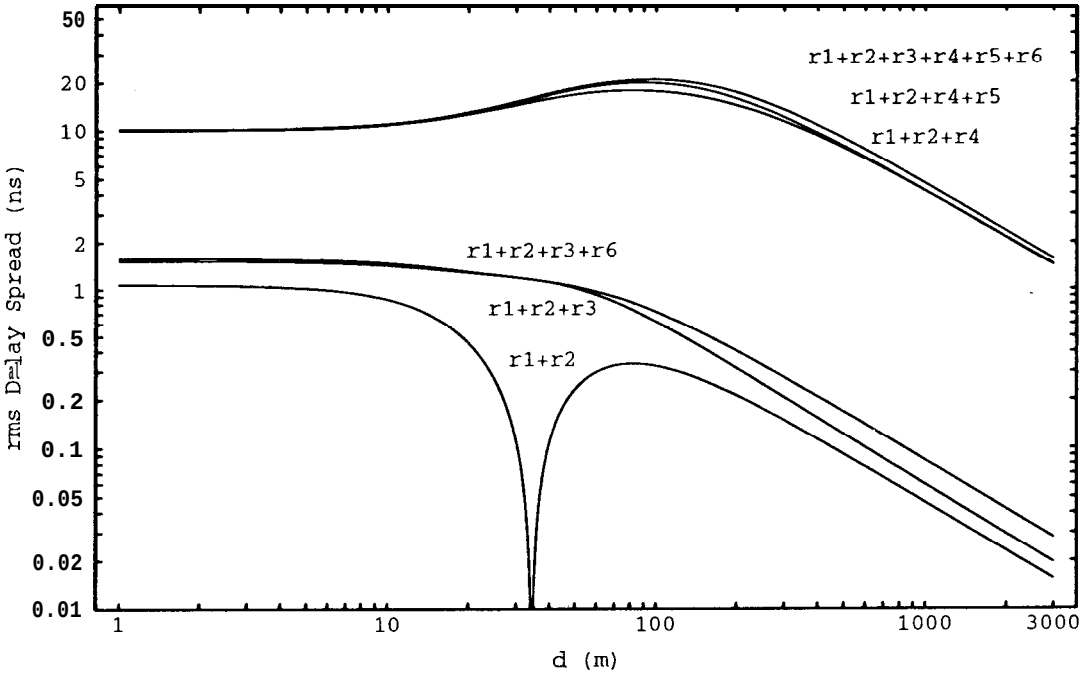

(b) Six-Ray versus Obstructed Rays with Second-Ray present

Figure 4.25: RMS Delay Spread for the Six-Ray Model and Ground Reflection

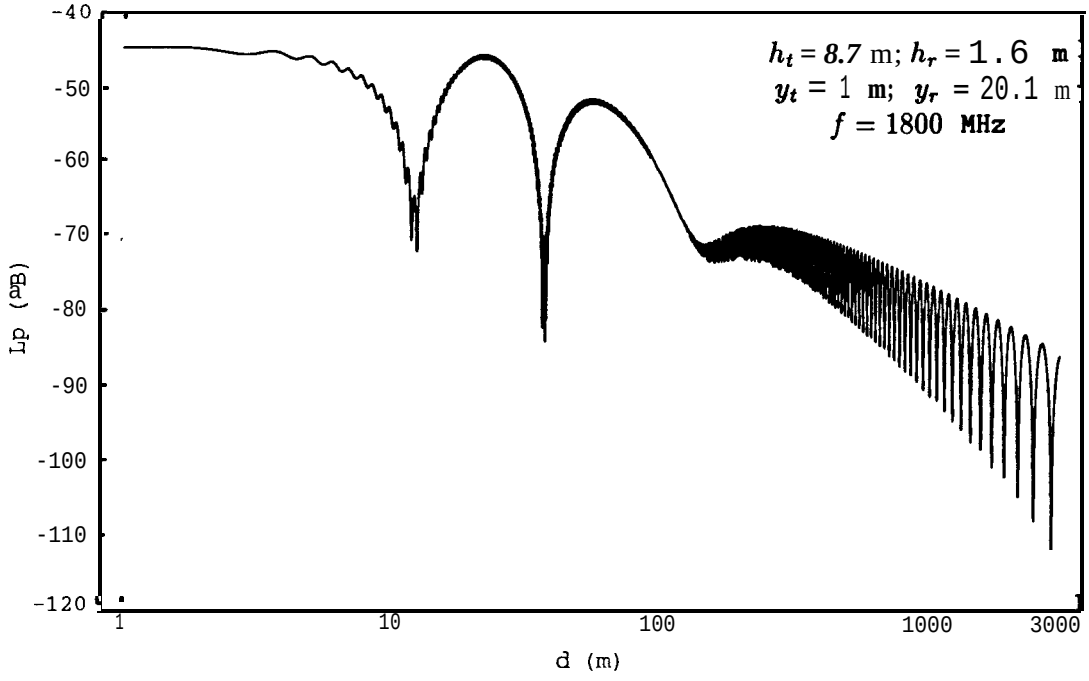

Figure 4.26: Path Loss for Reflection on the Hood/Trunk of a Car

Degenerate "Six"-Ray Models : Obstructed Specular Rays

The degenerate cases result from the non-existence of one or more of the specularly reflected rays. In the case of obstructed/non-existent third and sixth ray, i.e., reflection only on the far wall, the path loss curve is shown in Figure 4.27.

For the case of reflection only in the nearest wall (Figure 4.28), due to blockage/non-existence of the fourth and fifth rays, we obtain a much smoother path loss curve, as expected, since the involved path-length variations are much smaller in this case.

A most interesting case is that of reflection on the ground only (in fact a 2RM). As pointed in [7], the corresponding path loss curve gives the trend of the spatial average as a function of distance, without the details of the "fast fading" (see Figure 4.29). For the far region, however, it gives us a pessimistic estimate of the path loss (in comparison to the 6RM). The two-ray pattern is especially precise in the absence of the third and sixth rays, corresponding to far wall reflection (Figure 4.30).

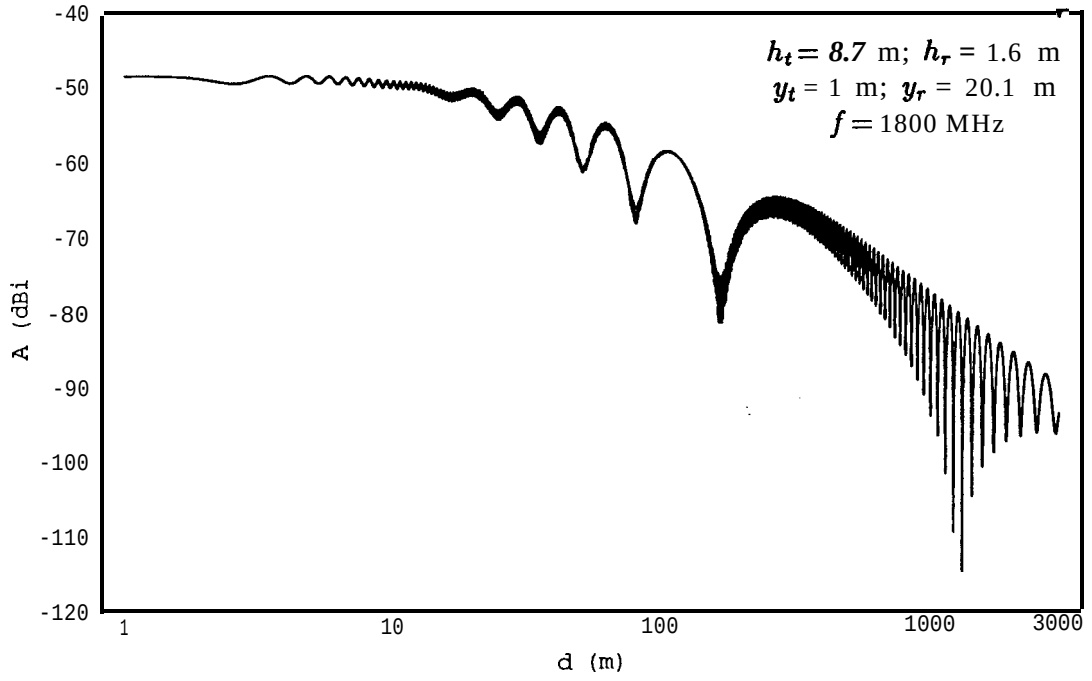

Figure 4.27: Path Loss for Reflection on the Ground and on the Far Wall

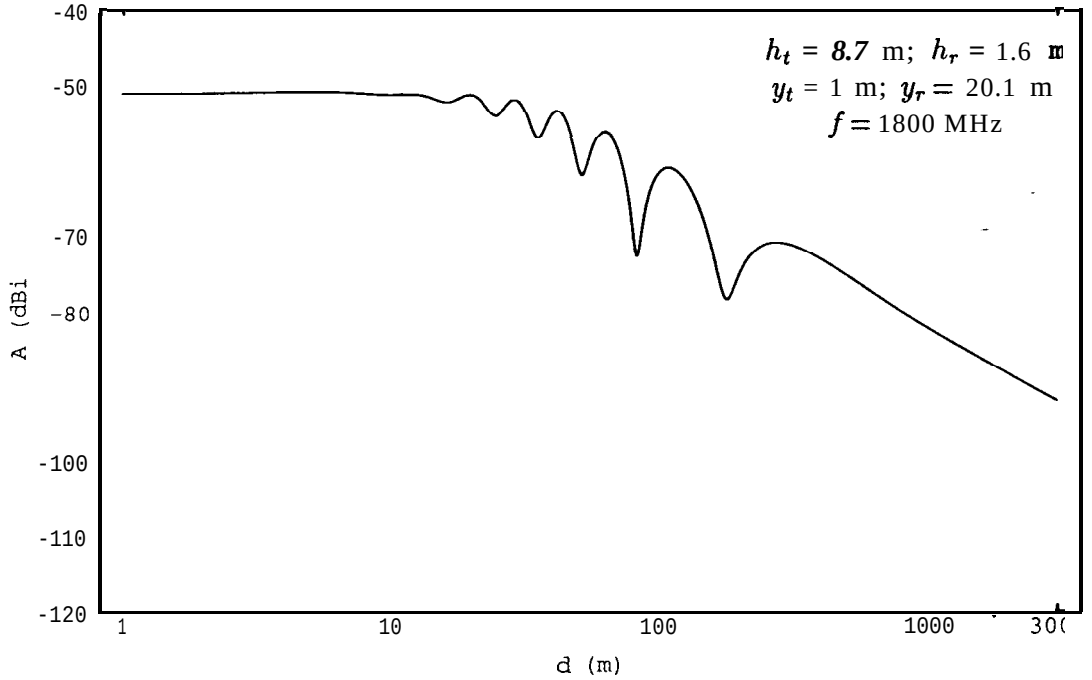

Figure 4.28: Path Loss for Reflection on the Ground and on the Nearest Wall

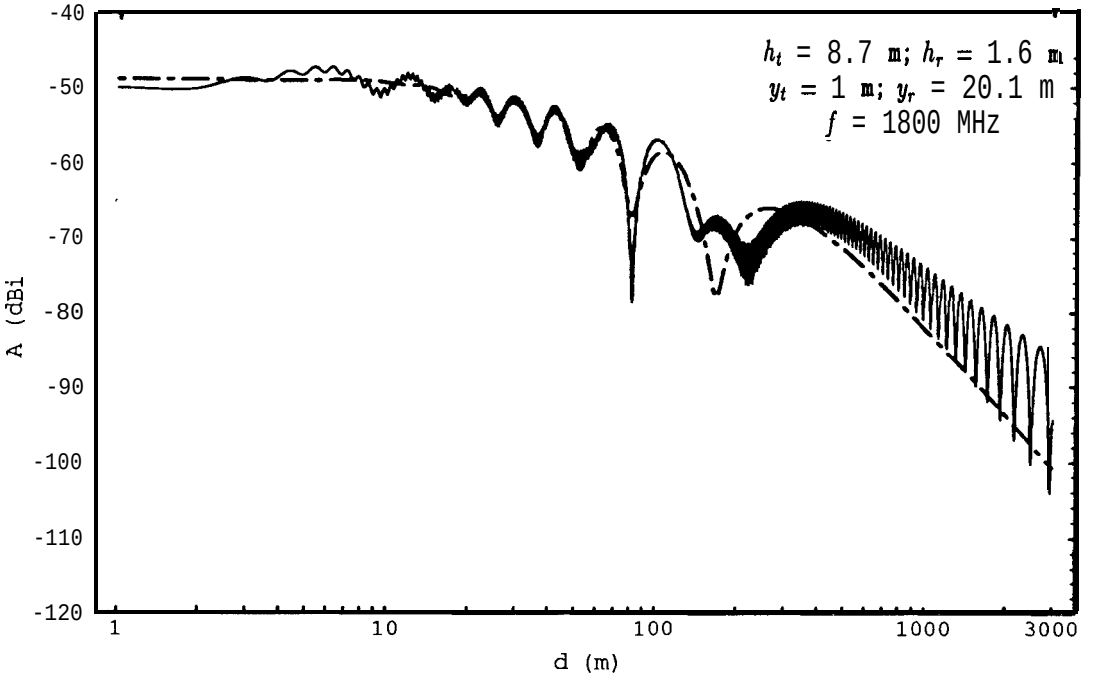

Figure 4.29: Path Loss – Two-Ray versus Six-Ray Model

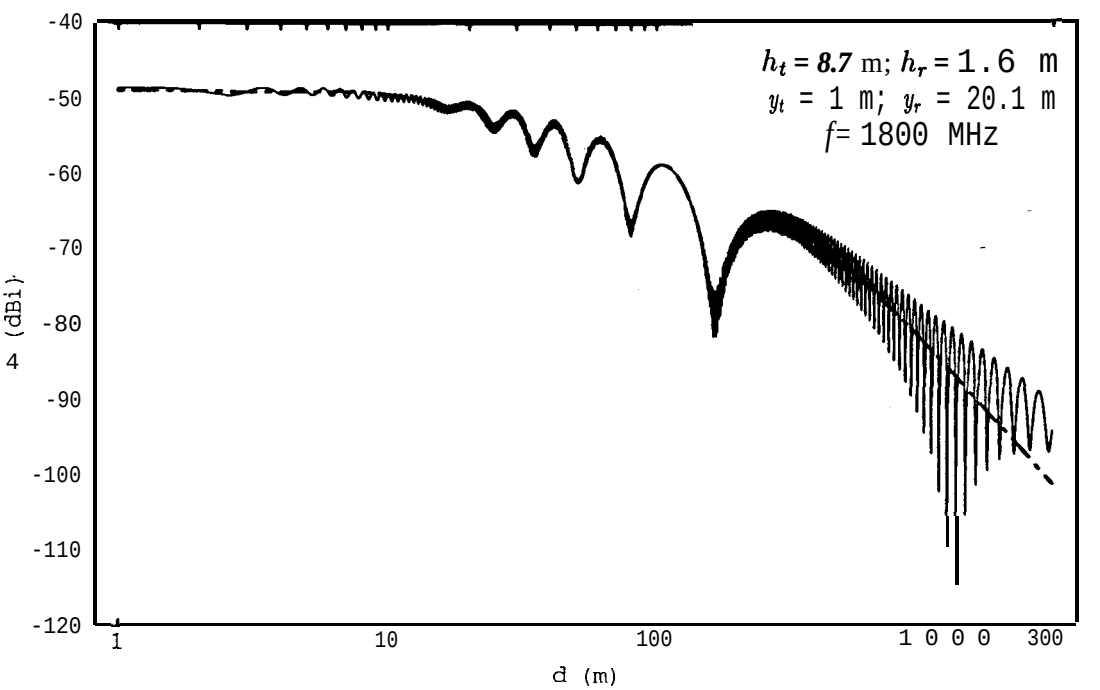

Figure 4.30: Two-Ray Model versus Ground and Far Wall Reflection

The match in terms of trend is worst when the obstructed rays are the fourth and fifth, corresponding to near wall reflection (Figure 4.31), reflecting mainly the fact that the third ray contributes much more than the fourth for the overall signal, since it suffers less path loss than the latter. Again, due to the involved double reflections, the effect of the fifth and sixth rays is usually negligible, except when the first reflection occurs on a metallicsurface (metallic reflector behind the BS antenna).

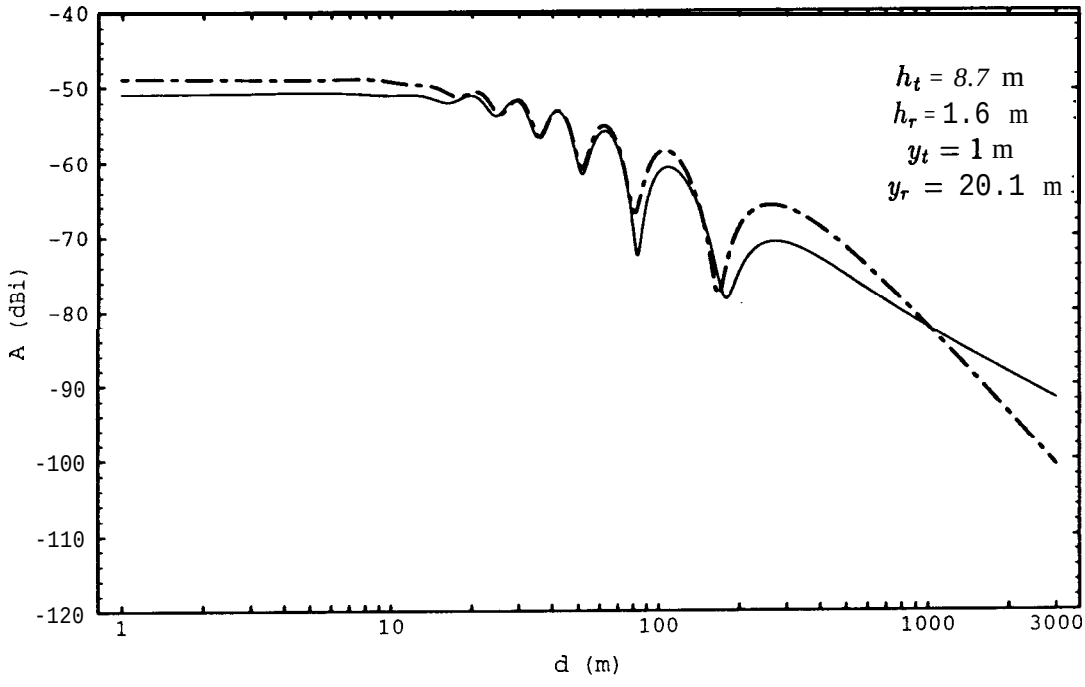

Figure 4.31: Two-Ray Model versus Ground and Near Wall Reflection

A case not to be forgotten is that of obstructed second-ray (Figure 4.32), one of the most energetic, due to vehicles in nearby lanes, a situation that can arise in all but the slowest lane near the BS antenna. More importantly, this will likely be the case for vehicles on the far side of the highway.

Finally, Figure 4.33 shows that, as expected, the 1RM, corresponding to LOS only, provides information on the trend of the spatial average of the path loss in the region very close to the BS, and is better than the 2RM in the far away region.

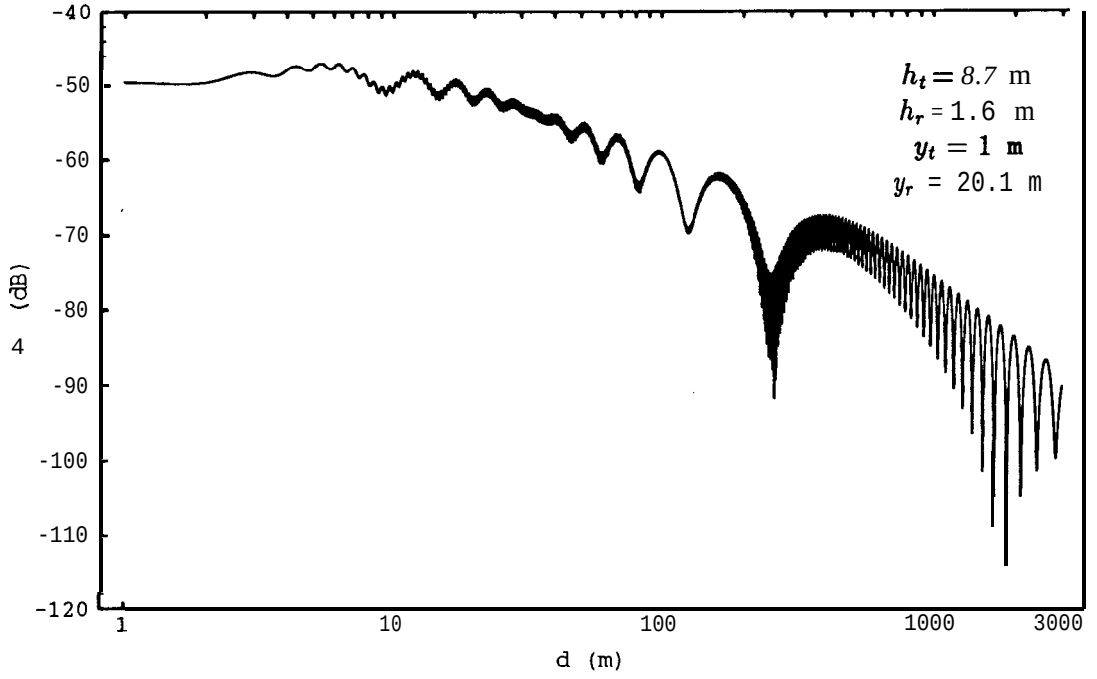

Figure 4.32: Path Loss with Obstructed Second-Ray

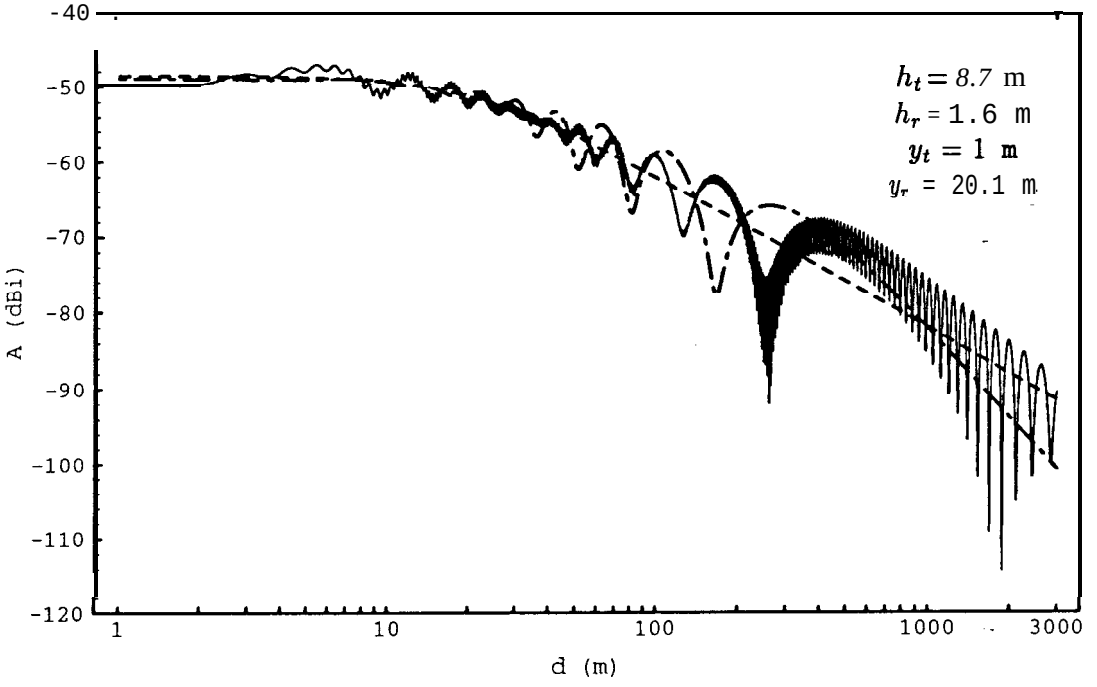

Figure 4.33: Obstructed Second Ray versus (- - -) Two-Ray and (- –) One-Ray Models

Four-Ray Model

The 4RM arising from inclined walls is a more complicated one. In fact, the vertical polarization will be seen **by** the inclined wall as a sum of vertical and horizontal polarizations, each one affected by the corresponding reflection factor.

The 4RM for a depressed highway is shown in Figure 4.34,

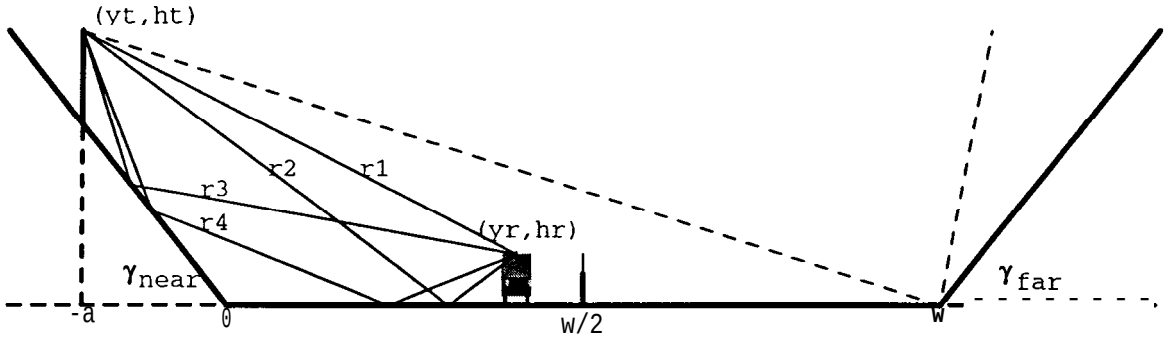

Figure 4.34: Four-Ray Model for Depressed Highways with Inclined Slopes showing Ray Divergence at the Far Slope

where

- a is the distance of the BS antenna from the side of the road;
- γ_{near} is the slope of the side of the highway where the BS antenna is located.

All other parameters are similar to those of the walled highway (Figure 4.24).

The resulting path loss plot (Figure 4.35) is similar to the one obtained for degenerate "six"-ray model with no fourth and no fifth rays (Figure 4.28), smoother (i.e., smaller fades) except for a deep null.

For completeness we also present the degenerate case of obstructed second-ray (Figure 4.36), which again has a smoother path loss curve than that of the corresponding degenerate "six"-ray model (Figure 4.32).

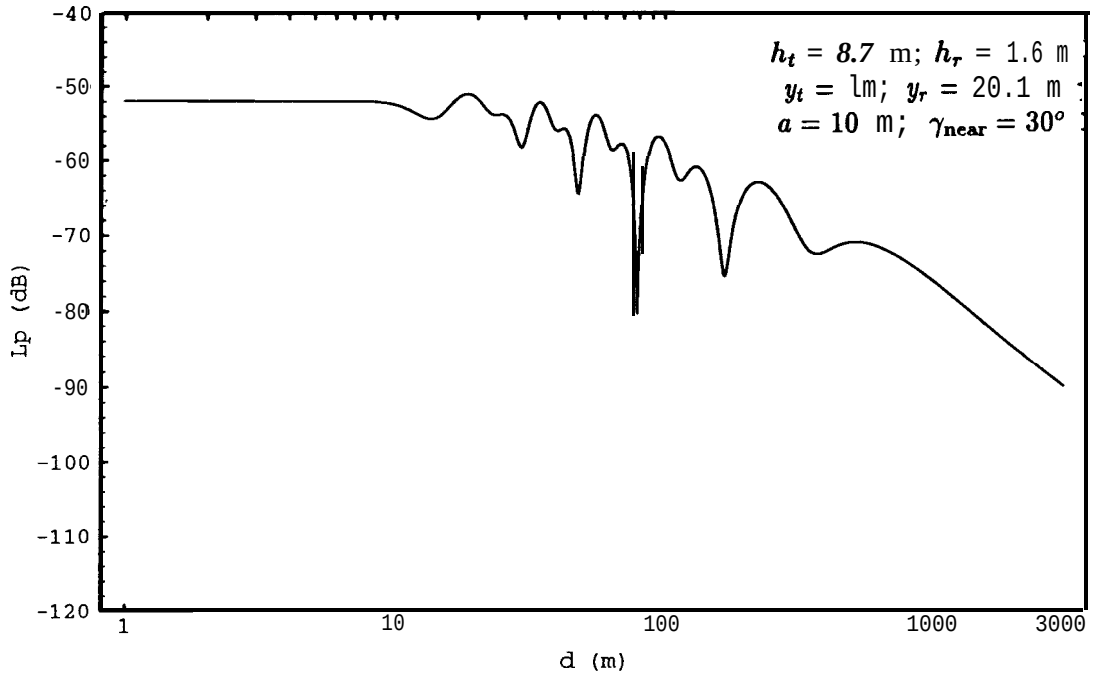

Figure 4.35: Path Loss for Inclined Walls

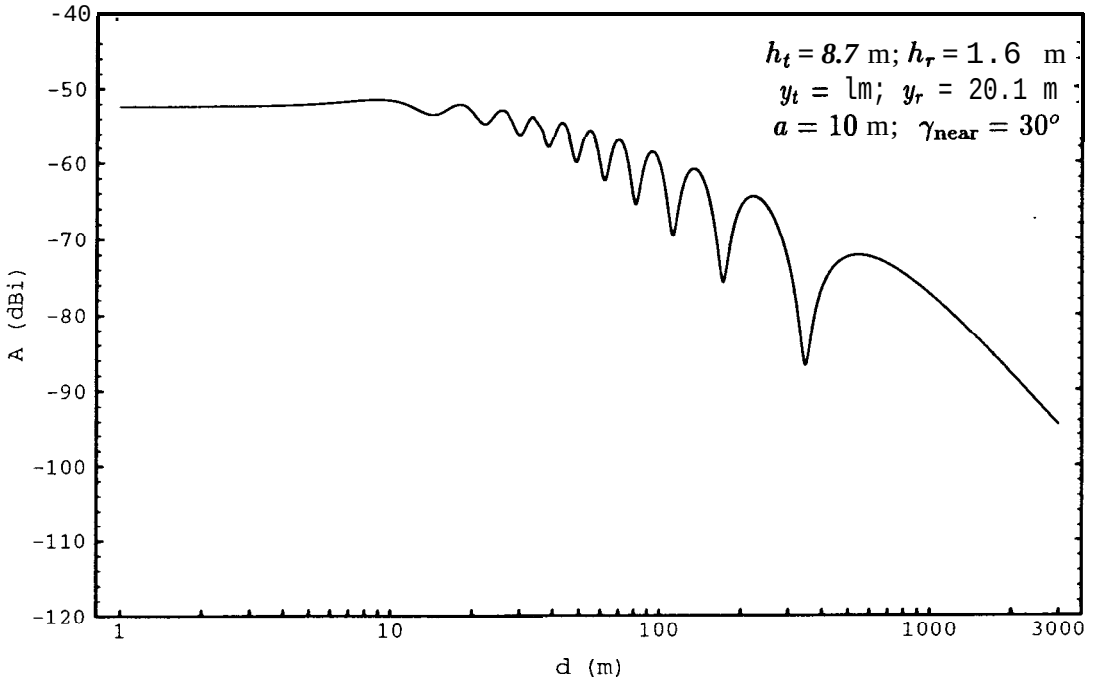

Figure 4.36: Path Loss for Inclined Walls with Obstructed Second-Ray

4.3.4 Middle-Of-The-Road Base Station Antennas

For MoR BS antennas, the situation is slightly simpler, especially for the case of inclined confinement (depressed highways), for which one does not expect reflection from the slopes. In fact, referring back to Figure 4.3.3, for a given α_{max},

$$\alpha_{max} = \arctan\left(\frac{h_t}{w}\right) , \tag{4.29}$$

in order to exist reflections from the other side of the road one must have

$$\gamma_{sides} > \frac{\pi}{2} - \alpha_{max} . \tag{4.30}$$

The MRM is now the 4RM[9] of Figure 4.37a, where the third and the fourth rays will not exist except for vertical confinement (walled or vertically depressed). In any other case, the model reduces from the 4RM to the 2RM of Figure 4.37b.

Comparing now the path loss results for MoR BS antennas with those for SoR positioning for the same highway profile and for the middle lane nearest to the SoR BS antenna, one observes (Figure 4.38) that the fading is somewhat less severe, except for the far region, but the similar trends do not warrant any immediate preference.

Again, it must be emphasized that a given vehicle, as it moves along within a Cell, will face a sequence of different channels depending upon the (non-)existence of obstructions in the path of the specular components. Thus, the path loss "seen" by the vehicle can come from one of the above curves (or from similar ones corresponding to other degenerate cases), with the selection based upon the verification of blockage of each ray.

[9] We can neglect the contribution of rays suffering Multiple Reflections not only due to the reflection losses associated with the reflection coefficient Γ, but also due to the differential path length involved.

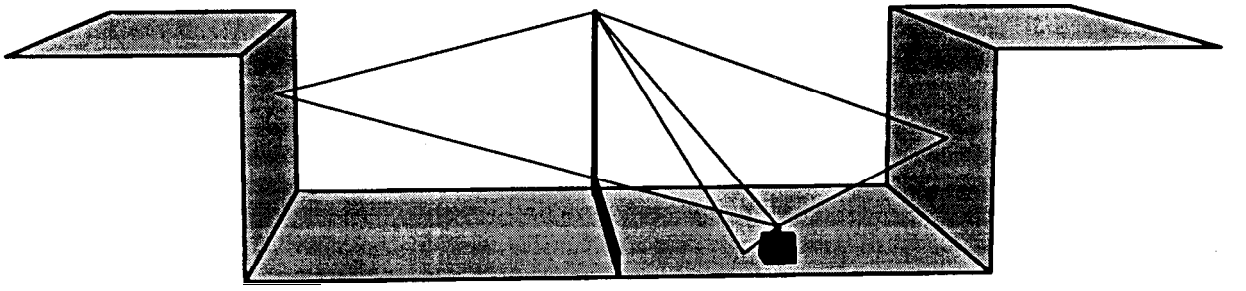

(a) Four-Ray Model for Vertical Confinement

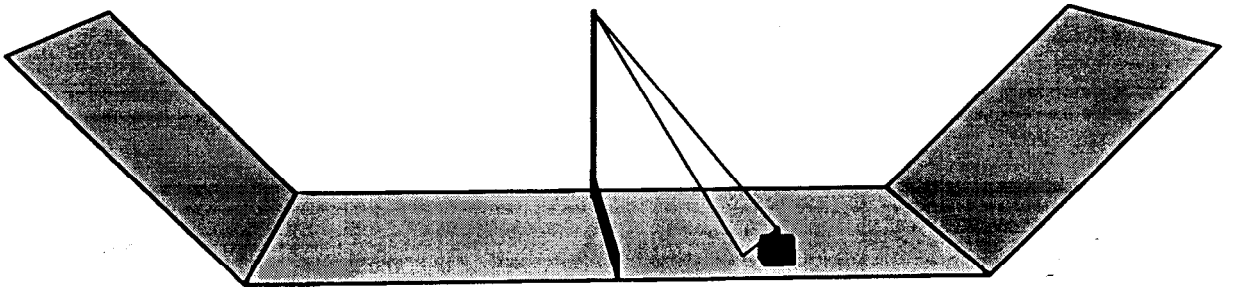

(b) Two-Ray Model for Inclined Confinement

Figure 4.37: Multi-Ray Model for Middle-Of-The-Road Base Station Antennas

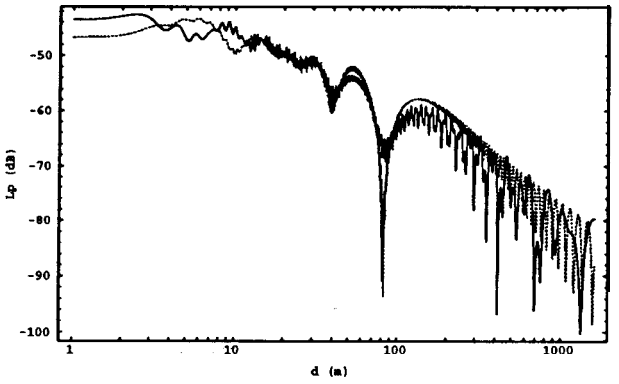

(a) Reflection on the Ground

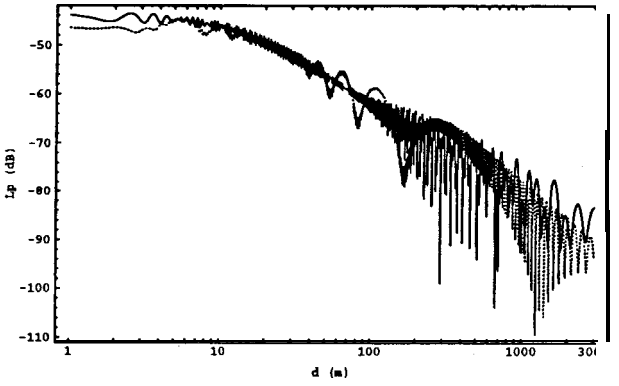

(b) No Second-Ray

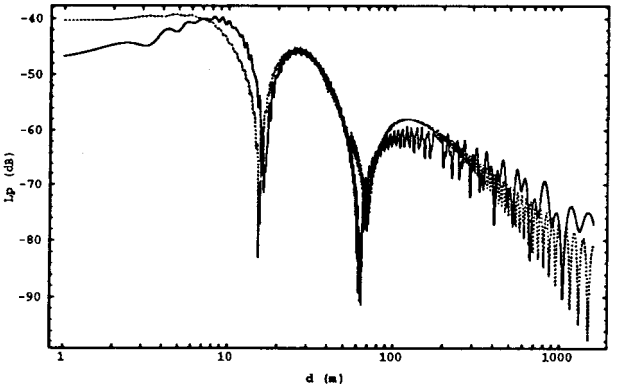

(c) Reflection on the Hood/Trunck of a nearby Car (an usually temporary situation)

Figure 4.38: Path Loss for (-) Middle-Of-The-Roadversus (···) Side-Of-The-Road BS Antennas

4.3.5 Effects of Base Station Antenna Patterns

The effects of antenna directivity (beam shaping) on signal attenuation are now investigated. Major emphasis is placed on the use of inexpensive antenna configurations. Therefore, the use of passive metallic reflectors, or of a pair of antennas, is analyzed first.

In a walled highway environment it is easy to put a reflector on the wall behind the BS antenna. The dimensions of the reflector should be such that they provide for both cell confinement and improved signal intensity profile inside the cell. The reflector must be reasonably small to be practical. If the reflector is small enough, then assembly would be practical even in absence of supporting walls or if the antenna is free standing.

Antenna plus Metallic Reflector

To get as low an attenuation as possible near the BS antenna, one should place the metallic reflector at a distance of X/4 from the antenna. Then, since the value of the reflection coefficient is $\Gamma(\alpha) \approx -1$, one obtains, for small ***d*** (see Figure 4.22), reinforcement from the reflected rays :

$$\text{small d} \Longrightarrow r_3 \approx r_1 + \frac{\lambda}{2}, \quad r_6 \approx r_2 + \frac{\lambda}{2}, \quad r_5 \approx r_4 + \frac{\lambda}{2}, \tag{4.31}$$

which leads, for example, to

$$\frac{\exp(-jkr_1)}{r_1} + \Gamma(\alpha_3)\frac{\exp(-jkr_3)}{r_3} \approx \frac{\exp(-jkr_1)}{r_1}[1 + (-1)\exp(-jk\frac{\lambda}{2})] = 2\frac{\exp(-jkr_1)}{r_1} \tag{4.32}$$

For points far from the antenna, i.e., large ***d,*** one gets

$$r_3 \approx r_1, \quad r_6 \approx r_2, \quad r_5 \approx r_4, \tag{4.33}$$

which leads, for example, to

$$\frac{\exp(-jkr_1)}{r_1} + \Gamma(\alpha_3)\frac{\exp(-jkr_3)}{r_3} \approx \frac{\exp(-jkr_1)}{r_1}[1 + (-1)] = 0, \tag{4.34}$$

i.e., the ray pairs r_3 and r_6, and r_4 and r_5, will almost cancel each other.

On the other hand, if the distance between the BS antenna and the metallic reflector is X/2 one obtains the inverse behavior, i.e., the ray pairs will almost cancel each other for small ***d,*** and they will reinforce each other for large ***d.***

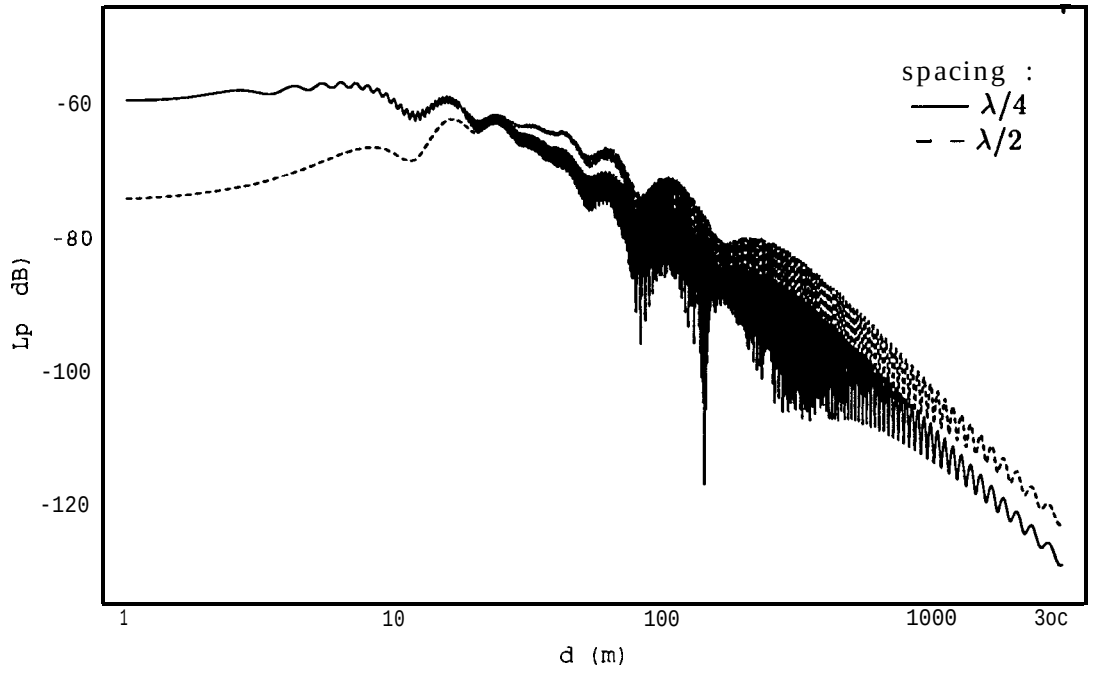

Figure 4.39: Path Loss for BS Antennas with Metallic Reflector

The most important feature of the path loss curves of Figure 4.39 is the somewhat reduced fading compared to the situation without reflector (omni-directional antenna – Figure 4.24), especially for the X/2 case.

Three regions of interest should be considered relative to the curves, namely

- near region - where the path loss for $\lambda/4$ is smaller than that for X/2;
- intermediate region - up to and perhaps a little past the break point, where the path loss for $\lambda/2$ is smaller than that for X/4;
- far region (possibly already in the next cell) - after the break point, where one would want as big a path loss as possible for signal confinement.

Correspondingly, the reflector surface could be composed of three portions (Figure 4.40.a), each associated with one of the above regions, if the objective is maximum cell confinement plus maximum signal intensity within the cell (the transitions need not to be abrupt), or be placed at X/2 to minimize the required dynamic range (Figure 4.40.b).

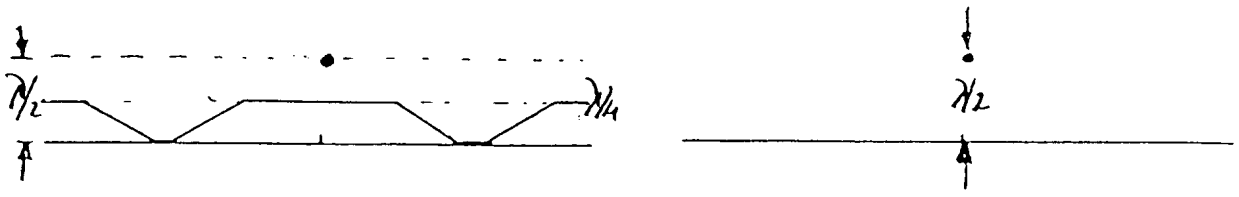

(a) Maximum Confinement plus Maximum Signal Intensity within the Cell (b) Minimum Dynamic Range

Figure 4.40: Suggested Reflector Structures

The longitudinal size of the reflector, $l_{\text{reflector}}$, as referred above, must insure coverage of the region up to the break point. This means that

$$\frac{d_{bp}}{y_{r_{min}} + y_t} = \frac{l_{\text{reflector}}}{y_t} \rightsquigarrow l_{\text{reflector}} = \frac{y_t}{y_{r_{min}} + y_t} d_{bp} \quad , \tag{4.35}$$

where $y_{r_{min}}$ is the minimum transversal distance of a M to the BS antenna, corresponding to the slow lane. Then, as seen from Figure 4.41 which illustrates the locus of the reflection points associated with each of the lanes, the required $l_{\text{reflector}}$ is a very small fraction of d_{bp}, since $y_t = \lambda/4, \lambda/2 \ll y_{r_{min}}$. Moreover, the required reflector height, $h_{\text{reflector}}$, is so small as to make the dimensions of the reflector impractical, and structurally unsound.

The above analysis, however, based upon ray-tracing techniques, ignores near-field effects, and those will determine the required dimensions of the reflector. Anyhow, the longitudinal size of the reflector is not expected to exceed by much $l_{\text{reflector}}$ above.

However, $l_{\text{reflector}}$ can still be impractically large. In that case one needs either to consider the effects of a "truncated" planar reflector or the use of a diverging reflector of smaller dimensions (the inherent divergence losses would, in our case, be small - Figure 4.42), although more sensitive to build and possibly more difficult to physically install.

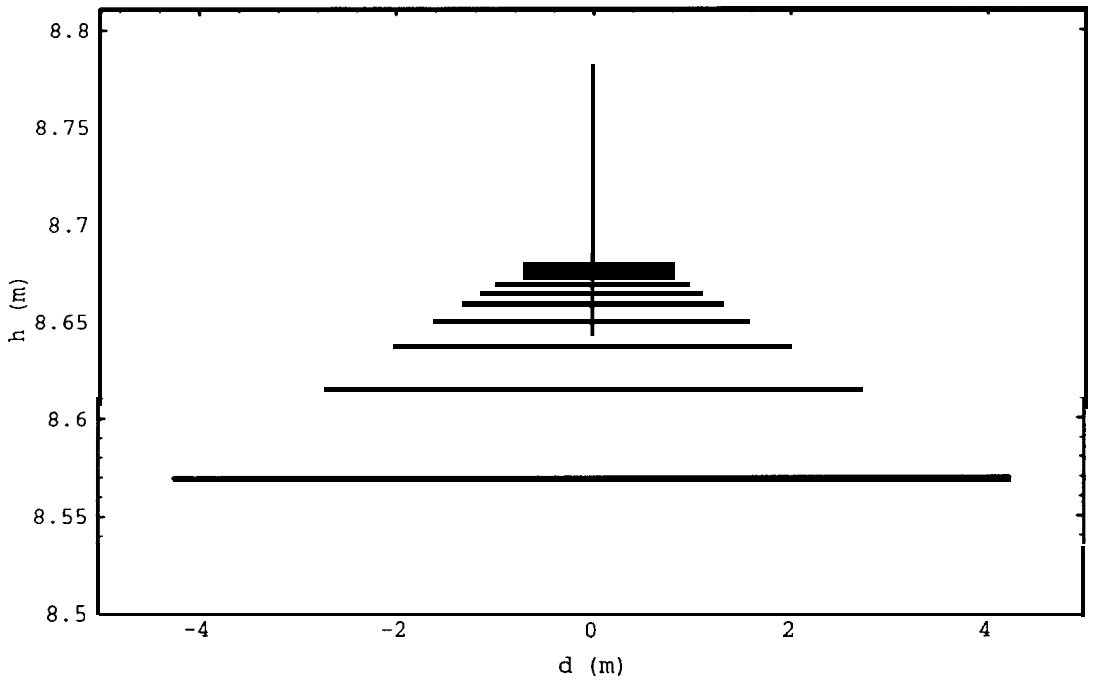

Figure 4.41: Locus of Reflection Points for X/2 spacing

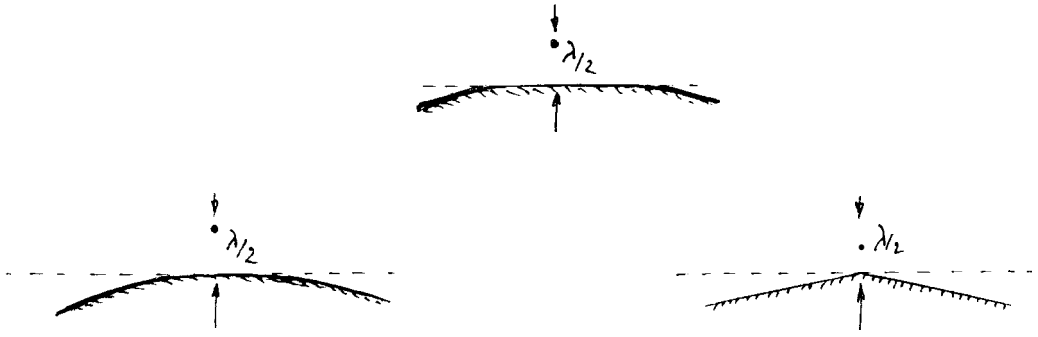

Figure 4.42: Diverging Reflector Structures

Pair of Antennas

Another beam shaping alternative, and one that needs to be considered for the case of MoR BS antennas is the use of arrays of antennas, obviously while trying to make them as cheap as possible. With that objective, the simplest possible array, one that has only two active elements and no metallic reflectors, was considered, both in the longitudinal and transversal positions.

In the case of a longitudinal array (LA), the shape of the path loss curve can be controlled by adjusting the distance and/or the phasing between the elements of the array. Hereafter only the spacing between the elements of the array was varied, assuming that the two elements are excited in phase. As it can be seen from Figure 4.43, where we left out the fast fading effect, in the near region the two fields will reinforce each other (almost independently of the distance between the elements of the array). At large distances they will almost cancel each other if the distance between the elements is close to $\lambda/2$.

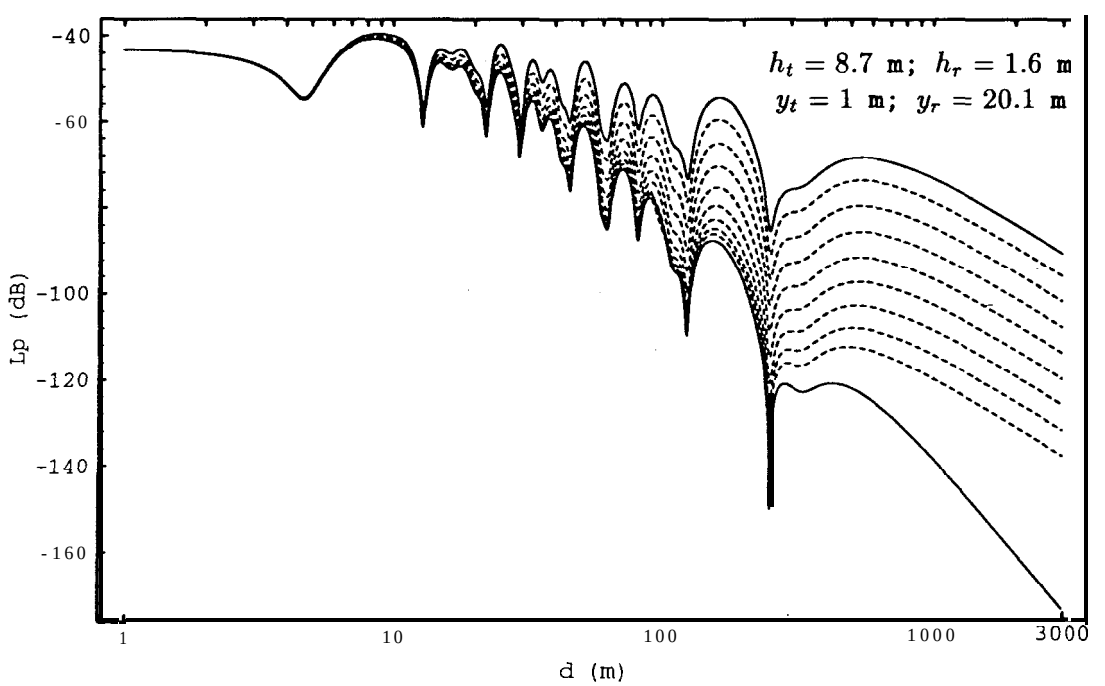

Figure 4.43: Path Loss for a Two-Element Longitudinal Array with In-Phase Excitation as a function of the Distance between Elements : $(2^{-1} - 2^{-i})\lambda, i = 2, \cdots, 10$; X/2

For the transversal array (TA), in order to get reinforcement for small ***d,*** one has to excite the elements of the array in phase opposition. Then, the fields in the far region will, again, almost cancel each other (Figure 4.44).

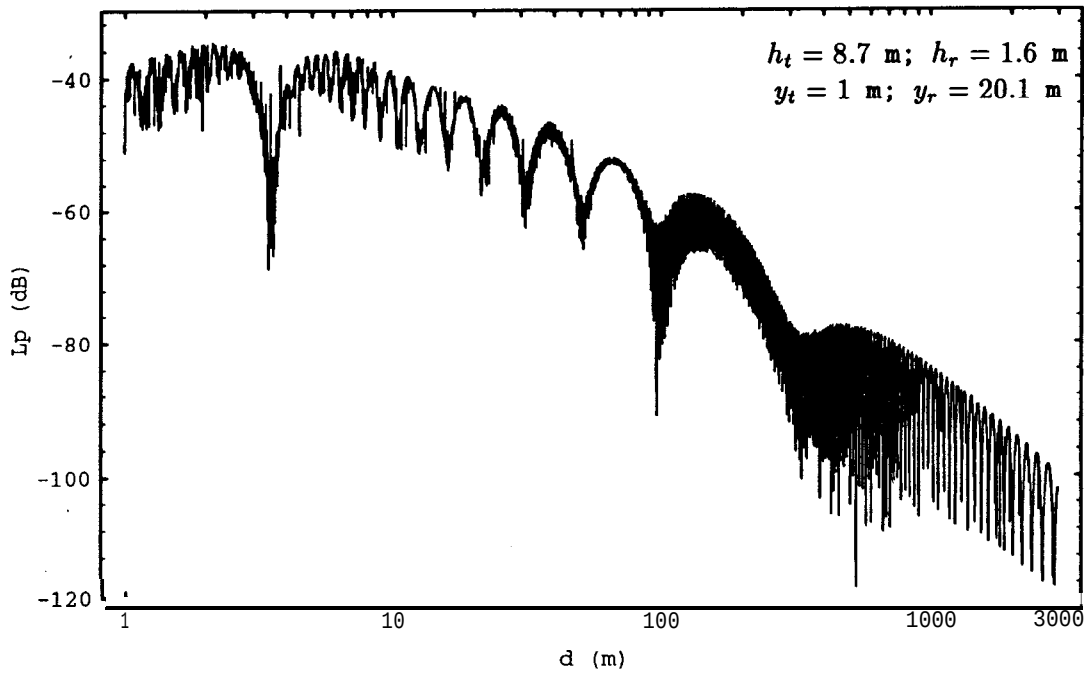

Figure 4.44: Path Loss for a Two-Element Transversal Array for a X/2 spacing of the Elements and Opposite Excitation

One must note, here, the sensitivity of the LA Path Loss curve to the spacing between the elements of the array. This may present some advantages in terms of cell size definition. Another aspect that needs to be analyzed is the effect of any misaiignment when positioning the array, such that they are neither transversally nor longitudinally installed.

4.3.6 IVHS Scenarios

Surface Streets

For surface streets, and antennas at street-lamp level positioned at main intersections [6], the turning point is typically located before the next intersection, as it would be expected from equation (4.4). In fact, building-guided propagation dominates within the first city block.

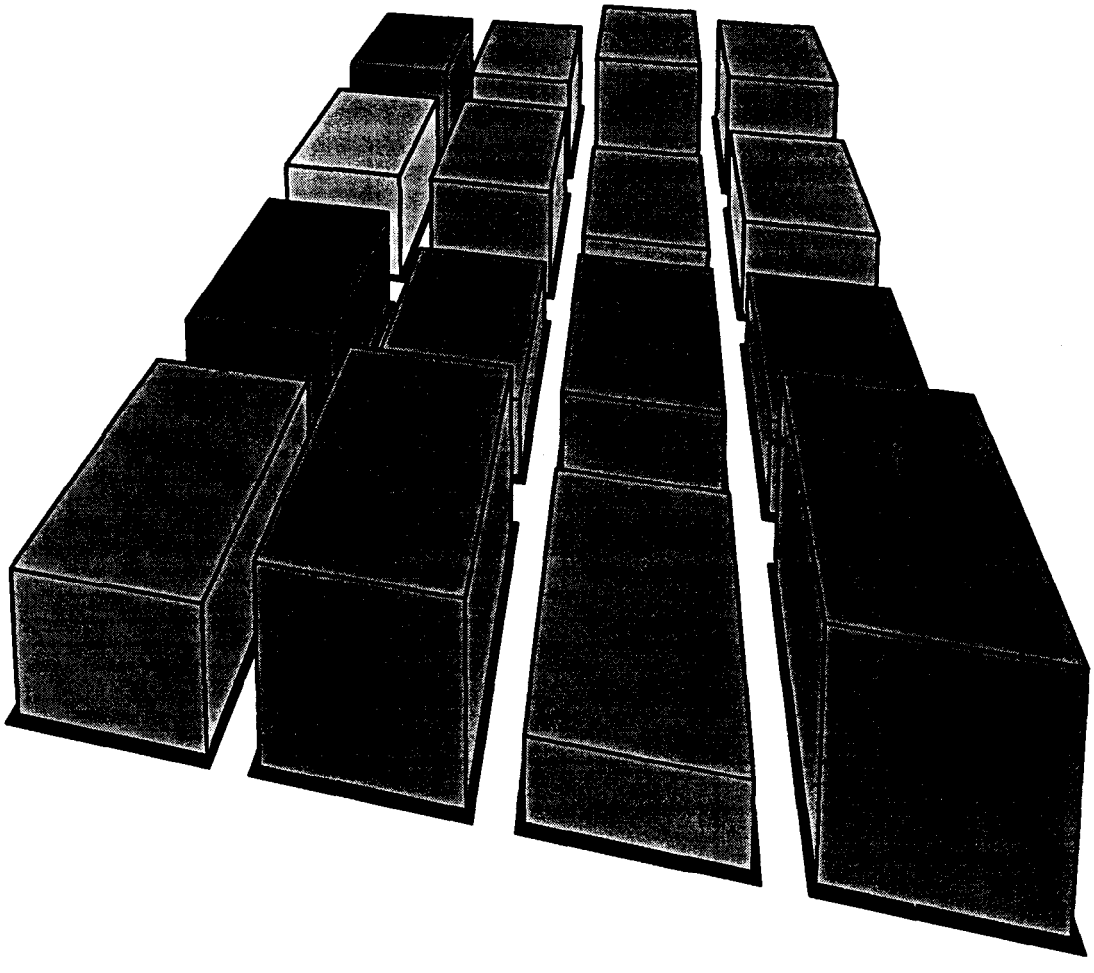

Figure 4.45: Examples of Surface Street Structures

Highways

For the highway case, purely geometric arguments account for the expected behavior. Having already discussed the Walled Highway and the Depressed Highway cases, we present in Figure 4.46, different highway cross-sections and (some of) their associated MRMs. The theory expanded in the previous Sections would obviously be applicable, requiring only the solution of the ray-tracing problem involved.

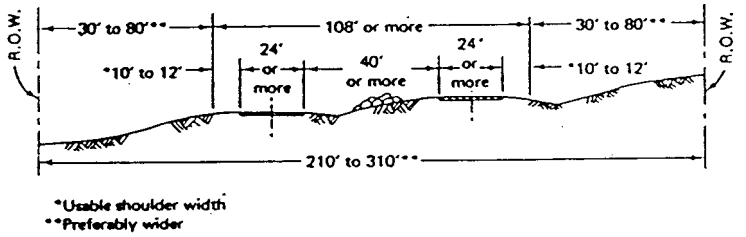

Rural, at-grade

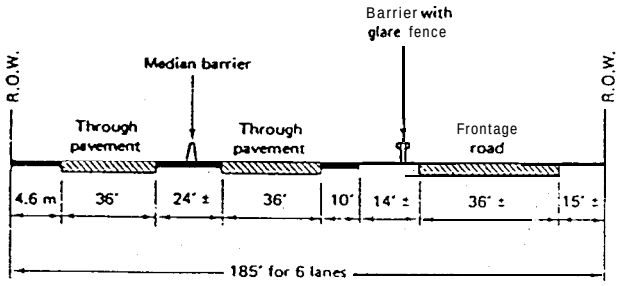

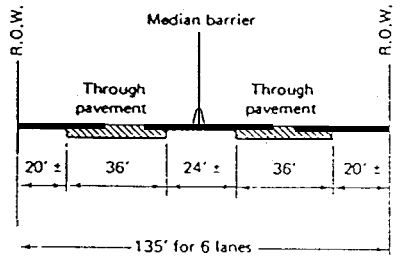

Suburban, urban at-grade

(a) Examples of Highways At Grade

Figure 4.46: Examples of Highway Structures [37]

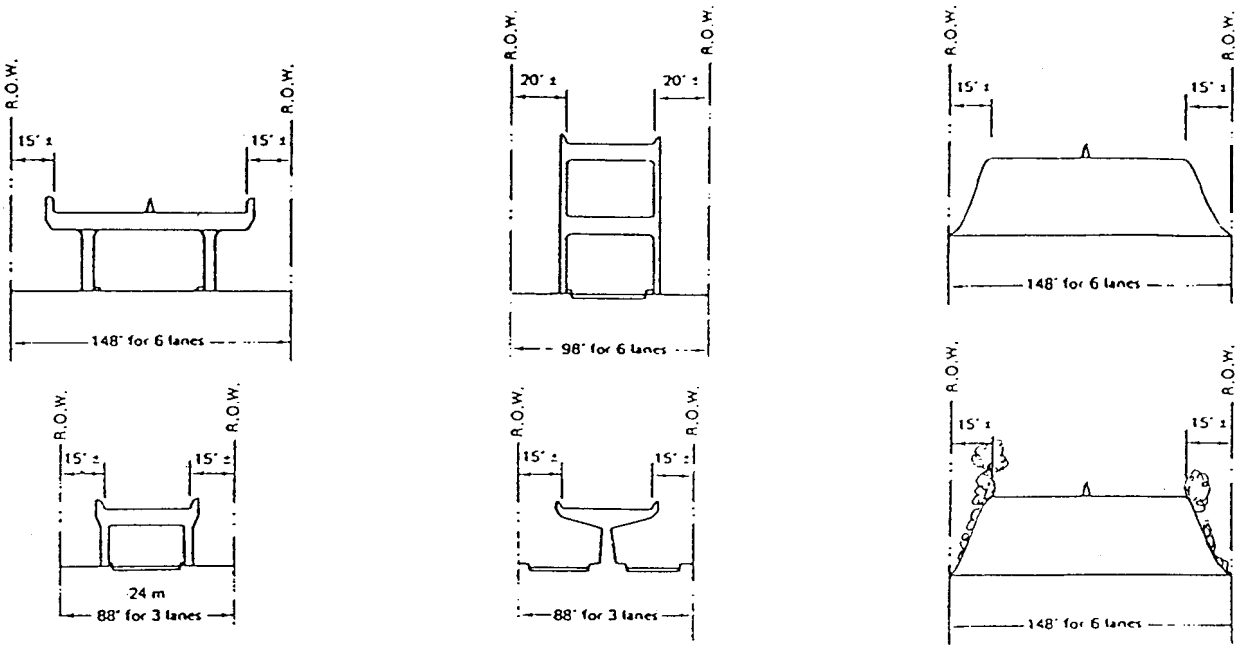

(b) Examples of Elevated Highways

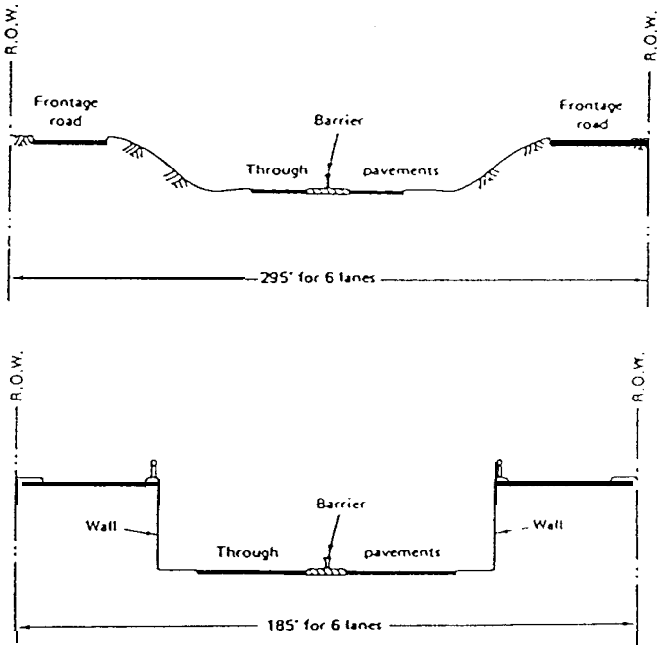

(c) Examples of Depressed Highways

Figure 4.46: Examples of Highway Structures [37] (Cont.)

4.4 Temporal Description of the Fading

It is now important to analyze the fading as a function of time, and a Section will be dedicated to that subject. The objective is to have an idea of the channel "seen" by a vehicle as it moves through the Cell, as a function of its location (lane), speed (function of the lane and of the traffic intensity), and of the overall traffic (i.e., all the neighboring vehicles). Given the complexity of the problem at hand, one will have to count on some kind of Monte Carlo simulation of traffic conditions in order to get statistical information on what happens to each of the meaningful specular components.

Assuming that the vehicle cruises at a fixed speed (usually function of the lane), it can be observed (Figure 4.47) that, **in absence of other vehicles** that might obstruct some of the rays, the temporal evolution of the path loss shows a piecewise linear trend independently of the lane and the speed of the vehicle. The effects of speed would show up only in terms of (time) scaling of the path loss curve.

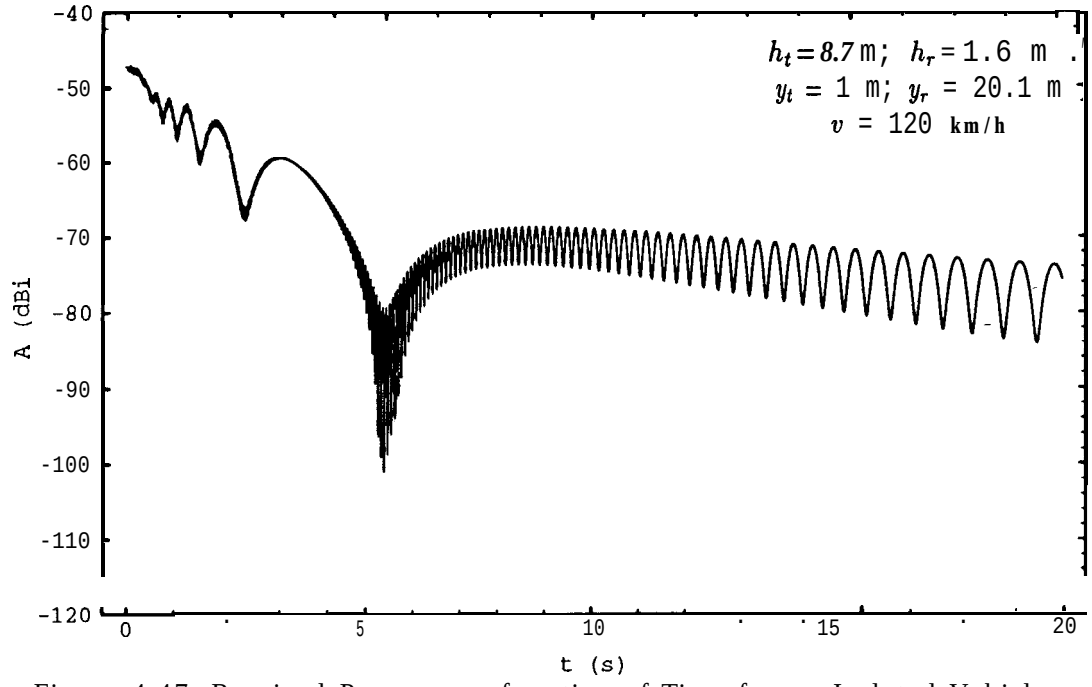

Figure 4.47: Received Power as a function of Time for an Isolated Vehicle

From Figure 4.47 one can immediately see that the channel is indeed slowly time-varying, with fading that gets slower as the vehicle moves away from the BS. At the

same time, the piecewise linear spatial average may eventually be used, even the region nearest to the BS, as a coarse indication for the AGC presumably required for power control.

Under more realistic conditions, i.e., **considering the presence of traffic,** one will notice the effect of obstruction of certain rays, especially the LOS (due to the interposition of trucks/buses between a car/van and the BS). Figure 4.48 corresponds to the simplest MRM, the 2RM. Therefore, when the LOS, and consequently the ground reflected ray, is obstructed one ends up with the limiting case of the Rician channel, i.e., with a Rayleigh channel.

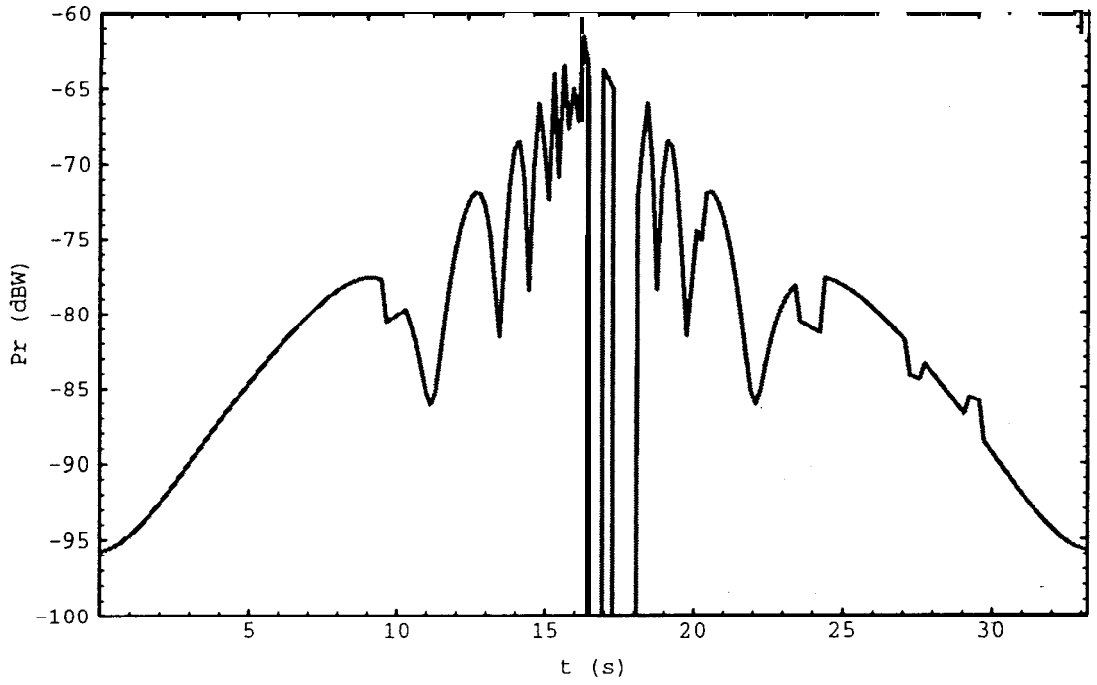

Figure 4.48: Received Power in the Slow Lane for Middle-Of-The-Road BS Antenna and Inclined Confinement (Geometry of Figure 4.37)

This simple model can nevertheless show some important aspects of fading in the IVHS scenario. From Figure 4.49 one can see that the effect of the obstruction of the ground reflected ray accentuates with distance : far from the BS, but yet before the break point, the absence of the second ray implies a very noticeable loss/gain of received power, which does not happen near the BS, where the difference between the 1RM and

the 2RM is much smaller.

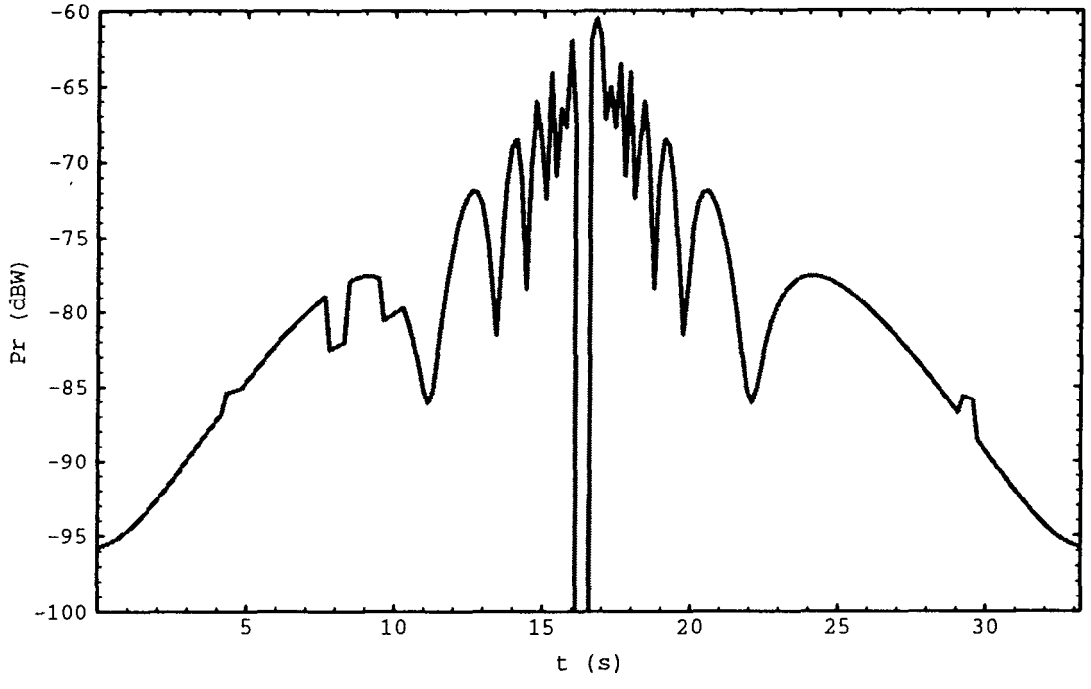

Figure 4.49: Received Power in the Slow Lane for Middle-Of-The-Road BS Antenna and Inclined Confinement – Effects of Distance

At the same time, as seen in Figure 4.50, the **duration of a fade,** defined as the duration of the deviation from what would be the received power without any obstructed rays, is obviously a function of the speed differential between the target and the interposing vehicles. It must be noticed that we have chosen, due to time constraints, not to show in Figures 4.49 and 4.50 the "fast fading" details one can notice in Figure 4.47.

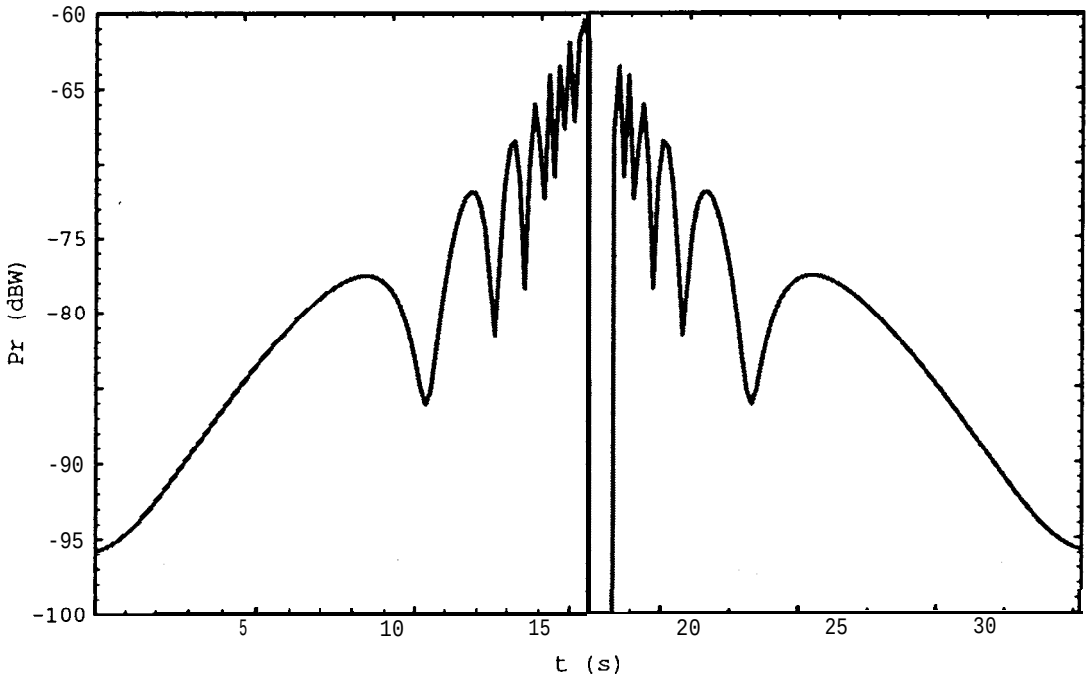

(a) Interposition of a "Slow" Truck/Bus

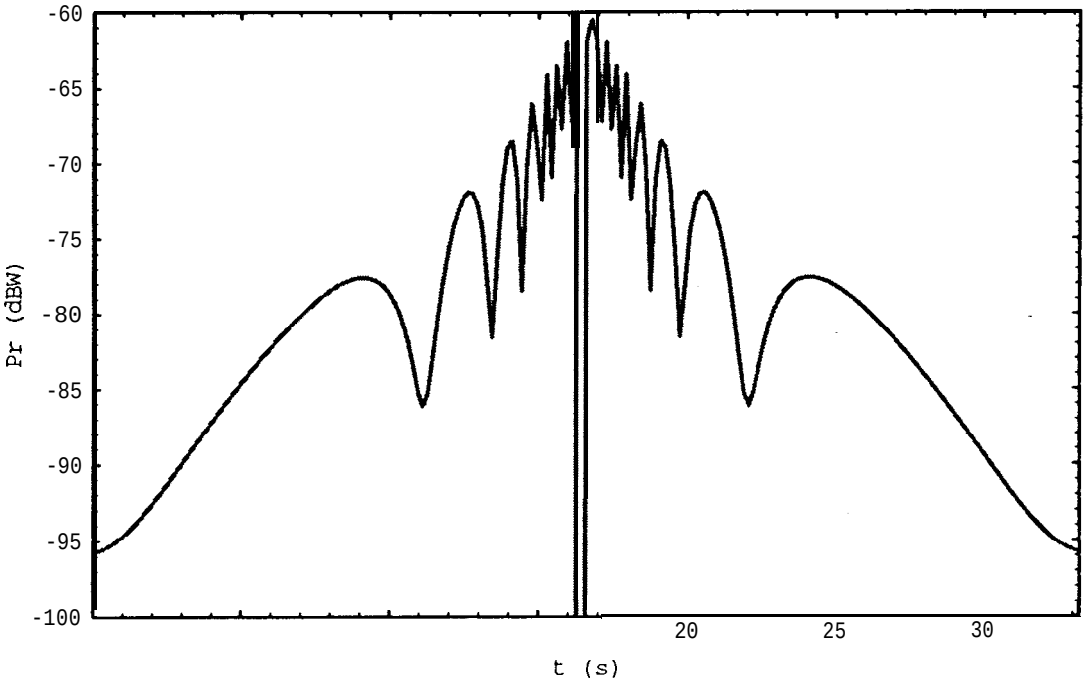

(b) Interposition of a "Fast" Truck/Bus

Figure 4.50: Received Power in the Slow Lane for Middle-Of-The-Road BS Antenna and Inclined Confinement – Effect of Speed Differentials

4.5 The CSI IVHS Package

In parallel with the development of the present Report, a new IVHS software package was developed by one of the authors (J.M.N. Pereira), at the *Communication Sciences Institute,* using the MATHEMATICA package. The CSI IVHS Package consists of three main parts, namely the definition of the MRMs, the animation of a section of highway, and the simulation of received power at the mobile under realistic traffic conditions.

4.5.1 Multi-Ray Models

The package contains the definition of all MRMs previously described, and it was used to obtain all the plots in this Report. A more interactive, and realistic (in terms of geometric characterization) version of this part of the package is under development. A more distant objective is to go from the ray-tracing (RT) analysis here employed to a full geometric theory of diffraction (GTD), taking into account the contribution of diffraction to the received electric fields.

4.5.2 Animation

The animation of a section of highway, that may be even bigger than a cell, given its geometry and the traffic conditions, was achieved under certain simplifications and using some heuristics :

- constant speeds, function of the lane where the vehicles cruise, and of the traffic intensity, but not of the type of vehicle – all vehicles in a given lane will have the same speed;
- no passing or lane changes allowed;
- geometric distribution of the distance between vehicles (function of the lane), but guaranteeing a minimum distance between vehicles (which is a function of the lane speed);

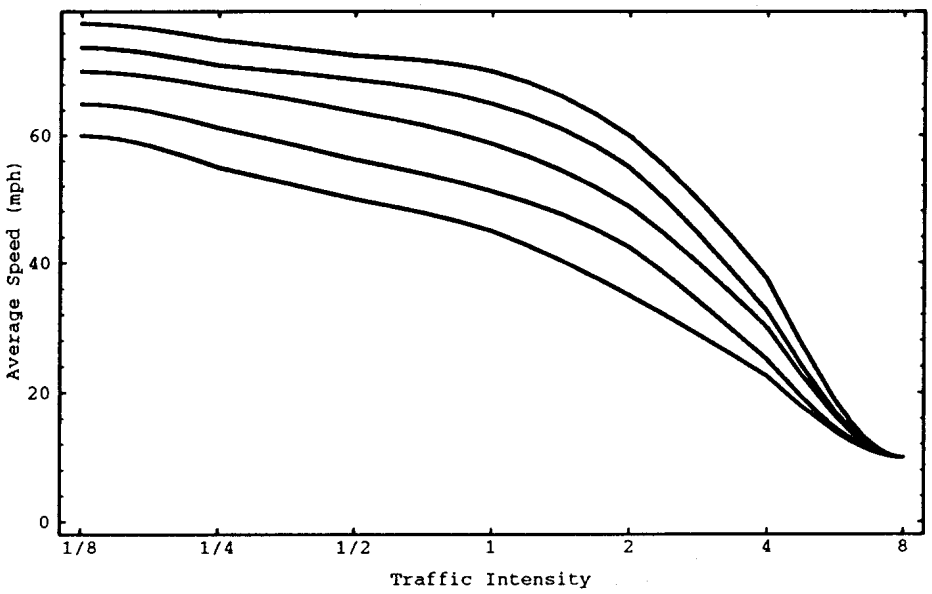

Figure 4.51: Lane Speeds as a function of Traffic Intensity (Heuristic)

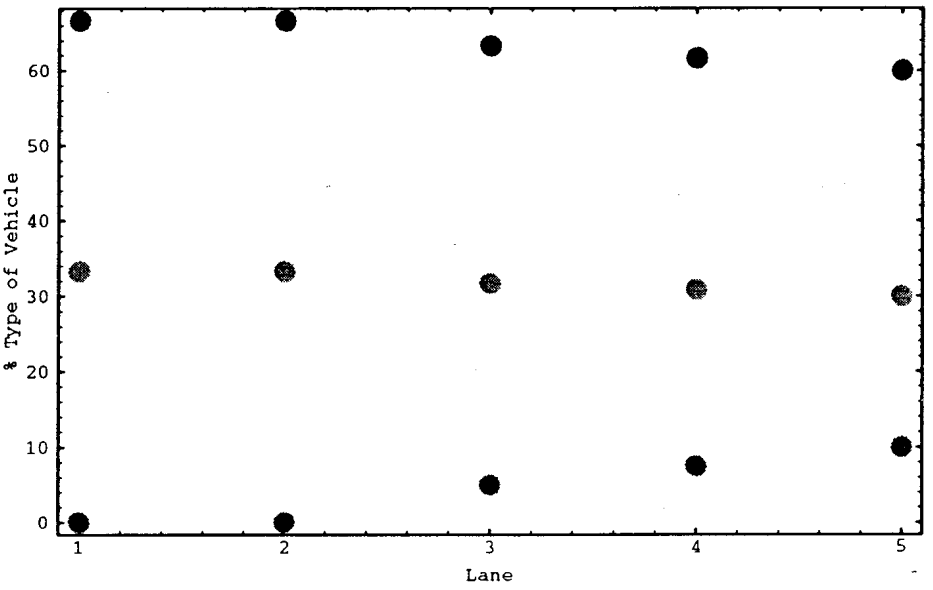

Figure 4.52: Percentage of Vehicles of each type in each Lane (Heuristic)

- only three types of vehicles, namely "car", "van", and "truck/bus", with fixed geometries;
- only a given percentage of the vehicles, function of traffic intensity, will be in communication with the BS,

where the **traffic intensity** figure is the ratio of the number of cars within the cell for given traffic conditions and the same number for average traffic.

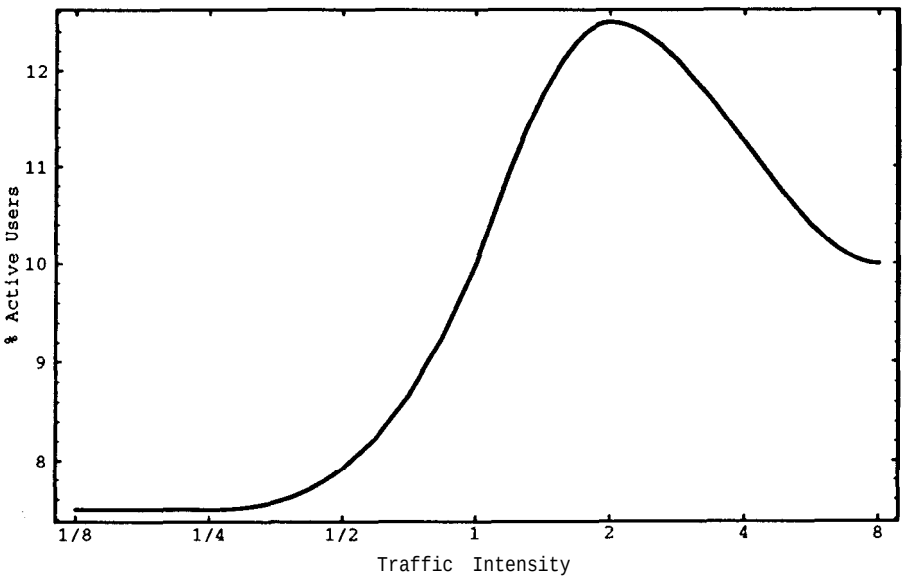

Figure 4.53: Percentage of Active Mobiles as a function of Traffic Intensity (Heuristic)

4.5.3 Channel Waveforms

The determination of the received power at the M, as a function of a specific (i.e., realistically simulated) traffic condition, proceeds as follows :

- for a given position of the mobile (function of a random initial position, lane speed and time)
  - * determine which vehicles are in position to obstruct any of the specularly reflected rays to expedite the search for really obstructing vehicles;
  - * verify if those vehicles in fact obstruct any of the rays;
  - * mark all obstructed rays;
- given the information on obstructed rays, compute the received power via a specific RMR.

4.6 References

[1] I. Korn, "GMSK with Limiter Discriminator Detection in Satellite Mobile Channel", ***IEEE Trans. Comm.,*** Jan 91

[2] R.J.C. Bultitude, G.K. Bedal, "Propagation Characteristics on Microcellular Urban Mobile Radio Channel at 910 MHz", ***IEEE J. Sel. Areas Comm.,*** Jan 89

[3] R. Steele, "The Cellular Environment of Lightweight Handheld Portables", ***IEEE Comm. Mug.,*** Jul 89

[4] S.A. El-Dolil, W.-C. Wong, R. Steele, "Teletraffic Performance of Highway Microcells with Overlay Macrocell", ***IEEE J. Sel. Areas Comm.,*** Jan 89

[5] "Urban Transmission Loss Models for Mobile Radio in the 900- and 1800-MHz Bands", Revision 2, COST 231 TD (91) 73, Sep 91

[6] P. Harley, "Short Distance Attenuation Measurements at 900 MHz and 1.8 GHz using Low Antenna Heights for Microcells", ***IEEE J. Sel. Areas Comm.,*** Jan 89

[7] H.H. Xia, H.L. Bertoni, L.R. Maciel, A. Lindsay-Stewart, R.Rowe, L. Grindstaff, "Radio Propagation Measurements and Modeling for Line-of-Sight Microcellular Systems", ***42nd IEEE Veh. Tech. Conf.***, May 92

[8] J.G. Proakis, ***Digital Communications***, 2nd Ed., McGraw Hill, 1989

[9] Y. Okumura et ***al.,*** "Field Strength and its Variability in VHF and UHF Land-Mobile Radio Service", ***Rev. Elec. Comm. Lab.,*** Sept-Ott 68

[10] K.L Blackard, M.J. Feuerstein, T.S. Rappaport, S.Y. Seidel, H.H. Xia, "Path Loss and Delay Spread Models as Functions of Antenna Height for Microcellular System Design", ***42nd IEEE Veh. Tech. Conf.,*** May 92

[11] W.C.Y. Lee, ***Mobile Communications Engineering,*** McGraw-Hill, 1982

[12] J.W. Ketchum, "Down-Link Capacity of Direct Sequence CDMA for Application in Cellular Systems", GTE Labs. Report (?)

[13] R. Steele, "The Cellular environment of lightweight handheld Portables", *IEEE **Comm. Mug.,*** Jul 89

[14] H.R. Reed, C.M. Russell, ***Ultra High Frequency Propagation,*** John Wiley & Sons, 1953

[15] K. Bullington, "Radio Propagation Fundamentals", *B.S.T.J.*, Vol. 36, May 57

[16] B.D. Popović, M.B. Dragović, A.R. Djordjevid, ***Analysis and Synthesis of Wire Antennas,*** Research Studies Press (John Wiley & Sons), 1982

[17] K.H.Awadalla, T.S.M. Maclean, "Monopole Antenna at the Centre of Circular Ground Plane : Input Impedance and Radiation Pattern", ***Trans. Antennas & Prop.,*** AP-27, 1979

[18] R.E. Collin, ***Antennas and Radiowave Propagation,*** McGraw-Hill, 1985

[19] D. Parsons, ***The Mobile Radio Propagation Channel,*** Halsted Press (John Wilay & Sons), 1992

[20] D.O. Reudink, "Properties of Mobile radio Propagation above 400 MHz", *IEEE **Trans. Veh. Tech., Nov 74***

[21] H. Suzuki, "A Statistical Model for Urban Radio Propagation", ***IEEE Trans. Comm.,*** July 77

[22] F.J. Mammano, J.R. Bishop,Jr., "Status of IVHS Technical Developments in the United States", *42nd **IEEE Veh. Tech.** Conf.*, May 92

[23] J. Dickerson, "Fuzzy Platoon Leader", *SIPI **Seminar,*** May 92

[24] Hughes Ground Systems, ***VRC Proposal***

[25] W.L. Stutzman (Ed.), R.M. Barts, C.W. Bostian, J.S. Butterworth, R. Campbell, J. Goldhirsh, W.J. Vogel, "Mobile Satellite Propagation Measurements and Modeling : a Review of Results for Systems Engineers", *Proc. **Mobile Satellite** Conf.*, May 88

[26] "Dual-Mode Mobile Station/Base Station Compatibility Standard", *EIA/TIA **Specification** IS-54*, Oct 90

[27] Research and Development Center for Radio Systems (RCR) Standard 27, Apr 91;

[28] H.L. Kazecki, J.C. Baker, "Digital Cellular Modem Field Results", ***42nd IEEE Veh. Tech. Conj.,*** May 92

[29] D.C. Cox, "910 MHz Urban Mobile Radio Propagation : Multipath Characteristics in New York City", ***IEEE Trans. Veh. Tech., Nov 73***

[30] T.S. Rappaport, S.Y. Siedel, R. Singh, "900 MHz Multipath Propagation Measurements for U.S. Digital Cellular Radiotelephone", ***IEEE Global Telecomm. Conj., Nov 89***

[31] S.Y. Siedel, T.S. Rappaport, S. Jain, L. Lord, "Path Loss, Scattering, and Multipath Delay Statistics in Four European Cities for Digital Cellular and Microcellular Radiotelephone", ***IEEE Trans. Veh. Tech., Nov*** 91

[32] COST 207 WG1, "Proposal on Channel Transfer Function to be used in GSM Tests Late 1986", Sep 86

[33] G.L. Turin, F.D. Clapp, T.L. Johnston, S.B. Fine, D. Lavry, "A Statistical Model for Urban Multipath Propagation", ***IEEE Trans. Veh. Tech.,*** Feb 72

[34] B. Vucetic, J. Du, "Channel Modeling and Simulation in Satellite Mobile Communication Systems", ***IEEE J. Sel. Areas Comm.,*** Oct 92

[35] P.A. Bello, "Characterization of Randomly Time-Variant Channels", ***IRE Trans. Comm. Systems,*** Dec 63

[36] A.A.R. Townsend, ***Digital Line-of-Sight Radio Links – A Handbook,*** Prentice Hall, 1988

[37] W.R. McShane, R.P. Roess, ***Traffic Engineering,*** Prentice Hall, 1990

[38] S.C. Schwartz, Y.S. Yeh, . . .

[39] P. Diaz, R. Agusti, "Analysis of a Fast CDMA Power Control Scheme in an Indoor Environment", ***42nd IEEE Veh. Tech. Conj.,*** May 92

[40] J. Chadwick, V. Patel, "Strategies for Acquiring Radio Frequencies for Intelligent Vehicle Highway Systems (IVHS)", ***42nd IEEE Veh. Tech. Conf.***, May 92

[41] K. Yamada, K. Daikoku, H. Usui, "Performance of Portable Radio Telephone using Spread Spectrum", ***IEEE Trans. Comm.,*** Jul 84

[42] A. Salsami, KS. Gilhousen, "On the System Design Aspects of Code Division Multiple Access (CDMA) Applied to Digital Cellular and Personal Communications Networks", ***41st IEEE Veh. Tech. Conj.,*** May 91

[43] K.K. Ho, "Architectural Design of a Code Division Multiple Access Cellular System", ***42nd IEEE Veh. Tech. Conj.,*** May 92

[44] J. Weitzen, J. Larsen, R. Mawrey, "Design of a Meteor Scatter Communication Network for Vehicle Tracking", ***42nd IEEE Veh. Tech. Conj.,*** May 92

[45] Caltrans, ***Proposed Additions to Title 21, Chapter 16, Articles 1 through 7 of the California Code of Regulations,*** Mar 92

Chapter 5

Multiple-Access Performance Analysis

5.1 Introduction

In this chapter, multiple-access (MA) techniques will be studied and their performance assessed for IVHS applications. Multiple-access, briefly speaking, is a way of resource sharing. In communications the resource usually consists of the channel or a given frequency band. The most commonly adopted multiple-access schemes are FDMA, TDMA, and CDMA. In this chapter, only performance measures for TDMA and CDMA for IVHS applications are considered, since FDMA is deemed too expensive due to the cost of the accurate frequency synthesizers needed. The performance measures include bit error rate (BER) and packet error rate (PER).

In TDMA, time is divided into slots. The users will be assigned slots to transmit their message. The number of user that can be supported (i.e., the system capacity) is limited in the TDMA case by the available bandwidth. In CDMA, every user is assigned a specific code and they can transmit their messages simultaneously. Any reduction in interference converts directly into increase in capacity. Thus CDMA is interference limited.

The remainder of this chapter is organized as follows. In Section 5.2, performance measures for several modulation and demodulation schemes for TDMA systems are de-

rived and some interesting results are discussed. In Section 5.3, we study the performance measures for CDMA systems. Conclusions and future challenges are given in Section 5.4.

5.2 Time Division Multiple-Access

5.2.1 Introduction

In this section, we are interested in the BER performance of a TDMA system over a Rician fading channel in IVHS short-range (microcellular type) communications. In the Rician fading channel, the received signal will include line-of-sight (LOS), specular, and scattered components [4]. In addition, the signal-to-noise ratio (SNR) can be very large in this kind of short-range communications. Binary PSK, FSK, and ASK modulations with LOS-coherent and noncoherent demodulation are considered and their BER performance compared.

This section is structured as follows. In Section 5.2.2, the Rician fading channel model is introduced. In Sections 5.2.3 and 5.2.4, the BER for LOS-coherent and noncoherent demodulation are respectively derived. PER is derived in Section 5.2.5. Numerical results were obtained and are discussed in Section 5.2.6. Section 5.2.7 provides some conclusions.

5.2.2 Channel Model

In the IVHS environment, the channel is AWGN with Rician envelope fading characteristics [4]. The lowpass equivalent complex impulse response, h(t), can be expressed as

$$h(t) = [1 + \beta \exp(j\xi)]\,\delta(t) , \tag{5.1}$$

where the constant represents the line-of-sight (LOS) component, and the random gain β and phase ξ of the scattered component have, respectively, a Rayleigh distribution with $E[\beta^2] = 2\sigma^2$, and a uniform distribution on $[0, 2\pi)$. These random gain and phase will be assumed constant over the bit interval. This model is a simplified version of that proposed in [4]. Here, we ignore the specular component because it strongly depends on

the dynamic traffic conditions and we can not account for it at this stage of our analysis. In addition, we use the fact that we can also ignore the effect of intersymbol interference (ISI) because the delay time spread of the received signal is very small compared with the bit interval (see Chapter 4).

The ratio,, K, of the LOS component power to Rayleigh scattered component power

$$K = \frac{1}{E[\beta^2]} = \frac{1}{2\sigma^2} \quad , \tag{5.2}$$

will play an important role in determining the BER performance. The range of K in IVHS communication is expected to be 10–20 dB, being determined by actual traffic conditions.

5.2.3 LOS-Coherent Demodulation

In this section, we will derive the BER for LOS-coherent demodulation of BPSK,BFSK, and ASK modulated signals. In LOS-coherent demodulation, we assume that the phase of the LOS component can be perfectly tracked, i.e., the LOS component is the desired term and the scattered component is treated as interference.

PSK

In BPSK modulation, the transmitted signals take the form

$$s(t) = \Re e\left\{b_i\sqrt{2P}\exp[j(2\pi f_c t + \theta)]\right\} \quad , \tag{5.3}$$

where b_i is the ith bit of the data signal whose values are equally likely ± 1, P is the received power, f_c is the carrier frequency, and θ is the phase angle of the system. If the channel is a Rician fading channel as described in Section 5.2.2, the received signal r(t) can be written as

$$r(t) = \Re e\left\{\sqrt{2P}b_i\{\exp(j\theta) + \beta\exp[j(\theta + \xi)]\}\exp[j2\pi f_c t]\right\} + n(t) \quad , \tag{5.4}$$

where n(t) is the AWGN introduced by the channel with two-sided power spectral density (PSD) $N_0/2$ W/Hz.

The receiver model for coherent BPSK is shown in Figure 5.1. Here, we assume the phase for the LOS component can be tracked perfectly. The decision variable Z_i for the ith bit can be derived as

$$\begin{aligned} Z_i &= \int_{iT_b}^{(i+1)T_b} 2r(t)\cos(\omega_c t + \theta)\,dt \\ &= b_i\sqrt{2P}T_b + b_i\sqrt{2P}T_b\beta\cos\xi + N \\ &= b_i\sqrt{2P}T_b + D + N \quad , \end{aligned} \tag{5.5}$$

where T_b is the bit interval, $\omega_c = 2\pi f_c$, N is a Gaussian random variable (r.v.) with zero mean and variance N_0T_b, and D is the interference due to the scattered component, also a Gaussian r.v. with zero mean and variance $2P\sigma^2T_b^2$.

The BER, P_b, can be represented as

$$P_b = \frac{1}{2}[\,\Pr(Z_i < 0 \mid b_i = +1) + \Pr(Z_i \geq 0 \mid b_i = -1)\,] \,. \tag{5.6}$$

Due to symmetry of this problem, $\Pr(Z_i < 0 \mid b_i = +1) = \Pr(Z_i \geq 0 \mid b_i =$ -1). Thus, the BER for coherent BPSK is

$$P_b = \Pr(Z_i \geq 0 \mid b_i = \text{-1}) = \mathrm{Q}\left[\frac{\sqrt{2P}T_b}{\sqrt{\mathrm{var}(D) + \mathrm{var}(N)}}\right] = \mathbf{Q}\left[\sqrt{\frac{2(E_b/N_0)}{1 + (E_b/N_0)2\sigma^2}}\right] , \tag{5.7}$$

where $\mathbf{Q}(x)$ is the complementary error function which is defined as

$$\mathbf{Q}(x) \triangleq \frac{1}{\sqrt{2\pi}}\int_x^\infty \exp(-\frac{y^2}{2})\,dy \quad , \tag{5.8}$$

and $E_b = PT_b$ is the bit energy.

Substituting $2\sigma^2 = 1/K$, P_b can be written as

$$P_b = \mathbf{Q}\left[\sqrt{\frac{2K(E_b/N_0)}{K + (E_b/N_0)}}\right] \tag{5.9}$$

Therefore, P_b is a function of E_b/N_0 and K. If $K = \infty$ (i.e., $\sigma = 0$, no scattered component), then $P_b = \mathrm{Q}\left(\sqrt{2E_b/N_0}\right)$ which is exactly the BER for coherent BPSK in an AWGN channel.

F S K

The signal set for BFSK modulation is as follows:

$$s_i(t) = \Re e\{ \sqrt{2P} \exp[j(w_i t + \theta)] \}, \quad 0 \le t \le T_b, \quad i = 1,2 \ . \tag{5.10}$$

For coherent BFSK signals, $s_1(t)$ and $s_2(t)$ should be orthogonal. Therefore, the minimum carrier spacing between f_1 and f_2 is $|f_1 - f_2| = 1/2T_b$ [9].

The receiver model for coherent BFSK is shown in Figure 5.2. There are two arms in the receiver, each matched to one of the possible signals. The decision circuit chooses the largest of the two decision variables, Z_1 and Z_2, as the actually transmitted signal. Utilizing the orthogonality of the signal set, it is easy to show that $Z_2 = N_2$ when $s_1(t)$ is sent, where N_2 is a Gaussian r.v. with zero mean and variance N_0T_b. Similarly, Z_1 should be:

$$Z_1 = \sqrt{2P}T_b + D_1 + N_1 \ , \tag{5.11}$$

where the D_1 and N_1 are both Gaussian r.v. with zero mean and variances $2PT_b^2\sigma^2$ and N_0T_b, respectively. Based upon the decision strategy just described, the BER can be derived as

$$P_b = \Pr[\sqrt{2P}T_b + D_1 + N_1 - N_2 < 0 \mid s_1] \ . \tag{5.12}$$

Because summation of independent Gaussian r.v.'s is still a Gaussian r.v., $D_1 + N_1 - N_2$ is a Gaussian r.v. with zero mean and variance $(2PT_b^2\sigma^2 + 2N_0T_b)$. Thus, the BER is

$$P_b = Q\left[\frac{\sqrt{2P}T_b}{\sqrt{2PT_b^2\sigma^2 + 2N_0T_b}}\right] = Q\left[\sqrt{\frac{2K(E_b/N_0)}{2K + (E_b/N_0)}}\right] \ . \tag{5.13}$$

Now, for $K = \infty$, the BER is equal to $Q(\sqrt{E_b/N_0})$ which is exactly the result of coherent BFSK in an AWGN channel.

A S K

For binary ASK modulation, the signal set is

$$\begin{cases} s_1(t) = \Re e\{ \sqrt{4P} \exp[j(\omega_c t + \theta)] & 0 \le t \le T_b \\ s_2(t) = 0 & 0 \le t \le T_b \end{cases} \ . \tag{5.14}$$

Note that we let the transmitted power of $s_1(t)$ be equal to $2P$ in order for the average transmitted power to be the same as in BPSK and BFSK cases. Only under this condition will the performance comparison between them be reasonable.

The receiver model for coherent ASK is shown in Figure 5.3. The decision variable Z when $s_1(t)$ is sent via the Rician channel is similar to equation (5.5) which is

$$Z = \sqrt{4P}T_b + D + N \quad , \tag{5.15}$$

and Z = N when $s_2(t)$ is sent. Here, we have to note that the noise power σ_1^2 when $s_1(t)$ is sent is $(N_0T_b + 4PT_b^2\sigma^2)$ which is larger than the noise power $\sigma_2^2 = N_0T_b$ when $s_2(t)$ is sent. Let us denote the pdf of Z given $s_1(t)$ is transmitted as $p(z|s_1)$, and similarly for $p(z|s_2)$. Then, $p(z|s_1)$ is a Gaussian pdf with mean $\sqrt{4P}T_b$ and variance σ_1^2, and $p(z|s_2)$ is also a Gaussian pdf with zero mean and variance σ_2^2, respectively.

Now, we have to determine the decision threshold α. For a maximum likelihood receiver, the optimal threshold α should satisfy

$$p(\alpha|s_1) = p(\alpha|s_2) \ . \tag{5.16}$$

To make the result dimensionless, let us define $\alpha' \triangleq \alpha/\sigma_2$. Then α' can be proved to be equal to (see Appendix 5.A)

$$\alpha' = \frac{\sqrt{a + (a/K)[2a + (1 + 2a/K)\log(1 + 2a/K)/2]} - \sqrt{a}}{(a/K)} \quad , \quad \sigma \neq 0 \ , \tag{5.17}$$

where a = E_b/N_0. If $\sigma = 0$, then $\alpha = \sqrt{P/2T_b}$ which is just one half of the mean of Z given s_1.

Once we know the value of α', the BER for coherent ASK is

$$\begin{aligned} P_b &= \frac{1}{2}\left[\int_{\alpha}^{\infty} p(z|s_2)\,dz + \int_{-\infty}^{\alpha} p(z|s_1)\,dz\right] \\ &= \frac{1}{2}\left[Q\left(\frac{\alpha}{\sigma_2}\right) + Q\left(\frac{\sqrt{4P}T_b - \alpha}{\sigma_1}\right)\right] \\ &= \frac{1}{2}\left\{Q(\alpha') + Q\left[\sqrt{\frac{K}{K + 2E_b/N_0}}\left(\sqrt{\frac{4E_b}{N_0}} - \alpha'\right)\right]\right\} \end{aligned} \tag{5.18}$$

Because the optimal threshold α is a function of K and E_b/N_0, it will be also a time-varying function depending on the traffic condition. Therefore, it is not easy for

the receiver to compute the optimal threshold in real time. Again, if $K = \infty$, then the BER for coherent ASK using the the optimal threshold is $\mathbf{Q}(\sqrt{E_b/N_0})$ which is exactly the BER of ASK in an AWGN channel.

5.2.4 Noncoherent Demodulation

In noncoherent detection of the received signals, it is assumed that only the carrier frequency is known. It means that we can only use the envelope of the received signals to determine which signal is transmitted. In the following, the BER performance for differential BPSK (DPSK), BFSK, and ASK will be derived.

DPSK

The signal set in DPSK takes the form

$$s(t) = \Re e\{ b_i\sqrt{2P}\exp[j(\omega_c t + \theta)] \} , \tag{5.19}$$

where b_i is the differentialy encoded version of the data sequence whose values are equally likely fl. The channel model is still the Rician fading channel of Section 5.2.2. The random gain β and phase ξ will be discussed for two cases: (1) β and ξ are constant over the bit interval but bit-to-bit independent (very fast fading – VFF); (2) β and ξ are invariant at least for two successive bits (slower fading – SF). In the first case, the scattered component can not be used to improve the BER performance. On the contrary, the scattered component in the second case can be utilized to reduce the decision error.

Very Fast Fading Under very fast fading (VFF) conditions, the gain and phase of the scattered component are modeled as bit-to-bit independent. The demodulator for DPSK is shown in Figure 5.4, where the bold type arrow represents a complex value. At the ith bit interval, the complex variable V_i is

$$\begin{aligned} V_i &= \int_{iT_b}^{(i+1)T_b} 2r(t)\exp(-j\omega_c t)\,dt \\ &= \sqrt{2P}T_b b_i \exp(j\theta) + \sqrt{2P}T_b\beta_i b_i \exp[j(\theta + \xi_i)] + N_i \\ &= S_i + D_i + N_i , \end{aligned} \tag{5.20}$$

where S_i is the desired term and both D_i and N_i are zero mean complex Gaussian r.v.'s. The variance of the real and imaginary parts of D_i and N_i are $2PT_b^2\sigma^2$ and N_0T_b, respectively. D_i and N_i now are treated as interference.

The decision variable Z_i can be written as

$$Z_i = \Re e[\, V_iV_{i-1}^* \,] = \frac{1}{2}[V_iV_{i-1}^* + V_i^*V_{i-1} \,] \quad , \tag{5.21}$$

where * denotes the complex-conjugate operation.

The result derived in [9] can be applied to compute the BER which is

$$P_b = \frac{1}{2}\exp\left[-\frac{2PT_b^2}{2(N_0T_b + 2P\sigma^2T_b^2)}\right] = \frac{1}{2}\exp\left[-\frac{K(E_b/N_0)}{K + E_b/N_0}\right] \quad . \tag{5.22}$$

We can check this result letting $K = \infty$. Then $P_b = \frac{1}{2}\exp(-E_b/N_0)$, which is exactly the BER of DPSK in an AWGN channel.

Slow Fading In the slower fading (SF) case, the gain and phase of the LOS component as well as the scattered component are invariant for at least two successive bits. The complex variable V_i now is

$$V_i = S_i + N_i \,, \tag{5.23}$$

where the desired term now is

$$S_i = \sqrt{2P}T_bb_i\{\exp(j\theta) + \beta\exp[j(\theta + \xi)]\} \quad . \tag{5.24}$$

Define the random SNR, R, as

$$R = \frac{|S_i|^2}{2N_0T_b} = \frac{E_b}{N_0}[1 + \beta^2 + 2\text{pcos } \xi] = \frac{E_b}{N_0}\chi \,, \tag{5.25}$$

where $\chi \triangleq [1 + \beta^2 + 2\beta\cos\xi]$.

Then, the conditional BER given χ, $P_b(\chi)$, is [10, equation (4.4.13)]

$$P_b(\chi) = \frac{1}{2}\exp\left(-\frac{E_b}{N_0}\chi\right) \quad . \tag{5.26}$$

According to [10, Chapter 1], χ has a noncentral chi-square pdf with 2 degree freedom, given by [10, equation (1.1.115)]),

$$p(\chi) = \frac{1}{\rho^2} \exp\left(-\frac{\chi+1}{2\rho^2}\right) I_0\left(\frac{\sqrt{\chi}}{\rho^2}\right) U(\chi) \quad , \tag{5.27}$$

where $\rho^2 = N_0 T_b$ and $U(x)$ is the unit-step function.

Therefore, the BER can be derived by integrating $P_b(\chi)$ with respect to $p(\chi)$, which is given by

$$P_b = \int_0^\infty P_b(\chi) p(\chi)\, d\chi = \frac{K}{2(K + E_b/N_0)} \exp\left[-\frac{K(E_b/N_0)}{K + E_b/N_0}\right] \quad . \tag{5.28}$$

Let us compare the results for the very fast and slower fading cases. In the former, the scattered component can not be utilized (under the assumption that we can not track both the phases θ and ξ simultaneously) to improve the performance. In the latter, on the contrary, the fading component can be employed to increase the total signal power. Comparing equations (5.22) and (5.28), we can see that

$$\frac{P_b(\text{DPSK/SF})}{P_b(\text{DPSK/VFF})} = 1 + \frac{1}{K}\frac{E_b}{N_0} . \tag{5.29}$$

This implies that the performance improvement in the SF condition over VFF depends on both the SNR and the K value. Of course, if $K = \infty$, then the ratio in equation (5.29) is 1 because no scattered component exists in either case.

F S K

The receiver model for noncoherent BFSK is shown in Figure 5.5. Again, there are two arms in the receiver, each arm having the same structure as the noncoherent ASK receiver shown in Figure 5.6. The decision logic is the same as in coherent BFSK. The minimum carrier spacing for noncoherent BFSK is $|f_1 - f_2| = 1/T_b$ which is two times the required for the coherent case [9].

When $s_1(t)$ is sent, the pdf $p(z_2|s_1)$ is a Rayleigh pdf which can be derived by the same procedure as in noncoherent ASK. Thus, the pdf is

$$p(z_2|s_1) = \frac{z_2}{\sigma_2^2} \exp\left(-\frac{z_2^2}{2\sigma_2^2}\right) U(z_2) \quad , \tag{5.30}$$

where $\sigma_2^2 = N_0 T_b$.

Similarly, the pdf $p(z_1|s_1)$ is a Rician pdf

$$p(z_1|s_1) = \frac{z_1}{\sigma_1^2} \exp\left(-\frac{z_1^2 + m^2}{2\sigma_1^2}\right) I_0\left(\frac{m z_1}{\sigma_1^2}\right) U(z_1) \quad , \tag{5.31}$$

where m $= \sqrt{2P}T_b, \sigma_1^2 = N_0 T_b + 2PT_b^2\sigma^2$, and $I_0(x)$ is the modified Bessel function of order zero.

According to the decision logic, the BER can be derived as follows:

$$\begin{aligned} P_b &= \Pr(Z_2 > Z_1 \mid s_1) \\ &= \int_0^\infty p(z_1|s_1)\left[\int_{z_1}^\infty p(z_2|s_1)\, dz_2\right] dz_1 \\ &= \int_0^\infty \frac{z_1}{\sigma_1^2} \exp\left(-\frac{z_1^2 + m^2}{2\sigma_1^2}\right) I_0\left(\frac{z_1 m}{\sigma_1^2}\right) \exp\left(-\frac{z_1^2}{2\sigma_2^2}\right) dz_1 \\ &= b^2 \int_0^\infty y \exp\left(-\frac{y^2 + \tilde{m}^2}{2}\right) I_0(by\tilde{m})\, dy \quad , \end{aligned} \tag{5.32}$$

where $b = \sqrt{\sigma_2^2/(\sigma_2^2 + \sigma_1^2)}$ and $\tilde{m} = m/\sigma_1$.

Now, let $m_0 = b\tilde{m}$. Then, P_b can be expressed by

$$\begin{aligned} P_b &= b^2 \left\{ \int_0^\infty y \exp\left(-\frac{y^2 + m_0^2}{2}\right) I_0(y m_0)\, dy \right\} \exp\left(\frac{m_0^2 - \tilde{m}^2}{2}\right) \\ &= b^2 \exp\left(\frac{m_0^2 - \tilde{m}^2}{2}\right) \\ &= \frac{K}{2K + (E_b/N_0)} \exp\left[-\frac{K(E_b/N_0)}{2K + (E_b/N_0)}\right] \quad . \end{aligned} \tag{5.33}$$

If $K = \infty$, then $P_b = \frac{1}{2}\exp\left[-\frac{1}{2}E_b/N_0\right]$, which is exactly the BER of noncoherent BFSK in an AWGN channel.

A S K

The receiver model for noncoherent ASK is shown in Figure 5.6. When $s_2(t)$ is sent, the received signal r(t) will be equal to $n(t)$ (i.e., no signal is transmitted). Therefore, X = N_c and Y = N_s, where N_c and N_s are all Gaussian r.v.'s with zero mean and

variance N_0T_b. In this situation, the pdf $p(z|s_2)$ is a Rayleigh pdf which is given by

$$p(z|s_2) = \frac{z}{\sigma_2^2}\exp\left(-\frac{z^2}{2\sigma}\right) U(z) \ , \qquad \textbf{(5.34)}$$

where $\sigma_2^2 = N_0 T_b$.

Now, when s_1 (t) is sent, the received signal becomes

$$r(t) = \Re e\{\sqrt{4P}\{\exp(j\theta) + \beta\exp[j(\theta + \xi)]\}\exp(j\omega_c t)\} + n(t) \ , \qquad \textbf{(5.35)}$$

and, in this case, the variable X is

$$x = \int_0^{T_b} 2r(t)\cos(\omega_c t)\,dt = \sqrt{4P}T_b[\cos\theta + \beta\cos(\theta + \xi)] + N_c = \sqrt{4P}T_b\cos\theta + D_c + N_c \ . \qquad \textbf{(5.36)}$$

X now is a Gaussian r.v. with mean equal to $\sqrt{4P}T_b\cos\theta$ and variance $\sigma_1^2 = (4PT_b^2\sigma^2 + N_0T_b)$. The same procedure can be applied to derive Y which is also a Gaussian r.v. with mean $\sqrt{4P}T_b \sin\theta$ and variance σ_1^2.

In this case, the pdf $p(z|s_1)$ is a Rician pdf which is given by

$$p(z|s_1) = \frac{z}{\sigma_1^2}\exp\left(-\frac{z^2+m^2}{2\sigma_1^2}\right) I_0\left(\frac{zm}{\sigma_1^2}\right) U(z) \ , \qquad \textbf{(5.37)}$$

where $m = \sqrt{4P}T_b$.

As in coherent ASK case, the optimal threshold α should satisfy the equation $p(\alpha|s_1) = p(\alpha|s_2)$, i.e.,

$$\frac{\alpha}{\sigma_2^2}\exp\left(-\frac{\alpha^2}{2\sigma_2^2}\right) = \frac{\alpha}{\sigma_1^2}\exp\left(-\frac{\alpha^2+m^2}{2\sigma_1^2}\right) I_0\left(\frac{\alpha m}{\sigma_1^2}\right) \ . \qquad \textbf{(5.38)}$$

The above equation can be replaced by

$$\left(\frac{\sigma_1}{\sigma_2}\right)^2\exp\left\{\frac{1}{2}\left(\frac{m}{\sigma_1}\right)^2 + \frac{1}{2}\left[\left(\frac{\alpha}{\sigma_1}\right)^2 - \left(\frac{\alpha}{\sigma_2}\right)^2\right]\right\} = I_0\left[\left(\frac{\alpha}{\sigma_1}\right)\left(\frac{m}{\sigma_1}\right)\right] \ . \qquad (5.39)$$

Defining the normalized optimal threshold $\tilde{\alpha} = \alpha/\sigma_1$, and replacing σ_1 and σ_2 by their actual values, we can find that $(\frac{\sigma_1}{\sigma_2})^2 = 1 + 2a/K, (\frac{\alpha}{\sigma_1})^2 - (\frac{\alpha}{\sigma_2})^2 = -(2a/K)(\tilde{\alpha})^2$, and $(\frac{m}{\sigma_1})^2 = 4Ka/(K + 2a)$, where $a = E_b/N_0$. Therefore, we have to solve the following nonlinear equation to derive the normalized optimal threshold $\tilde{\alpha}$:

$$\left(1 + \frac{2a}{K}\right)\exp\left(\frac{2Ka}{K+2a}\right) = \exp\left[\frac{a(\tilde{\alpha})^2}{K}\right] I_0\left(\sqrt{\frac{4Ka}{K+2a}}\tilde{\alpha}\right) \ . \qquad \textbf{(5.40)}$$

Because $I_0(x) \geq 1$, $\forall x \geq 0$ and is a monotonically increasing function, we can first set $I_0\left(\sqrt{2Ka/(K+2a)}\tilde{\alpha}\right) = 1$, and solve for the value of $\tilde{\alpha}$ in equation (5.40). Let the solution be $\tilde{\alpha}_{up}$, which is given by

$$\tilde{\alpha}_{up} = \sqrt{(K/a)[\log(1 + 2a/K) + 2Ka/(K + 2a)]} \quad . \tag{5.41}$$

The value of $\tilde{\alpha}$ will be in $(0, \tilde{\alpha}_{up})$. Thus, we can utilize the binary searching method to find the approximation of $\tilde{\alpha}$ with some prespecified error tolerance. When $a \gg 1$, $\tilde{\alpha}$ will be very close to 0, then $I_0\left(\sqrt{4Ka/(K+2a)}\tilde{\alpha}\right) \approx I_0(\sqrt{2K}\tilde{\alpha}) \approx 1$. Therefore, we can use $\tilde{\alpha}_{up}$ to approximate $\tilde{\alpha}$. Another way to solve the above nonlinear equation is to use the function 'fzero' provided by MATLAB with $\tilde{\alpha}_{up}$ as the initial point.

Based on the optimal threshold α, the BER can be computed by

$$P_b = \frac{1}{2}\int_{\alpha}^{\infty} p(z|s_2)\, dz + \frac{1}{2}\int_{0}^{\alpha} p(z|s_1)\, dz \quad . \tag{5.42}$$

The first integral is equal to $\exp[-\alpha^2/(2\sigma_2^2)]$. The second term is

$$\begin{aligned}\int_0^{\alpha} p(z|s_1)\, dz &= 1 - \int_{\alpha}^{\infty} \frac{z}{\sigma_1^2}\exp\left(-\frac{z^2+m^2}{2\sigma_1^2}\right) I_0\left(\frac{mz}{\sigma_1^2}\right) dz \\ &= 1 - \int_{\frac{\alpha}{\sigma_1}}^{\infty} y \exp\left[-\frac{y^2 + (m')^2}{2}\right] I_0(m'y)\, dy \\ &= 1 - \mathbf{Q}(m', \tilde{\alpha}) \quad , \end{aligned} \tag{5.43}$$

where $m' = m/\sigma_1$ and $\mathbf{Q}(a,b)$ is the Marcum-Q function which is defined as

$$\mathbf{Q}(a,b) \triangleq \int_b^{\infty} y \exp\left[-\frac{1}{2}(y^2 + a^2)\right] I_0(ay)\, dy \quad . \tag{5.44}$$

Therefore, the BER for noncoherent ASK can be written as

$$\begin{aligned} P_b &= \frac{1}{2}\exp\left(-\frac{\alpha^2}{2\sigma_2^2}\right) + \frac{1}{2}[1 - \mathbf{Q}(m', \tilde{\alpha})] \\ &= \frac{1}{2}\exp\left[-\left(\frac{K + 2E_b/N_0}{2K}\right)(\tilde{\alpha})^2\right] + \frac{1}{2}\left\{1 - \mathbf{Q}\left[\sqrt{\frac{4K(E_b/N_0)}{K + 2(E_b/N_0)}}, \tilde{\alpha}\right]\right\} . \end{aligned} \tag{5.45}$$

5.2.5 Packet Error Rate for TDMA Systems

In this section, the PER for TDMA systems in a Rician fading channel with very slow fading (VSF) will be derived. For VSF, we assume that the scattered component

remains fixed for the whole packet duration and is packet-to-packet independent. Suppose a packet of L bits is transmitted over a memoryless binary communication channel with BER equal o P_b. If the packet includes some block error control capacity, being able to correct t or fewer errors, then, assuming bit-to-bit independence, the PER becomes

$$P_E = \sum_{l=t+1}^{L} \binom{L}{l} P_b^l (1-P_b)^{L-l} \triangleq g(P_b; L, t) \quad . \tag{5.46}$$

If the scattered component is given, and since the AWGN is bit-to-bit independent, we can use the above equation to compute the conditional PER. Then, by unconditioning with respect to the scattered component, the PER can be easily found. In the following, we will derive the PER for some of modulation schemes we have been analyzing

LOS-Coherent PSK

From equation (5.5), the decision variable Z_i is

$$Z_i = \sqrt{2P}T_b + \sqrt{2P}T_b\beta\cos\xi + N \quad , \tag{5.47}$$

where we assume, without loss of generality given the symmetry of the problem, $b_i = 1$. Normalizing Z_i by $\sqrt{2P}T_b$, the decision variable will become

$$Z_i' = \frac{Z_i}{\sqrt{2P}T_b} = 1 + Y + N \quad , \tag{5.48}$$

where Y = $\beta\cos\xi$ which is a zero mean Gaussian r.v. with variance $\sigma^2 = 1/(2K)$ and n is also zero mean Gaussian r.v. with variance $1/(2a)$, and a = E_b/N_0.

Given Y, the conditional BER, $P_b(Y)$, is

$$P_b(Y) = \mathrm{Q}\left[\frac{1+Y}{\mathrm{var}(N)}\right] = \mathrm{Q}\left[\sqrt{2a}(1+Y)\right] \quad . \tag{5.49}$$

Therefore, the conditional PER for LOS-coherent BPSK given Y is

$$P_E(Y) = \sum_{l=t+1}^{L} \binom{L}{l} P_b(Y)^l [1 - P_b(Y)]^{L-l} \quad . \tag{5.50}$$

Finally, averaging over Y, we can evaluate the PER as

$$P_E = \int_{-\infty}^{\infty} P_E(y) f_Y(y)\, dy \quad , \tag{5.51}$$

where $f_Y(y)$ is given by

$$f_Y(y) = \frac{1}{\sqrt{2\pi}\sigma} \exp\left(-\frac{y^2}{2\sigma^2}\right) = \sqrt{\frac{K}{\pi}} \exp(-Ky^2) \ . \qquad (5.52)$$

DPSK and Noncoherent FSK

By the same method, we can find the PER for both the DPSK and noncoherent BFSK. For DPSK with very slow fading, the conditional BER, $P_b(\gamma)$, is given by

$$P_b(\gamma) = \frac{1}{2} \exp[-a\gamma^2] \ , \qquad (5.53)$$

where γ is a Rician distributed r.v. with pdf as

$$f(\gamma) = 2K\gamma \exp[-K(\gamma^2 + 1)] I_0(2K\gamma)\, U(\gamma) \ . \qquad (5.54)$$

Similarly, the conditional BER for noncoherent BFSK is given by

$$P_b(\gamma) = \frac{1}{2} \exp\left(-\frac{a}{2}\gamma^2\right) \ . \qquad (5.55)$$

By applying equation (5.50), we can find the conditional PER for DPSK and noncoherent BFSK. By unconditioning, the PER is given by

$$P_E = \int_0^\infty P_E(\gamma) f(\gamma)\ d\gamma \ . \qquad (5.56)$$

5.2.6 TDMA Numerical Results

Let us summarize the BER derived in previous sections in Table 5.1.

where a = E_b/N_0, $\tilde{\alpha}$ is the normalized optimal threshold for noncoherent ASK, and

$$\alpha' = \frac{\sqrt{a + (a/K)[2a + (1 + 2a/K)\log(1 + 2a/K)/2]} - \sqrt{a}}{a/K}$$

In Figure 5.7, the BER for LOS-coherent and noncoherent BPSK, BFSK, and ASK are shown for $K = 10$ dB. For LOS-coherent demodulation, when a = E_b/N_0 is small,

the BER of ASK and BFSK are almost the same and both are about 3 dB worse than BPSK. This is the same result as for an AWGN channel because thermal noise now is the major interference. As a increases, the interference from the scattered component also increases, gradually becoming dominant. Under this situation, the performance of coherent BPSK and BFSK will converge to $Q\left(\sqrt{2K}\right) = Q\left[\sqrt{2(1/2\sigma^2)}\right]$. This can be thought as the BER of BPSK in an AWGN channel with $a = 1/2\sigma^2$. We also notice that as a >> 1, the BER of coherent ASK converges to $\frac{1}{2}Q\left(\sqrt{2K}\right)$ which is just one half of the asymptotic ($a \to \infty$) BER of BPSK and BFSK. This can be interpreted as follows: for ASK, the threshold α is proportional to a, but the noise power σ_2^2 is fixed. Thus, as a becomes larger, the conditional error probability given $s_2(t)$ is sent becomes smaller and will approach zero. On the other hand, the conditional error probability given $s_1(t)$ is sent is nearly the same as that of BPSK and BFSK. Therefore, in average, the asymptotic BER of ASK is only half that of BPSK and BFSK, i.e., ASK is asymptotically better.

For noncoherent detection, we find an interesting phenomenon for $a \gg 1$, the BER for DPSK/SF, BFSK, and ASK are inversely proportional to a. This results from the fact that in noncoherent detection, part of the scattered component power can be used to improve performance. The asymptotic BER is shown in Table 5.2.

For DPSK, if the bit-to-bit correlation relationship is between 0 (VFF) and 1 (SF), then its BER performance should also be in between, i.e., the BER for DPSK/VFF and DPSK/SF will behave as upper and lower bounds, respectively.

The BER for $K=12$ dB is shown in Figure 5.8. The asymptotic BER for each case is about 2 orders of magnitude better than for the $K=10$ dB case.

Figures 5.9 and 5.10 show the PER for LOS-coherent BPSK, DPSK, and noncoherent BFSK for $K=10$ and 13 dB, respectively. No error correction function is used, i.e., $t = 0$. In this case, $g(x; L, t) = 1-(1-x)^L$ which is a concave function for $0 \le x \le 1$. Using Jensen's inequality [13]

$$g(E(P_b); L, t) \ge E[g(P_b; L, t)] \qquad (5.57)$$

where the latter term is just the average PER that we have derived in Section 5.2.5.

The former term in the above equation can be viewed as an upper bound of the

average PER for slow fading. It can be treated as the PER accounting for the fast fading cases since the BER is bit-to-bit independent, i.e., the scattered component is bit-to-bit independent. The reason why the PER for fast fading case without error correction is worse than slow fading can be interpreted as follows. Without error correction, the whole packet is useless even only one bit of the packet is in error. For fast fading, the bit error will happen more uniformly than slow fading. Therefore, its PER is worse. In these figures we see that DPSK and noncoherent BFSK for slow fading are still better than LOS-coherent BPSK for large E_b/N_0. In addition, the Rician factor K has great impact on the PER performance.

5.2.7 TDMA Conclusions

In this section, we have derived the BER of a TDMA system using binary PSK, FSK, and ASK modulation with LOS-coherent and noncoherent demodulation over the Rician fading channel typical of short-range IVHS communications. For this kind of short-range communications, the receiver SNR can be very large. LOS-coherent BPSK can provide the best BER performance for small E_b/N_0 but will be limited by the K value as E_b/N_0 becomes large. For slow fading, DPSK and noncoherent BFSK seem to be the best candidates for this application. In addition, the value of K has great impact on the BER performance.

	LOS-coherent	Noncoherent	
BPSK	$Q\left[\sqrt{2Ka/(K+a)}\right]$	DPSK/VFF	$\frac{1}{2}\exp[-Ka/(K+a)]$
		DPSK/SF	$\frac{K}{2(K+a)}\exp[-Ka/(K+a)]$
BFSK	$Q\left[\sqrt{2Ka/(2K+a)}\right]$	$\frac{K}{2K+a}\exp[-Ka/(2K+a)]$	
ASK	$\frac{1}{2}\left\{Q(\alpha') + Q\left[\sqrt{\frac{K}{K+2a}}(\sqrt{4a}-\alpha')\right]\right\}$	$\frac{1}{2}\exp[-(\frac{K+2a}{2K})(\tilde{\alpha})^2] + \frac{1}{2}\left[1 - Q\left(\sqrt{\frac{4Ka}{K+2a}}, \tilde{\alpha}\right)\right]$	

Table 5.1: BER for LOS-Coherent and Noncoherent Demodulation of BPSK, FSK, and ASK with the same Average Transmission Power

	LOS-Coherent	Noncoherent	
BPSK	$Q(\sqrt{2K})$	DPSK/VFF	$\frac{1}{2}\exp(-K)$
		DPSK/SF	$\frac{K}{2}\exp(-K)$
BFSK	$Q(\sqrt{2K})$	$\frac{K}{2}\exp(-K)$	
ASK	$\frac{1}{2}Q(\sqrt{2K})$	$\frac{1}{2}\exp[-\frac{a}{K}(\tilde{\alpha})^2] + \frac{1}{2}[1 - Q(\sqrt{2K}, \tilde{\alpha})]$	

Table 5.2: Asymptotic BER for LOS-Coherent and Noncoherent Demodulation of BPSK, BFSK, and ASK with the same Average Transmission Power

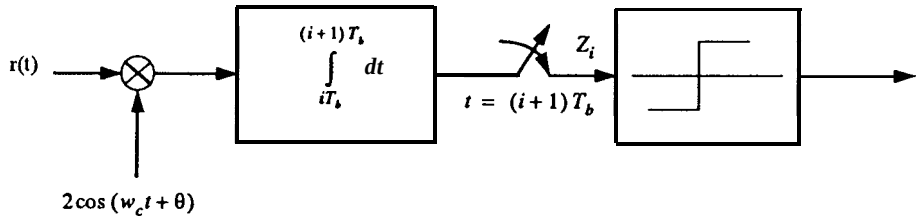

Figure 5.1: TDMA System Receiver Model for LOS-Coherent PSK

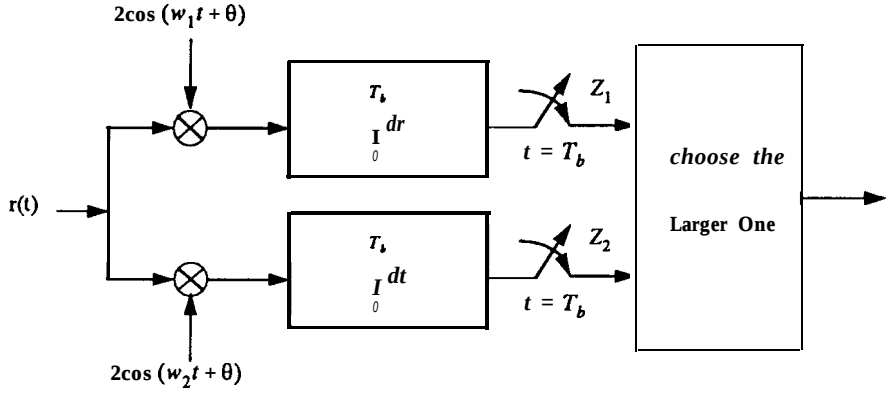

Figure 5.2: TDMA System Receiver Model for LOS-Coherent FSK

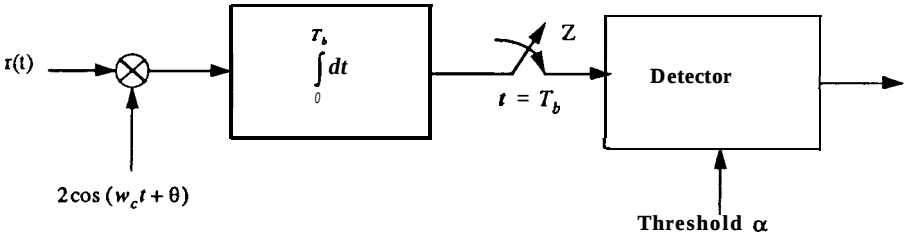

Figure 5.3: TDMA System Receiver Model for LOS-Coherent ASK

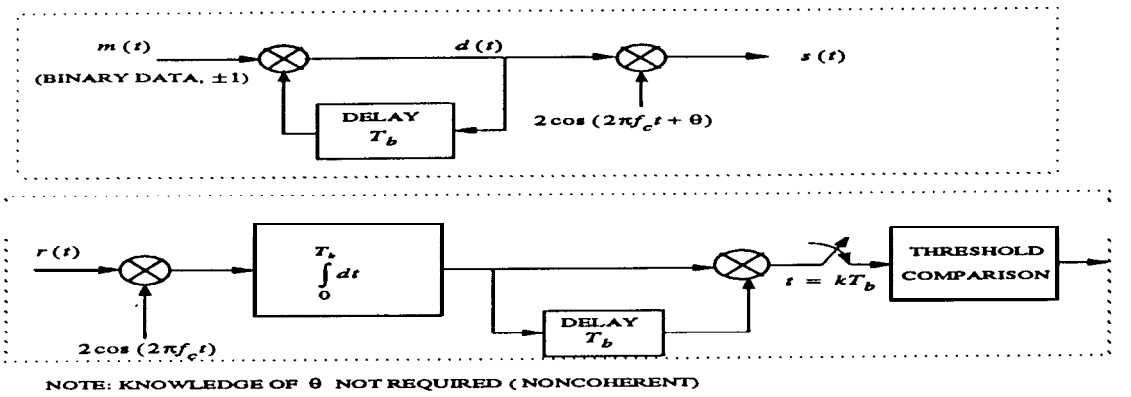

Figure 5.4: TDMA System Receiver Model for DPSK

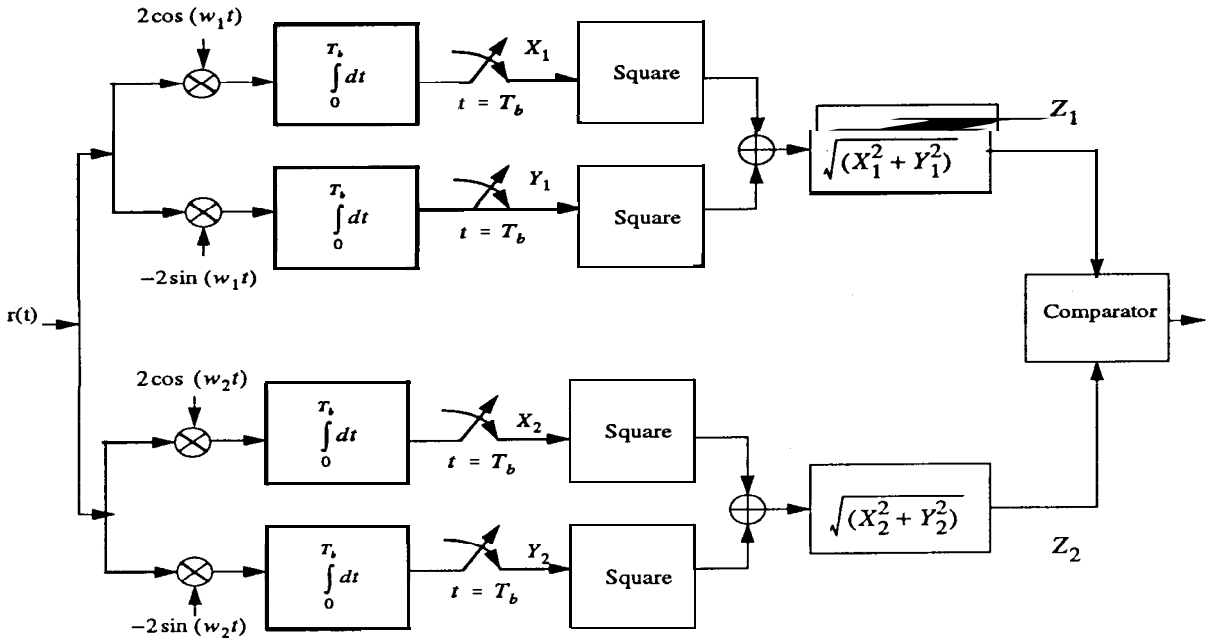

Figure 5.5: TDMA System Receiver Model for Noncoherent FSK

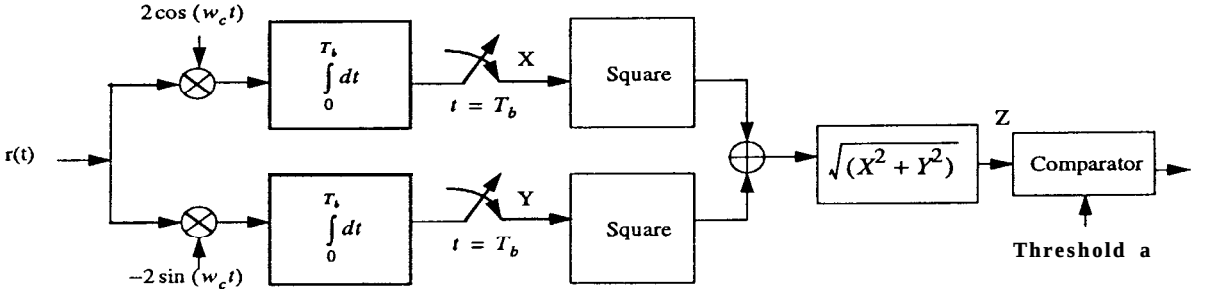

Figure 5.6: TDMA System Receiver Model for Noncoherent ASK

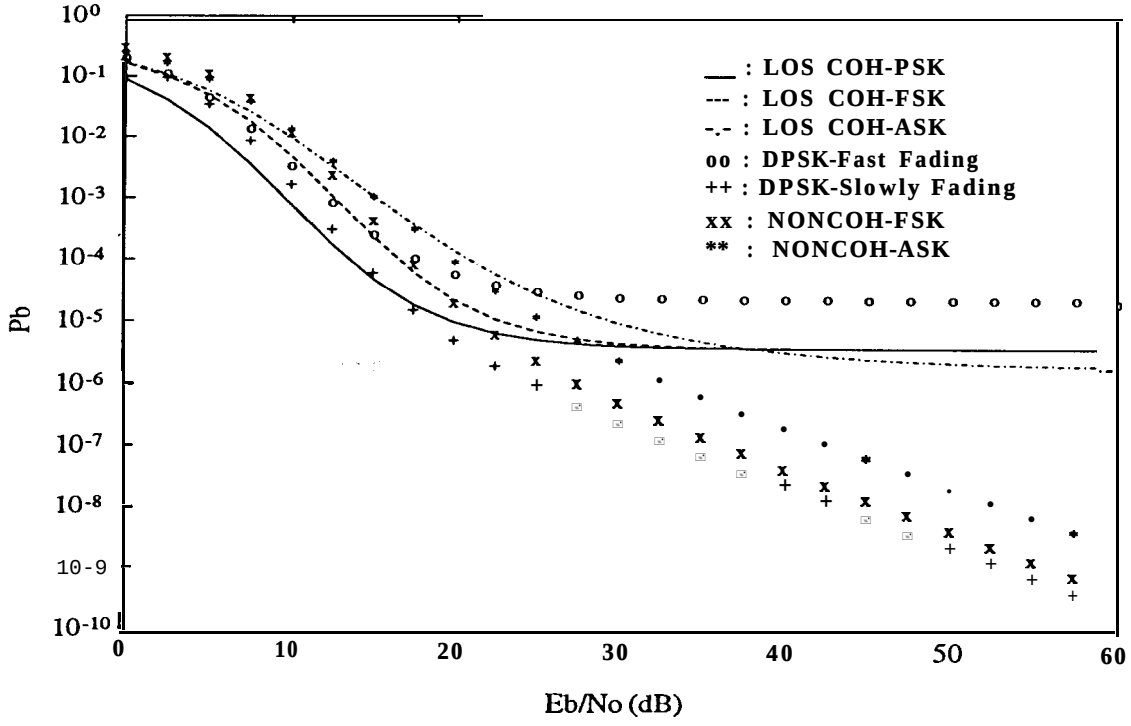

Figure 5.7: BER for TDMA Systems @K=10 dB

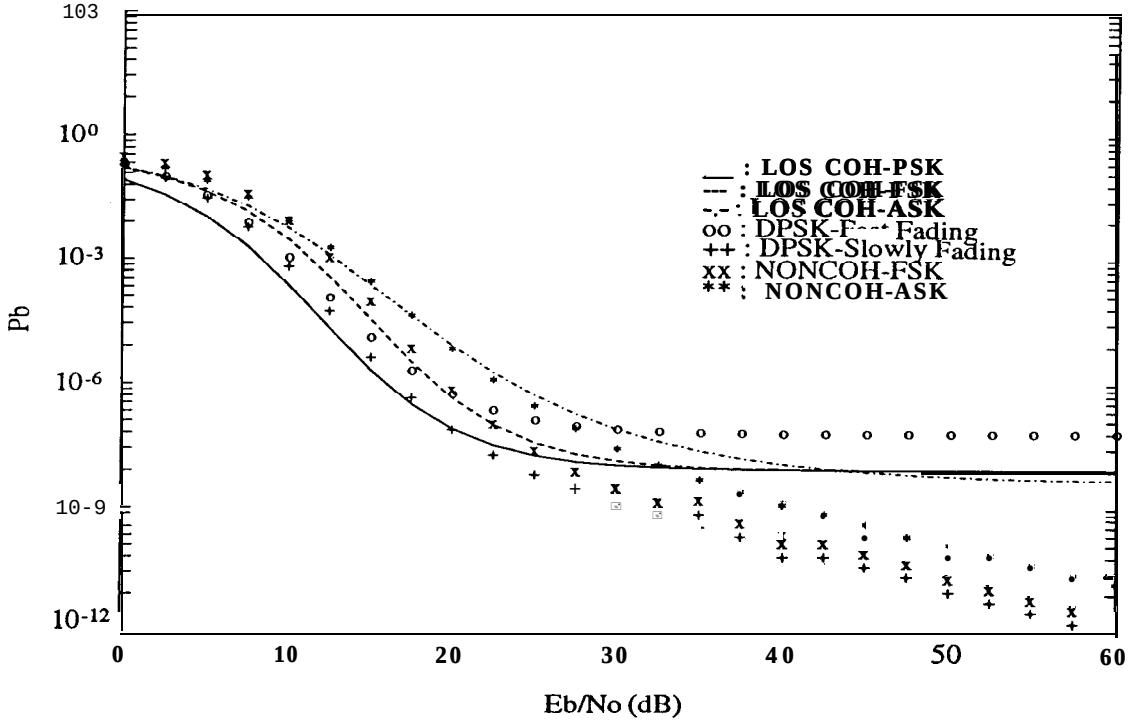

Figure 5.8: BER for TDMA Systems @K=12 dB

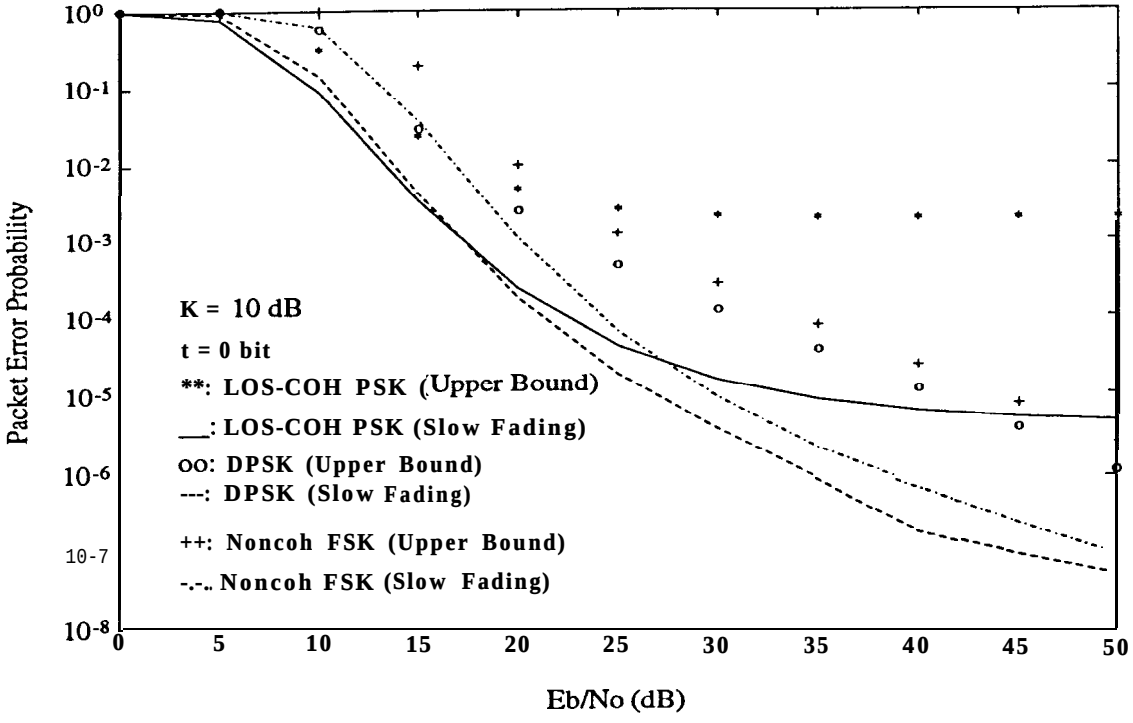

Figure 5.9: PER for TDMA Systems for LOS-Coherent PSK, DPSK, and Noncoherent FSK @K=10 dB@ t=O bit

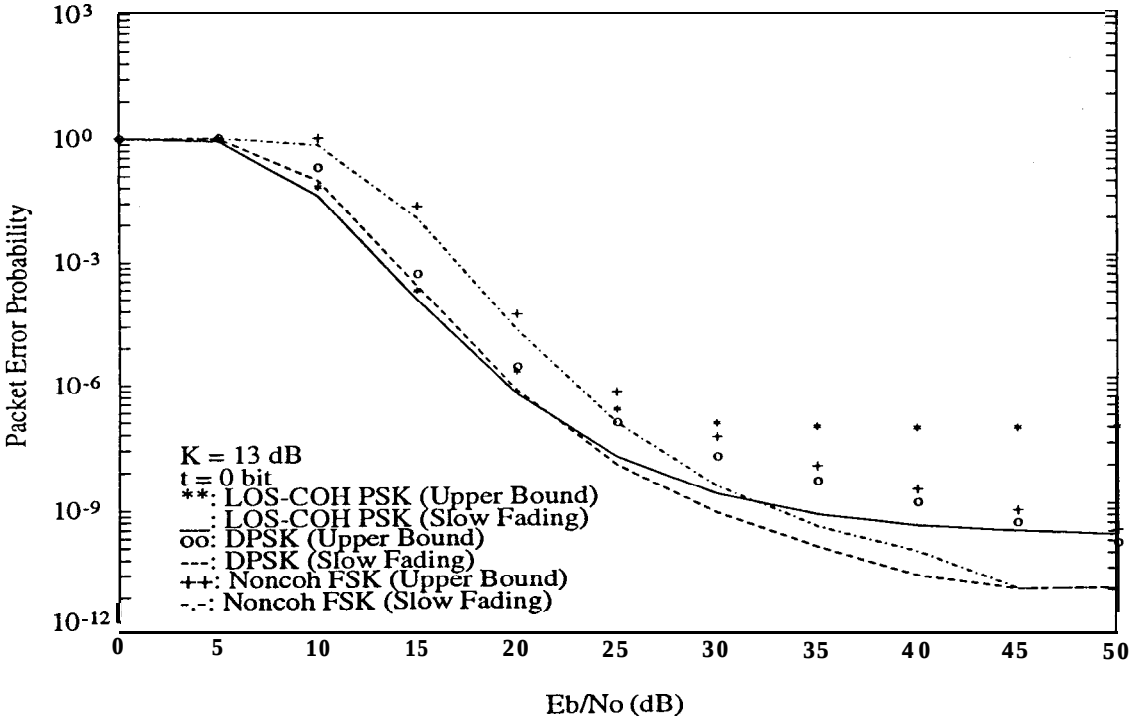

Figure 5.10: PER for TDMA Systems for LOS-Coherent PSK, DPSK, and Noncoherent FSK @K=13 dB@ t=O bit

5.3 Code Division Multiple-Access

5.3.1 Introduction

In this section, we will consider the BER and PER performance of an asynchronous direct-sequence code-division multiple-access (DS/CDMA) system in a Rician fading channel in an IVHS communications environment. Existing techiques to evaluate the BER and PER for a DS/CDMA system employing random signature sequences are (1) the standard Gaussian method (SGA) [1], (2) the bounding technique [3], (3) the improved Gaussian method (IGA) [5], and (4) the simple but accurate approximation of the IGA method (SIGA) in [7]. In the above referred works, an AWGN channel and perfect power control were assumed, and BPSK modulation scheme with rectangular chip pulse shape was employed. In this analysis, we will extend the analysis to Rician fading channel, applying the SIGA method to derive the BER and PER. Both BPSK and DPSK modulation schemes are considered. In addition, expressions for BER and PER are generalized for arbitary chip pulse shapes, not limited to rectangular. Therefore, we can investigate the effect of chip pulse shape on system performance.

The remainder of this section is organized as follows. The system model is introduced in Section 5.3.2. Derivation of the BER and PER for arbitary chip pulse shape for BPSK and DPSK are in Sections 5.3.3 and 5.3.4, respectively. In Section 5.3.5, we discuss some numerical results. Conclusions and future challenges are presented in Section 5.3.6.

5.3.2 System Model

The asynchronous binary DS/CDMA system in a Rician fading channel to be considered is shown in Figure 5.11 for N users. The model used in this report is an extension of that in [1] which has been used in most of the recent performance analysis for asynchronous binary DS/CDMA communications (e.g., [2],[3]). In the following sections we present the different components of this system, namely the transmitter, the channel, and the receiver.

Transmitter Model

The waveform $s_k(t)$ transmitted by the kth user of a CDMA system employing DS/BPSK or DS/DPSK **is** given by

$$s_k(t) = \sqrt{2P_k}b_k(t)a_k(t)\cos(2\pi f_c t + \theta_k) , \quad 1 \leq k \leq N , \tag{5.58}$$

where f_c is the common carrier frequency, P_k is the transmitted signal power of the kth user, θ_k is the phase of the kth modulator, and N is the total number of users. In the case of BPSK modulation, the kth data signal $b_k(t)$ is the kth user's information sequence, whereas for DPSK modulation, $b_k(t)$ is a differentialy encoded version of the kth user's information sequence. The data signal $b_k(t)$ can be expressed as

$$b_k(t) = \sum_{-\infty}^{\infty} b_j^{(k)} p(t - jT) , \tag{5.59}$$

where $b_j^{(k)}$ is the jth data bit in the binary information sequence for the user k and p(t) is a rectangular pulse whose value equals to unity in $0 \leq t \leq T$ and zero outside this interval. The information sequence $b_j^{(k)}$ is modeled as an i.i.d. sequence of with equally likely fl.

The spreading waveform $a_k(t)$ for user k can be expressed as

$$a_k(t) = \sum_{j=-\infty}^{\infty} a_j^{(k)} \psi(t - jT_c) , \tag{5.60}$$

where $a_j^{(k)} = \pm 1$ is the jth chip of the kth user's signature sequence and $\psi(t)$ accounts for the arbitary chip pulse shape. The only restriction is that $\psi(t) = 0$ except for $0 \leq t \leq T_c$, where T_c^{-1} is the chip rate of the DS/CDMA system. The chip pulse shape is normalized to have energy equal to T_c, that is $\int_0^{T_c} \psi^2(t)dt = T_c$. In this work, $\{a_j^{(k)}\}$ is assumed to be random; thus it is not periodic. Moreover, all $\{a_j^{(k)}\}$ sequences are independent of each other for all k and j. In other words, each transmitter sends a truly random binary sequence $\{a_j^{(k)}\}$ for the whole transmission period, and the intended receiver is assumed to have complete knowledge of it. We will assume that each bit is encoded with η chips, i.e., $T = \eta T_c$, and that perfect alignment exists between bits and chips. η is called the spreading ratio.

Channel Model

The lowpass equivalent complex impulse response for the kth user can be written as

$$h_k(t) = [1 + \beta_k \exp(j\xi_k)]\delta(t - \tau_k) \ , \tag{5.61}$$

where the time-delay parameter τ_k which accounts for the propagation delay and lack of synchronism between the users is uniformly distributed over [0, T). We assume that the data streams $\{b_j^{(k)}\}$, the spreading sequences $\{a_j^{(k)}\}$, the system phase angles $\{\theta_k\}$, and the channel parameters (which include random gain $\{\beta_k\}$, phases $\{\xi_k\}$, and time-delays $\{\tau_k\}$) associated with different transmitted signals are mutually independent.

Receiver Model

For simplicity, we do not consider the effect of adjacent cell interference in this work. Also, the base station is assumed to control the average transmission power, within its particular cell, to overcome the near/far problem. Therefore, the received signal $r(t)$ can be expressed as

$$r(t) = \sum_{k=1}^{N} \sqrt{2P}\Re e\{[1 + \beta_k \exp(j\xi_k)] \exp[j(\omega_c t + \phi_k)]\} a_k(t - \tau_k) b_k(t - \tau_k) \ , \tag{5.62}$$

where P is the power received from any user, and $\phi_k = \theta_k - \omega_c \tau_k$.

Because of the symmetry of the model, we need to consider only the receiver that is listening to the first transmitter. In the next sections, we will derive the BER and PER for LOS-coherent BPSK and DPSK demodulation schemes by applying the SIGA method.

5.3.3 BER and PER for LOS-Coherent BPSK

For LOS-coherent BPSK demodulation, we assume that only the phase of the LOS component can be tracked by the receiver. Once only relative delays and phases are important, we can set $\tau_1 = \phi_1 = 0$. The receiver model considered here is shown in

Figure 5.12. The decision statistic Z_1 for user 1 is expressed by

$$\begin{aligned} Z_1 &= \int_0^T 2r(t)\cos(\omega_c t)a_1(t)\,dt \\ &= \sqrt{2P}Tb_0^{(1)} + \sqrt{2P}Tb_0^{(1)}\beta_1 \cos\xi_1 + n_1 \\ &\quad + \sqrt{2P}\sum_{k=2}^{N}[\cos\phi_k + \beta_k\cos(\phi_k+\xi_k)]\int_0^T a_k(t-\tau_k)b_k(t-\tau_k)a_1(t)dt \quad , \end{aligned} \tag{5.63}$$

where n_1 is a zero mean Gaussian r.v. with variance N_0T.

It is easy to show that $\cos\phi_k + \beta_k\cos(\phi_k+\xi_k) = \gamma_k\cos\Phi_k$, where Φ_k is a r.v. which is uniformly distributed over $[0, 2\pi)$ and γ_k is a Rician distributed r.v. whose pdf is given by

$$f_\gamma(x) = \frac{x}{\sigma^2}\exp\left(-\frac{x^2+1}{2\sigma^2}\right) I_0\left(\frac{x}{2\sigma^2}\right) \mathrm{U(z)} = 2Kx\exp[-K(x^2+1)]\, I_0(2Kx)\, U(x) \quad . \tag{5.64}$$

If we divide both sides of equation (5.63) by $\sqrt{2PT}$, then $Z_1' = Z_1/(\sqrt{2PT})$ can be written (in Appendix 5.B) as follows

$$Z_1' = 1 + D + n_1^* + \sum_{k=2}^{N}\gamma_k W_k\cos\Phi_k = 1 + D + n_1^* + \sum_{k=2}^{N} I_k(S_k,\Phi_k) \quad , \tag{5.65}$$

where $\sum_{k=2}^{N} I_k(S_k,\Phi_k)$ is called the multiple access interference (MAI), $D = \beta_1\cos\xi_1$ is a zero mean Gaussian r.v. with variance $\sigma^2 = 1/(2K)$, corresponding to the scattered component interference (SCI), and n_1^* is also a zero mean Gaussian r.v. with variance $N_0/(2E_b) = 1/(2a)$. E_b is the bit energy which is equal to PT, and W_k is given by

$$W_k = \frac{1}{T}[P_k R_\psi(S_k) + Q_k\hat{R}_\psi(S_k) + X_k f_\psi(S_k) + Y_k g_\psi(S_k)] \quad , \tag{5.66}$$

where P_k and Q_k are equally likely fl, and X_k and Y_k can be treated as the summation of $(\eta-1)/2$ independent unbiased Bernoulli trials. In addition, P_k, Q_k, X_k, and Y_k are conditionally mutually independent given the desired (user 1) signature sequence. From equation (5.65), we see that the total interference for the desired user include AWGN, MAI, and SCI.

In order to apply the SIGA method to derive the BER, we first have to find the conditional AWGN and MA1 variance Ψ which is defined as

$$\Psi = \mathrm{var}\left[n_1^* + \sum_{k=2}^{N}\gamma_k W_k\cos\Phi_k \,\middle|\, \underline{\gamma}, \underline{\Phi}, \underline{S}\right] \quad , \tag{5.67}$$

where $\underline{\gamma} = [\gamma_2, \ldots, \gamma_N]$, $\underline{\Phi} = [\Phi_2, \ldots, \Phi_N]$, and $\underline{S} = [S_2, \ldots, S_N]$ are random vectors. We show in Appendix 5.C that ψ can be written as

$$\Psi = \frac{1}{2a} + \sum_{k=2}^{N} \gamma_k^2 Z_k \quad , \tag{5.68}$$

where the Z_k are identically distributed and conditionally independent given $\underline{\gamma}, \underline{s}$, and $\underline{\Phi}$. Thus, for some k, $Z = Z_k$ is

$$Z = UV \quad , \tag{5.69}$$

where

$$U = 1 + \cos(2\Phi) \, , \tag{5.70}$$

and

$$V = \frac{1}{2T^2}\left[R_\psi^2(S) + \hat{R}_\psi^2(S) + \left(\frac{\eta-1}{2}\right) f_\psi^2(S) + \left(\frac{\eta-1}{2}\right) g_\psi^2(S)\right] \quad . \tag{5.71}$$

It is proved that as $\eta \to \infty$, given $\underline{\gamma}, \underline{S}$, and $\underline{\Phi}$, the MA1 can be accurately approximated by a Gaussian r.v.[5]. Therefore the conditional BER, $P_b(\Psi, D)$, is given by

$$P_b(\Psi, D) = \mathbf{Q}\left(\frac{1+D}{\sqrt{\Psi}}\right) \, , \tag{5.72}$$

where $\mathbf{Q}(x)$ is the complementary error function previously defined.

Finally, the average BER, $\overline{P}_b$, can be approximated by (see Appendix 5.D)

$$\overline{P}_b \approx \frac{2}{3}\mathbf{Q}\left[\frac{1}{\sqrt{\frac{1}{2K} + \mu_\psi}}\right] + \frac{1}{6}\mathbf{Q}\left[\frac{1}{\sqrt{\frac{1}{2K} + \mu_\psi + \sqrt{3}\sigma_\psi}}\right] + \frac{1}{6}\mathbf{Q}\left[\frac{1}{\sqrt{\frac{1}{2K} + \mu_\psi - \sqrt{3}\sigma_\psi}}\right] \, , \tag{5.73}$$

where $\mu_\psi = E(\Psi)$ and $\sigma_\psi^2 = \mathrm{var}(\Psi)$.

For arbitrary chip pulse shape, μ_ψ and σ_ψ^2 can be computed as follows (see detailed derivation in Appendix 5.E) :

$$\mu_\psi = \frac{1}{2a} + \left(1 + \frac{1}{K}\right)(N-1)\left(\frac{m_\psi}{\eta}\right) \quad , \tag{5.74}$$

$$\sigma_\psi^2 = (N-1)[\, \mathsf{E}\,(\gamma^4 z^2) - \mathsf{E}^{\,2}(\gamma^2 z)\,] \, , \tag{5.75}$$

where

$$E(\gamma^4 z^2) = \left(1 + \frac{4}{K} + \frac{2}{K^2}\right)\left(\frac{3}{2}\right)\left(\frac{1}{\eta^2}\right)\left\{\frac{1}{4}E\,[f_n^4(w)] - E\,[f_n^2(w)R_n(w)\hat{R}_n(w)] + E\,[R_n^2(w)\hat{R}_n^2(w)]\right\} \, , \tag{5.76}$$

and

$$E(\gamma^2 z) = \left(1 + \frac{1}{K}\right)\left(\frac{m_\psi}{\eta}\right) \quad . \tag{5.77}$$

In the above equations, we normalize the chip pulse shape such that $T_c = 1$ to facilitate the computation, not to worry with the actual value of T_c. In this situation, $\psi_n(t)$ is zero except for $0 \leq t \leq 1$. $\hat{R}_n(w) = \int_w^1 \Psi_n(t)\Psi_n(t-w)\,dt$, and R,(w) = $\hat{R}_n(t-w)$. Similarly, $f_n(w) = \hat{R}_n(w) + R_n(w)$ and $g_n(w) = \hat{R}_n(w) -$ R,(w).

In addition, m_ψ is defined as

$$m_\psi = E\,[\,\hat{R}_n^2(w)\,] = E\,[\,R_n^2(w)\,] \,. \tag{5.78}$$

For rectangular chip pulse shape, $m_\psi = 1/3$. For a half-sine chip pulse shape of the form $\psi_n(t) = \sqrt{2}\sin(\pi t)$, $m_\psi = (15 + 2\pi^2)/(12\pi^2)$. For a raised-cosine chip pulse shape of the form $\psi_n(t) = \sqrt{\frac{2}{3}}[1 - \cos(2\pi t)]$, $m_\psi = 1/6 + 35/(48\pi^2)$.

Finally, let us compare the result of $\overline{P}_b$ in equation (5.73) with that by the SGA method, $\overline{P}_{b,g}$ which assumes the MA1 are Gaussian r.v.'s and can be shown to be

$$\overline{P}_{b,g} = Q\left(\frac{1}{\sqrt{\frac{1}{2K} + \mu_\psi}}\right) \quad . \tag{5.79}$$

We see that $\overline{P}_{b,g}$ is just the first term of $\overline{P}_b$ without the coefficient $2/3$. In Appendix 5.B, we have shown that the MA1 components are only conditionally independent given $\underline{\gamma}$, $\underline{S}$, and $\underline{\Phi}$. But in SGA, these MA1 are modeled as Gaussian r.v.. Because the interference, in fact, are uncorrelated which implies they are unconditionally independent. This is where the error of the SGA comes from. Therefore, the $\overline{P}_b$ derived by the SIGA method can be viewed as improving the SGA method by adding another two terms shown in equation (5.73) and using appropriate weighting coefficients.

Next, we want to derive the PER for LOS-coherent BPSK. Suppose a packet of L bits is transmitted over a memoryless binary communication channel with BER equal to P_b. If the packet includes some block error control capacity and is able to correct t or fewer errors, then, assuming bit-to-bit independence, the PER becomes

$$P_E = \sum_{l=t+1}^{L} \binom{L}{l} P_b^l (1 - P_b)^{L-l} \triangleq g(P_b; L, t) \quad . \tag{5.80}$$

From equations (5.65) and (5.66), and the fact that if conditioning is done on $\underline{\gamma}, \underline{S}$, and $\underline{\Phi}$, then the MA1 becomes independent from bit-to-bit within the packet. This allows for finding the conditional PER using (5.80). Then, by unconditioning, the PER can be easily found.

Assume that each γ_k, S_k, and Φ_k is selected at random at the start of a desired packet, but remains constant for the duration of the packet. Then each $\Psi = \psi$ of the conditional variance is produced by a specific $1/(2a), \underline{\gamma}, \underline{S}$, and $\underline{\Phi}$. Hence, $P_b(\Psi, D) = \mathrm{Q}\left[\frac{1+D}{\sqrt{\Psi}}\right]$ is an accurate approximation of the BER and g $\left(\mathrm{Q}\left[\frac{1+D}{\sqrt{\Psi}}\right]; \boldsymbol{L}, t\right)$ is an accurate approximation of the conditional PER [5]. Unconditioning g $\left(\mathrm{Q}\left[\frac{1+D}{\sqrt{\Psi}}\right]; \boldsymbol{L}, t\right)$ and applying the SIGA, PER can be approximated by (see Appendix 5.F)

$$\begin{aligned} P_E &= E_{\Psi,D}\left\{ g\left(\mathrm{Q}\left[\frac{1+D}{\sqrt{\Psi}}\right]; L, t\right)\right\} \\ &\approx \int_{-\infty}^{\infty}\left\{\frac{2}{3} g\left(\mathrm{Q}\left[\frac{1+y}{\sqrt{\mu_\psi}}\right]; L, t\right) + \frac{1}{6} g\left(\mathrm{Q}\left[\frac{1+y}{\sqrt{\mu_\psi + \sqrt{3}\sigma_\psi}}\right]; L, t\right)\right. \\ &\qquad \left. + \frac{1}{6} g\left(\mathrm{Q}\left[\frac{1+y}{\sqrt{\mu_\psi - \sqrt{3}\sigma_\psi}}\right]; L, t\right)\right\} f_D(y)\, dy \quad (5.81) \end{aligned}$$

where $f_D(y) = \sqrt{K/\pi}\exp(-Ky^2)$.

5.3.4 BER and PER for DPSK

For DPSK demodulation a possible implementation of the differentialy-coherent match filter receiver for a DS/CDMA system is shown in Figure 5.13 [9]. The demodulator has two branches: the first matches the in-phase component and the other matches the quadrature component. Consider the reception of the data bit $b_0^{(1)}$. The in-phase decision statistic Z_c is given by

$$Z_c = \int_0^T 2r(t)a_1(t)\cos(\omega_c t)\, dt\,, \qquad (5.82)$$

where $r(t)$ is defined in equation (5.62).

The decision statistic Z_s is defined by equation (5.82) with the [cos(·)] term replaced by [-sin(.)]. The receiver forms the statistic $Z_c Z_{c,d} + Z_s Z_{s,d}$ and compares it to a zero threshold. Similarly to the LOS-coherent BPSK case, we let $\tau_1 = 0$ and $b_0^{(1)} = 1$. Then,

Z_c is given by

$$Z_c = \sqrt{2P}T\cos\phi_1 + \sqrt{2P}T\beta_1\cos(\phi_1+\xi_1) + n_1 + \sum_{k=2}^{N}\sqrt{2P}\gamma_k B_{k,1}(\tau_k)\cos\Phi_k$$
$$= \sqrt{2P}T\gamma_1\cos\Phi_1 + n_1 + \sum_{k=2}^{N}\sqrt{2P}\gamma_k B_{k,1}(\tau_k)\cos\Phi_k \quad . \tag{5.83}$$

Let $Z_c' = Z_c/\sqrt{2P}T$. Then,

$$Z_c' = \gamma_1 cos\Phi_1 + n_1^* + \sum_{k=2}^{N}\gamma_k W_k\cos\Phi_k \quad , \tag{5.84}$$

where γ_1 is a Rician distributed r.v. with pdf as shown in equation (5.64).

For DPSK demodulation, we assume, without loss of generality, that the phase Φ_1 does not change over the duration of two adjacent data bits. If $\underline{\gamma}, \underline{S}$, and $\underline{\Phi}$ are given, the MA1 are conditionally bit-to-bit independent, then the conditional BER, $P_b(\Psi,\gamma_1)$, for DPSK is given by [10]:

$$P_b(\Psi,\gamma_1) = \frac{1}{2}\exp\left(-\frac{\gamma}{2\Psi}\right) \quad , \tag{5.85}$$

Averaging over γ_1, we can find the conditional BER, $P_b(\Psi)$, as

$$P_b(\Psi) = \int_0^\infty P_b(\Psi,\gamma_1)f(\gamma_1)\,d\gamma_1 = \frac{K}{\Psi^{-1}+2K}\exp\left(-\frac{\Psi^{-1}K}{\Psi^{-1}+2K}\right) \quad . \tag{5.86}$$

Finally, the BER for DPSK can be approximated by using the SIGA method as

$$\overline{P}_b = \int_0^\infty P_b(\psi)f_\Psi(\psi)\,d\psi \tag{5.87}$$
$$\approx \frac{2}{3}\frac{K}{A_1+2K}e^{-\frac{A_1K}{A_1+2K}} + \frac{1}{6}\frac{K}{A_2+2K}e^{-\frac{A_2K}{A_2+2K}} + \frac{1}{6}\frac{K}{A_3+2K}e^{-\frac{A_3K}{A_3+2K}} \quad ,$$

where $A_1 = 1/\mu_\psi$, $A_2 = 1/(\mu_\psi+\sqrt{3}\sigma_\psi)$, and $A_3 = 1/(\mu_\psi-\sqrt{3}\sigma_\psi)$, respectively.

Similarly, the PER for DPSK can be derived by

$$P_E = \int_0^\infty\int_0^\infty g(P_b(\psi,\gamma_1);L,t)f_\Psi(\psi)f(\gamma_1)\,d\psi\,d\gamma_1 \tag{5.88}$$
$$\approx \int_0^\infty \left\{\frac{2}{3}g(P_{b1}(\gamma_1);L,t) + \frac{1}{6}g(P_{b2}(\gamma_1);L,t) + \frac{1}{6}g(P_{b3}(\gamma_1);L,t)\right\} f(\gamma_1)d\gamma_1 \quad ,$$

where $P_{bi}(\gamma_1) = 1/2\exp(-A_i\gamma_1^2/2), i = 1,2,3.$

5.3.5 CDMA Numerical Results

The BER versus E_b/N_0 for LOS-coherent BPSK and DPSK evaluated via the SIGA and the SGA methods for three chip pulse shapes are shown in Figure 5.14 and Figure 5.15, respectively. The spreading ratio is η = 511, K = 10 dB, and N = 45. We see that the BER derived by SIGA and SGA are very close, even when E_b/N_0 is large, which is not necessarly true for an AWGN channel. In an AWGN channel, as E_b/N_0 becomes large, the MA1 will play the dominant role to cause decision errors. In that situation, we know that the BER evaluated by SGA is very optimistic [5] compared with SIGA because of the Gaussian assumption for MA1 used in the SGA method. However, in a Rician fading channel, as E_b/N_0 gets large, the SCI, i.e., the D term in equation (5.65), is dominant, covering the effect of mismodeling of the MA1 in the SGA method. In the same figures, we can also see the effect of different chip pulse shapes on BER performance. When E_b/N_0 is large, raised-cosine can provide the best performance while rectangular is the worst because the latter possesses the largest MA1 power.

In Figures 5.16 and 5.17, we compare the BER performance of LOS-coherent BPSK with that of DPSK. It is found that for N = 45 LOS-coherent BPSK is better than DPSK for the whole E_b/N_0 range from 0 to 50 dB and is about 3 dB better than DPSK at $P_b = 10^{-3}$. However, when N = 10, the above observation is no longer true. When E_b/N_0 is less than 20 dB, LOS-coherent BPSK is better than DPSK and conversely for E_b/N_0 larger than 20 dB. The reason is that when N = 10, the MA1 is small compared with the SCI. At high values of E_b/N_0, DPSK can utilize part of the power of the SCI (we have also found this phenomenon in TDMA system), while LOS-coherent BPSK treats the SCI just as noise.

Figures 5.18 and 5.19 show the BER versus total users, N, of LOS-coherent BPSK for $K = 10$ and 13 dB, respectively. Here, we assume $E_b/N_0 \to \infty$, i.e., we can ignore the thermal noise which is just the situation in IVHS short range communications. In these two figures, we first find that the effect of chip pulse shape on the system capacity (total number of users can be supported at the same value of P_b). For instance, at η = 511 and $P_b = 10^{-4}$, the system can support about 44 users using raised-cosine pulse shape while only 32 users can be supported if rectangular chip pulse shape is employed.

CDMA system is interference limited. More smooth chip pulse shapes can reduce the total multiple-access interference, and then increase the system capacity. Secondly, the value of K has great impact on the BER performance. For rectangular chip pulse shape, $P_b = 10^{-4}$, and k = 10 dB, about 32 users can be accommodated by the system. While 68 users can be supported at K = 13 dB which is twice compared to the former case. Therefore, precise K value for realistic IVHS communications has to be measured to achieve a satisfactory system design. Figures 5.20 and 5.21 are for DPSK case and same phenomenon as in LOS-coherent BPSK can be found. Figures 5.22 to 5.25 are the same situations as above except that the spreading ratio is now η = 255. The effect of K on the BER performance is similar to that for η = 511.

In Figure 5.26, the BER for LOS-coherent BPSK and DPSK using the rectangular chip pulse shape is compared. Again, we can observe that when N is less than 17, DPSK has a better performance than LOS-coherent BPSK and conversely for larger number of users. The system designer should make decision which demodulation scheme is appropriate by trading off system complexity for system capacity.

We show the PER performance of LOS-coherent BPSK and DPSK in Figures 5.27 and 5.28, respectively, both employing rectangular chip pulse shape and with L= 512 bits. In these figures, we also demonstrate the power of error correcting coding for t=5 and 10 bits versus t=0. Finally, the PER performance for LOS-coherent BPSK and DPSK is shown in Figure 5.29 for rectangular chip pulse shape.

Finally, we compare the PER for LOS-coherent BPSK of slow fading and its upper bound without error correction in Figure 5.30. This bound is evaluated by

$$P_E^U = g\left(E_{D,\Psi}\left[Q\left(\frac{1+D}{\sqrt{\Psi}}\right)\right];L,0\right). \tag{5.89}$$

In this expression, since the bit-to-bit error dependence is ignored, the PER will be worse than tha actual situation [6]. Meanwhile, it also accounts for the situation that the scattered component is bit-to-bit independent. Given these two curves, we can see range of the performance will be if the actual channel fading is between fast (SF) and very slow fading (VSF).

5.3.6 CDMA Conclusions

We have derived the BER and PER of an asynchronous DS/CDMA system employing random signature sequences in a Rician fading channel by applying the SIGA method. Both LOS-coherent BPSK and DPSK modulation schemes have been considered. In addition, the expressions for BER and PER have been generalized for arbitrary chip pulse shapes. In a Rician fading channel, the BER derived via SGA and SIGA are very close even for high E_b/N_0 value. The value of Rician factor K has great impact on the system capacity. Accurate value of K has to be measured in realistic IVHS communications to achieve a satisfactory system design. In general, raised-cosine pulse shape can provide the best performance, half-sine next, and rectangular the worst. When system load is high, i.e., total number of users N is large, the performance of LOS-coherent BPSK is usually better than DPSK independent of the value of E_b/N_0. However, when system load is low and E_b/N_0 is high, DPSK may have better performance than LOS-coherent BPSK. This phenomenon was also found for narrowband modulation in TDMA systems. Finally, in a Rician fading channel, error correcting coding can greatly improve the system capacity.

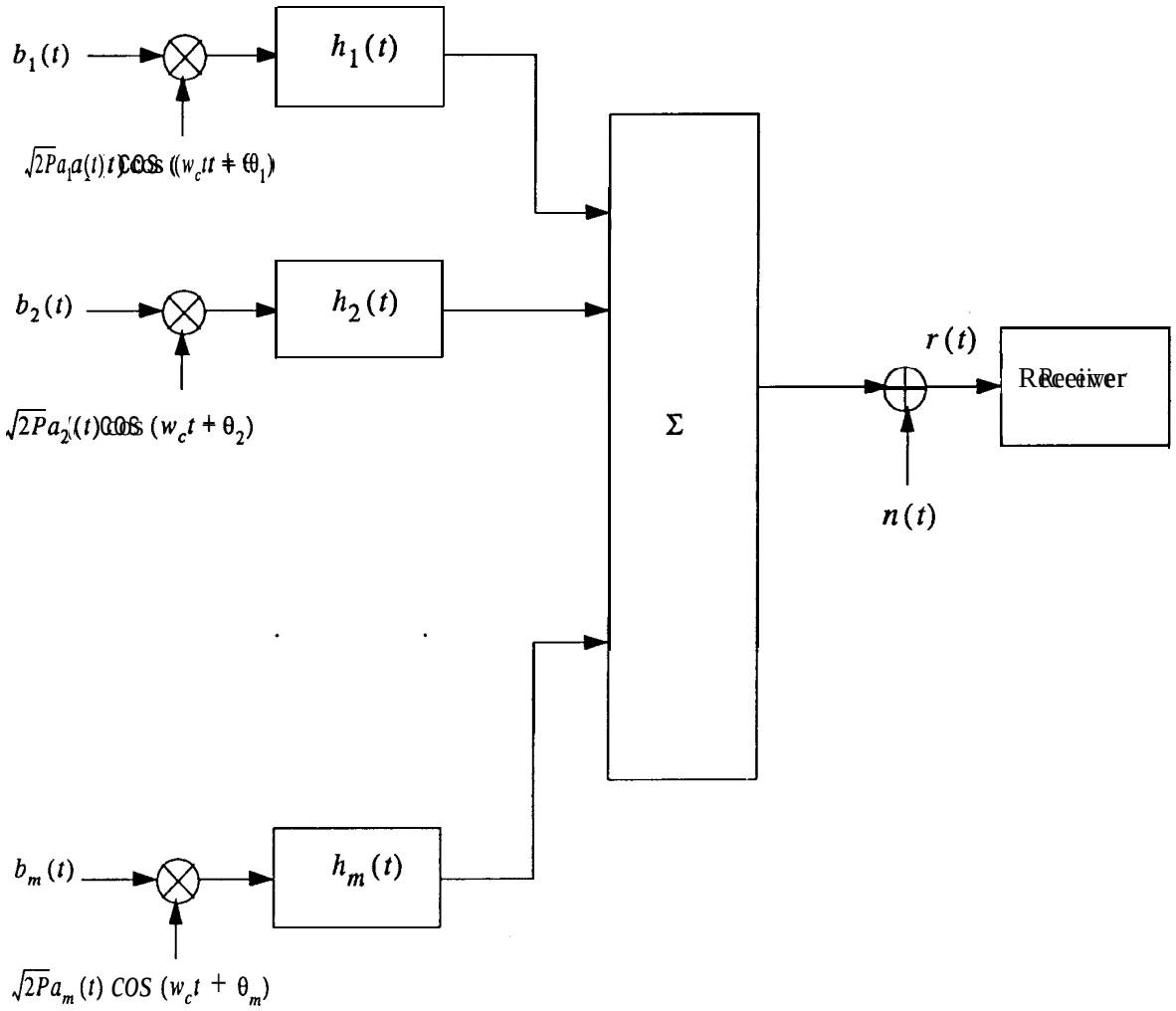

Figure 5.11: Asynchronous DS/CDMA System Model

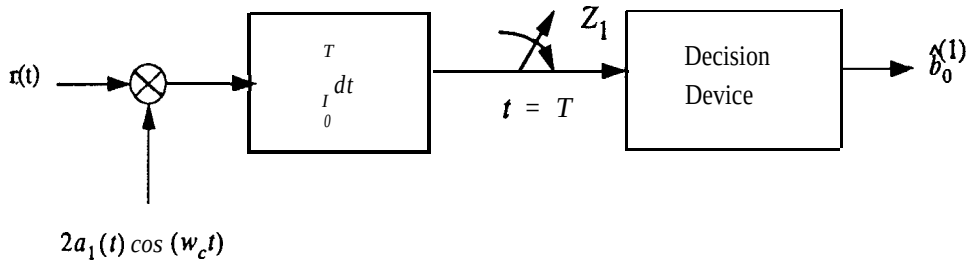

Figure 5.12: Asynchronous DS/CDMA System Receiver Model for LOS-Coherent PSK

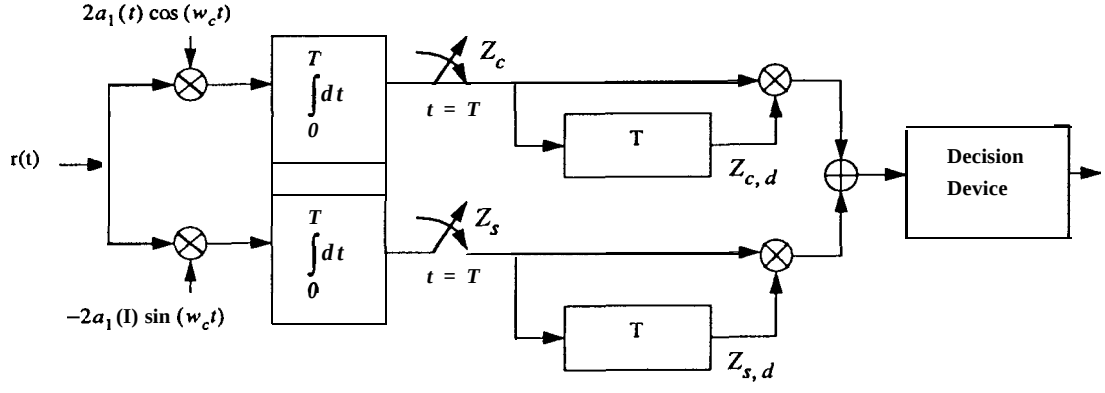

Figure 5.13: Asynchronous DS/CDMA System Receiver Model for DPSK

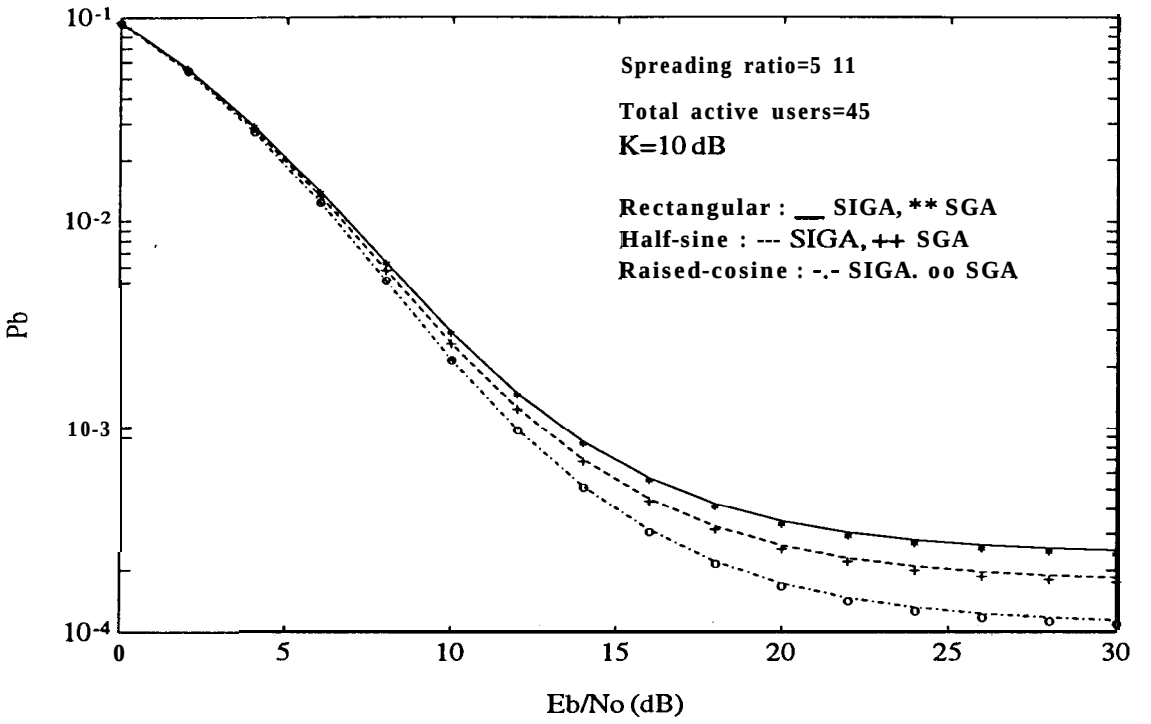

Figure 5.14: BER versus E_b/N_0 using the SIGA and SGA Methods in a Rician Fading Channel with K=10 dB for LOS-Coherent PSK employing three Pulse Shapes

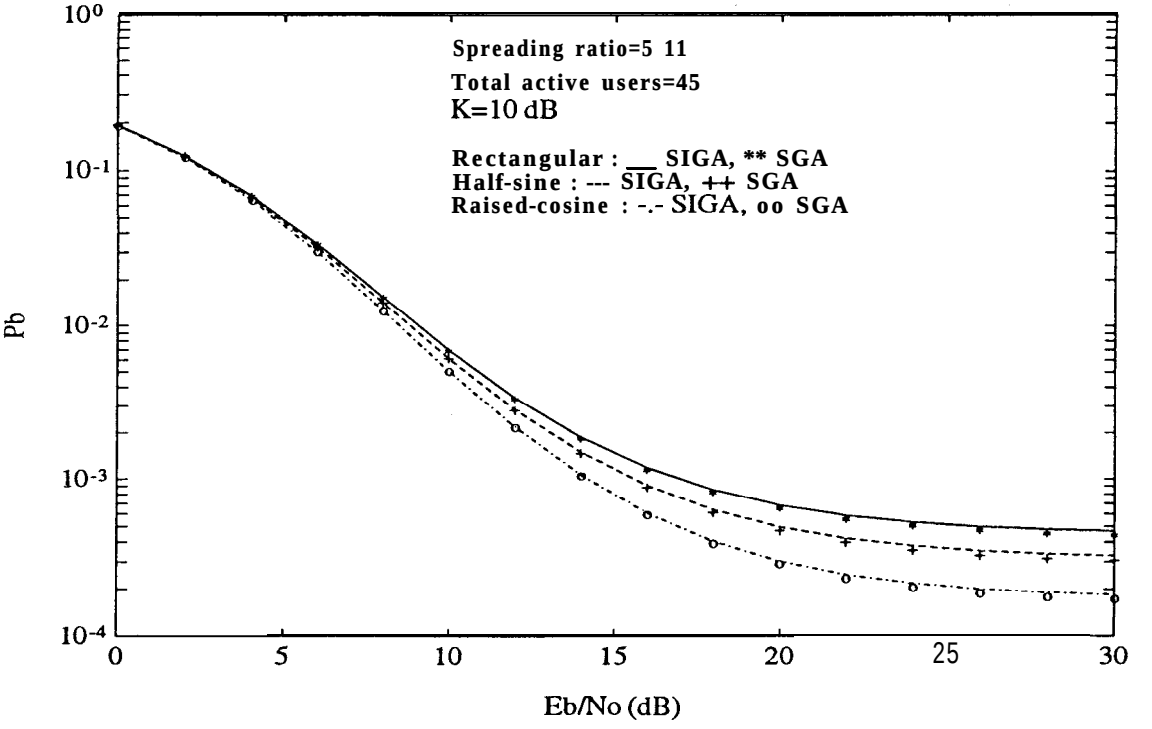

Figure 5.15: BER versus E_b/N_0 using the SIGA and SGA Methods in a Rician Fading Channel with K=10 dB for DPSK employing three Pulse Shapes

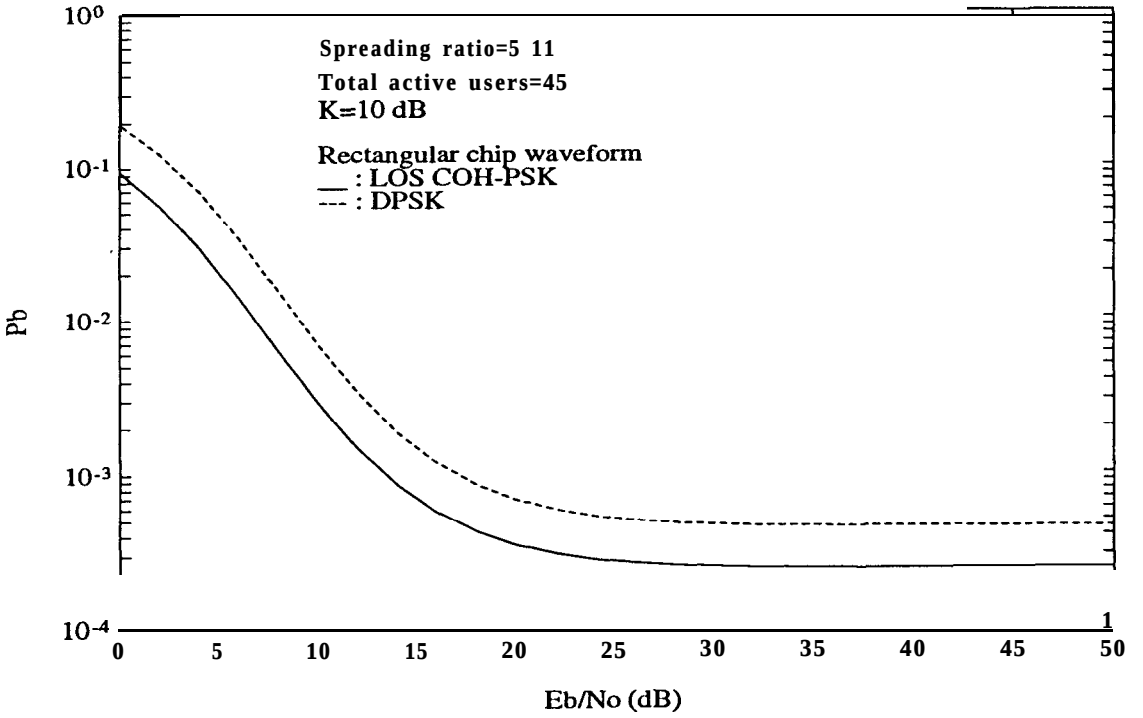

Figure 5.16: BER versus E_b/N_0 for LOS-Coherent PSK compared with DPSK using Rectangular Pulses; N=45

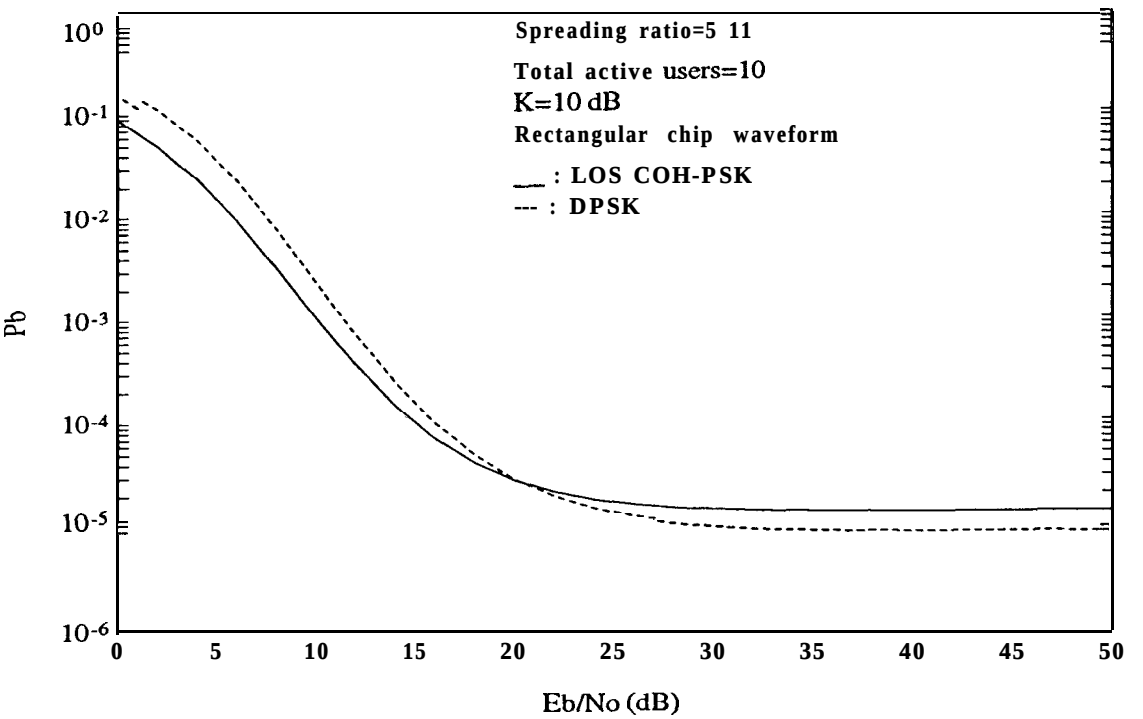

Figure 5.17: BER versus E_b/N_0 for LOS-Coherent PSK compared with DPSK using Rectangular Pulses; N=10

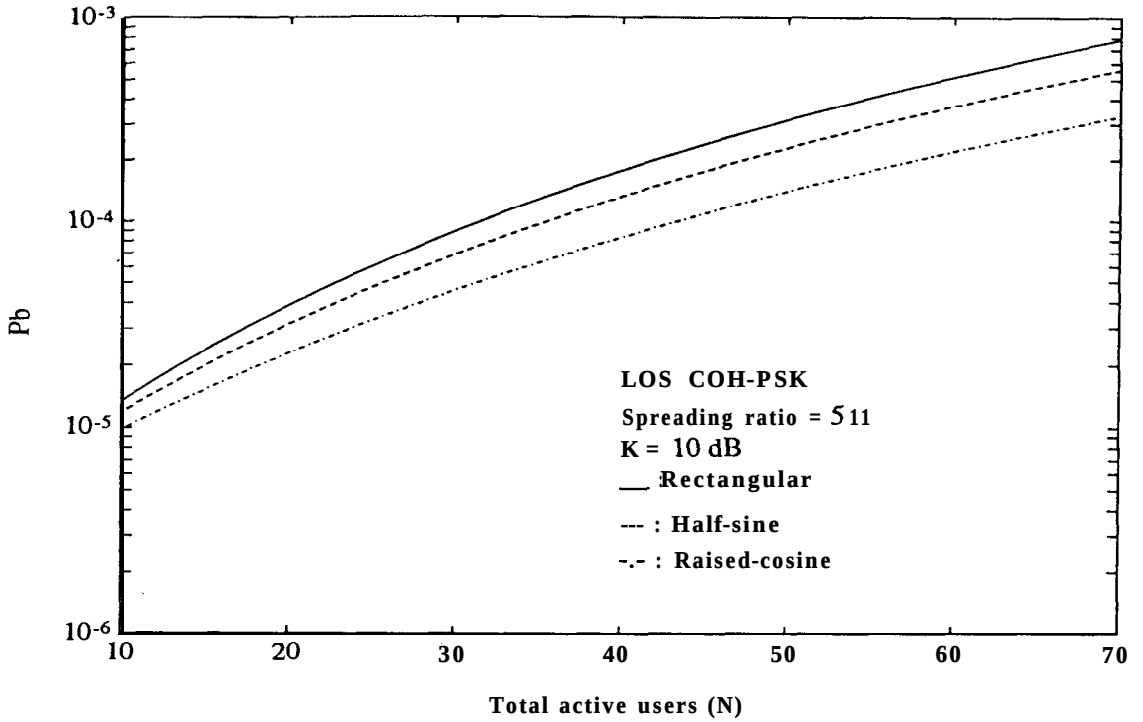

Figure 5.18: BER versus N using the SIGA Method in a Rician Fading Channel with K=10 dB for LOS-Coherent PSK employing three Pulse Shapes; E_b/N_0 = *oo.*

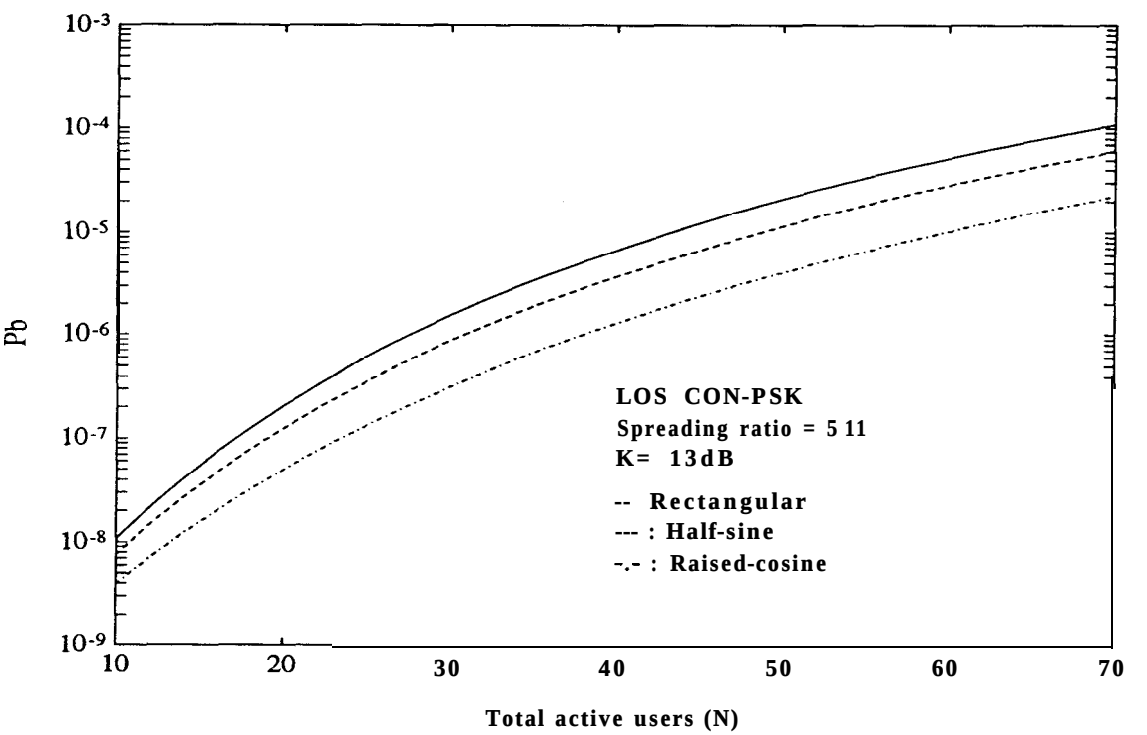

Figure 5.19: BER versus N using the SIGA Method in a Rician Fading Channel with K=13 dB for LOS-Coherent PSK employing three Pulse Shapes; $E_b/N_0 = \infty$.

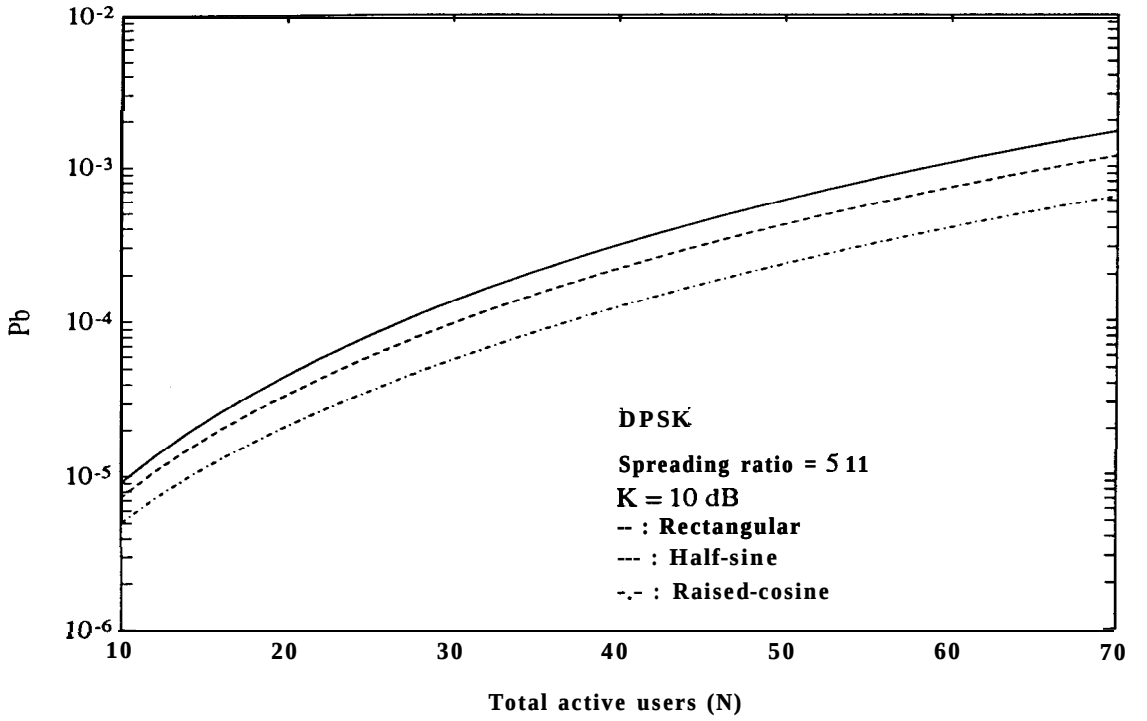

Figure 5.20: BER versus N using the SIGA Method in a Rician Fading Channel with K=10 dB for DPSK employing three Pulse Shapes; $E_b/N_0 = \infty$.

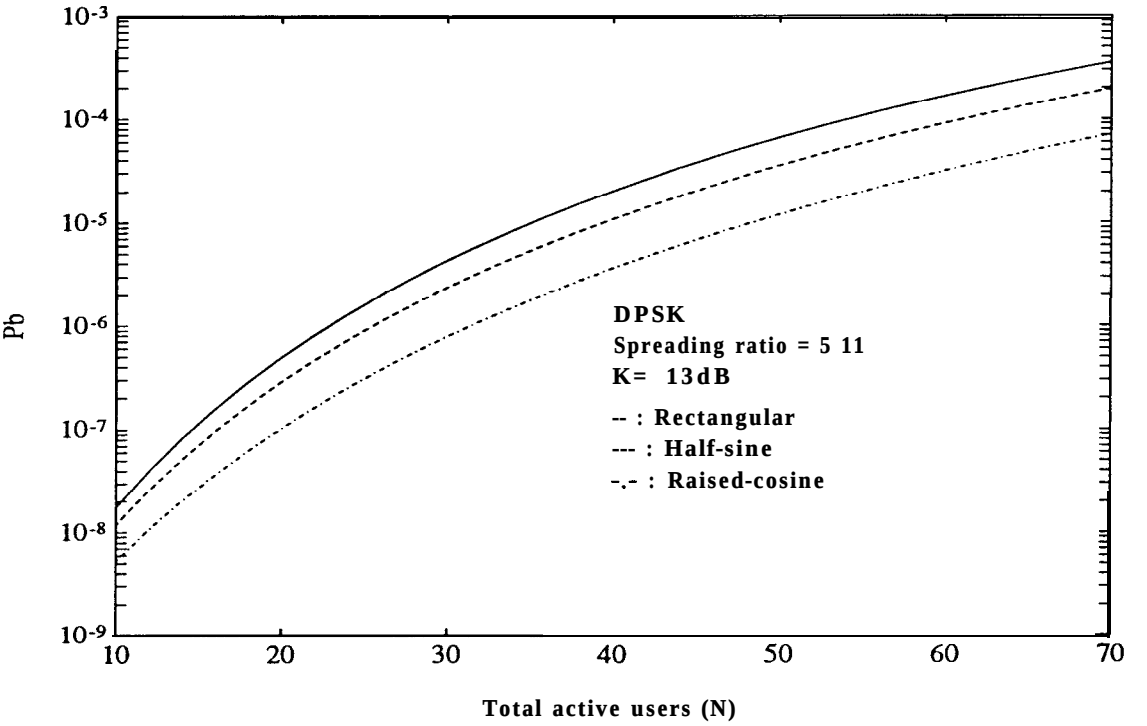

Figure 5.21: BER versus N using the SIGA Method in a Rician Fading Channel with K=13 dB for DPSK employing three Pulse Shapes; $E_b/N_0 = \infty$.

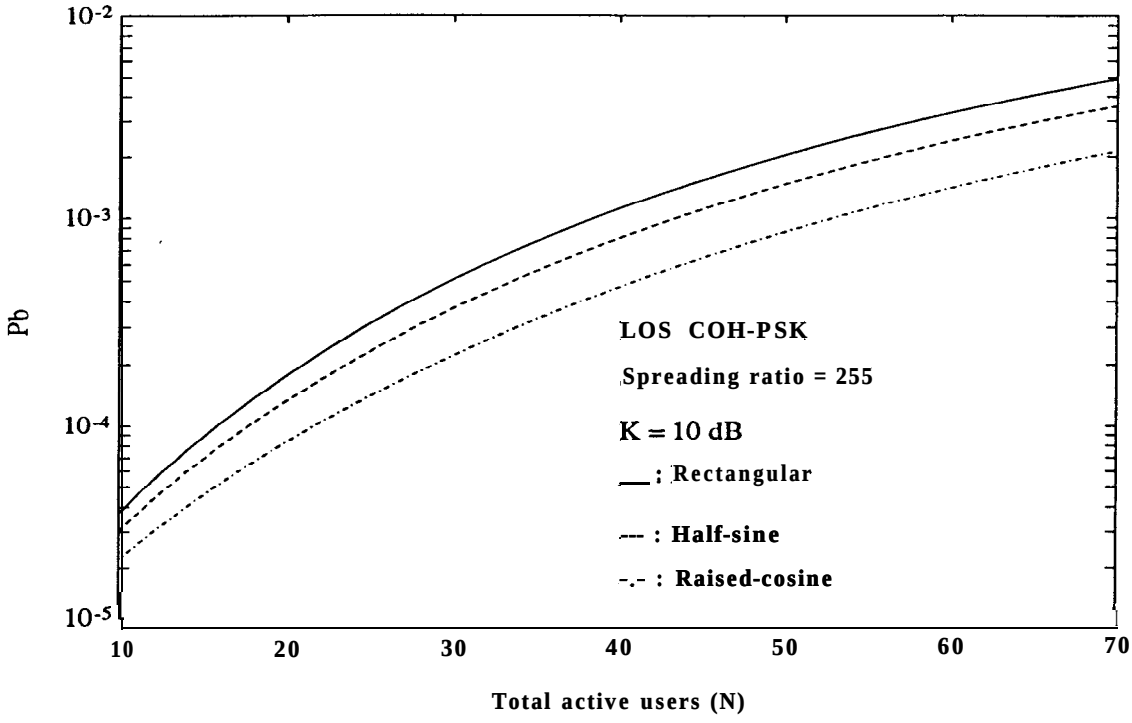

Figure 5.22: BER versus N using the SIGA Method in a Rician Fading Channel with K=10 dB for LOS-Coherent PSK employing three Pulse Shapes; E_b/N_0 = *co.*

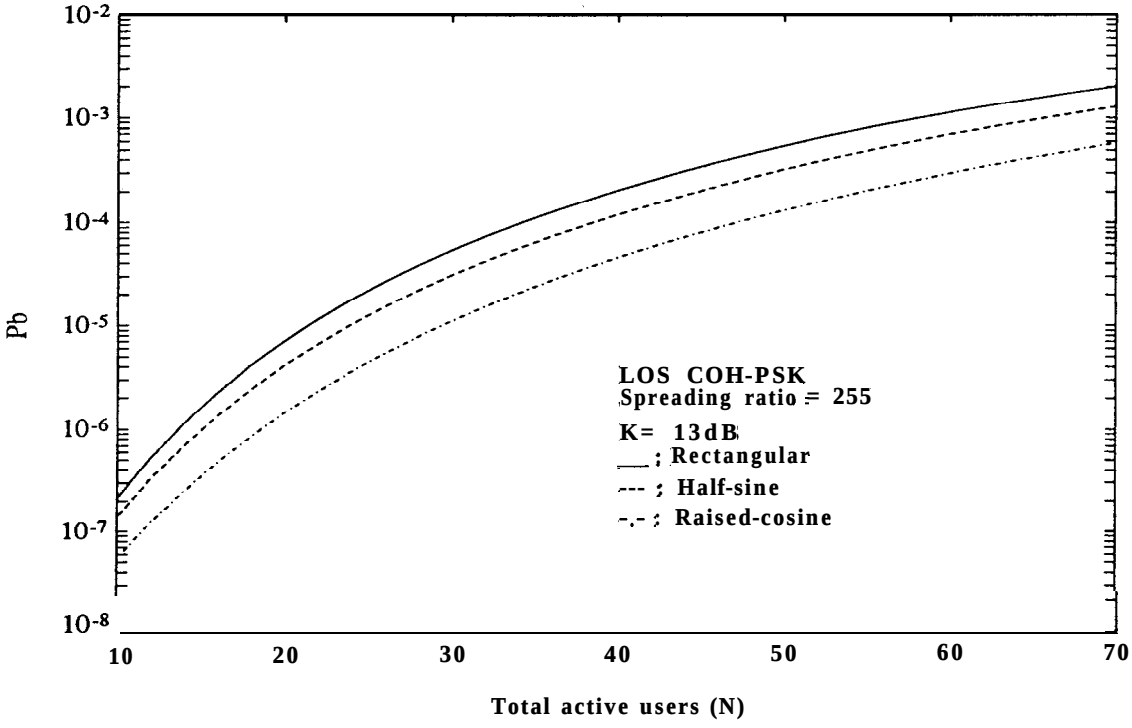

Figure 5.23: BER versus N using the SIGA Method in a Rician Fading Channel with K=13 dB for LOS-Coherent PSK employing three Pulse Shapes; E_b/N_0 = ∞.

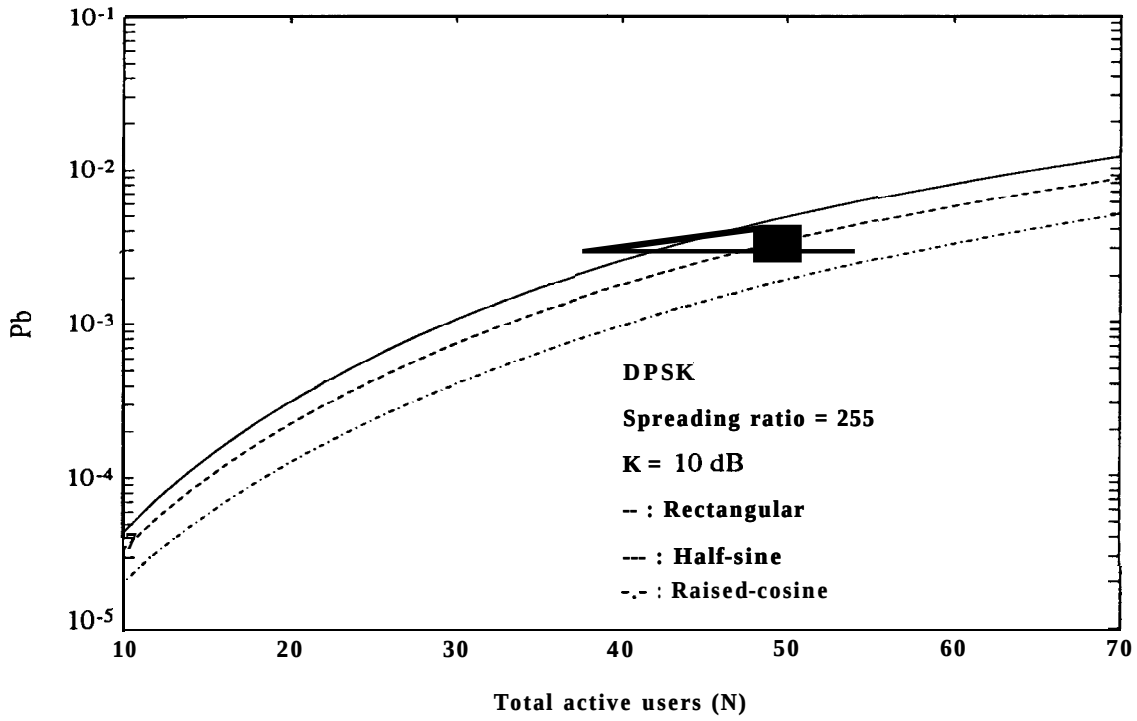

Figure 5.24: BER versus N using the SIGA Method in a Rician Fading Channel with K=10 dB for DPSK employing three Pulse Shapes; $E_b/N_0 = \infty$.

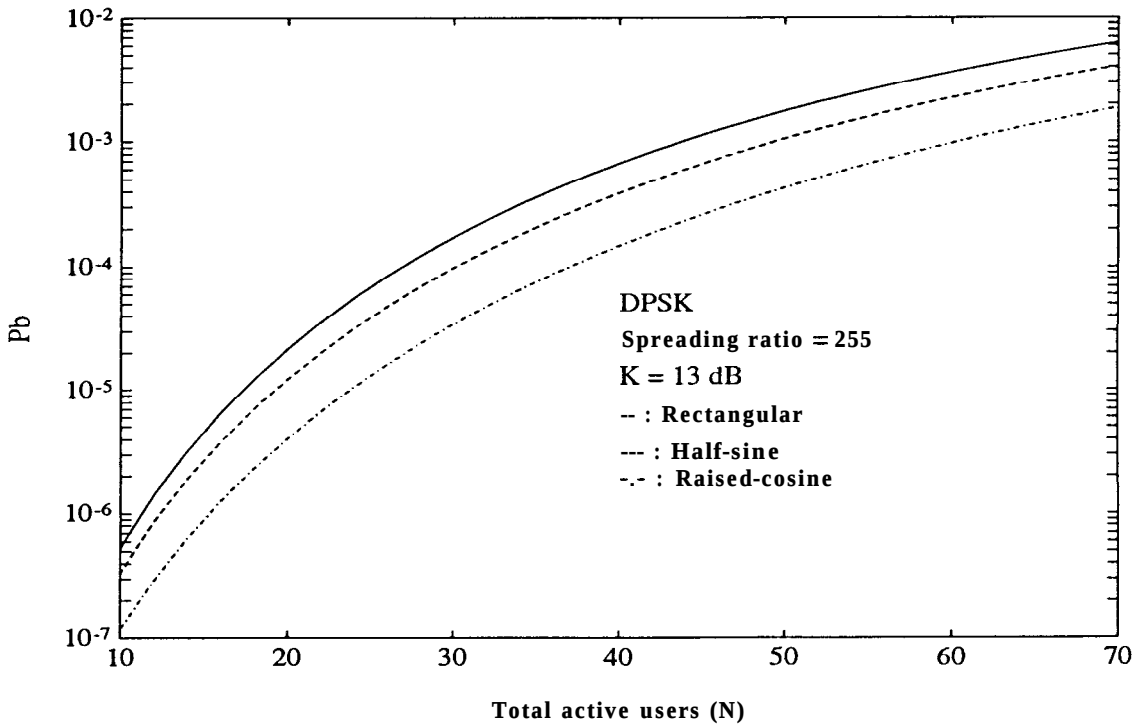

Figure 5.25: BER versus N using the SIGA Method in a Rician Fading Channel with K=13 dB for DPSK employing three Pulse Shapes; $E_b/N_0 = co.$

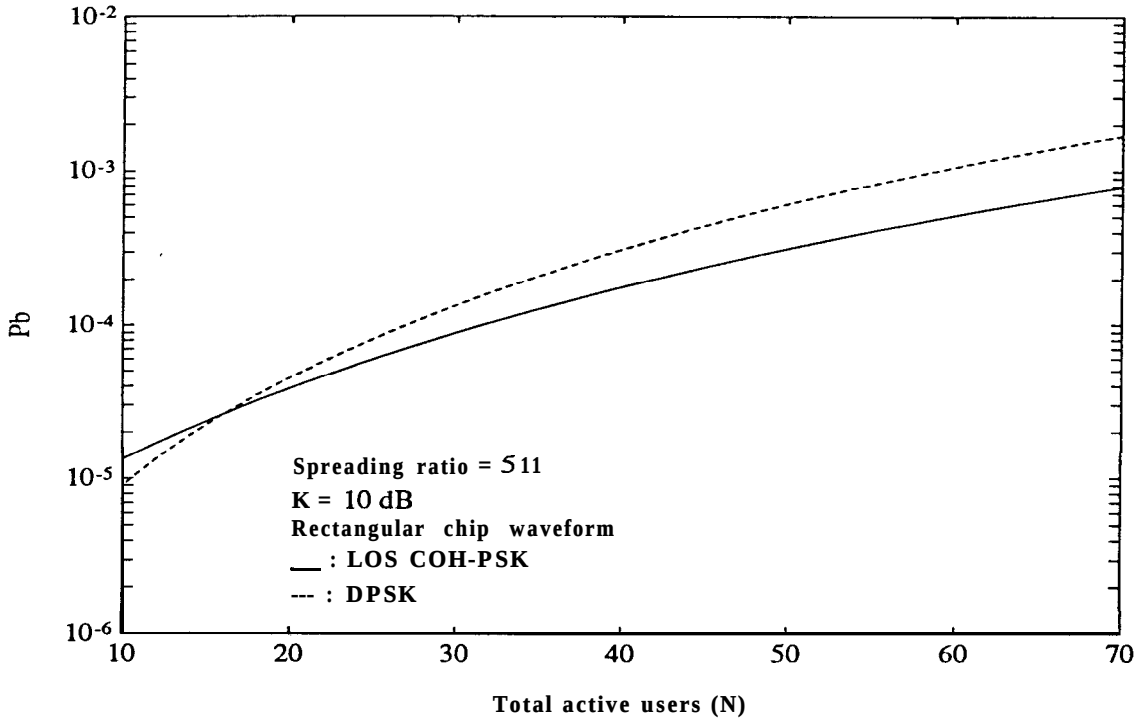

Figure 5.26: BER versus N in a Rician Fading Channel with $K=10\,dB$ for LOS-Coherent PSK compared with DPSK using Rectangular Pulses; $E_b/N_0 = \infty$.

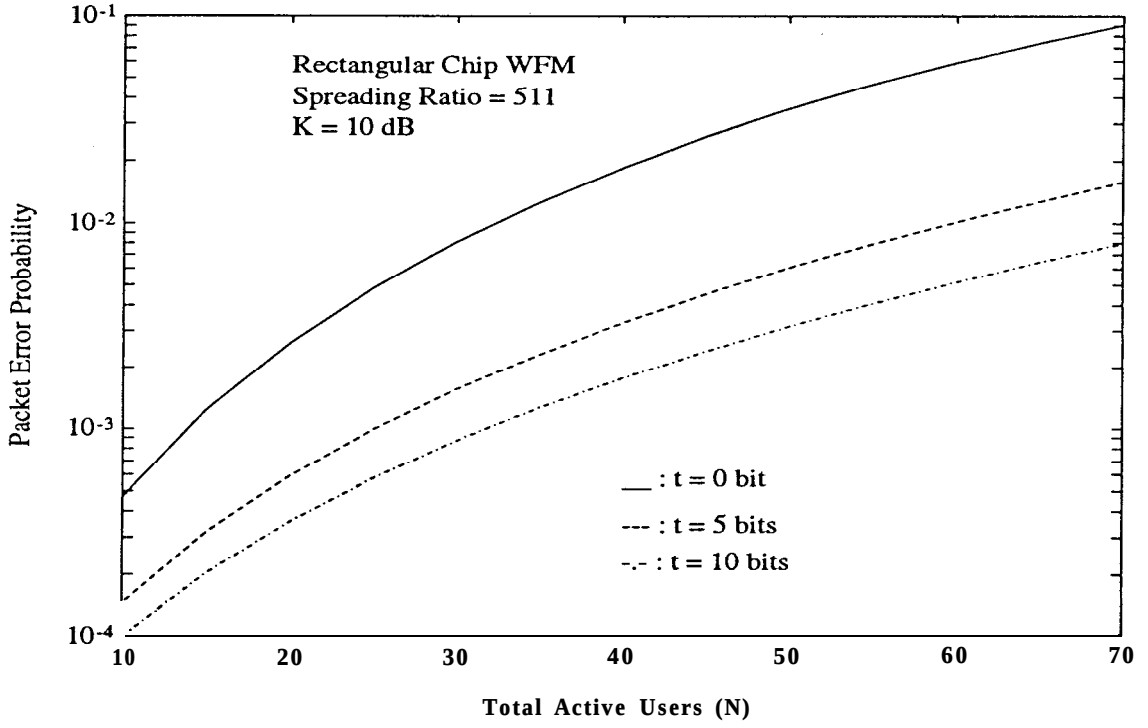

Figure 5.27: PER versus N using the SIGA Method in a Rician Fading Channel with $K=10\,dB$ for LOS-Coherent PSK employing Rectangular Pulses; $E_b/N_0 = \infty$; $\eta = 511$

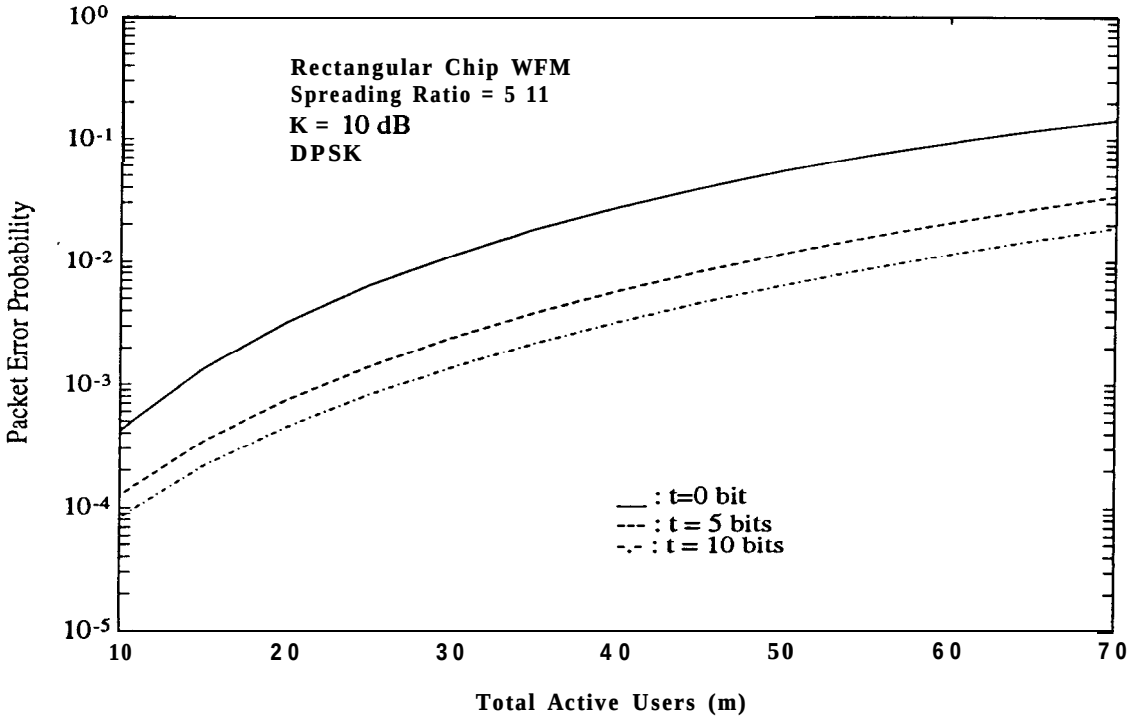

Figure 5.28: PER versus N using the SIGA Method in a Rician Fading Channel with K=10 dB for DPSK employing Rectangular Pulses; $E_b/N_0 = \infty; \eta = 511$

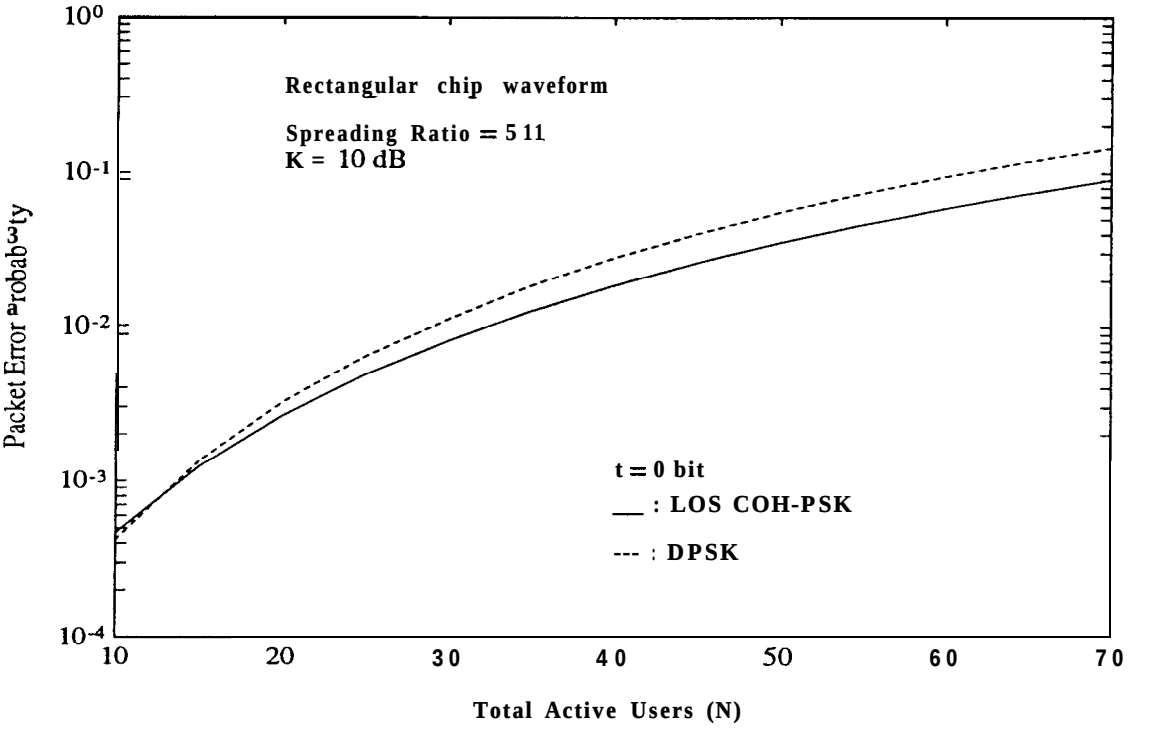

Figure 5.29: PER versus N in a Rician fading channel with K=10 dB for LOS-Coherent PSK compared with DPSK using Rectangular Pulses; $E_b/N_0 = \infty; \eta = 511$

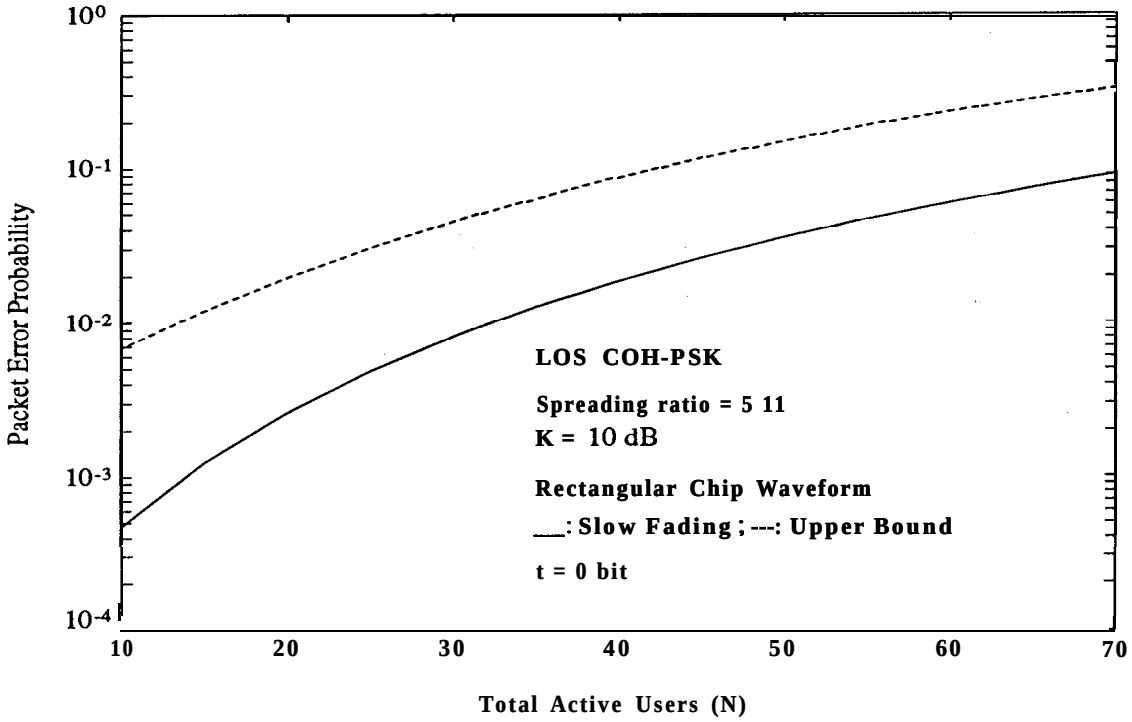

Figure 5.30: PER in a Rician Fading Channel with K=10 dB for LOS-Coherent PSK with Slow Fading and its Upper Bound using Rectangular Pulses; $E_b/N_0 = \infty; \eta = 511;$ $t = 0$ bit

5.4 Conclusions and Future Challenges

In this chapter, we have first derived the BER for binary PSK, FSK, and ASK modulations with LOS-coherent and noncoherent demodulation over a Rician fading channel for a TDMA system. In that part of the analysis, we found that DPSK and noncoherent BFSK are appropriate for slow fading short range IVHS communications. Secondly, we investigate the BER and PER performance for an asynchronous DS/CDMA system in a Rician fading channel by applying the SIGA method. Both LOS-coherent BPSK and DPSK are employed. The results were generalized for arbitrary chip pulse shape. The performance of raised-cosine, half-sine, and rectangular pulse shapes is compared. In general, raised-cosine can provide the best results. Finally, the value of Rician factor K has great impact on system performance both for TDMA and CDMA systems.

In this work, we did not consider the interference from neighboring cells which would further degrade the BER and PER performance of the system. Therefore, we need to find appropriate models, for both TDMA and CDMA systems, to take into account the interference from other cells. Then we will have a more precise estimate of the system capacity.

Chapter 5.A

Derivation of the Normalized Optimal Threshold α' for LOS-Coherent ASK

Because α satisfies equation (5.16),

$$\frac{1}{\sqrt{2\pi}\sigma_2}\exp\left(-\frac{\alpha^2}{2\sigma_2^2}\right) = \frac{1}{\sqrt{2\pi}\sigma_1}\exp\left[-\frac{(\alpha-\sqrt{4P}T_b)^2}{2\sigma_1^2}\right] . \tag{5.A.1}$$

Let $m = \sqrt{4P}T_b$. Then, the above equation can be simplified since

$$\log\left(\frac{\sigma_1}{\sigma_2}\right) = \frac{\alpha^2}{2\sigma_2^2} - \frac{(\alpha-m)^2}{2\sigma_1^2} . \tag{5.A.2}$$

But σ_1/σ_2 is

$$\sigma_1/\sigma_2 = \sqrt{\frac{N_0T_b + 4P\sigma^2T_b^2}{N_0T_b}} = \sqrt{1+2a/K} . \tag{5.A.3}$$

Then, multiplying both sides of equation (5.A.2) by $2\sigma_2^2$ and making some manipulations, we can get the following equation:

$$(2a/K)\alpha^2 + 2m\alpha - (m^2 + C) = 0 , \tag{5.A.4}$$

where $C = \sigma_2^2(1+2a/K)\log(1+2a/K)$.

Thus, α can be derived by solving equation (5.A.4) to be

$$\alpha = \frac{\sqrt{m^2 + (2a/K)(m^2+C)} - m}{(2a/K)} \quad , a \neq 0 \tag{5.A.5}$$

To remove the dependence of T_b in α, we define $\alpha' = \alpha/\sigma_2$. Therefore, α' can be expressed as

$$\alpha' = \frac{\sqrt{a + (a/K)[2a + (1 + 2a/K)\log(1 + 2a/K)/2]} - \sqrt{a}}{(a/K)}, \quad a \neq 0 \qquad (5.A.6)$$

Chapter 5.B

MA1 Distribution Analysis

If we divide both sides of equation (5.63) by $\sqrt{2PT}$, then $Z_1' = Z_1/(\sqrt{2PT})$ becomes

$$Z_1' = b_0^{(1)} + D + n_1^* + \frac{1}{T}\sum_{k=2}^{N} \gamma_k \cos\Phi_k B_{k,1}(\underline{b}_k, \tau_k) \quad , \tag{5.B.1}$$

where $B_{k,1}(\underline{b}_k, \tau_k)$ is given by

$$\begin{aligned} B_{k,1}(\underline{b}_k, \tau_k) &= \int_0^T a_k(t-\tau_k) b_k(t-\tau_k) a_1(t) dt \\ &= b_{-1}^{(k)} \int_0^{\tau_k} a_k(t-\tau_k) a_1(t) dt + b_0^{(k)} \int_{\tau_k}^{T} a_k(t-\tau_k) a_1(t) dt \\ &= b_{-1}^{(k)} R_{k,1}(\tau_k) + b_0^{(k)} \hat{R}_{k,1}(\tau_k) \quad , \end{aligned} \tag{5.B.2}$$

and the continuous partial cross-correlation functions $R_{k,n}(\tau)$ and $\hat{R}_{k,n}(\tau)$ are given by

$$R_{k,n}(\tau) = \sum_{j=0}^{l-1} a_{j-l}^{(k)} a_j^{(n)} \hat{R}_\psi(\tau - lT_c) + \sum_{j=0}^{l} a_{j-l-1}^{(k)} a_j^{(n)} R_\psi(\tau - lT_c) \quad , \tag{5.B.3}$$

and

$$\hat{R}_{k,n}(\tau) = \sum_{j=l}^{\eta-1} a_{j-l}^{(k)} a_j^{(n)} \hat{R}_\psi(\tau - lT_c) + \sum_{j=l+1}^{\eta-1} a_{j-l-1}^{(k)} a_j^{(n)} R_\psi(\tau - lT_c) \, , \tag{5.B.4}$$

where $\hat{R}_\psi(\tau) = \int_\tau^{T_c} \psi(t)\psi(t-\tau)\, dt$ and $R_\psi(\tau) = \hat{R}_\psi(T_c - \tau)$, and $l = \lfloor \tau/T_c \rfloor$, and $\lfloor x \rfloor$ is the largest integer not greater than x. Therefore, l is uniformly distributed over $\{0, \ldots, \eta - 1\}$. If we let $S_k = \tau_k - lT_c$, then S_k is uniformly distributed over $[0, T_c]$.

Because the signature sequence is random, the time delay τ_k needed to be known only to the nearest chip (i.e., we can let $l = 0$), and the value of $B_{k,1}$ is independent of $\underline{b}_k$

[11]. Therefore, the continuous partial cross-correlation functions $R_{k,1}(S)$ and $\hat{R}_{k,1}(S)$ becomes

$$R_{k,1}(S) = a_{-1}^{(k)} a_0^{(1)} R_\psi(S) \quad , \tag{5.B.5}$$

and

$$\hat{R}_{k,1}(S) = \sum_{j=0}^{\eta-1} a_j^{(k)} a_j^{(1)} \hat{R}_\psi(S) + \sum_{j=1}^{\eta-1} a_{j-1}^{(k)} a_j^{(1)} R_\psi(S) \quad . \tag{5.B.6}$$

Substituting &r(S) and $\hat{R}_{k,1}(S)$ into equation (5.B.2), $B_{k,1}(S)$ becomes

$$B_{k,1}(S) = a_{-1}^{(k)} a_0^{(1)} R_\psi(S) + a_{\eta-1}^{(k)} a_{\eta-1}^{(1)} \hat{R}_\psi(S) + \sum_{j=0}^{\eta-2} a_j^{(k)} [a_j^{(1)} \hat{R}_\psi(S) + a_{j+1}^{(1)} R_\psi(S)] \quad . \tag{5.B.7}$$

If we condition on the reference sequence $a_j^{(1)} = \hat{a}_j^{(1)}$ for $j \in \{0, 1, \ldots, \eta-1\}$ and using the fact that $(\hat{a}_j)^2 = 1$, $B_{k,1}(S)$ becomes

$$B_{k,1}(S) = a_{-1}^{(k)} \hat{a}_0^{(1)} R_\psi(S) + a_{\eta-1}^{(k)} \hat{a}_{\eta-1}^{(1)} \hat{R}_\psi(S) + \sum_{j=0}^{\eta-2} a_j^{(k)} \hat{a}_j^{(1)} \left[\hat{R}_\psi(S) + \hat{a}_j^{(1)} \hat{a}_{j+1}^{(1)} R_\psi(S) \right] \quad . \tag{5.B.8}$$

Further simplification is possible by noting that $\hat{a}_j \hat{a}_{j+1} =$ fl. Let the sets α and β be defined as

$$\alpha = \{ j : \hat{a}_j \hat{a}_{j+1} = +1 \} \quad , \tag{5.B.9}$$

and

$$\beta = \{ j : \hat{a}_j \hat{a}_{j+1} = -1 \} \quad , \tag{5.B.10}$$

for $j \in \{0, 1, \ldots, (\eta - 2)\}$.

After rearranging terms, $B_{k,1}(S)$ becomes

$$B_{k,1}(S) = P_k R_\psi(S) + Q_k \hat{R}_\psi(S) + X_k f_\psi(S) + Y_k g_\psi(S) \quad , \tag{5.B.11}$$

where $P_k = a_{-1}^{(k)} \hat{a}_0^{(1)}$ and $Q_k = a_{\eta-1}^{(k)} \hat{a}_{\eta-1}^{(1)}$ are equally likely ± 1 r.v.'s, X_k is

$$X_k = \sum_{j \in \alpha} a_j^{(k)} \hat{a}_j^{(1)} \quad , \tag{5.B.12}$$

and Y_k is

$$Y_k = \sum_{j \in \beta} a_j^{(k)} \hat{a}_j^{(1)} \quad , \tag{5.B.13}$$

and $f_\psi(S) = \hat{R}_\psi(S) + R_\psi(S)$, $g_\psi(S) = \hat{R}_\psi(S) - R_\psi(S)$.

Suppose now that A and B are the cardinalities of α and β, respectively. Then X_k and Y_k are the sum of umbiased Bernoulli trials given by

$$P_{X_k}(j) = \binom{A}{\frac{j+A}{2}} 2^{-A} \quad , \; j \in \{-A, -A+2, \ldots, A-2, A\} \; , \tag{5.B.14}$$

and

$$P_{Y_k}(j) = \binom{B}{\frac{j+B}{2}} 2^{-B} \quad , \; j \in \{-B, -B+2, \ldots, B-2, B\} \; . \tag{5.B.15}$$

From the definitions of α and β, it is obvious that $A + B = \eta - 1$. Also, $A - B = C$, where C = $C_{1,1}(1)$ is the aperiodic auto-correlation of the signature sequence of user 1 with offset by one chip. Therefore, $A = (\eta - 1 + C)/2$ and $B = (\eta - 1 - C)/2$. Note that if any two of the four quantities A, B, C, and η are known, the other two can be found. The r.v. C is given by

$$C = \sum_{j=0}^{\eta-2} a_j^{(1)} a_{j+1}^{(1)} \; , \tag{5.B.16}$$

which is the sum of $\eta - 1$ umbiased Bernoulli r.v.'s, so that the density of C is given by

$$P_C(j) = \binom{\eta - 1}{\frac{j+\eta-1}{2}} 2^{1-\eta} \quad , \; j \in \{1-\eta, 3-\eta, \ldots, \eta-3, \eta-1\} \; . \tag{5.B.17}$$

Since the r.v.'s P_k, Q_k, X_k, and Y_k are composed of disjoint set of symmetric Bernoulli trials for a particular desired signature sequence, they are conditionally independent given B (or C).

Because of the symmetry of the distribution of the n_1^*, D, and $B_{k,1}(S_k) \cos \Phi_k$, the conditional BER given $b_0^{(1)}$ does not depend on the value of $b_0^{(1)}$, so we take it to be $+1$. Combining equation (5.B.1) and (5.B.11), Z_1' can be expressed in the simplified form

$$Z_1' = 1 + D + n_1^* + \sum_{k=2}^{N} \gamma_k W_k \cos \Phi_k = 1 + D + n_1^* + \sum_{k=2}^{N} I_k(S_k, \Phi_k) \quad , \tag{5.B.18}$$

where W_k is given by

$$W_k = \frac{1}{T}[P_k R_\psi(S_k) + Q_k \hat{R}_\psi(S_k) + X_k f_\psi(S_k) + Y_k g_\psi(S_k)] \; , \tag{5.B.19}$$

and the term $\sum_{k=2}^{N} I_k(S_k, \Phi_k)$ is called the multiple access interferences (MAI) which is the total interference caused by the other users in the system.

Morrow and Lehnert [5] invoke the central limit theorem to show that if the relative delays and phases between the desired and interfering users are fixed, and if a particular autocorrelation property of the desired signature sequence (i.e., the value of C or B of desired user) is also fixed, then the MA1 can be accurately modeled as a Gaussian r.v. when all interfering signature sequences are randomly generated. By using a characteristic function approach [6], however, they also showed that the MA1 also converges in distribution to a Gaussian r.v. for desired signature sequences that are completely random, provided once again that the relative delays and phases between the desired and interfering signals are fixed. This important result is also discussed in [11]. We can interpret this result as follows: when $\eta \rightarrow \infty$, the coefficient of variation of B goes to zero. This suggests that the mean of $B, (\eta - 1)/2$, can be used and conditioning is unnecessary. The question remains as to the effect of not conditioning on B and using only its mean for small η when the coefficient of variation of B is not small. Simpson [12] showed that the difference of BER and PER between conditioning on B and not conditioning on B is negligible even for η = 7. Therefore, we can just set $B = (\eta - 1)/2$ which will simplify the computation.

Based on the above arguments, we can say that P_k and Q_k are equally likely fl. X_k and Y_k can be treated as the summation of $(\eta - 1)/2$ independent unbiased Bernoulli trials. In addition, P_k, Q_k, X_k, and Y_k are conditionally mutually independent given the desired (user 1) signature sequence.

Chapter 5.C

Derivation of the Conditional Variance Ψ

In order to apply the SIGA method to derive the BER, we first have to find the conditional AWGN and MA1 variance Ψ which is defined as

$$\Psi = \text{var}\left[n_1^* + \sum_{k=2}^{N} \gamma_k W_k \cos(\Phi_k) \;\middle|\; \underline{\gamma}, \underline{\Phi}, \underline{S} \right] \quad , \tag{5.C.1}$$

where $\underline{\gamma} = [\gamma_2, \ldots, \gamma_N]$, $\underline{\Phi} = [\Phi_2, \ldots, \Phi_N]$, and $\underline{S} = [S_2, \ldots, S_N]$ are random vectors.

Since the r.v.'s P_k, Q_k, X_k, and Y_k are zero mean and conditionally independent. Moreover, n_1^* is also zero mean and independent of the MA1 terms. Using the fact that variance of summations of independent r.v.'s equals to the summations of the variance of each r.v., thus Ψ is given by

$$\begin{aligned}
\Psi &= \text{var}(n_1^*) + \text{var}\left[\sum_{k=2}^{N} \gamma_k W_k \cos\Phi_k \;\middle|\; \underline{\gamma}, \underline{\Phi}, \underline{S} \right] \\
&= \frac{1}{2a} + E\left\{ \left[\sum_{k=2}^{N} \gamma_k W_k \cos\Phi_k \right]^2 \;\middle|\; \underline{\gamma}, \underline{\Phi}, \underline{S} \right\} \\
&= \frac{1}{2a} + \sum_{k=2}^{N} \gamma_k^2 E[W_k^2 | S_k] E[(\cos\Phi_k)^2 | \Phi_k] \\
&= \frac{1}{2a} + \sum_{k=2}^{N} \frac{\gamma_k^2}{2} [1 + \cos(2\Phi_k)] \text{var}[W_k | S_k] \quad .
\end{aligned} \tag{5.C.2}$$

The conditional variance where $W = W_k$ can be computed as follows,

$$\text{var}[W_k | S_k] = \frac{1}{T^2} \{ E \quad [P^2 R_\psi^2(S) | S] + E \quad [Q^2 \hat{R}_\psi^2(S) | S] + E[X^2 f_\psi^2(S) | S] + E[Y^2 g_\psi^2(S) | S] \} . \tag{5.C.3}$$

Since P and Q are equally likely ± 1, their variance is 1. The variance of X can be found by expressing X as a sum of $(\eta-1)/2$ independent symmetric Bernoulli trials and noting that

$$E\,[X^2 f_\psi^2(S)|S] = \left(\frac{\eta-1}{2}\right) f_\psi^2(S)\,. \tag{5.C.4}$$

By similar reasoning,

$$E\,[Y^2 g_\psi^2(S)|S] = \left(\frac{\eta-1}{2}\right)\; g_\psi^2(S)\,. \tag{5.C.5}$$

Combining the above yields

$$\Psi = \frac{1}{2a} + \sum_{k=2}^{N} \gamma_k^2 Z_k \quad , \tag{5.C.6}$$

where the Z_k are identically distributed and conditionally independent given $\underline{\gamma}, \underline{S}$, and $\underline{\Phi}$, thus Z where $Z = Z_k$ for some k is specified by

$$Z = UV \quad , \tag{5.C.7}$$

where

$$U = 1 + \cos(2\Phi), \tag{5.C.8}$$

and

$$V = \frac{1}{2T^2}\left[R_\psi^2(S) + \hat{R}_\psi^2(S) + \left(\frac{\eta-1}{2}\right) f_\psi^2(S) + \left(\frac{\eta-1}{2}\right) g_\psi^2(S)\right] \quad . \tag{5.C.9}$$

Chapter 5.D

Derivation of BER for LOS-Coherent BPSK

The average BER, $\overline{P}_b$, can be evaluated by

$$\begin{aligned}\overline{P}_b &= E\left[\mathrm{Q}\left(\frac{1+D}{\sqrt{\Psi}}\right)\right] \\ &= \int_0^\infty \int_{-\infty}^\infty \mathrm{Q}\left(\frac{1+D}{\sqrt{\Psi}}\right) f_D(y) f_\Psi(\psi)\, dy\, d\psi \\ &= \int_0^\infty \mathrm{Q}\left[\frac{1}{\sqrt{\frac{1}{2k}+\psi}}\right] f_\Psi(\psi) d\psi \quad . \end{aligned} \tag{5.D.1}$$

The above integration can be interpreted as follows. If the r.v. Y equals $1 + X_1 + X_2$, where both X_1 and X_2 are zero mean Gaussian r.v.'s with variances σ_1^2 and σ_2^2, respectively, the probability $\Pr(Y < 0) = \mathrm{Q}\left[1/\sqrt{\sigma_1^2 + \sigma_2^2}\right]$. On the other hand, we can first condition on $X_1 = x_1$ and compute the conditional probability $\Pr(Y < 0 \mid X_1 = x_1) = \mathrm{Q}\,[(1 + x_1)/\sigma_2]$. Then, averaging over x_1 we should get the same result.

Because $(\eta - 2)$ fold convolutions are needed to evaluate the pdf of $f_\Psi(\psi)$ which becomes intractable as η becomes large, we can directly apply the SIGA method [8] to simplify the computation of P_b in equation (5.D.1). The idea of SIGA is that let $f(\theta)$ is a real function of θ which is a r.v. with mean μ_θ and variance σ_θ^2. Assume all the derivatives of $f(\theta)$ exist. Then, $E\,[f(\theta)]$ can be approximated by

$$E\,[f(\theta)] \approx \frac{2}{3} f(\mu_\theta) + \frac{1}{6} f(\mu_\theta + \sqrt{3}\sigma_\theta) + \frac{1}{6} f(\mu_\theta - \sqrt{3}\sigma_\theta) \quad , \tag{5.D.2}$$

which, in fact, is exact for fifth-degree polynomials and normally distributed 6'[7].

Applying the above result, the $\overline{P}_b$ can be approximated by

$$\overline{P}_b \approx \frac{2}{3}\mathbf{Q}\left[\frac{1}{\sqrt{\frac{1}{2k}+\mu_\psi}}\right] + \frac{1}{6}\mathbf{Q}\left[\frac{1}{\sqrt{\frac{1}{2k}+\mu_\psi+\sqrt{3}\sigma_\psi}}\right] + \frac{1}{6}\mathbf{Q}\left[\frac{1}{\sqrt{\frac{1}{2k}+\mu_\psi-\sqrt{3}\sigma_\psi}}\right], \tag{5.D.3}$$

where $\mu_\psi = E(\Psi)$ and $\sigma_\psi^2 = \mathrm{var}(\Psi)$.

Chapter 5.E

Derivation of μ_ψ and σ_ψ^2 for Arbitrary Chip Pulse Shapes

From equation (5.68),

$$\Psi = \frac{1}{2a} + \sum_{k=2}^{N} \gamma_k^2 U_k V_k \quad , \tag{5.E.1}$$

where

$$U_k = 1 + \cos(2\Phi_k) \ , \tag{5.E.2}$$

$$\begin{aligned} V_k &= \frac{1}{2T^2}\left[R_\psi^2(S_k) + \hat{R}_\psi^2(S_k) + \left(\frac{\eta-1}{2}\right) f_\psi^2(S_k) + \left(\frac{\eta-1}{2}\right) g_\psi^2(S_k)\right] \\ &= \frac{1}{2T^2}\left[\eta R_\psi^2(S_k) + \eta \hat{R}_\psi^2(S_k)\right] \ , \end{aligned} \tag{5.E.3}$$

Therefore, the mean value of Ψ, μ_ψ, is given by

$$\begin{aligned} \mu_\psi &\triangleq E\ [\Psi] \\ &= \frac{1}{2a} + \sum_{k=2}^{N} E\,[\gamma_k^2] E\,[1 + \cos(2\Phi_k)] \left(\frac{1}{2T^2}\right) \{\eta E\,[R_\psi^2(S_k)] + \eta E\,[\hat{R}_\psi^2(S_k)]\} \\ &= \frac{1}{2a} + \left(1 + \frac{1}{K}\right)(N-1)\left(\frac{\eta}{2T^2}\right)\{E\,[R_\psi^2(S)] + E\,[\hat{R}_\psi^2(S)]\} \ , \end{aligned} \tag{5.E.4}$$

where $0 \leq S \leq T_c$.

To facilitate the computations, we let $T_c = 1$. Then,

$$\frac{1}{T^2} E\,[\,\hat{R}_\psi^2(S)\,] = \frac{1}{\eta^2} E\,[\,\hat{R}_n^2(w)\ 1 \ , \tag{5.E.5}$$

where the normalized chip pulse shape $\psi_n(t)$ is zero except for $0 \leq t \leq 1$ and $\hat{R}_n(w) = \int_w^1 \psi_n(t)\psi_n(t-w)dt$ where $0 \leq w \leq 1$.

Now let $m_\psi = E[\hat{R}_n^2(w)] = E[R_n^2(w)]$, then μ_ψ is given by

$$\mu_\psi = \frac{1}{2a} + \left(1 + \frac{1}{K}\right)(N-1)\left(\frac{m_\psi}{\eta}\right) \quad . \tag{5.E.6}$$

Next, let us derive the variance of Ψ, σ_ψ^2, which is given by

$$\sigma_\psi^2 = \text{var}(\Psi) = (N-1)[\,E(\gamma^4 Z^2) - E^2(\gamma^2 Z)\,] \; . \tag{5.E.7}$$

Since 7 and Z are independent, $E(\gamma^4 Z^2) = E(\gamma^4)E(Z^2)$. It is not difficult to find that $E(\gamma^4) = (1 + \frac{4}{K} + \frac{2}{K^2})$. In addition, $E(Z^2) = E(U^2V^2) = E\{[1+\cos(2\Phi)]^2 E(V^2)\} = \frac{3}{2}E(V^2)$ which is given by

$$\begin{aligned} E(V^2) &= \left(\frac{1}{T^4}\right) E\left\{\left(\frac{\eta^2}{4}\right)[f_\psi^2(S) - 2R_\psi(S)\hat{R}_\psi(S)]^2\right\} \\ &= \left(\frac{\eta^2}{4T^4}\right)\{E[f_\psi^4(S)] - E[f_\psi^2(S)R_\psi(S)\hat{R}_\psi(S)] + E[R_\psi^2(S)\hat{R}_\psi^2(S)]\} \\ &= \left(\frac{1}{\eta^2}\right)\{\frac{1}{4}E[f_n^4(w)] - E[f_n^2(w)R_n(w)\hat{R}_n(w)] + E[R_n^2(w)\hat{R}_n^2(w)]\} \end{aligned} \tag{5.E.8}$$

For rectangular chip pulse shape $\hat{R}_n(w) = 1 - w$ and $f_n(w) = 1$. Then, $E(Z^2)$ becomes

$$E(Z^2) = \left(\frac{7\eta^2}{40}\right)\left(\frac{1}{\eta^4}\right) \; . \tag{5.E.9}$$

In [7], $E(Z^2) = (7\eta^2 + 2\eta - 2)/40$. Compare with the above result, the difference results from (1) Holtzman making the normalization in the decision statistic in equation (5.65) which accounted for the factor $1/\eta^4$; and (2) treating B mentioned in Appendix 5.B as a r.v., which is just a constant $(\eta - 1)/2$ in this analysis, thus adding the terms $(2\eta - 2)$ to the numerator.

Therefore, $E[\gamma^4 Z^2]$ can be expressed as

$$E(\gamma^4 Z^2) = \left(1 + \frac{4}{K} + \frac{2}{K^2}\right)\left(\frac{3}{2}\right)\left(\frac{1}{\eta^2}\right)\left\{\frac{1}{4}E[f_n^4(w)] - E[f_n^2(w)R_n(w)\hat{R}_n(w)] + E[R_n^2(w)\hat{R}_n^2(w)]\right\} . \tag{5.E.10}$$

It is straightforward to compute the values of $I_1 = E[f_n^4(w)]$, $I_2 = E[f_n^2(w)R_n(w)\hat{R}_n(w)]$, and $I_3 = E[R_n^2(w)\hat{R}_n^2(w)]$ by using numerical method. These values for three commonly used pulse shapes are listed in Table 5.E.1.

Finally, $E(\gamma^2 Z)$ is given by

$$E(\gamma^2 Z) = E(\gamma^2)E(U)E(V) = \left(1 + \frac{1}{K}\right)\left(\frac{m_\psi}{\eta}\right) \quad . \qquad (5.E.11)$$

	I_1	I_2	I_3
Rectangular	1	$1/6$	$1/30$
Half-Sine	0.497	0.217×10^{-1}	0.324×10^{-2}
Raised-Cosine	0.350	0.185×10^{-2}	0.190×10^{-3}

Table 5.E.1: Values of I_1, I_2, and I_3 for Rectangular, Half-Sine, and Raised-Cosine Pulse Shapes

Chapter 5.F

Derivation of PER for LOS-Coherent BPSK

Averaging $g\left(\mathrm{Q}[(1+D)/\sqrt{\Psi}];L,t\right)$ over D and Ψ yields the unconditional PER as

$$P_E = E_{\Psi,D}\left\{g\left(\mathrm{Q}\left[\frac{1+D}{\sqrt{\Psi}}\right];L,t\right)\right\} = \int_{-\infty}^{\infty}\int_{0}^{\infty} g\left(\mathrm{Q}\left[\frac{1+y}{\sqrt{\psi}}\right];L,t\right) f_{\Psi}(\psi)\, f_D(y)d\psi\, dy\,. \tag{5.F.1}$$

Notice that g $\left(\mathrm{Q}[(1+D)/\sqrt{\Psi}];L,t\right)$ is a real function of the r.v. Ψ. Another application of (5.D.2) yields a computationally simple approximation for the conditional PER, $P_E(D)$, as

$$\begin{aligned} P_E(D) &= \int_0^{\infty} g\left(\mathrm{Q}\left[\frac{1+D}{\sqrt{\Psi}}\right];L,t\right) f_{\Psi}(\psi)\, d\psi \qquad (5.F.2)\\ &\approx \frac{2}{3}g\left(\mathrm{Q}\left[\frac{1+D}{\sqrt{\mu_\psi}}\right];L,t\right) + \frac{1}{6}g\left(\mathrm{Q}\left[\frac{1+D}{\sqrt{\mu_\psi+\sqrt{3}\sigma_\psi}}\right];L,t\right) + \frac{1}{6}g\left(\mathrm{Q}\left[\frac{1+D}{\sqrt{\mu_\psi-\sqrt{3}\sigma_\psi}}\right];L,t\right)\,. \end{aligned}$$

Therefore, the PER for LOS-coherent BPSK can be approximated by

$$\begin{aligned} P_E &\approx \int_{-\infty}^{\infty} P_E(y) f_D(y)\, dy \qquad (5.F.3)\\ &= \int_{-\infty}^{\infty}\left\{\frac{2}{3}g\left(\mathrm{Q}\left[\frac{1+D}{\sqrt{\mu_\psi}}\right];L,t\right) + \frac{1}{6}g\left(\mathrm{Q}\left[\frac{1+D}{\sqrt{\mu_\psi+\sqrt{3}\sigma_\psi}}\right];L,t\right) + \frac{1}{6}g\left(\mathrm{Q}\left[\frac{1+D}{\sqrt{\mu_\psi-\sqrt{3}\sigma_\psi}}\right];L,t\right)\right\} f_D(y)\, dy\,, \end{aligned}$$

where $f_D(y) = \sqrt{K/\pi}\exp(-Ky^2)$.

5.5 References

[1] M.B. Pursley, "Performance Evaluation for Phase-Coded Spread-Spectrum Multiple-Access Communication – Part I : System Analysis", *IEEE Trans. Comm.*, Vol. COM-25, pp. 795-9, Aug 77

[2] E.A. Geraniotis, M.B. Pursley, "Error Probability for Direct-Sequence Spread-Spectrum Multiple-Access Communications-Part II : Approximations,, , *IEEE Trans. Comm.*, Vol. COM-30, pp. 985-95, May 82

[3] J. Lehnert, M.B. Pursley, "Error Probability for Bonary DS Spread-Spectrum Communications with Random Signature Sequences", *IEEE* Trans. *Comm.*, Vol. COM-35, pp. 87-98, Jan 87

[4] J.M.N. Pereira, "Modeling of Fading Channels in the IVHS Environment", Univ. *South. Cal.*, Aug 92

[5] R. K. Morrow, J. S. Lehnert, "Bit-to-Bit Error Dependence in Slotted DS/SSMA Packet Systems with Random Signature Sequences", *IEEE Trans. Comm.*, Vol. COM-37, pp. 1052-61, Oct 89

[6] ———, "Packet Throughput in Slotted ALOHA DS/SSMA Radio Systems with Random Signature Sequences", *IEEE Trans. Comm.*, Vol. COM-40, pp. 1223-30, Jul 92

[7] J.M. Holtzman, "A Simple Accurate Method to Calculate Spread-Spectrum Multiple-Access Error Probabilities", *IEEE Trans. Comm.*, Vol. COM-40, pp. 461-4, Mar 92

[8] ——, "On Using Perturbation Analysis to do Sensitivity Analysis: Derivatives versus Differences", *IEEE Truns. Avt. Control*, Vol. AC-37, pp. 243-7, Feb 92

[9] B. Sklar, *Digital Communications —Fundamental and Applications*, Prentice-Hall, 1988

[10] J. Proakis, *Digital Communication*, 2nd Ed., McGraw-Hill, 1989

[11] M. Georgiopoulos, "Packet Error Probabilities in Direct-Sequence Spread-Spectrum Radio Networks", ***IEEE T***runs. ***Comm.,*** Vol.COM-38, pp. 1599-606, Sep 90

[12] F. D. Simpson, Direct Sequence *CDMA* ***Performance Analysis*** Methodologies, Ph.D. Dissertation, Rutgers Univ., 1992

[13] W. Feller, ***In Introduction to Probability Theory and its Application,*** Vol. II, New York: John Wiley, 1966

Chapter 6

Simulation for IVHS Communications

6.1 Introduction

The objective of IVHS simulation is to develop a software simulation tool to substantiate the conceptual design for IVHS communications which consists of the infrastructure layout, the mobility of vehicles, the channel characteristics, and the network protocol as depicted in Figure 6.1.

In general, performance data can be obtained by mathematical analysis or software simulation. Software simulation of IVHS communications, however, is by necessity the primary analytic tool due to the following intangible factors in IVHS communications which render mathematical analysis intractable:

- the huge number of mobiles;
- the subtle fading effects which depend on the location of the vehicles on the highway and on the infrastructure layout;
- the probabilistic nature of the network protocol used for sending messages; and
- the intricate combination of all the above.

Software simulation can generate the performance data of IVHS communication systems. With the performance data, we can validate the conceptual design and then optimize them. The success of the design process cannot be guaranteed without this tool.

This Chapter will describe the simulation approach in Section 6.2, the models and assumptions of the simulation in Section 6.3, the structure of the simulation program in Section 6.4, some instruction for using the program in Section 6.5, examples and performance results from the simulation in Section 6.6, and finally, prospective extensions for IVHS simulations in Section 6.7.

6.2 Simulation Approach

Software simulation tools can be implemented either by in-house efforts, by using commercially available simulation packages, or a combination of both. During the initial stage of this project, we surveyed several existing simulation packages, such as OPNET, MODSIM, etc., and analyzed their advantages and disadvantages. The advantages are summarized as follows.

- Reducing the time and the effort to develop the program *if* the problem is ***suitable for the simulation*** package.
- Writing the simulation program may become standard, which other people can easily proceed.
- The packages usually have well developed graphical interfaces which can be used for education and demonstration purposes.

However, we also found some critical shortcomings of the commercial packages.

- These packages do not provide sufficient library functions to simulate an IVHS system, especially the vehicles' mobility and the fading channel.
- Training overheads are necessary to learn how to use the packages.

- Auxiliary programs would have to be written to compensate the deficiency of the packages, and interface problems during software linkage can be an issue.
- The packages require long computational times and large memory spaces. Table 6.1 shows a comparison between the requirement of using OPNET and a program written in C language for simulating an M/M/l queue.
- The packages provide few or limited debugging tools, rendering the development of the simulation difficult.
- The packages are not portable because they are required to be developed and run in licensed computers.

Due to the limited survey of the packages and the tight schedule of this Project, it was decided to implement an internal interim simulation program in the C language. This program will be a prototype of IVHS simulation and will help in building a complete software simulation tool even if it is decided to use a commercial package.

6.3 Modeling and Assumptions

The software development attempts to implement a model of IVHS communications in the following three major functional parts:

- Mobility: simulation of the movement of vehicles.
- Channel: simulation of the channel effects including multipath fading, noise, and multi-access interference.
- Network: simulation of the multi-access network protocols in which the multiple users send messages via a common channel.

A full blown simulation of IVHS is a very complex undertaking, well beyond the scope of Phase I of this Project. The simulation prototype developed relies on an array of simplifying assumptions as a first step. These assumptions are described below for the three areas identified above.

6.3.1 Mobility

The objective of Mobility is to simulate the movement of the vehicles in a sector of a highway, called the cell. The cell has the following structure in the simulation :

- The cell consists of one direction and several lanes. (The actual number of lanes, ***lanenumber,*** and the distance between the center of each lane to the highway boundary, $yr[l], l = 1, \cdots,$ ***lanenumber,*** should be given as inputs to the simulation.)

- Each lane has the same end-to-end distance. (The actual distance, $cell\_size$, should be given as input.)

The vehicles travel through the cell, and the following is assumed:

- The vehicles will follow the geometry depicted in Figure 6.2, and will be assumed identical and pointlike (i.e., zero size).

- The vehicles will enter the cell in a given cell from one end, according to independent Poisson processes such that the distance between two successive vehicles in a particular lane is exponentially distributed. (The actual average distances, $ave\_car\_distan[l], l = 1, \ldots,$ ***Zunenumber,*** should be given as inputs to the simulation.)

- The vehicles will be inactive (i.e., keep radio silence) after they reach the center of the cell at which the base station is located.

- Each vehicle in the cell keeps constant speed, and the speed of all vehicles in a particular lane is the same. (The actual speed of each lane, $car\_speed[l], l = 1, \cdots,$ ***lanenumber,*** should be given as input to the simulation.)

- The vehicles will not change lane or overtake other vehicles.

6.3.2 Channel

Here, we attempt to simulate the error status of each bit and each packet due to channel effects, including fading, noise, and multiple-access interference for the given communication link from the vehicle to the base station. Channel models for TDMA and CDMA are developed separately. Their common assumptions include:

- The base station is located at the intersection of the center of the cell and the highway boundary.
- For transmissions, a given carrier frequency is used to provide the appropriate bit rate. (The actual carrier frequency, $freq$, and bit rate, bit_rate, should be given as inputs to the simulation.)
- The base station's receiving antenna has a specific antenna height and antenna gain. (The actual antenna height, h_r, and antenna gain, $gain\_r$, should be given as inputs.)
- The power of radio signals attenuates as the inverse square of the distance.
- Noise is combined urban and thermal noise with a Gaussian distribution.
- Fading is Rician consisting of the line-of-sight component and Rayleigh scattered components. (The actual power ratio between the line-of-sight and the scattered components is defined as the K-factor, k_factor, given as input parameter of the simulation.)
- The received power due to Rayleigh-scattered fading is assumed independent from packet to packet but remains fixed within the packet.
- Bit errors within a frame or a slot are statistically independent; so are packet errors independent.
- The base station can have some error-correcting capability and full error-detecting capability. (The actual error-correctable number of bits per packet, $correc\_length$, should be given as input of simulation.)

For specifics of TDMA and CDMA, the following must be noted. The TDMA case involves the following additional assumptions:

- Noncoherent FSK modulation is used.
- Both the urban noise and the Rician fading contribute to the bit and packet errors. (The actual noise temperature is fixed at 31547.3°K., i.e., . . . dB above KT_0B.)

The CDMA case has the following additional assumptions:

- Direct-sequence spread spectrum is used. (The actual spreading ratio of the direct-sequence system, ***spread-ratio,*** should be given as an input to the simulation.).
- The base station and vehicle transmitter possess a power control mechanism to maintain the received line-of-sight power at a certain fixed signal-to-noise ratio irrespective of its location. (The actual signal-to-noise, ***eb-over-n,*** should be given as input to the simulation.)
- Noise, fading, and multiple-access interference due to other users in this common channel contribute to bit and packet errors.
- The above effects are assumed to be statistically independent at the different spread spectrum receivers at the base station.

6.3.3 Network

Here, we attempt to simulate the protocol which controls the packet transmissions via this common channel. The data traffic is assumed as follows:

- Each vehicle needs to send a message in a fixed packet length (initially set to be one packet) to the base station. (The actual number of bits per packet, ***pktlength,*** should be given as an input to the simulation.)
- Each vehicle initiates its channel access when it enters the cell, and ends after successfully finishing transmission or when leaving the cell.

For specifics of TDMA and CDMA, the following is noted. The TDMA protocol uses reservation ALOHA with the following assumptions:

- The schedule of packet transmission is divided into a sequence of frames. Each frame consists of several data slots and activation slots (i.e., request slots) as in Figure 6.3. Each data slot is allocated for the transmission of one data packet while the activation slot is used for sending the control packet to inform the base station to reserve a data slot for transmitting a data packet. (The actual frame size, ***frame-size,*** number of data slots in a frame, *data_slot_number*, and number of activation slots in a frame, *activa_slot_number*, should be given as inputs to the simulation.)

- Each vehicle with a data packet to send should first send a control packet randomly in one of the activation slots of the current frame.

- If no collision occurs, the base station will reserve a data slot in one of the future frames on a first come first served basis and will inform the vehicle of the timing of transmission; otherwise, the vehicle re-sends the control packet in the same way until it succeeds.

- Once it finishes this reservation procedure, the data packet will be sent in the assigned data slot of the assigned frame.

- Channel fading and noise may corrupt the data packet transmitted in the data slot; transmissions of control, handshaking, and acknowledgement messages are assumed to be free of errors.

- If a data packet is received with errors at the base station, the base station will reserve another data slot in the next frame for retransmission.

The CDMA protocol uses slotted-ALOHA with the following assumptions.

- The base station has an infinite number of CDMA receivers and an infinite number of available orthogonal code sequences.

- Each vehicle is assigned a code sequence different from those assigned to the other vehicles and keeps using the given code until its transmission finishes.
- Noise, fading, and other vehicles' interference may corrupt the transmission of a particular data packet.
- An error packet should be retransmitted in any subsequent slot with a certain retransmission probability until its transmission succeeds. (The actual retransmission probability, *retx_prob*, should be given as an input to the simulation.)

6.4 Structure and Operation of the Simulation

In general, a simulation program can only simulate the state of a continuous-time system in sequence of discrete instants. One of two sampling techniques can be used: periodic or event-driven. In our simulation, the network protocol operates synchronously with the frame in TDMA or the slot in CDMA. In addition, the position of the moving vehicles and the fading channel will change little between two consecutive frames or slots. Therefore, the program will simulate the system state only at the boundaries of the frame in TDMA or the slot in CDMA. All the events are assumed to occur at these periodic sampling instants; the events happening between two consecutive instants are moved to the earliest sampling instant.

The simulation program is organized in several parts as shown in the Figure 6.4 (with each of the blocks implementing several functions):

1. Input and Initialization:
   Inputs data $(Input())$, preprocesses the input data $(Pre\_Calcul())$, and initializes the state variables of the simulation machine $(Initia())$.
2. Mobility:
   Simulates the entrance/exit of the vehicles in/from the cell, and calculates the position of the vehicles ***(Mobile()).***
3. Channel:

Calculates the signal-to-noise ratio (*Signal_To_Noise*()), the error probability of a received bit (*Bit_Error_Rate*()), and the error status of a received packet (*Packet_Error_Stati*

4. Network:
   Simulates the request (*Reques*()), reservation (*Reserv*()) and transmission/retransmission (*Transm*()) procedures.

5. Probing and Output:
   Collects the performance data, calculates the statistical average (*Statis*()), and outputs the results (*Output*()).

6. Clock and Stochastics:
   Generates the samples of the random variables involved (*Random_Number*(), *Expone*()), and simulates the progress of time (*main*()).

6.4.1 Input and Initialization

This part includes *Input*, *Precal*(), and *Initia*(). *Input* is for inputing data. Common to both CDMA and TDMA simulations are :

- *seed*: initial value of the random number generator;
- *time_limit*: length of real time simulated;
- *cell_size*: cell size;
- *lane_number*: number of lanes;
- $car\_speed[l], l = 1, \cdots, lane\_number$: speed of vehicles on each lane;
- $ave\_car\_distan[l], l = 1, \cdots, lane\_number$: average distance between two consecutive vehicles on each lane;
- *bit_rate*: data rate;
- k_factor: K-factor of Rician fading;
- $frame\_size$: frame cycle time;

- *pkt_length*: number of bits per packet; and
- *correc_length*: number of error-correctable bits per packet.

For TDMA, the following specific input data is also required:

- ***freq:*** carrier frequency;
- $yr[l], l = 1, \cdots,$ ***lane-number:*** transversal distance from the center of the lane to the base station;
- *h_tx*: vehicle's antenna height;
- *h_rx*: base station's antenna height;
- ***power-tx:*** vehicle's transmitting power;
- ***gain-tx:*** vehicle's antenna gain;
- gainrx: base station's antenna gain;
- *activa_slot_number*: number of request slots per frame;
- *data_slot_number*: number of data slots per frame;
- excessloss: additional loss in the system.

For CDMA, the following input data is required.

- ***eb-over-n:*** signal-to-noise ratio of the received signal at the base station;
- ***spread-ratio:*** spreading ratio;
- *retx_prob*: retransmission probability;

Precal() calculates the average time delay between two consecutive vehicles on each lane by their average distance. *Initia*() computes the time when the initial vehicle arrives for each lane, clears the arrays which store the location information and history of the vehicles, and resets the counters for statistical analysis.

6.4.2 Mobility

This part involves the following key variables:

- Each vehicle has an ID, $(l,$ j), whichmeans that the vehicle comes in the order of j on lane ***1.*** (j should be module $LANESIZE$ to prevent this number from being too large to save the memory size where $LANESIZE$ is the assumed maximum number of vehicles on each lane.) To save memory space, the ID may be encoded in one number, ***k = 1 * LANSIZE + j.***

- $car\_status[l][j]$: the transmission status of the vehicle with ID = (l,j): ***status*** = -1 means that this variable is empty; ***status*** = 0 means that a vehicle just enters and its transmission has not been reserved yet; ***status*** = 1 means that a vehicle has been scheduled for transmission; and ***status*** = ∞ means that a vehicle has finished its transmission and is currently timed-out.

- $time\_next\_car\_arrive[l]$: the time when the next vehicle will arrive on lane ***1;***

- $time\_car\_enter\_cell[l][j]$: the ime when the existing vehicle with ID = (l,j) entered the cell;

- $time\_car\_exit\_cell[l][j]$: the ime when the existing vehicle with ID = (l,j) will pass the center of the cell and become inactive.

- $list\_new\_car[i]$: the list of the ID's of the vehicles generated in the latest frame.

This part of the simulation proceeds in the following way:

1. If the current time, ***time,*** is greater than $time\_next\_car\_arrive[l]$, then the program should generate a new vehicle for lane ***1,*** issue an ID, (l,j), and initialize a set of variables to store the information of this new vehicle.

2. The entrance time of the newly generated vehicle is stored in ***time-cur-enter-cell[l]Ij]*** and the exit time in $time\_car\_exit\_cell[l][j]$ calculated from $car\_speed[l]$ and ***cell-size.***

3. The program should update the time the next vehicle will arrive, $time\_next\_car\_arrive[l]$, by a random sample from exponentially distributed random number generator $Expone()$.

4. Collect all the new vehicles in the list of $list\_new\_car[i]$ for future use by Channel and Network.

5. If current time, time, is greater than $time\_car\_exit\_cell[l][j]$, then the program should collect the statistical data contributed by the vehicle with ID = (l, j), and update the overall performance measures, including average number of vehicles per lane, throughput, reservation delay, transmission delay, and probability of escape. Then the vehicle's ID and the associated variables will be cleared and returned for future reuse.

6.4.3 Channel

This part of the simulation proceeds in this way:

1. The program calculates the signal-to-noise ratio, snr, using the position of the vehicles in the highway via $Signal\_To\_Noise()$.

2. The program generates the random sample of the Rician fading used for the current packet in $Bit\_Error\_Rate()$.

3. The program calculates the bit error probability by using the bit error rate formula for the above generated fading strength via $Bit\_Error\_Rate()$.

4. The program simulates the error status of each bit in a packet by generating a sequence of Bernoulli trials using the above bit error rate in $Packet\_Error\_Status()$ as the parameter.

5. The program generates the error status of a packet by the error status of its bits via $Packet\_Error\_Status()$: if the number of the error bits is greater than the number of correctable bit errors, then there is a packet error, i.e., ***status*** = 1; otherwise, $status$ = 0.

TDMA and CDMA have specific *Signal_To_Noise*() and *Bit_Error_Rate*() functions. In *Signal_To_Noise*() for TDMA, the received signal-to-noise ratio is calculated from

$$\begin{aligned} \frac{E_b}{N_0}\,(\mathrm{dB}) &= \frac{E_b}{N_e} - L\ (\mathrm{dB})\ , \\ \frac{E_b}{N_e} &= \frac{P_r T_b}{N_e}\ , \\ P_r &= P_t g_t \left(\frac{c}{4\pi f_c d}\right)^2 g_r\ , \\ d &= \sqrt{x^2 + y^2 + (ht - h_r)^2}\ , \end{aligned} \tag{6.1}$$

where

- E_b/N_e is the signal-to-overall-noise ratio,
- L is the additional system loss,
- P_t is the vehicle's transmitter power,
- P_r is the the base station's received power,
- g_t is the vehicle's transmitter antenna gain,
- g_r is the base station's receiver antenna gain,
- h_t is the vehicle's transmitter antenna height,
- h_r is the base station's receiver antenna height,
- T_b is the data rate,
- f_c is the carrier frequency,
- c = 3 x 10^8 m/s is the speed of the light in free space,
- $T_b = 31547.3^0 K$ is the effective system noise temperature,
- d is the distance between the vehicle and the base station, and
- x, y are the coordinates of the vehicle assuming that the base station is at the origin (see Figure 6.2).

In *Bit_Error_Rate()* for TDMA, the per bit error probability employing noncoherent FSK is calculated by

$$P_b = \frac{1}{2}\exp\left(-\frac{E_b}{2N_0}\gamma^2\right), \tag{6.2}$$

where $\gamma^2 = (1 + x_c)^2 + x_s^2$, x,, $x_s \sim \mathcal{N}\left(0, \frac{1}{2K}\right)$ are components of the Rician fading. K is the K-factor of the Rician fading. A Gaussian random variable x of zero mean and variance σ^2 may be generated by $x = \sqrt{z}cos(\theta)$ where z is the random variable of $2\sigma^2$-mean exponential distribution and 19 is a random variable uniformly distributed over $[0,2\pi]$.

CDMA does not need *Signal_To_Noise()* since the signal-to-noise ratio is fixed by the receiver power control mechanism. *Bit_Error_Rate()* will calculate the per bit error probability from

$$\begin{aligned} P_b &= \mathbf{Q}\left(\frac{1+D}{\sqrt{\Psi}}\right), \\ D &\sim \mathcal{N}(0,\sigma^2) = \mathcal{N}\left(0,\frac{1}{2K}\right), \\ \Psi &= \frac{1}{2a} + \frac{1}{2N}\sum_{k=2}^{m}\gamma_k^2(1+cos2\Phi_k)(1-2S_k+2S_k^2), \end{aligned} \tag{6.3}$$

where

- P_b is the bit error rate,
- $\mathbf{Q}(x)$ is the Q function obtained by $Qf()$.
- $1 + D$ is the in-phase component of the Rician fading with Gaussian distribution with variance $\frac{1}{2K}$.
- Ψ is the conditional variance due to AWGN and multiple-access interference.
- $\frac{E_b}{N_0}$ is specified by the signal-to-noise ratio in *Input()*.
- m is the total number of users present in the current slot in *Mobile()*.
- $\gamma_k^2 = (1 + x_{ck})^2 + x_{sk}^2$ is a noncentral χ^2 where $x_{ck}, x_{sk} \sim \mathcal{N}\left(0, \frac{1}{2K}\right)$.
- $\Phi_k \sim$ uniform distribution over $[0, 2\pi]$, and
- $S_k \sim$ uniform distribution over [0, 1].
- N is the spreading ratio.

6.4.4 Network

There are some key variables in this part.

- *list_new_car*[]: the list of the IDs of the vehicles generated in the latest frame from *Mobile*(); *n-new* is the number of elements in this linear list.
- *reques_queue*[]: the queue of the IDs of each vehicle having requested for sending message; *nreques* is the number of elements in this queue.
- *reserv_queue*[]: the queue of the IDs of the vehicles with reservation being made for transmission in the TDMA protocol or those vehicles ready to transmit or retransmit in the coming slot in the CDMA protocol; *n_reserv* is the number of elements in this queue.

TDMA operational specifics are as follows.

1. Add the newly arrived vehicles to the request queue; each of these vehicles sends a control packet in one of the randomly selected activation slots in the frame (*Reques*()).
2. Check which of those vehicles sending the control packets to the base station can succeed in contending for these activation slots, and include the IDs of those vehicles in the reservation queue (*Reserv*()).
3. Check which vehicles in the reservation queue should transmit in the current frame and determine if each of their transmissions is correctly received by the base station. If it is, remove the ID from the request and the reserve queues; otherwise, leave the reservation as is for retransmission in the next frame (*Transm*()).

CDMA operational specifics are as follows.

1. Add the the newly arrived vehicles to the request queue (*Reques*()).

2. Check which vehicles should send data packets in the coming frame: for a new vehicle which never transmitted a data packet, allow it to transmit immediately; otherwise, decide whether or not it should retransmit its packet by comparing the sample of a [0,1] uniformly distributed random number generator and the retransmission probability ($Reserv()$).

3. Check which vehicles can succeed in transmitting the data packets. If one does, remove its ID from the request and the reservation queues; otherwise leave the reservation for retransmission in the a coming frame ($Transm()$).

6.4.5 Output

This part includes $Statis()$ and $Output()$. $Statis()$ calculates the statistics of the performance measures, including average number of vehicles per lane, average signal-to-noise ratio (TDMA only), average probability of bit error, average packet error rate, average transmission delay, average reservation delay (TDMA only), and probability of escape. $Output()$ displays these performance measure.

6.5 Limitations and I/O

The program is written in the C language which is highly portable. The program needs less than 200 kbytes of memory space and the execution time is one fiftieth of the real time simulated when running in a SPARC ELC work station.

6.5.1 Limitations

The limitations on the simulation program are set by the constants at the beginning of the program:

- *LANESIZE:* maximum number of simultaneous vehicles per lane that the program can handle;

- *LANENUM:* maximum number of lanes in the cell;
- *MAXACTSLO:* maximum number of activation slots per frame (TDMA only); and
- *MAXNEW*: maximum number of new vehicles generated in a frame;
- *MAXQUE:* maximum number of elements in the request or the reservation queue.

By modifying these constants, the limitations on the program can be altered.

6.5.2 Input and Output

The input and output are set from or to the standard I/O, i.e., the keyboard and the monitor, respectively. In a computer with the unix operating system, the input and the output can be directed to two chosen files. For example, the command "a.out<in>out" means that the simulation program with the executable code "a.out" will input from the file "in" and output to the file "out".

6.6 Examples and Results

A typical example of input and output values corresponding to the normal highway condition follows. The input for TDMA is

- initial value of the random number generator: 60000;
- real time simulated: 3600 sec;
- sampling interval: 0.00958 sec;
- cell size: 1 mile;
- number of lanes: 5;
- speed of vehicles on each lane: 45, 52.5, 60, 67.5, 75 mph; and

- average distance of two consecutive vehicles on each lane: 8, 16, 16, 20, 30 m;
- distance from the center of each lane to the base station: 5, 9, 13, 17, 21 m;
- carrier frequency: 900 MHz;
- data rate: 500 Kbps;
- vehicle's antenna height: 1.6 m;
- base station's antenna height: 8.7 m;
- vehicle's transmitting power: 10 mW;
- vehicle's transmitting antenna gain: 0 dB;
- base station's receiving antenna gain: 3 dB;
- K-factor of Rician fading channel: 10 dB;
- frame cycle time: 0.00958 sec;
- number of activation slots per frame: 16;
- number of data slots per frame: 4;
- packet length: 512 bits;
- error correcting capability per packet: 0 bit;
- additional loss: 1 dB;

The following output results are generated:

- average number of vehicles in each lane: 99.3, 50.3, 50.4, 40.9, 27.3;
- average signal-to-noise ratio: 19.0 dB;
- average bit error rate: 0.000045;
- packet error rate: 0.0025;
- average reservation delay: 0.000037 sec;

- average transmission delay: 0.0096 sec; and
- probability of escape: 0.

The input for CDMA is

- initial value of the random number generator: 60000;
- real time simulated: 3600 sec;
- sampling interval: 0.012 sec;
- cell size: 1 mile;
- number of lanes: 5;
- speed of vehicles on each lane: 50, 55, 60, 65, 70 mph;
- average distance between two consecutive vehicles on each lane: 8, 16, 16, 20, 30 m;
- distance from the center of each lane to the base station: 5, 9, 13, 17, 21 m;
- data rate: 48.387 Kbps;
- signal-to-noise ratio at the base station: 13 dB;
- K-factor of Rician fading channel: 10 dB;
- slot cycle time: 0.012 sec;
- spreading ratio: 31;
- retransmission probability: 1.0;
- packet length: 512 bits; and
- error correcting capability per packet: 0 bit;

The program generates the following output results:

- average number of vehicles on each lane: 96.9, 50.6, 48.4, 40.4, 26.4;
- average bit error rate: 0.00014;
- packet error rate: 0.015;
- average transmission delay: 0.01216 sec; and
- probability of escape: 0.

We now present some performance results for a simple IVHS communications scenario using either TDMA or CDMA. We assume that each message consists of one packet, which is the case for Automatic Vehicle Identification (AVI) application. Table 6.2 shows the delay performance of TDMA while Table 6.3 shows that of CDMA. The input parameters are those of the above section with slight modification for different cases of the highway traffic: light, medium, or heavy. The results indicate that the delay varies little even for different highway traffic intensities. In addition, it shows that the TDMA has a slightly shorter delay than CDMA. This is because of the shorter frame cycle time, i.e. 9.58 ms, in TDMA (cf. 12 ms in CDMA).

6.7 Extensions

In this phase, we have successfully implemented a simple simulation program for the performance of IVHS communications and tested a few examples to compare the performance of TDMA and CDMA protocols. The current cases of simulation implement only a simple case of IVHS communications, but it can be extended to simulating any IVHS system of interest. Extensions of current work to more general IVHS communication simulations include:

- Mobility :

  A more intricate and realistic highway traffic model will be considered. The vehicles will be able to change their speeds, change their lanes, pass other vehicles, etc. The physical dimensions of the vehicles should be nonzero and function of vehicle types.

- Channel:

  An efficient simulation method will be sought to expedite our simulation for the complex channel fading effects (for the models givens in Chapter 4) which depend on the position of the vehicles in the highway. Interference due to adjacent cells will be considered.

- Network:

  A more general model for the messages will be considered, and priority schemes will be included in the communication services. Various kinds of multiple-access communication protocols will be implemented. Inter-cell communications will also be considered.

	Execution Time	Memory Space
OPNET	205 **sec**	893 **k**
C	**1.3 sec**	33 **k**

Table 6.1: Comparison of OPNET and C for simulating an M/M/l queueing system

Vehicle Speed (mph)	Average Inter-Vehicle Distance (m)	Transmission Delay (ms)
90,95,100,105,110	16,32,32,40,60	9.605
50,55,60,65,70	8,16,16,20,30	9.600
10,10,10,10,10	2,2,2,2,2	9.616

Table 6.2: Average delay of TDMA protocol for AVI communications (5 lanes)

Vehicle Speed (mph)	Average Inter-Vehicle Distance (m)	Transmission Delay (ms)
90,95,100,105,110	16,32,32,40,60	12.173
50,55,60,65,70	8,16,16,20,30	12.163
10,10,10,10,10	2,2,2,2,2	12.181

Table 6.3: Average delay of CDMA protocol for AVI communications (5 lanes)

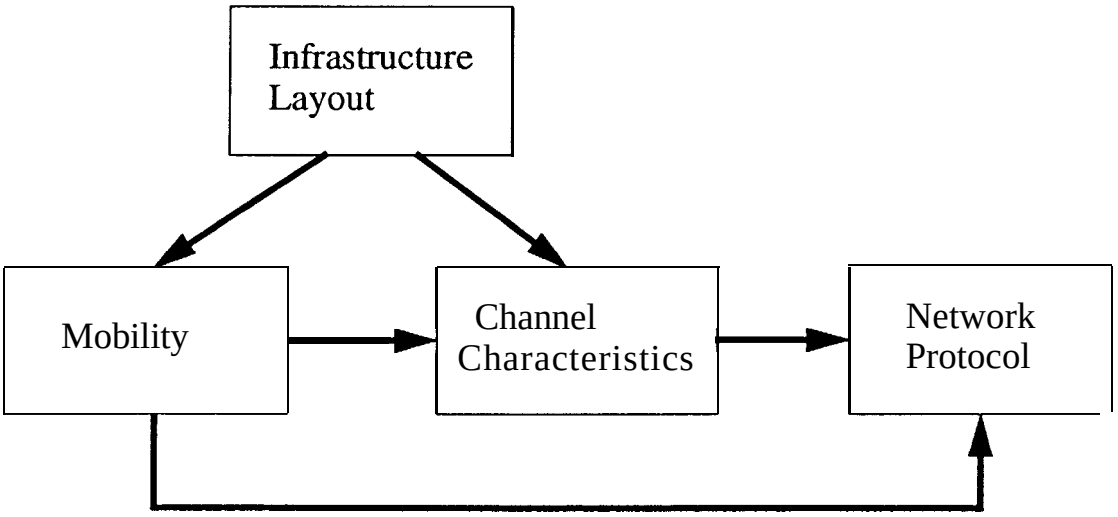

Figure 6.1: Functional block diagram of IVHS communications

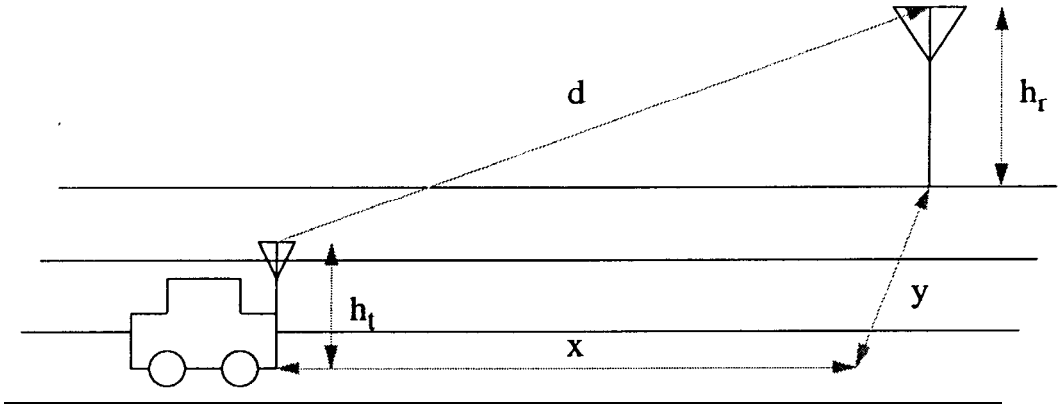

Figure 6.2: Physical configuration of the vehicle in the cell

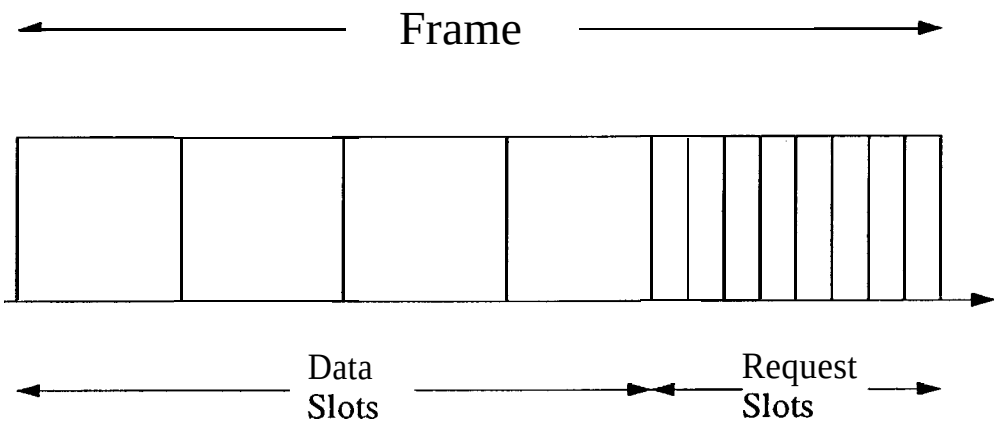

Figure 6.3: Frame structure for the reservation-ALOHA TDMA network protocol

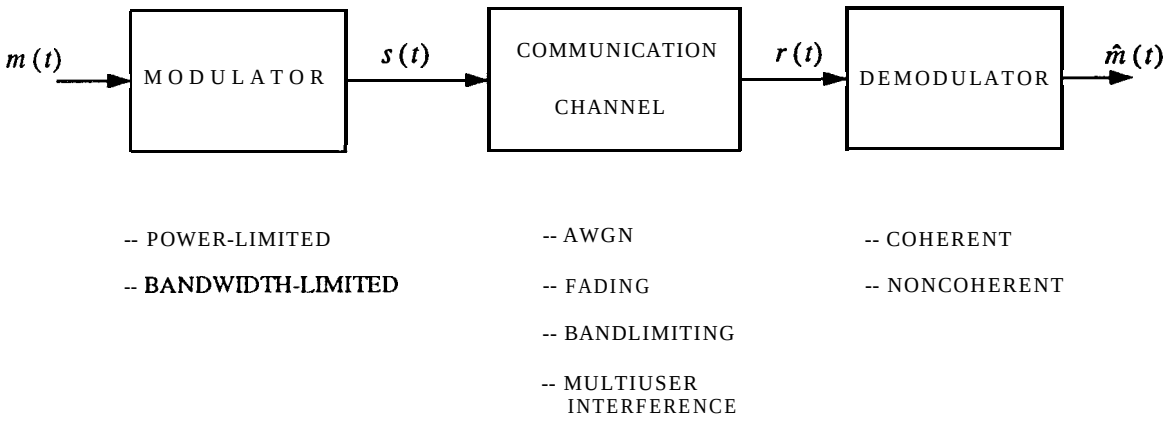

Figure 6.4: Functional block diagram of the IVHS simulation program

Chapter 7

System Layout and Architectural Tradeoffs

7.1 Introduction

In Chapter 4 we developed an extensive set of channel models that have exposed a substantial number of parameters that can be traded-off in system design. In chapter 5 we derived a number of performance results for both the TDMA and CDMA access approaches that could be adopted in IVHS communication system design. Among the host of parameters are base station (BS) location, BS antenna configuration, highway geometry, cell size, frequency band, transmit power, modulation schemes, mobile (M) antenna positioning, etc. Among the constraints are receiver dynamic range and sensitivity which are dictated by low complexity and low cost. Among the access-layer variables are frame and slot sizes, code rates and spreading ratios, interference mitigation approaches such as the use of different frequencies in different cells, power control, etc. The layout problem is a multi-dimensional one, the objective here is to provide the reader with an understanding of the communication system design issues in ADIS design and lay the groundwork for the more thorough and in-depth treatment of Phase II research.

We start by discussing the implications of the physical channel. We follow that by a discussion of the access schemes and how they are defined for the link layer of ADIS. We address specifically the division between the basic components that need to be addressed in Phase I and the important details that will be the subject of the more in-depth

treatment of Phase II. We next proceed to build some candidate access architectures which satisfy the projected system requirements discussed in Chapter 3. We then contrast the preliminary results that we arrive at for the different candidates and use them to provide insight into the required resources. In the process we identify the various areas which affect performance that require more refined analysis and simulation.

7.2 Implications of the ADIS Propagation Environment

The many figures provided in Chapter 4 have illustrated the general behavior of the ADIS propagation environment. We aim here to illustrate the fundamental implications this type of environment has on system design. We select a typical highway example from the Southern California landscape, and apply to it a set of BS antenna configurations. We also look at effects related to M antenna placement. We focus on four cases that we designate Cl through C4 (for Configurations 1 through 4) and retain them throughout the tradeoffs in this Chapter. These configuration will serve as a demonstration tool for the various trades and limitations imposed by the parameters of the physical link.

Figure 7.1 depicts the path loss for a roadside BS along a walled highway using an antenna that is non-directive in the azimuthal plane, like a dipole. Such an antenna has directivity in the vertical plane. It has a "doughnut"-shaped pattern with approximately 3 dB of gain in the horizontal plane. The M antenna is assumed to be a simple monopole with about 1 dB of gain. This case is designated Cl in the remainder of this Chapter.

Figure 7.2 depicts the path loss for the same BS configuration but assuming the M antenna is in the middle of the roof, thereby modeled by a dipole due to the reflecting metallic plane. The associated gain is roughly 3 dB. This case is referred to as C2. There are two differences between the two scenarios: (1) the M antenna gain; and (2) the channel model: the full six-ray model (6RM) is presumed for Cl, while a 5RM is used for C2 because the ground reflection (the so-called second ray) is blocked by the roof of the vehicle (i.e., the second ray is highly attenuated – see Figure 4.7)

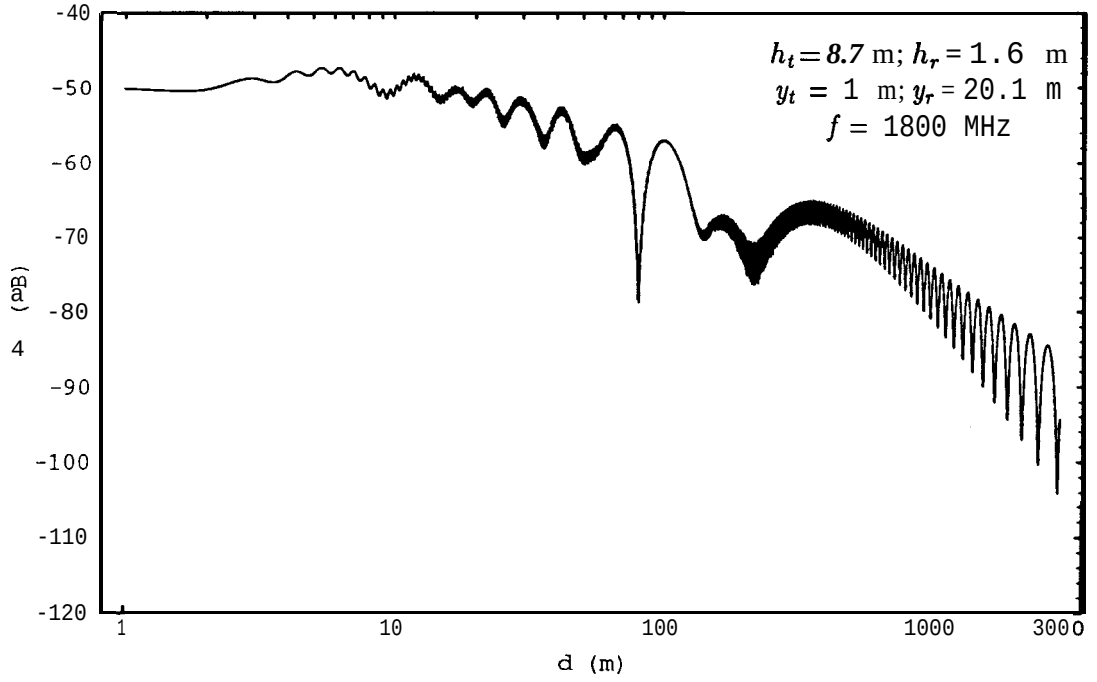

Figure 7.1: Cl : Path Loss for Reflection on the Ground

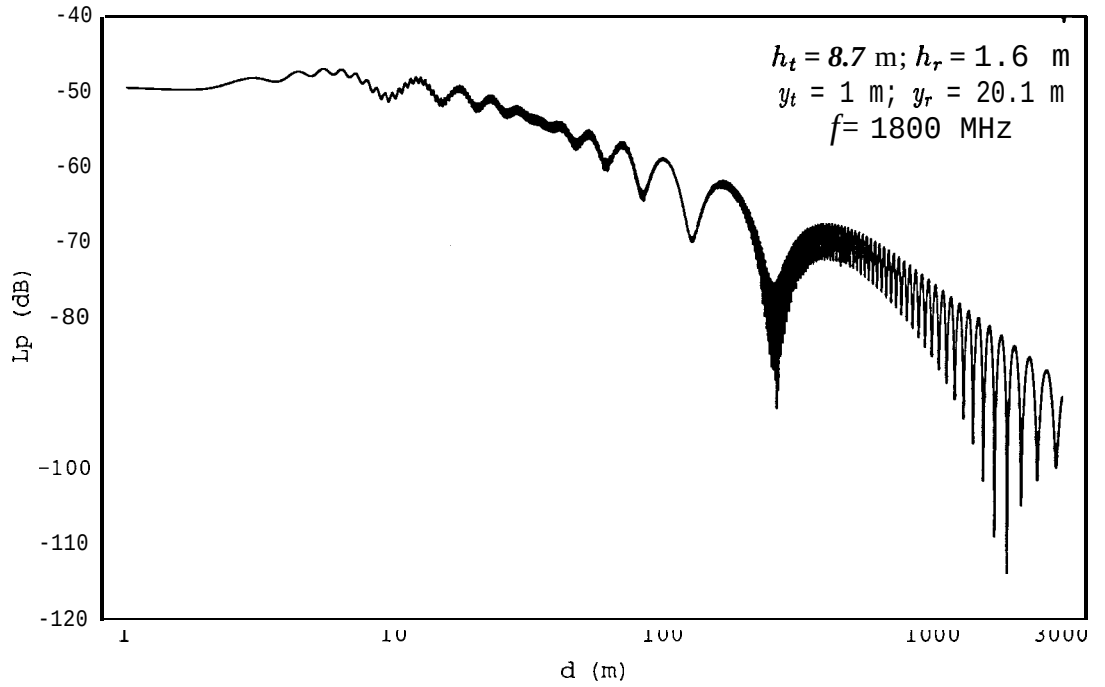

Figure 7.2: C2 : Path Loss for Second-Ray "Blocked" by the Receiver Antenna

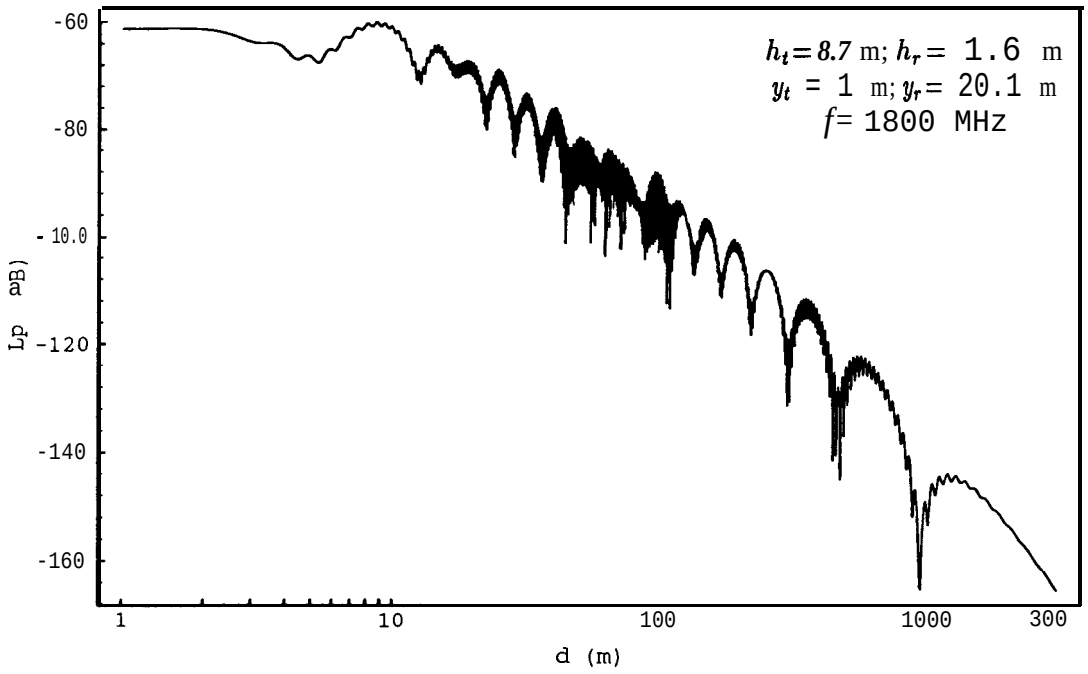

Figure 7.3: C3 : Path Loss for a Two-Element Longitudinal Array with In-Phase Excitation and X/2 spacing between the Elements

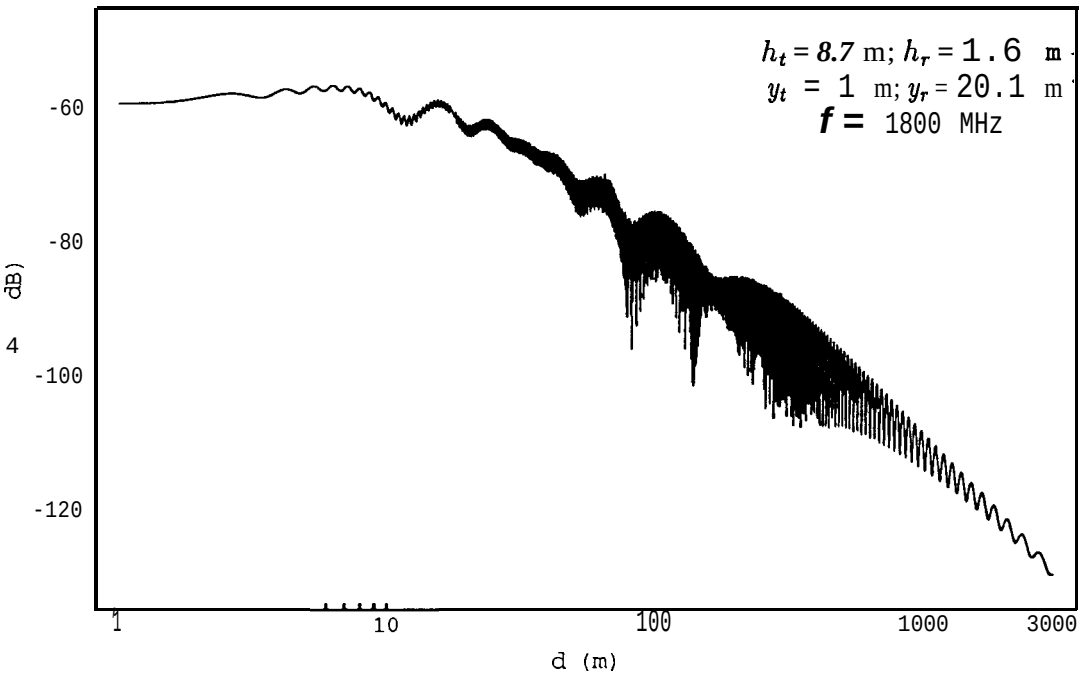

Figure 7.4: C4 : Path Loss for BS Antenna with Metallic Reflector X/2 away

Figure 7.3 provides the path loss for C3 where a roadside BS antenna array of two dipoles X/2 apart is placed longitudinally relative to the highway. The gain of such an antenna array relative to a single element is included in the path-loss computations by employing ray tracing which accounts for the rays emanating from the two elements.

Finally, Figure 7.4 gives the path loss for roadside BS antenna configuration wherein a dipole is placed with a metallic reflector behind it, with the reflector plane parallel to the direction of the highway. The distance between he dipole and the plate is chosen to be X/2. Additional directivity relative to the dipole alone is accounted for in the ray tracing computations. This case is referred to as C4.

In the "short" range application at hand, cell size is determined in most cases by the dynamic range of a mobile receiver which has to operate anywhere along the cell. From cellular telephony experience, a dynamic range of 30 to 40 dB is typical for an inexpensive unit. Allowing for at least some improvement in mass produced technology, we assume that a dynamic range in the neiborhood of 40 dB is acceptable. We use this in setting the limit on the range of signal variation that is acceptable at the mobile receiver.

Another factor that is related to cell size and transmit power is the implied receiver sensitivity. Naturally, the receiver at the M rather than at the BS is the one whose complexity or cost must be minimized. Accordingly, we focus in this paragraph on the forward link, i.e., the one from the BS to the M. If we assume by way of example a 100 mW BS transmitter feeding a 3 dB gain dipole antenna, a 1 dB gain M antenna, and a 100 dB path loss at 1800 MHz (for some given channel), the field strength computed at the vehicle using equation (2.1) is found to be 2.3 mV/m. This is lower than what is mentioned in Chapter 2 for the AVI proposals. There, the driver was to protect against interference from nearby cells by setting an artificially high minimum sensitivity threshold. A typical receiver used in the mobile environment, such as in cellular telephony, will operate satisfactorily as long as the useful received signal is above the noise floor. This consideration is incorporated in the link budgets which are computed for every cell and/or BS antenna choice. In other words, a candidate cell configuration and the corresponding channel must yield sufficient signal to noise ratio for the vehicular receiver to perform properly, even at the points farthest from the BS. If in certain cases it is

found that not enough signal is available at the edge of the cell relative to noise, then the designed transmit power would need to be increased. This is usually a feasible but not attractive solution for the short range problem. As we shall see, this is rarely a concern since interference from adjacent cells rather than background noise tends to be the performance limiting factor.

After developing this fundamental understanding of the issues related to cell size determination, we can address the important effects of the BS antenna configuration. The metallic reflector or the array of two elements alter the shape of the field along the highway, and have most influence at long distances from the BS. In the "far" region, the rays emanating from the two elements (or those emitted from the one element and then reflected off the metallic reflector) tend to cancel and thereby significantly reduce the available power far from the BS. This obviously confines the range of the cell and reduces the interference to or from neighboring cells.

The most important characteristic that governs this co-channel interference from neighboring cells is the slope of the path loss curve past the break point, as discussed at length in Chapter 4. If we assume that the cells along the highway have equal transmit power then the carrier to interference ratio, C/I, at a certain point within the cell (say, 800 m from the center of the cell) is only a function of the path loss curve for the assumed BS configuration and operating frequency, and is independent of the actual transmit power. Thus, curves like those for Cl or C3 in Figures 7.1 or 7.3, respectively, would completely determine the C/I in those cases. As we shall see in Section 7.3, C/I is a critical parameter that will limit the performance of the communication channel in most cases.

Cell confinement, although important, does not come without a price. The array whose path loss is shown in Figure 7.3 is very effective in accomplishing cell confinement. Yet, a closer look at the figure shows that, as a side effect, the size of the cell is reduced significantly relative to the other cases. Typically, a reduction by a factor of 4 is experienced. Moreover, due to the sharp cutoff at cell boundary, increasing the BS transmit power by a factor of 4 (6 dB) results only in an increase in the cell radius by less than 50% (see Figure 4.10). This means that increasing the transmit power is not an effective

solution to offset the cell radius reduction caused by antenna configuration selection.

Another important factor that impacts cell size through dynamic range besides the BS antenna configuration is the frequency selected. In Chapter 4 it was explained that doubling the frequency from 900 to 1800 MHz results in cell expansion due to dynamic range reduction. It was also pointed out that that is achieved at the cost of 6 dB more transmitted power to achieve a given received power at the mobile location.

From the foregoing discussions we see that determination of the appropriate cell size involves delicate tradeoffs among various factors, most notably BS antenna configuration, system frequency and transmit power. In Section 7.4 we explore in more detail (through the paradigms provided by the four configurations Cl-C4) the interrelations among these various factors, within the additional context of the candidate multiple-access architectures.

7.3 Implications of the ADIS Signal and Access-Protocol Design

The previous Section examined in some detail the impact that the propagation environment has in the proper selection of the cell layout and the associated sub-selections of BS and M antennas, operating frequency, etc. We can think of these choices as the "electrophysical elements" of the design, namely those components and parameters which affect performance via their electromagnetic behavior. The next major layer of architectural choice is in the "microelectronic/software" sphere of transceiver design, namely the adopted modulation/demodulation, error- and channel-coding/decoding, spreading/despreading (if any), and link-access protocol design, a necessary ingredient of any dynamic multi-user environment.

A dynamic, multi-user, bursty radio environment like the present one is without doubt a complicated one to design, perhaps even more so than high-speed optical-fiber networks with their problems of access, congestion and flow control, etc. The reason of this complexity is simple: the elements or "layers" of such a radio network interact in a

strong fashion and choices at one layer have a profound impact on the other choices for optimized system behavior; this will become clearer through the following examples of Section 7.4. These examples purport to convey a flavor of that complexity and pave the way for the subsequent research to be performed at USC/CSI in the follow-up contract; they are by no means absolute recommendations for system architecture, neither do they exhaust the architectural possibilities. We are mostly concerned here with identifying these components of the design problem that create "first-order", major effects and must be chosen, positioned and traded-off very carefully for achieving acceptable and efficient operation. The finer aspects of the design and their impact will be examined at much greater length in the future.

As envisioned in the system layout of the previous Section, the infrastructure will involve a backbone network of BSs, well connected amongst themselves with wider-band communication means (that can be dedicated lines or even another radio system), and also communicating with a central facility or computer for overall real-time system management. We do not concern ourselves in this Report with that portion of the overall communication; we concentrate on the wireless portion between the BSs and the M units; at a later phase, communication between Ms will be added as a consideration (AVCS).

Mobile radio networks exhibit many facets and require many design choices. For the benefit of the reader, we summarize some of them in Appendix 7.A. It suffices, for the present discussion, to list the salient choices in the first two layers, namely:

- *On the Physical Layer :*
  - modulation
  - forward error correction (FEC) coding
  - channel equalization
  - signal quality measurements
  - synchronization
  - automatic gain and power control

- ***On the Data Link (or Link Access) Layer :***

  * error detection
  * retransmission mechanism
  * channel accessing mechanism
  * signaling issues (packet, frame and slot structure, link control)

The particular combination of choices made at this level interacts with (a) the system layout as previously discussed, (b) the channel/multipath profile, and (c) the generated data traffic, in order to provide a certain performance level, namely the number of supportable users on the average at a certain deliverable bit rate and delay, and for a specific cost per unit.

Let us note here that a favorable trend which facilitates the choice of ever more sophisticated design choices is the continuing drop in price of the electronic component of the design; thus, it becomes feasible to shift responsibility for improved system performance to intelligent processing, control and software, as opposed to expensive hardware such as RF portion, amplifiers, etc. Furthermore, logical integration and time-sharing for multiple tasks (information exchange, warnings, measurements, positioning, paging, etc.) becomes a much more feasible and cost-effective task when performed at the software level within the same unit, rather than superimposing physically distinct designs on the same vehicle (say, different radios or radar/optical systems).

As explained in Appendix 7.A., the three broad categories of multiple-access schemes are FDMA, TDMA and CDMA. FDMA has enjoyed acceptance in traditional system designs because of its conceptual simplicity and is still in wide use in commercial (mostly point-to-point) communication systems. Examples include mobile cellular telephony (e.g., the AMPS standard) and mobile satellite systems (e.g., those of INMARSAT and AMSC). With the dramatic increase in the popularity of mobile communications, and concomitant rise in demand for services, system architects and service providers have turned their attention to newer access concepts which permit substantially higher capacities while maintaining inexpensive consumer equipment and cost of service. The TDMA cellular standard IS-54 has already been in place and some cellular carriers have already

started shifting capacity from FDMA to TDMA. On the other hand, Qualcomm Inc. has developed a CDMA cellular system which it successfully demonstrated in various parts of the country and abroad. It is claimed that, for cellular telephony, CDMA can achieve several times more capacity than TDMA. This is one of the most hotly debated issues in mobile communications and has not been resolved, and may not be in the near future. The extension of the battle in the Personal Communication Services (PCS or PCN) arena in the indoor environment has only added to the ferocity of the battle.

The main issue at stake is the most appropriate format for a multi-user, bursty-traffic, multipath-degraded application such as wireless radio for urban environments. It is appropriate at this point to explain, in the briefest of terms, why such a crucial choice is not so obvious. In a structured, distortionless channel, where each user demands a portion of the channel capacity for a significant and continuous portion of the time (heavy use), there is not much of a debate : any reservation/fixed capacity allocation scheme, such as TDMA or FDMA will do best and provide an almost full use of channel capacity. The multiplexed satellite channel is the classical example here (barring any other restrictions, like power flux density, which might dictate a different choice). Most of these channels are TDMA nowadays. The situation changes dramatically when (a) users are many and very bursty, so that each one is on and off in an unpredictable and bursty fashion (although the aggregate traffic from all of them might be large), and (b) the channel is itself unpredictable, as is the notoriously challenging, multipath fading urban (or highway, in our case) channel. Then, reservation schemes might have a hard time following the quick and fluctuating user demands, the channels might not be able to support accessing-enhancement schemes like Carrier-Sense Multiple-Access (CSMA), and the channel demands multipath compensation schemes in order to deliver a satisfactory bit-error-rate (BER). CDMA is being advocated as a way of alleviating all these problems in a single package and, in principle at least, this appears feasible, under the caveat that certain technological difficulties such as power control will be solved effectively and cost/complexity issues will be resolved (CDMA is indeed a sophisticated design). On the other hand, novel schemes like extended-TDMA reservation and strong equalization algorithms are being explored in a flurry of activity from the complementary camp in an effort to counter the aforementioned problems. It might well turn out that the resolution of the conflict will come from business and regulatory (i.e., non-technical)

considerations; nonetheless, the technical ambivalence is there.

It should be emphasized here that the ADIS problem with short-range short-length data messages is sufficiently different from general cellular telephony that conclusions gained from that experience have to be substantially revised and adapted to IVHS problems. Nevertheless, one trend that applies in both cases is that more efficient resource utilization, expressed in terms of higher capacities for given bandwidth, infrastructure and user equipment costs, favors a move from pure FDMA to either CDMA or TDMA, or hybrids of either with frequency division multiplexing (FDM) and reuse. Hence, in Section 7.3 we shall concentrate on these latter options.

In summary, the main system driver which will determine the range of architectural options of signal and access-protocol design is the need to deliver heterogeneous, bursty, randomly generated, packetized data in a topologically dynamic and unpredictable multi-user environment, and do so in a stable and efficient fashion with a reasonable component cost. Whether a reservation (TDMA) or a random access (CDMA) mechanism (plus all the associated signal and link design sub-choices) is the right way to go can only be determined after an analysis of their corresponding throughput/delay capabilities. A first cut at this issue will be taken in the examples of Section 7.4, wherein we compute the ability of specific options to support certain numbers of simultaneous users. We must emphasize, however, that this is only indicative of the corresponding system capacity. A fuller and more rounded insight into performance must account for the interplay between throughput and corresponding delay; we look at such questions in Chapter 8, aided by the results of Chapter 5. Still, the results of Chapter 8 are far from a complete understanding of the problem and its solution: we only perform approximate analysis for single-shot type of transactions, like AVI. The development of a full, all-encompassing theory for multi-packet transactions in such mobile environments is relegated to the next research phase.

7.4 Some Layout Options and Examples

Even within the TDMA and CDMA frameworks a host of possible architectural layouts can be applied to the ADIS problem. In the following paragraphs we highlight a few then we focus on two examples; one for TDMA and one for CDMA.

In a TDMA system, all the users in a cell share the transmission time slots within a TDMA frame. All such transmissions make one combined signal, occupying a given frequency band, which exists within the cell, but which also exists at somewhat lower levels (as determined by the propagation path loss curves of Chapter 4) in its neighboring cells. The need to separate adjacent cells is obvious, for otherwise the unwanted signals from the neighboring cells would create an interference that could even be stronger than. the desired signals within the cell. Adjacent cells could use different frequency "slots" or sub-bands. This would be a frequency division multiplexed (FDM)/TDMA layout. If the composite data rate within the cell is not too high, say of the order of 100 kbps, then the signals in the adjacent cells could be multiplexed in time as well, i.e., there could be one super-frame structure for the entire system where certain groups of slots are assigned to the users in a given cell. Those slots would be made available again to the users in cells that are sufficiently physically removed. This would be a time division multiplexed (TDM)/TDMA architecture.

With either of the above access architectures, one more aspect of choice exists. In traditional FDMA cellular telephony, as well as in the more recent TDMA cellular standard (IS54), the signals on the "forward" link (from the BS to the Ms) and those on the "return" link (from the Ms to the BS) are transmitted in different frequency bands all together. This does have some practical significance and implications on the equipment, but is not essential. Because of the very small propagation delays in short range systems, either frequency or time duplexing could be used with a TDMA architecture. Such a decision would have to be faced if one is building an architecture from ground zero, unincumbered by backward compatibility. Such questions are starting to be asked in emerging areas like the so-called Future Public Land Mobile Telecommunication System (FPLMTS) to exist within the 1800 - 2200 MHz band, possibly before the end of the century.

A host of analogous architectural options exists for CDMA. Again, adjacent cells could be assigned different frequency sub-bands, and then they do not have to if the CDMA system is designed with sufficient spreading to accommodate co-channel interference from adjacent cells. Both approaches require spectrum to support the required separation of the users in the adjacent cells. Yet, in one case they are separated in the code space, whereas in the other, they are separated in the frequency space. The frequency requirements are likely to be different. The complexity issues of equipment and network level protocol, like inter-cell handoff, are also likely to be different. Unfortunately, a very detailed, wide reaching analysis would be required before the overall "best" choice could be made.

Within the above CDMA options, still another set of layout choices exists. For example, in a given cell, should different vehicles be assigned different (orthogonal) codes, or would reliance on time shifts of the same code suffice (common code). Also, should the adjacent cells be designed to be able to close a link well into the adjacent cell for the so-called soft handover or only to its boundary. Both questions require very detailed analyses to be answered adequately, and will therefore be relegated to Phase II of the research effort.

In what follows we select two architectural design cases for more detailed analysis. The objective will be exposing the various design tradeoffs, and making a broad assessment of the feasibility of each architectural choice in supporting the requirements of ADIS as outlined earlier in Section 2.2.

7.4.1 Example 1. An FDM/TDMA Architecture

Here a TDMA protocol is used for serving all the users within a cell. In each cell the tranmissions from the BS to the Ms, i.e., the forward link, are separated in time and share the different time slots within a TDMA frame structure. All these transmissions occupy the same frequency band, that of the composite TDMA signal. The transmissions of the Ms back to the BS (the return link) are also grouped in time to share the slots of a TDMA frame. The frame structures for the forward and return links need not be identical. The forward and return link transmissions are assumed to be in different frequency bands as

is commonly used in mobile systems for practical considerations.

In the present architectural example adjacent cells use different frequency bands to reduce the interference from adjacent cells. If no such frequency division were used the TDMA signals within any cell would coincide in frequency with those in the adjacent cells and the interference would actually exceed the desired signals- obviously an unworkable situation. A very key question is how many frequencies should be used, or stated differently, every how many cells should a frequency be reused. This determines how much overall bandwidth the system requires. The answer intuitively is the minimum amount that results in the required capacity and acceptable interference levels. Those are the levels of interference that would permit data transmission at a tolerable error rate which would result in smooth, efficient protocol operation, and would meet any maximum delay requirements imposed by the services provided.

In the analysis and Tables to follow, results that have been obtained in Chapters 4 and 5 on the physical and access layers are combined to determine acceptable cell sizes, BS configurations and powers, as well as carrier to interference (C/I) ratios and frequency reuse. The data links are assumed to be half duplex, that is with transmission in one direction or the other at a given time. (This is in contrast to voice where both speakers can talk on the same link simultaneously). We will focus attention on the more demanding direction of transaction flow which is from the infrastructure to the M. This does not mean that we will only consider information flow in one direction, but rather base our analyses on the data requirements in that direction. Acknowledgements and responses could and would be flowing in the return direction.

For the set of four channel configurations Cl-C4 we shall provide two sets of designs one at 900 MHz and the other at 1800 MHz. The rationale for these two selections is that there are potential frequency bands that can accommodate IVHS-type applications in both frequency regions. Examples are the 902 to 928 MHz band and the 240 MHz or so in the 1800 to 2200 MHz band recently allocated by WARC'92 and the FCC to emerging technologies and services such as PCS.

In both frequency bands we restrict the BS transmit power to 0.1 W and assume that its basic antenna is a dipole with 3 dB gain in the horizontal direction. The basic

receive antenna is assumed to be a monopole with 1 dB gain. For the case of C2 this antenna is placed in the middle of the roof of the vehicle and its effective gain is then assumed to be 3 dB. For the M receiver we require a simple, inexpensive receiver. From the present trends in the advancement of mass producible technology it is predicted [JP private communication] that a 6 dB receiver noise figure will be well at hand in the next 2 or 3 years.' We therefore assume this number in the link computations. We assume also 3 dB of hardware losses. The background urban noise is one of the factors that change between the two frequency bands. Following [1] and [1, Chapter 1, Ref. 5] we assume that it is 18 dB above KT_0B at 900 MHz and 10 dB above KT_0B at 1800 MHz, with T_0 taken to be 300°K.

For either case we assume also the following traffic scenario which is tilted towards the worst case. We assume that the highway section follows a straight line with 5 lanes in each direction and that the vehicles are moving at 10 mph with only 6 m between successive vehicle centers; i.e, densely packed or "bumper to bumper" traffic. Under this condition there is there are 266 cars (worst case assumption also) per lane per mile. For a five lane highway each side then has 1330 cars per mile.

As for the data transactions we make the following assumptions which we believe are demanding yet not exaggerated. We assume transactions of the three broad categories discussed in Chapter 3: 1 kbits (AVI, road pricing, advisory messages, MAYDAY, probe, etc.); 5 kbits (route guidance, in-vehicle signing, dispatch, etc.) and 64 kbits (e.g., maps). We assume a lot of the short transactions, a moderate amount of the medium ones and only a few of the very long ones. Corresponding to the case of congested traffic and impatient motorists we use one 1 kbits transaction per vehicle per minute, and one of the 5 kbits transactions every 3 minutes per vehicle. We also assume that 5 % of the mobiles would require a very long transaction every 3 minutes. This yields 3.73 kbits per vehicle per minute on the average.

If we tailor a design to a one mile diameter cell then for the highway with 5 lanes on each side both in very congested traffic the total data requirement is 165.5 kbps. If we additionally assume a 50 % TDMA overhead, including slots for access and control, guard and dead times, and say 10% retransmission of corrupted packets (more on that

later) we arrive at a composite TDMA data rate of 248.2 kbps which we round up to ***250*** kbps. For a smaller cell it is fair to assume that proportionally less data traffic and composite data rate will be required. For example, if the cell diameter is 1200 m then only $3/4$ of the the above rate will be required.

It is important to realize that what determines the cell size here is a practical dynamic range which is tightly related to the choice of antenna configuration and frequency. Yet, for a certain cell configuration interference from other cells may be unacceptably high. All of these parameters are largely independent of the data rate requirement as long as performance is not background noise limited, which is usually the case as we shall see shortly.

Figure 5.7 provides the BER performance for a TDMA system in a Rician channel with K = 10. We use the curves in that Figure keeping in mind that K = 10 is a conservative assumption for the desired signal in a short range system on the highway. The curves indicate that for a 10^{-4} BER the E_b/N_e should be in the range of 14 to 17 dB depending on the modulation scheme use whereas the range is 18 to 22 dB for a 10^{-5} BER. In the design of the FDM/TDMA architecture we target these ranges of performance in selecting the frequency reuse and cell sizes.

Tables 7.1 and 7.2 provide the physical link design parameters for the FDM/TDMA architecture applied to channels Cl-C4 at 1800 and 900 MHz, respectively. The equivalent noise spectral density N_e includes background urban and thermal noises and receiver noise, but does not include interference. C/I includes only co-channel interference and it is computed from the two nearest cells of the same frequency (one on each side) and assumes the same channel configuration and transmit parameters in all cells. It should be noted that C/I and C/N, are computed near the edge of the cell which is the worst case. Moreover, whereas K = 10 may be pessimistic for the desired signal it could well be too generous for the interference which comes from significantly more distance and is likely to suffer more multipath and shadowing attenuation. Thus the results in the Tables should be interpreted cautiously and as first cut worst case analysis.

The design we select which is reflected in the two Tables adopts a 3 frequency plan as shown in Figure 7.5. The performance for this choice is generally interference rather

than noise limited. In fact a modest increase in BS transmit power would insure that this is always the case. (Note that C/I in this set up is insensitive to transmit power.) The choice of this frequency plan is of course driven by the desire to minimize the overall bandwidth required by the system. Assuming that non-coherent FSK is selected for simplicity, the bandwidth required for a cell would be approximately twice the data rate, viz., 500 kHz. The total bandwidth would then be 1.5 MHz, which is 3 times 500 kHz due to the reuse factor.

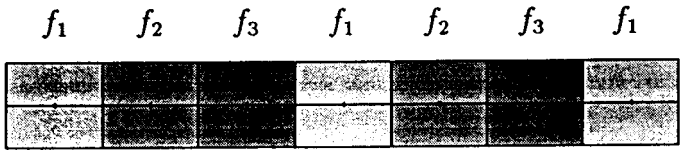

Figure 7.5: Frequency Plan for Reuse Factor 3

Of the four cell/BS configurations examined at 1800 MHz, C4 appears to be the best choice based on range (1 mile diameter) and its acceptable C/I and E_b/N_e performance. C4 provides a good balance between these requirements. C3 is a rather interesting case. It has stellar C/I and E_b/N_e performance but at a steep cost – one fourth the range, which basically means four times as much infrastructure cost.

The situation is basically the same for an implementation in the 900 MHz band. However, the cells will be somewhat smaller, and the C/I slightly worse. This indicates that an 1800 MHz system would generally be preferable.

If we go one last step in assessing performance, we would assume for a first estimate that interference has an impact on system BER as Gaussian noise. We would then conclude that a TDMA BER performance in the range 10^{-4}–10^{-5} is achievable under worst case conditions. A TDMA protocol using slotted ALOHA with a 512 bit frame would require less than 0.5% retransmissions at a 10^{-4} BER (see Figures 5.7 and 5.9). This is well within the 50% overhead allocation assumed above.

We conclude that an FDM/TDMA architecture with 3-frequency reuse, operating at 250 kbps for a l-mile cell diameter, occupying 1.5 MHz of bandwidth, using a simple BS antenna with a metallic reflector and 0.1 W transmitter power is very likely to meet fairly demanding ADIS requirements. This conclusion, we must emphasize, does not address

higher level issues such as networking, signalling, and base station costs. Also the details of the communication protocol would need to be worked out.

Cell Config.	Radius R (m)	Dynamic Range (dB)	Path Loss L_p (dB)	C/I Range @R (dB)	C/N_e* dB.Hz	Data Rate Req. (kbps)	E_b/N_e (dB)
C1	800	25	89.0	11-20	93	250	39
c 2	800	29	91.4	5-21	92	250	38
c 3	200	41	103	39-44	84	62.5	36
c 4	800	28	102	21-28	77	250	23

* P_t = 0.1 W; g_t = 3 dB; F_r = 6 dB; effects of thermal and urban noise included

Table 7.1: Physical Link Parameters for an FDM/TDMA Architecture with a 3-Frequency Plan @ 1800 MHz

Cell Config.	Radius R (m)	Dynamic Range (dB)	Path Loss L_p (dB)	C/I Range @R (dB)	C/N_e* dB.Hz	Data Rate Req. (kbps)	E_b/N_e (dB)
C1	600	29	87	9-17	89	250	37
c 2	600	30	88	10-20	88	250	36
c 3	150	41	91	26-30	87	62.5	41
c 4	600	28	97	20-30	79	250	27

* P_t = 0.1 W; g_t = 3 dB; F_r = 6 dB; effects of thermal and urban noise included

Table 7.2: Physical Link Parameters for an FDM/TDMA Architecture with a 3-Frequency Plan @ 900 MHz

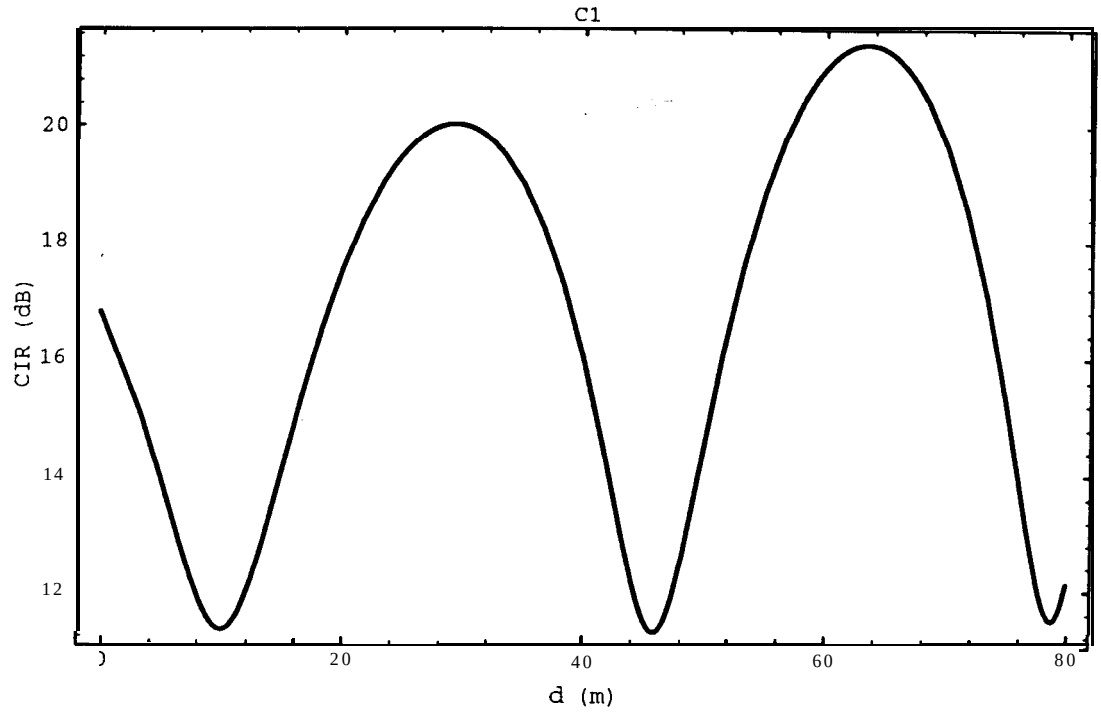

Figure 7.6: C/I Range for Configuration Cl @ 1800 MHz near the edge of the Cell

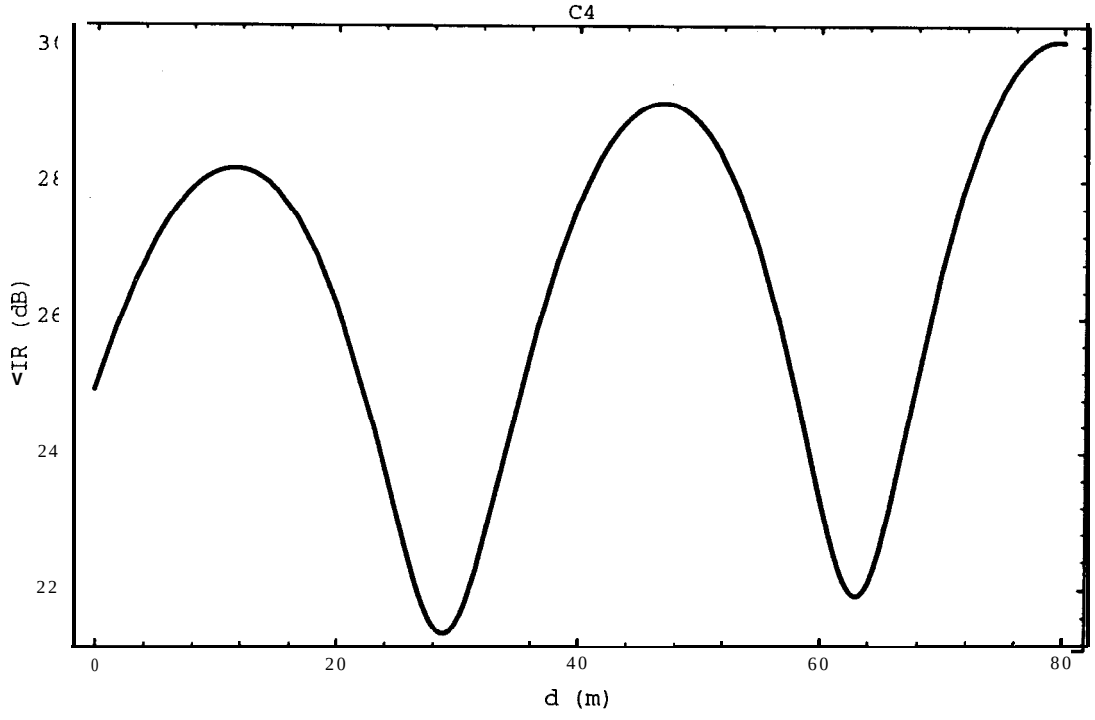

Figure 7.7: C/I Range for Configuration C4 @ 1800 MHz near the edge of the Cell

7.4.2 Example 2. A CDMA Architecture

As mentioned above, two of the broad architectural options are: (a) using the same frequency in all cells and in the CDMA case relying solely on code isolation to protect against adjacent cell interference; and (b) using different frequencies in the different cells with frequency reuse, i.e., FDM/CDMA, where the extent of frequency reuse can be traded-off versus the bandwidth required for CDMA in a cell, and the spreading and isolation this provides. In what follows we examine the former case. CDMA systems tend to be more involved in their analysis than TDMA and therefore only a very preliminary examination will be possible within the scope of Phase I of this research.

To provide a fair comparison with TDMA we use the traffic and data models developed under the TDMA analysis. We also start with the same overall bandwidth arrived at. The total raw data rate (before overheads) is 165 kbps, whereas the assumed TDMA overhead boosts that to 250 kbps. The overall bandwidth is 1.5 MHz.

For the purposes of a preliminary CDMA feasibility analysis we can assume that the total raw data rate could be viewed as 33 simultaneous users, each transmitting at 5 kbps. We assume a slotted system with a random-access mechanism (ALOHA). The size of the slot is taken to be 512 bits. The critical parameter is, of course, the spreading ratio. We assume a 1.275 Mcps code, which could easily fit into 1.5 MHz of bandwidth with Nyquist-type pulse shaping. The spreading ratio would then be 1.275 Mcps/5 Kbps = 255, one of the numbers used in the curves of Chapter 5. From Fig. 5.22 for CDMA BER performance in a Rician K = 10 channel, with high SNR and perfect power control, we find that a 2 x 10^{-4} BER is obtainable. If double the bandwidth is total bandwidth were available (i.e., 3 MHz) the spreading ratio wouldbe 511 and the BER from Fig 5.18 would be 6 x 10^{-5}. It should be noted here that CDMA results are sensitive to the value of K assumed.

There are two complicating factors that impact the performance of this architecture. They are the actual performance of the power control mechanism within the cell under consideration, and the interference contributed by users in adjacent cells, which would be power controlled relative to the BS in their own cells. The first factor has been a

subject of extensive debate in the cellular telephony literature. A rough rule of thumb is that a power control scheme with 1 to 2 dB accuracy results in a loss of roughly 20% capacity. We reiterate that the problem here is not that of cellular telephony, so this figure is only for illustrative purposes. A different "number" would need to be established for the data application at hand. This will be undertaken as part of Phase II research activities. As for interference from other cells, that again has been the subject of debate for cellular telephony. In the conventional planar cellular pattern (as opposed to linear along a highway), some authors report a two-third increase in the equivalent number of simultaneous users in the given cell due to those in the surrounding cells. Again, such an assertion would have to be completely reexamined and derived for the highway architecture and application at hand. We expect the result to be significantly lower than two-thirds by virtue of the linear, rather than planar, nature of the highway layout. Both of these CDMA complicating factors require very detailed modeling, analysis, and simulation. They are, therefore, beyond the scope of Phase I of this research, and will be addressed as part of Phase II activities.

What we can do here is essentially very tentative and crude, and we do it to investigate the capability of CDMA under such degraded conditions. We can postulate an increase in the number of simultaneous users within a cell to attempt to account for the effects of adjacent cells and power control. If we assume an equivalent 20% increase in the number of users inside the cell to account for imperfect power control and then add another 30% for the effect of adjacent cells along the highway, we have an increase from 33 to 52 users. What would be the performance of CDMA in the Rician fading environment if this equivalent representation were true? The answer can again be obtained from Figures 5.18 and 5.22. A BER of about 9×10^{-4} would prevail if the total available bandwidth were 1.5 MHz and 1.5×10^{-4} would be obtained if the bandwidth were 3 MHz at K = 10. This would indicate that to match the TDMA BER and bandwidth performance of the above example, simple forward error correction (FEC) may need to be included in the CDMA system to somewhat improve its performance (see Figures 5.27 and 5.28). This would perhaps translate the problem into the equipment cost tradeoff area. This and other complex power control/interference trades will be addressed in detail in Phase II.

Chapter 7.A

Classification/Review of Mobile Radio Networks

It is instructive to attempt a coarse classification of the various features that distinguish different classes of multi-user networks, in order to put the present proposal into perspective. Some of the possibilities associated with the network users, who from now on will be referred to as the "communicators", are the following:

(I) Number of Hops : In the systems under consideration messages are transmitted only one hop away (*monohop* type networks) implying that all source/destination pairs are within hearing distance from each other. References on the topic include [19], [20], [21], [25], [22], [11], [2].

(II) Connectivity : A multi-node network can be either Fully-Connected or Partially-Connected. A fully-connected network means that each base station can hear all transmitters in the locality of interest, although not necessarily with the same quality. Although standard problem formulations inherently assume a star topology (i.e., one single base station at the center of the cell or region under consideration), it is sometimes useful to consider the more general case of a communicator being heard by more than one base stations, as is the case, for instance, at the boundaries between cells and during hand-off procedures. A prerequisite for full connectivity is a monohop network; when the network under consideration is multihop, it is necessarily partially connected, exactly because there is at least one source/destination pair that cannot communicate directly. However,

there exist monohop networks that are not fully connected. Most of the references in [11] are about full connectivity (see also the models and references in [14],[12],[23]). An example of a partially connected monohop network can be found in [24].

(III) **TR/RCVR Format** : The issue here is whether TRs and RCVRs act in a dedicated or non-dedicated fashion. This is particularly important in a dynamic multi-user environment without a central coordinator or a reservation system, such as a vehicle-to-vehicle communication sub-system which relies on a simple random-access mechanism in order to communicate messages in the immediate neighborhood and receive from it. Obviously, this classification is not an issue in a star type of topology, where the base station (reader, roadside unit, etc) is the undisputed center and all other communicators (vehicles, in our case) relate their messages directly to it and receive from it.

A dedicated TR or RCVR performs just the respective function and no other. Contrary to that, a non-dedicated modem switches between the two functions according to some prespecified protocol. The latter case is more commonly known ***as*** the ***half-duplex*** case. Here, the modem can have a **TR-mode** priority or a **RCVR-mode** priority, depending on which function is preferred over the other at a particular point in time. Such a conflict can be of particular importance in an **unslotted** random-access system operation, where the need for a transmission and a reception job for a particular modem can overlap in time. In **slotted** operation, this issue can be resolved rather easily: whenever an active transmission is scheduled in a slot, the modem switches to its TR mode. In all other (non-transmitting) slots, it remains an "active" RCVR (see below for terminology).

It is sometimes thought (erroneously) that the opposite of the half-duplex case is the ***full-duplex*** one, whereby a modem can perform both functions simultaneously. In other words, a unit consists of a separate TR plus a RCVR at the same time. In reality, however, the full-duplex case is just a special example of the dedicated scenario. To explain this further, we should distinguish between the concepts of ***potential*** and ***active*** TRs or RCVRs. Any unit that ***can*** and, at some time, will transmit, belongs to the set of "potential" TRs, whose size is fixed at NT; the same goes for potential RCVRs (fixed size NR). The term "active" is reserved for those units which indeed act in either capacity at a particular slot. For a random access model, the number of ***active*** TRs in

any slot is a random variable denoted by MT; thus, in general, MT will be different than NT. On the other hand, the picture regarding the number of active RCVRs is a bit more complicated: if the network is built with dedicated TRs and RCVRs, then active and ***potential*** RCVRs are identical notions, i.e., MR = NR. A hierarchical type of network with devoted or "central" nodes (base stations), whose only job is to receive messages at all times,would fit in this category. If the units are non-dedicated, then obviously the number of active RCVRs is itself a random variable, and the equality MT+MR=U holds. Within this framework, ***full-duplex*** units correspond to a special case of dedicated networks where the total number of units U = NT = NR, each including a potential TR and RCVR. In general (i.e., for an arbitrary network), NT will not equal NR; this is the case, for instance, in the single-star or connected-star topology. References on this topic include [25], [11], [12], [13]. We emphasize that the distinction delineated above **is** crucial if one is interested in studying many types of multi-access links in a single theoretical framework, including centralized as well as distributed communication. Vehicle-to-roadside communication can be perceived as a case of the former, whereas vehicle-to-vehicle communication without a central reservation/coordination scheme can be interpreted as a case of the latter.

(IV) **Physical-Level Modem Structure :** This refers to the particular choice of the modulation-Forward Error Correction (FEC) coding-spreading (if any) combination employed in the design.

For wireless applications, constant-envelope modulations are typically preferred due to the general desire to employ low power transmission levels and efficient (saturated) amplifiers, which in turn implies the undesirability of envelope fluctuations and the resulting AM/PM conversion. For example, the European TDMA/GSM second-generation digital mobile cellular system (and other similar systems under current development in the USA and Japan) **employ offset** QPSK and/or its variants (MSK), all of which are constant-envelope. The alternative CDMA proposals for the same application employ either BPSK or QPSK with pulse-shaping of constant envelope. Both coherent or differentialy coherent modulations have been discussed, depending on the receiver's desired complexity and its ability to derive a coherent reference from the received data via either a phase-tracking loop or batch-processing type of phase estimation. These possibilities

are currently topics of intense interest and research worldwide.

When it comes to FEC coding, both block and convolutional codes are being included. Coding (with appropriate interleaving, for error randomization) is typically considered indispensable in the presence of multipath fading, although certain simplified designs avoid it altogether because of its perceived contribution to the final cost. In general, we should distinguish between fixed and **adaptive** coding schemes. In the latter case, which might be incorporated into the design for the purpose of mitigating the effects of a temporarily severe channel due to fading, man-made noise and multi-user interference, we distinguish further between TR-adaptivity, where the FEC rate is adjusted to the channel conditions [8], and the RCVR-adaptivity, such as the code-combining techniques [9].

Another fundamental architectural choice is whether to employ spreading (i.e., a spread-spectrum or CDMA system) or not. Spread-spectrum is a familiar by now military technique employed for mitigating the effects of undesirable narrowband interference. It entails the spreading of the useful-information spectrum over a spectral band much larger than the minimum necessary for reliable communication, and is achieved by straightforward signal design mechanisms. The key component is a spreading code, a digitally generated sequence of symbols known to the communicator and the friendly receiver only, but not to the interceptor or the jammer. Recently, the same designs have been employed as a multi-user channel-resource sharing mechanism in the commercial arena also. Users are separated in the code domain (as opposed to time or frequency), hence the name code-division multiple-access. The pros and cons of such a concept versus more traditional techniques like TDMA (see paragraph VI below) have been debated hotly lately, and the debate has carried itself in the IVHS domain too.

(V) **Buffering :** In the case of packetized transmission, there is still the choice between packet switching versus virtual-circuit switching. For the former case, there is the issue whether the different nodes in the network contain buffers which store packets before transmission, and what is the capacity of these buffers. The buffering capability is important for the following two tasks: (a) storing newly generated packets before their first attempted transmission, or transient packets on their way to a final destination (that

is when the node acts as a relay in a multihop network), and (b) storing packets that have failed their first transmission and are scheduled to be retransmitted (the so-called backlogged packets). The issue of buffer occupancy has been addressed extensively in [2], extending the models of [21],[25]. An analysis of interacting queues can be found in [4], but not for CDRA.

(VI) **Access Protocol :** This refers to the way that a communicator accesses the common channel. In reservation schemes, there is a central controller responsible for assigning a portion of the channel capacity (such as a time slot on TDMA) to each requesting user. The slot is reassigned whenever this particular communicator goes idle. The initial "hand-shaking" or request phase from a communicator to the center is handled via a random access scheme such as ALOHA. As mentioned above, reservation schemes are efficient and meaningful whenever each session between two users (or, equivalently, between the communicator and the base station or center) lasts for a long time (downloading a map or other long strings of data might be such an application).

Contrary to the above, a random-access scheme can be used for the totality of the communication, especially when the communication is short and bursty by nature. Such random access schemes of the ALOHA type can be combined with any type of modulation, but code-division seems to be a very natural candidate for this case due to the inherent quasi-orthogonality between the codes of different users, which reduces the impact of packet "collisions" to an additive noise effect.

In the standard ALOHA scheme, an available packet will be transmitted in a specific slot with a certain probability p, which can be different for first transmission versus the retransmission of a backlogged packet. If such a distinction is not made and all packets are transmitted with the same probability, we call it an ***uncontrolled access protocol,*** the opposite of which is ***controlled*** accessing. In the latter case we distinguish between **static control** and **adaptive control** techniques. For static control, the new-packet transmission probability is denoted by po, whereas the backlogged-packet transmission probability is denoted by pr. Both po and pr are fixed throughout the system operation, although they can be chosen optimally [10],[3],[16],[11],[2],[12],[13]. Contrary to that, the probability pr changes continuously with time in the "adaptive-control" case,

according to some channel observables (traffic levels, channel conditions, etc.) [5].

Before we proceed, a word about the value of the rather simple ALOHA protocol is due. Although it is well known that more elaborate random accessing schemes, such as tree-algorithms, carrier-sense, etc., can deliver stable throughputs that are higher than ALOHA (over or about 50% utilization, as opposed to 36% for slotted ALOHA), we must emphasize that these more elaborate schemes rely on a continuous monitoring of the channel, as well as a shared and flawless knowledge of the state and the collision history of the channel by all users. Contrary to that, ALOHA schemes depend only on each user knowing. the status of their individual transmission (successful or failed), which can be obtained by a very simple acknowledgement mechanism from the intended receiver. This totally decentralized nature of ALOHA, which imposes minimal monitoring requirements on each user, is very appealing for applications that (a) have to be simple in order to be cost effective and (b) are robust in the presence of unreliable fading channels which can distort the channel feedback obtained by different users and thus result in non-robust accessing algorithms. Is it our belief that controlled-access ALOHA (wherein the retransmission mechanism is optimized in a static or quasi-static fashion) represents a judicious compromise between robustness and system optimization for the application at hand.

(VII) **Code Distribution :** This is an issue only in CDMA. As explained in [15], [11], the networks can employ either a *common code,* a *TR-based* or a *RCVR-based* code system. *Hybrids* of those are also possible, wherein one set of codes are used in the synchronization preamble (such as a common code heard by all or a RCVR-based code for the destination of a particular packet), and then another is used in the data portion (for instance, a TR-based code). Code distribution also affects the overall network topology, as detailed in [11].

(VIII) **Accessing Observables :** In adaptive channel accessing, the action undertaken by each communicator is dictated by what this tansmitter observes in a particular time slot. An important is to identify the appropriate channel-quality monitoring schemes. Typical such measures are the channel signal-to-noise ratio, the bit- or word- or packet-error rate over some observation interval, the number of retransmissions required

to send a packet successfully, etc. These are obviously not unrelated statistics, and the selection of a proper subset of those upon which to base a channel-quality estimate is an important open issue.

(IX) **Data Traffic Profile** : The traffic requirements of a particular network, i.e., the amount of packets per second (or per slot) that the network can support on the average, is application-specific and can vary widely. The nature of traffic is mostly a modeling issue, having to do with how traffic is being generated at the various nodes of the network. As such, it is closely related to certain flow-control considerations. The two immediate issues affecting performance evaluation are the statistics of the traffic and its priority *level.* With regard to statistics, typical models are the **Bernoulli** (for finite-user models) and the **Poisson** (for very large or infinite user-models). On the other hand, the notion of "prioritized traffic" refers to the case of integrated services, where both **digitized voice** and **data** are to be transported through the network.. Such integration imposes different constraints on these heterogeneous traffic sources: voice can tolerate higher error rates (up to 10^{-3} BER are typical for digitized voice), but it is very stringent on the delay requirements. For data transfer, these constraints are effectively reversed.

7.5 References

[1] W.C. Lee, Mobile Communications Engineering, McGraw-Hill, 1982

[2] U. Cheng, "Static and Dynamic Jamming of Networks", Interim Technical Report No. R8712-6, Axiomatix Corp., Dec 87

[3] D. H. Davis and S. A. Gronemeyer, "Performance of Slotted ALOHA Ramdom Access with Delay Capture and Randomized Time of Arrival", IEEE Trans. Comm., Vol. COM-28, No. 5, May 80, pp. 703-10

[4] A. Ephremides and R. Zhu, "Delay Analysis of Interacting Queues with an Approximate Model", IEEE Trans. Comm., Vol. COM-35, No. 2, Feb 87, pp. 194-201

[5] B. Hajek, "Recursive Retransmission Control: Application to a FH Spread-Spectrum System", Proc. CISS, Princeton, pp. 116-20, 1982

[6] J. Jubin, "Current Packet Radio Network Protocols", Proc. INFOCOM 85, pp. 86-92, Apr 85

[7] R. Kahn, S. Gronemeyer, J. Burchfiel, and R. Kunzeman, "Advances in Packet Radio Technology", Proc. IEEE, vol. 66, pp. 1468-96, Nov 78

[8] T. Ketseoglou and A. Polydoros, "Spread-Spectrum Random Access Monohop Networks With Adaptive Packet Protection", Proc. CDC'87, Los Angeles, CA, pp.717-20, Dec 87

[9] T. Ketseoglou and A. Polydoros, "Code Combining With Convolutional Coding and Sequential Decoding for CDMA Slotted Networks", 1990 Int. Symp. Inf. Theory, San Diego, CA, Jan 90

[10] L. Kleinrock and S. Lam, "Packet Switching in a Multiaccess Broadcast Channel: Performance Evaluation", IEEE Trans. Comm., Vol. COM-23, pp. 410-23, Apr 75

[11] A. Polydoros and J. Silvester, "Slotted Random Access Spread-Spectrum Networks", IEEE J. Sel. Areas Comm., Vol. SAC-5, No. 6, pp. 989-1002, Jul 87

[12] N. Pronios and A. Polydoros, "Spread-Spectrum, Slotted-ALOHA,Fully-Connected Networks in Jamming", submitted to *IEEE Trans. Comm.*; see also preliminary version in *Proc. MILCOM 87*

[13] A. Polydoros and U. Cheng, "Topology-Selective Jamming of Fully-Connected, CDRA Networks", Interim Technical Report No. R8906-3, Axiomatix Corp., Dec 87: also, submitted to *IEEE Trans. Comm.*

[14] M. B. Pursley, "Frequency-Hop Transmission for Satellite Packet Switching and Terrestrial Packet Radio Networks", *IEEE Trans. Inf. Theory,* Vol. IT-32, No. 5, pp. 652-67, Sep 86

[15] M. B. Pursley, "The Role of Spread Spectrum in Packet Radio Networks", *Proc. IEEE,* Vol. 75, No. 1, pp. 116-34, Jan 87

[16] D. Raychaudhuri, "Performance Analysis of Random Access Packet-Switched Code Division Multiple Access Systems", *IEEE Trans. Comm.,* Vol. COM-29, No. 6, pp. 895-901, Jun 81

[17] P. F. Sass, "Army Spread Spectrum-Evolution or Revolution", *Proc. MILCOM '82,* pp 4.1.1-8, Boston, MA, Oct 82

[18] N. Shacham and J. D. Tornow, "Future Directions in Packet Radio Technology", *Proc. INFOCOM* 85, pp. 93-8, Apr 85

[19] J. A. Silvester and L. Kleinrock, "On the Capacity of Muliple Slotted ALOHA Networks with Regular Structure", *IEEE Trans. Comm.,* Vol. COM-31, No. 8, pp. 974-82, Aug 83

[20] J. A. Silvester and L. Kleinrock, "On the Capacity of Single-Hop Slotted ALOHA Networks for Various Traffic Matrices and Transmission Strategies", *IEEE Trans. Comm.,* Vol. COM-31, No. 8, pp. 983-91, Aug 83

[21] J. A. Silvester and I. Lee, "Throughput/Delay Performance of Multi-Hop Slotted ALOHA Networks", Technical Report CSI-83-09-01, Univ. Southern California, Sep 83

[22] M. K. Simon, J. K. Omura, R. A. Scholtz and B. K. Levitt, ***Spread Spectrum Communications,*** Computer Science Press, 1985

[23] J. S. Storey and F. A. Tobagi, "Throughput Performance of an Unslotted Direct-Sequence SSMA Packet Radio Network", ***IEEE Trans. Comm.,*** Vol. 37, No. 8, pp. 814-823, Aug 89

[24] Szu-Lin Su and V. 0. K. Li, "Performance Analysis of a Slotted Code Division Multiple Access (CDMA) Network", *Proc. MILCOM '84,* pp. 23.3.1-5, Los Angeles, CA, Oct 84

[25] Szu-Lin Su and V. 0. K. Li, "An Iterative Model to Analyze Multihop Packet Radio Networks", *Proc. 23rd Allerton* ***Conj. Comm., Control and Computing,*** Monticello, Ill., Oct 85

Chapter 8

Throughput /Delay Analysis

8.1 Introduction

This chapter will present throughput/delay analyses of IVHS communications based on TDMA and CDMA techniques. The results of the analysis will be compared with those obtained by using the simulation program developed at USC/CSI, and described in Chapter 6. The analysis will consider the compound effects of the mobility of the vehicles, channel characteristics, and protocol specifics on the throughput and delay performance.

The contributions of mathematical analysis to this project include:

- Propose and develop a simple but effective analytical tool to provide for approximate performance values.
- Use the results thus obtained to verify the accuracy of the developed simulation programs.
- Open a new dimension to this project, which introduces the throughput/delay performance measure as a valuable research topic in the area of IVHS communications.

Multiple-access communication is key to IVHS communications. In IVHS communication, the expected traffic generated by each vehicle is low, and thus multiple-access communication techniques, such as TDMA, CDMA, etc., are used to enable the multiple users to share a single communication channel. Due to the conflict resolving capabilities

of these techniques, the success of transmission can usually be guaranteed in spite of possible collisions on transmission. Throughput (i.e. the number of successful transmission per unit time) and delay (i.e., time delay in sending a message) analysis are needed to measure the performance of the given system. Compared to simulation, whenever tractable, mathematical analysis has the advantage of simplicity, fast data generation, and offering insights into system behavior.

Nevertheless, throughput and delay analysis becomes an intricate problem due to the complicated mobile dynamics, channel characteristics, and network protocols involved. In the following, we facilitate analysis by proper selection of simplifying assumptions. A key approximation is assuming the data traffic to be Poisson (e.g., the sum of new traffic and retransmission traffic, and the output of a particular stage in a cascade system). These assumptions make the model Markov, thereby easy to analyze. We only provide average results; higher-order statistics will be obtained at a later stage. Despite the approximations, we can still see clear resemblance between our analytical results and those from a more realistic simulation.

The remainder of this Chapter is organized as follows. The analysis of TDMA and CDMA will be presented in Sections 2 and 3, respectively. Conclusions will be given in Section 4.

8.2 T D M A

8.2.1 Delay Analysis

The reservation-ALOHA TDMA protocol is used to control the transmissions of packet by the vehicles. Let each frame have m data slots, n request slots, and a fixed duration T. The vehicles will enter the cell in one of the l lanes. The total arrival rate per frame is

$$\lambda = \sum_{i}^{l} \frac{v_i}{d_i} T \quad , \tag{8.1}$$

where v_i and d_i, respectively, are the speed of the vehicles and the average distance between two successive vehicles in lane i. Suppose that the total average network delay D is decomposed into two components, the average reservation delay D_r and the average transmission delay D_t. Reservation delay is defined as the time difference between the entrance of the vehicle in the cell and the successful reservation of transmission of the vehicle's packet by the base station. Transmission delay is defined as the time difference between the reservation of transmission and the successful transmission of a particular packet. These two delay components are derived separately.

Reservation Delay

A fairly simple calculation is used to compute the reservation delay. Assume that a tagged vehicle begins the transmission of its request packet in a certain request slot. The reservation delay is a function of whether or not other vehicles contend for the given request slot. The total rate of attempted transmissions in the selected request slot should be X/n since n request slots are available per frame. Let us approximate the total number of attempted transmissions in this particular request slot by a Poisson distribution. Then, the probability of successful transmission of the control packet by the tagged vehicle should correspond to the probability of no transmissions from other vehicles in the chosen slot, i.e.,

$$P_s = e^{-\frac{\lambda}{n}} \quad . \tag{8.2}$$

Assume that the number of retransmissions **is** geometrically distributed with parameter P_s. Then, the total number of transmissions of the request packet of the tagged vehicle should be $\frac{1}{P_s}$, yielding the reservation delay

$$D_r = \left(\frac{1}{P_s} - 1\right) T = \left(e^{\frac{\lambda}{n}} - 1\right) T \quad , \tag{8.3}$$

if the first transmission of the request packet is not included in the total network delay.

Transmission Delay

Queuing analysis is used to derive the transmission delay. A queue is used to emulate the transmission of data packets, which accounts for the time between successful transmission of the request packet and the time of successful transmission of the data packet. The input of the queue is actually the output of the reservation procedure. Therefore, the total arrival rate of the transmission queue is λ per frame since the flow of packets is assumed constant (equilibrium). We approximate the packet arrivals by a Poisson process with rate λ per frame, i.e., we assume independent arrivals in each lane. The probability that i packets arrive in a frame is

$$a_i = \frac{e^{-\lambda}\lambda^i}{i!}, \quad \mathbf{i} = 0, 1, \cdots \tag{8.4}$$

Assume that the error status of a transmitted packet is independent from that of any other, and thus that it can be modeled as a Bernoulli trial with paremeter P_e, the packet error rate. Then, the evolution of the number of packets waiting for transmission in the queu can be modeled as a discrete-time homogeneous Markov chain, with the number of packets in the queue as the state variable.

The number of packets departing from the queue per frame depends on the total number of enqueued packets. So, the conditional probability that k packets are successfully transmitted given that i packets were in the transmission queue at the beginning of a particular frame is given by

$$d_{i,k} = \begin{cases} C(m,k)P_e^{m-k}(1-P_e)^k & \text{if } m < \mathbf{i} \\ C(i,k)P_e^{i-k}(1-P_e)^k & \text{if } 0 \le i \le m \end{cases}, \quad i \ge k \ge 0 \tag{8.5}$$

where

$$C(i, \mathrm{j}) \triangleq \frac{i \cdot (i-1) \cdot \ldots (\mathbf{i} - \mathbf{j} + \mathbf{1})}{1 \cdot 2 \cdots j} \quad , \quad i \ge j \ge 0 \ .$$

The state transition probability $P_{i,j} \triangleq Prob\{x_1 = j | x_0 = i\}$ follows as

$$P_{i,j} = \sum_{k=\max(0,i-j)}^{i} a_{k+j-i} d_{i,k}, \quad i,j \geq 0 \tag{8.6}$$

The steady-state probability distribution can be obtained by solving the following balanced equations

$$\sum_{i=0}^{B} \pi_i P_{i,j} = \pi_j, \quad 0 \leq i \leq B \tag{8.7}$$

where, to faciliate the calculations, B is the bound of the indices truncated to cut the infinite dimension into the finite one. Given the steady state probabilities, $\pi_i, 0 \leq i \leq B$, the transmission delay should be

$$\frac{T \sum_{i=0}^{B} \left\{ \sum_{k=1}^{B} \left[\frac{1}{k} \sum_{j=1}^{k} \left\lceil \frac{i+j}{m} \right\rceil \right] \frac{k a_k}{\lambda} \right\} \pi_i}{1 - P_e} \tag{8.8}$$

We weigh the group of k arrivals with ka_k/λ while the average delay per transmission is $\frac{1}{k}\sum_{j=1}^{k}\lceil \frac{i+j}{m} \rceil$ for that group where $\lceil x \rceil$ is the least integer not less than x. Retransmission is taken into account by multiplying the average per-transmission delay by the additional factor $1/(1-P_e)$

8.2.2 Numerical Examples

Figures 8.1, 8.2, and 8.3 compare the delay obtained by simulation and analysis. These figures assume five lanes on the freeway, m = 2 and n = 4, SNR = 10 dB (thus packet error probability equals 0.6172), vehicle speeds of 100 mph, identical average inter-vehicle distance on each lane, the truncation factor B = 12. The cell size is assumed as 2 miles to increase the transmission distance and to decrease the signal-to-noise ratio. The inter-vehicle distance is used as the independent variable to plot the delay.

The curves show that the results of the simulation are close to those of the analysis. In Figure 8.1, the discrepancy is flat with various traffic load. In Figure 8.2, analysis matches well simulation especially for light freeway traffic. For heavy traffic loading, the deviation is expected to be larger due to the inaccurate Poisson arrival model. In the real case, the traffic is regulated by the contention procedure of reservation, so the traffic tends to be smooth. Accordingly, the delay obtained via the simulation should be

smaller than that obtained by the analytical method which assumes a more congested arrival model. From these results, we confirm the integrity of the developed simulation program.

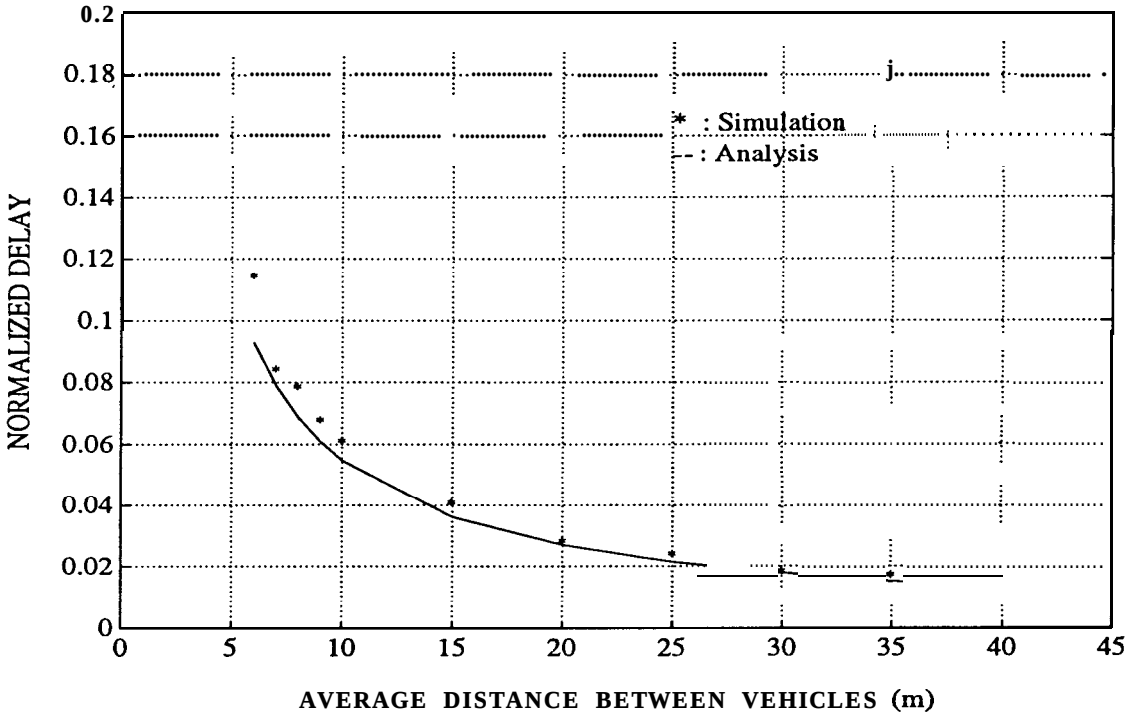

Figure 8.1: TDMA Reservation Delay : Simulation versus Analysis

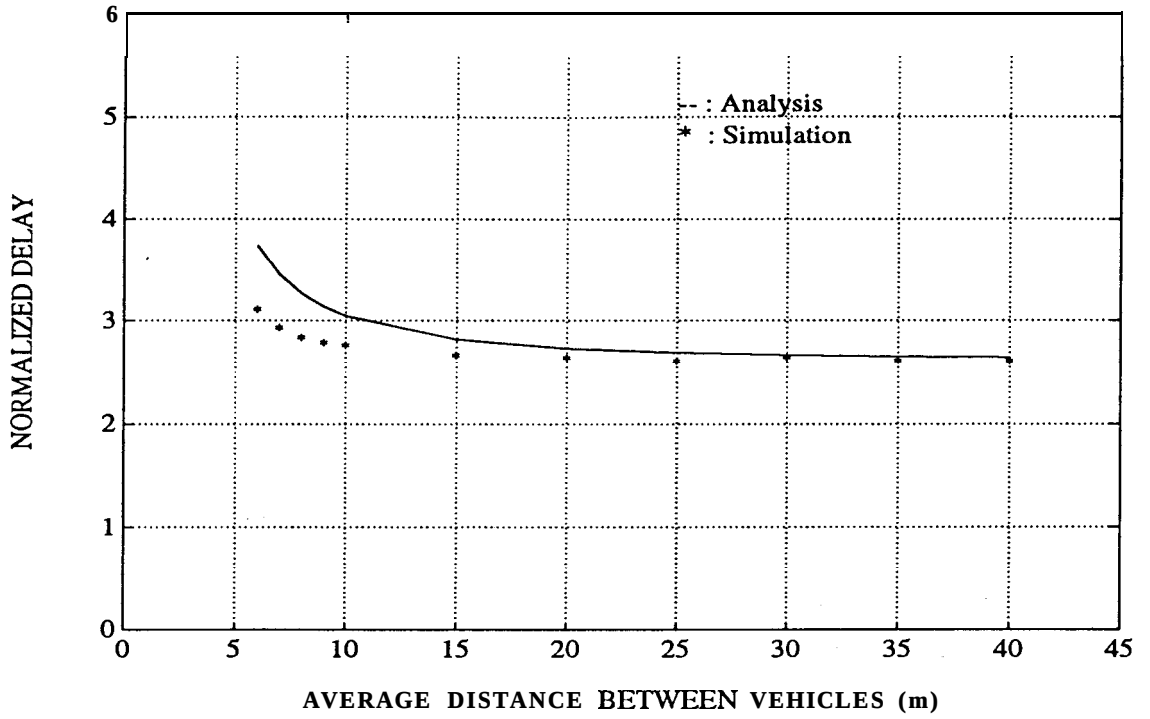

Figure 8.2: TDMA Transmission Delay : Simulation versus Analysis

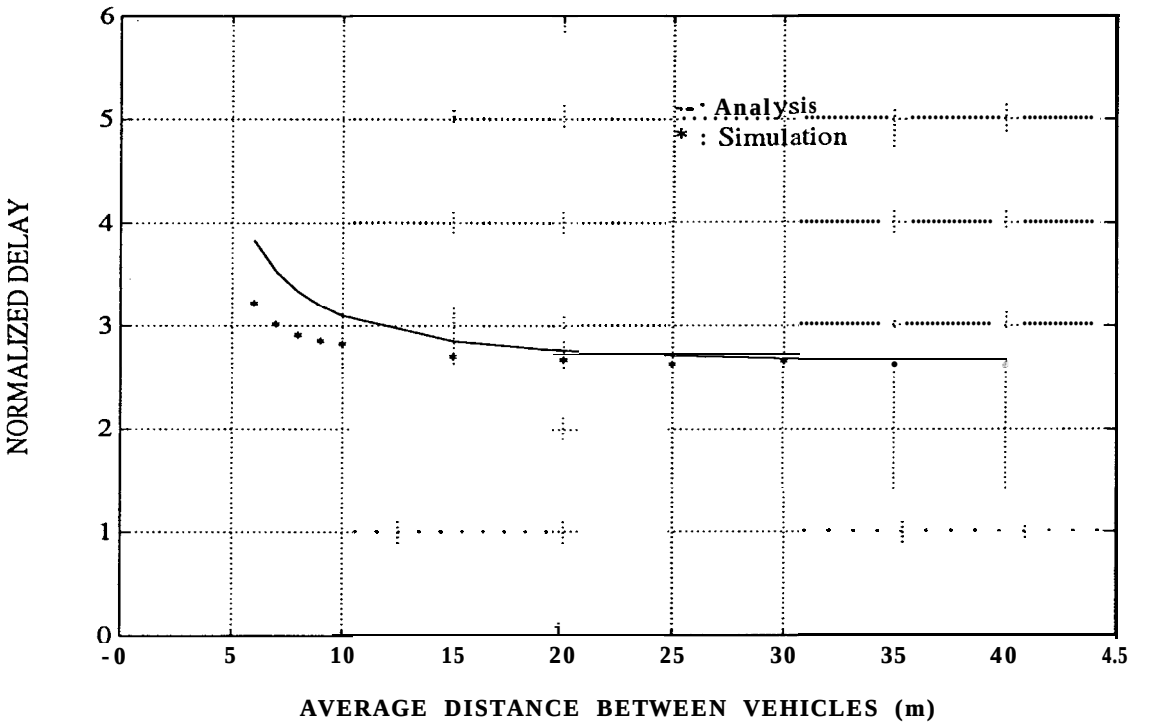

Figure 8.3: TDMA Total Network Delay : Simulation versus Analysis

8.3 C D M A

8.3.1 Throughput/Delay Analysis

In this section, we will derive the throughput/delay performance for DS/CDMA system. The slotted-ALOHA (S-ALOHA) random access [1] protocol is used to control the transmission of a message. In S-ALOHA, the time axis is divided into slots. When a vehicle enters a cell, we assume it can synchronize perfectly with the system clock and transmit its message at the beginning of the slot. If the message fails to be transmitted to the base station due to corruption by noise and multiple-access interference from other users, the vehicle will retransmit its message immediately in the next slot until the message is successfully received by the base station. After finishing the transaction, the vehicle will keep silent until it leaves the cell. The following are some important assumptions in this analysis.

1. One packet can be transmitted each slot and each vehicle transmits one packet only (AVI application).

2. The arrival process of vehicles at the cell is assumed to be a Poisson process with rate λ.

3. The new arrivals' transmission and retransmission probabilities are set to 1. We will assume that the composite (transmission and retransmission) arrival process is also Poisson with rate λ_c.

Based on the above assumptions, the throughput β of this system can be expressed as [2]

$$\beta = \sum_{m=1}^{\infty} mP_s(m)f_M(m) \quad , \tag{8.9}$$

where P,(m) is the packet success probability given m active vehicles in the system which is a function of the spreading ratio, the Rician factor K, and the signal to noise ratio E_b/N_e, and can be evaluated by the method discussed in Section 5.2. $f_M(m)$ is the pdf of the composite arrival traffic (average number of attempted transmissions per time slot)

which is given by

$$f_M(m) = \lambda_c^m \exp(-X,)/m! \quad . \tag{8.10}$$

The question is given the new arrivals rate λ, how can one compute the throughput and retransmission delay of the system? For a stable system, the throughput should be equal to the new arrivals rate. Therefore, let $\beta = \lambda$ and solve the nonlinear equation (8.9) to find the composite arriving rate λ_c. Corresponding to a given λ_c and β, the number of retransmissions has a geometric distribution with average $r_{av} = (\lambda_c/\beta - 1)$ [3]. The average retransmission delay, D_{av}, experienced by a packet is therefore

$$D_{av} = r_{av}F_r = \left(\frac{\lambda_c}{\beta} - 1\right) F_r \quad , \tag{8.11}$$

where F_r is the slot length.

If the new arrival transmission probability is not equal to the retransmission probability, the Poisson assumption for the composite arrival process is no longer true. In this case, we have to use the Markov model to evaluate the probabilistic distribution $f_M(m)$ of the composite arrival process and then compute the throughput of the system.

8.3.2 Numerical Examples

In this section, we will compare the theoretical results with the simulation results obtained from the simulation program discussed in Chapter 6. For the AVI case study, we let the spreading ratio be 31. The Rician factor K is set to 10 dB and the signal-to-noise ratio (E_b/N_e) is also assumed to be 10 dB. Given the velocity of the vehicle and the average distance between the vehicles, we can compute the new arrivals rate λ by using equation (1). For instance, if v_i = 100 miles/h and d_i= 10 meters, then λ = 0.267 vehicles (or packets) per slot. In Figure 8.4, both the theoretical and simulation average retransmission delays (normalized by slot length) v.s. average distance between vehicles are presented. We see that the simulation results for several traffic conditions are close to the theoretical results. The worst error is no more than 8%. This demonstrates that the simulation program for CDMA system is accurate. Figure 8.5 shows the throughput β as a function of composite traffic λ_c by using equation (8.9). The capacity for this system is 2.73 vehicles/slot at traffic about 6.73 vehicles/slot. In this design, we only utilize a

small portion of the capacity of the system. Finally, we show the average numbers of retransmission delays v.s. throughput in Figure 8.6.

Figures 8.7 to 8.9 show the same curves as discussed above except that the E_b/N_e is replaced by 6 dB. Both the simulation and theoretical results are also very close. However, the capacity for the system now is only 0.78 vehicles/slot because the packet success probability in this case is much smaller compared with that for the E_b/N_e = 10 dB case. Thus, in low SNRs, the average number of retransmissions dramatically increases.

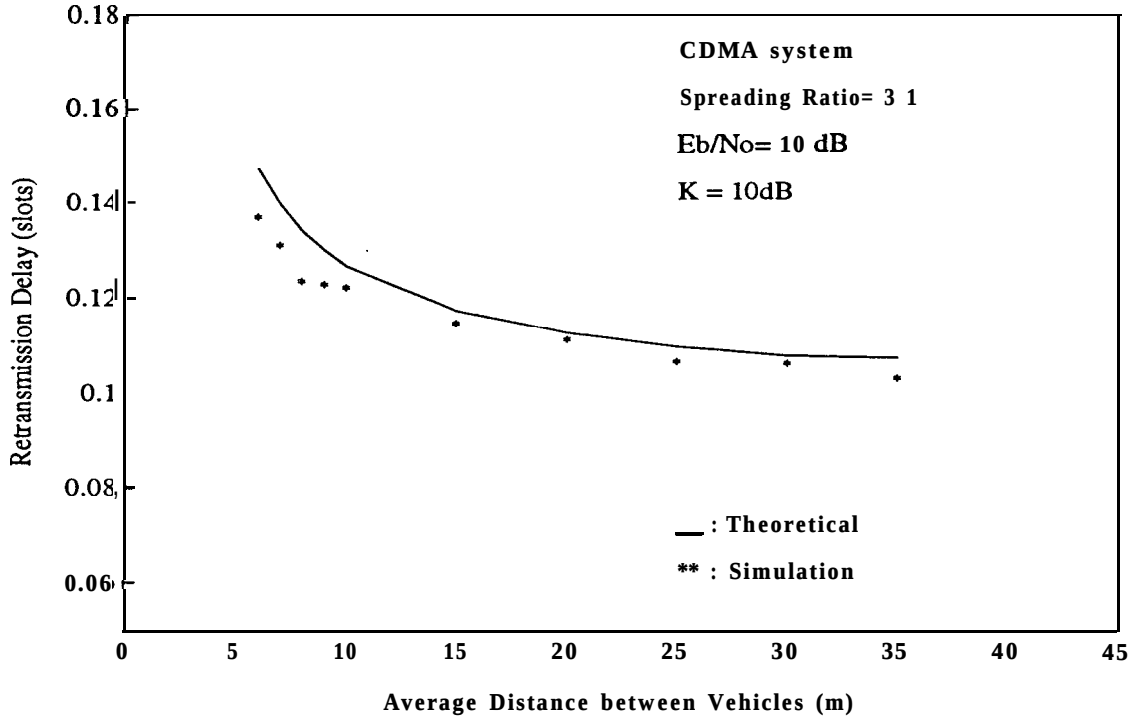

Figure 8.4: CDMA Average Retransmission Delay versus Average Distance between Vehicles

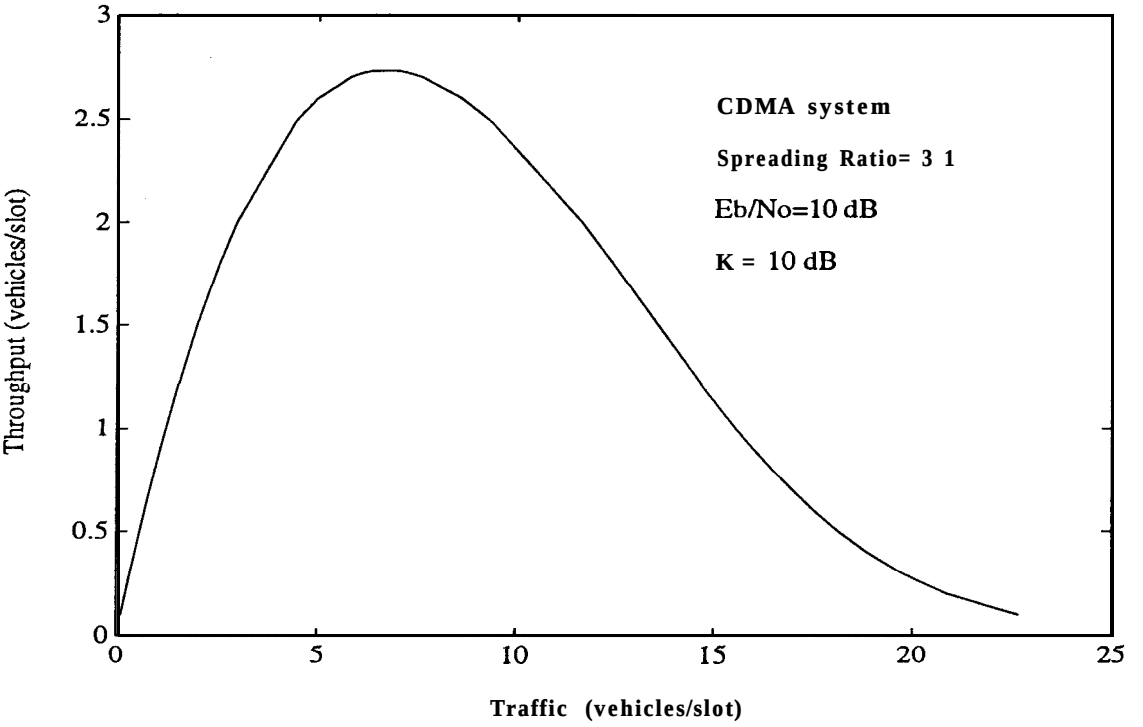

Figure 8.5: CDMA Throughput versus Traffic (Vehicles or Packets per Slot)

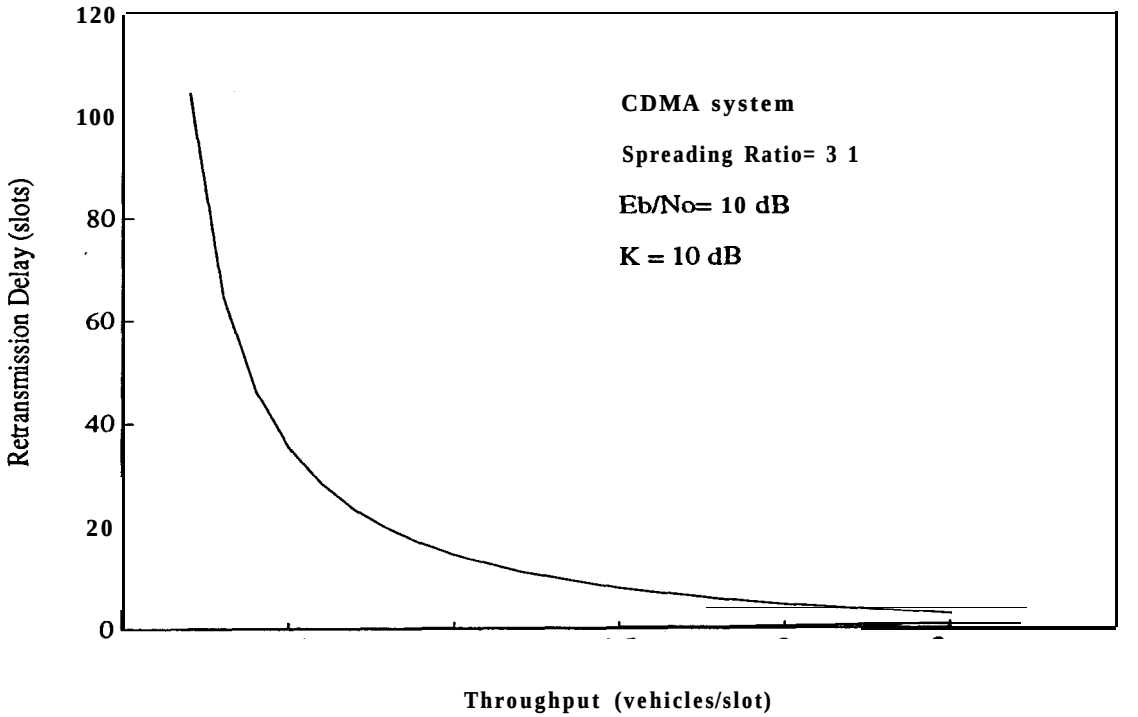

Figure 8.6: CDMA Average Retransmission Delays versus Throughput

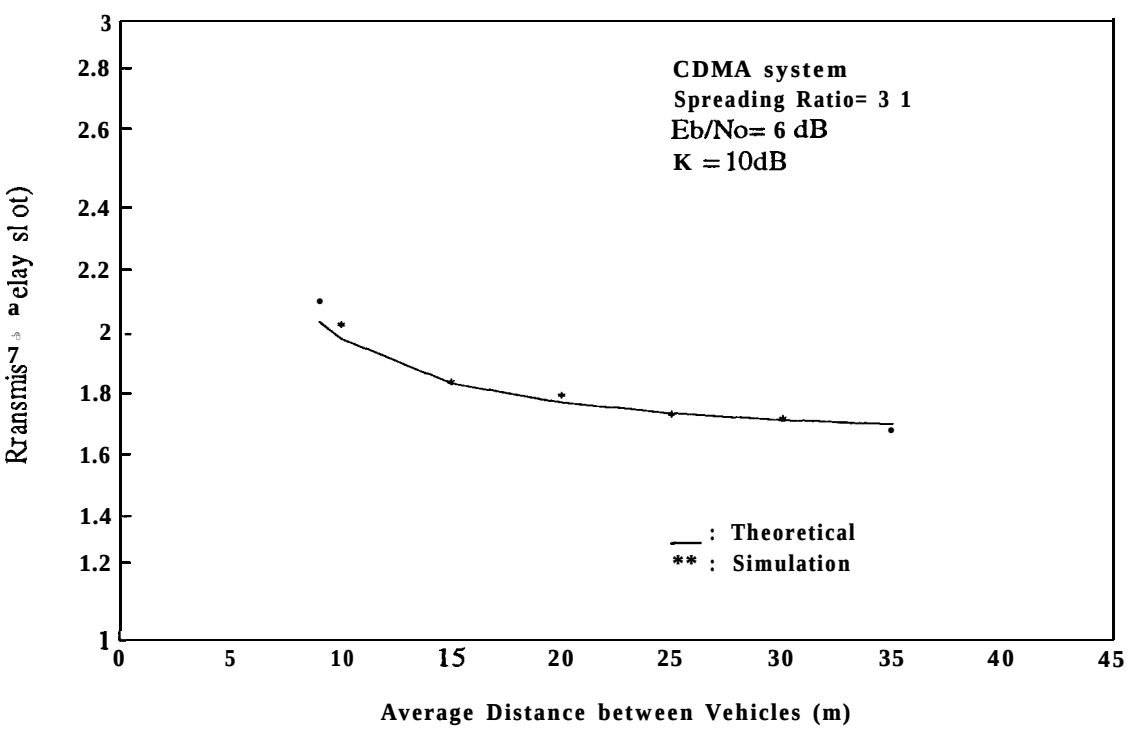

Figure 8.7: CDMA Average Retransmission Delay versus Average Distance between Vehicles

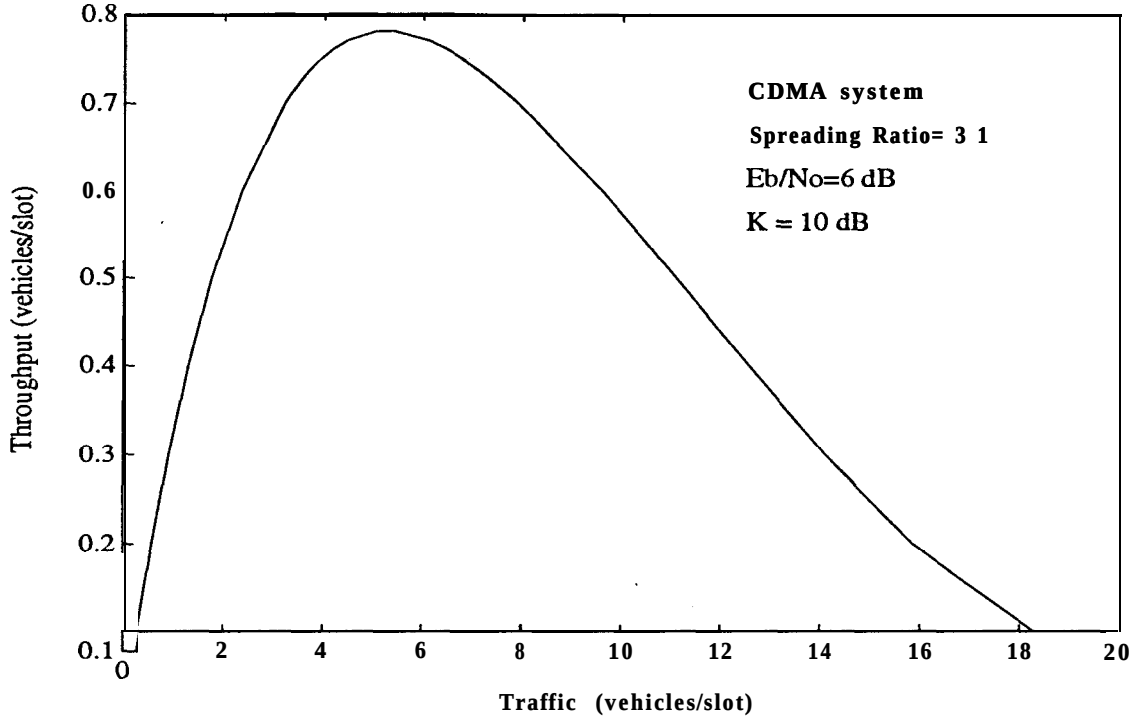

Figure 8.8: CDMA Throughput versus Traffic (Vehicles or Packets per Slot)

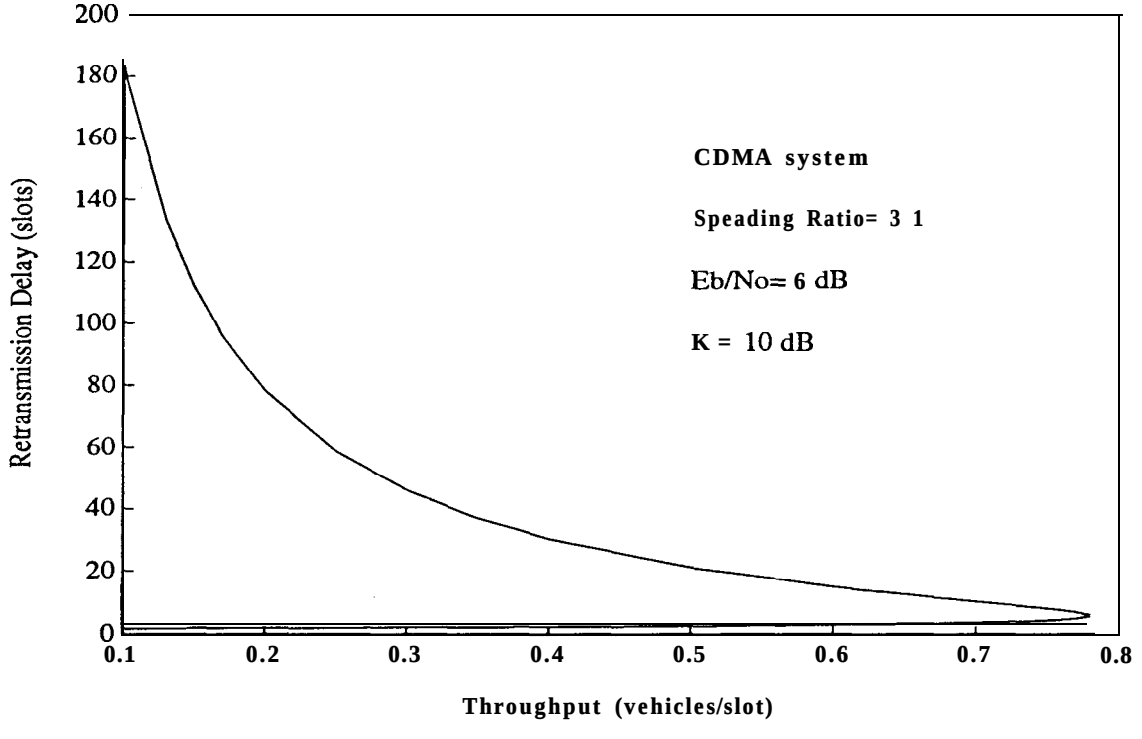

Figure 8.9: CDMA Average Retransmission Delay versus Throughput

8.4 Conclusion

In this chapter, we presented an approximate mathematical analysis of throughput and delay performance for TDMA and CDMA for a simple case of IVHS communications. The analytical results for the AVI application are compared with those obtained via the simulation program. The results match under some simplified assumptions enabling us to verify the correctness of the simulation program. They also demonstrate that the approximate, analytical model retains behavioural features of real systems, and provides meaningful performance estimates despite the approximations made.

The analysis conducted in this Chapter is the starting point of our future mathematical analysis. Eventually, we would like to develop a general and accurate mathematical technique for the performance analysis. This area is challenging since a good mathematical analysis should incorporate the mobility of vehicles and pertinent channel characteristics in the computation of network throughput and delay performance. We expect this to be a new and fertile research area in IVHS communications.

8.5 References

[1] B. Sklar, ***Digital Communications — Fundamentals and Applications,*** Prentice-Hall, 1988

[2] A. Polydoros, J. Silvester, "Slotted Random Access Spread-Spectrum Networks: An Analytical Framework", ***IEEE J. Sel. Areas Comm.,*** Vol. SAC-5, pp. 989-1002, Jul 87

[3] D. Raychaudhuri, "Performance Analysis of Random Access Packet-Switched Code Division Multiple Access Systems", ***IEEE Trans. Comm.,*** Vol. COM-29, pp. 895-901, Jun 81

Chapter 9

Conclusions, Recommendations, and Future Work

In this chapter we summarize the conclusions drawn in the preceding seven chapters of this report. We also provide a set of recommendations that are based on those conclusions, and more generally, on the experience gained in undertaking this study. We close with a discussion of the open issues, and the areas that require significant future effort to achieve refined, mature IVHS communication system designs that go beyond the preliminary examples provided so far.

9.1 Conclusions and Recommendations

9.1.1 AVI

Conclusions The proposed systems and specifications for AVI are tailored to the narrow application wherein a very brief information exchange takes place at a very short range. Consequently, they are in general unsuited to meet the far broader communication requirements of the wide span of services envisioned in IVHS. This is particularly true for the Interface Specification proposed by Caltrans/LLNL. The Specification has a series of shortcomings (e.g., one antenna per lane – see Chapter 2 for others) that make it virtually impossible to adapt to accommodate most IVHS requirements. The VRC system proposed by Hughes Aircraft, on the other hand, is an overkill for mere AVI,

yet it suffers from a protocol and some physical specifications that make it ill suited for transactions that are longer than in AVI .

Recommendations Make AVI upward compatible by (a) using architectures that permit multi-lane coverage with a single BS, and (b) enhancing the signaling and protocol aspects to accommodate many simultaneous users over a wide area of the highway. The result of such upgrades would be equivalent to including AVI as one of the many functions of ADIS. In fact, AVI transactions fit nicely into the category of short (< 1 kbit) transactions defined in Chapter 3 under generic ADIS communication requirements. It is obviously advantageous to have a single system that provides a wide range of IVHS services. Such a system would be fully capable of supporting AVI as well as many other applications.

9.1.2 Functional Requirements for IVHS Communications

Conclusions There are many proposals for presumed requirements but no final or mature state of general agreement on communication requirements. Nevertheless, there seems to be a commonality of classifying the messages which leads to 3 categories according to size: small (< 1 kbits), medium (5 - 10 kbits), and large (~ 64 kbits). There also seems to be agreement on the priority classification of the message types, namely high, medium and low. Short transactions tend to be of higher priority that longer ones, particularly very long ones.

Recommendations A concentrated effort should be dedicated to the assessment of the implications of the service classifications on broad features required in the communication architectures and protocols. This ranges from frame and slot sizes, to their level of flexibility, to such operations like discarding low priority messages if they are not received correctly the first time, etc. Generally speaking, the constraints on the architectures and protocols created by the requirements need to be articulated.

9.1.3 The Physical Channel

Conclusions Because of the confined, quasi-linear geometry of a highway segment, the propagation profile of the channel is unlike that of free-space propagation and unlike that of the traditional, macrocellular model. In ADIS communications the propagation channel is characterized by distinct slopes for the "near" and "far" ranges. The slope of the path loss curve in the far region is a strong function of the BS antenna configuration, and it plays a critical role in determining adjacent cell co-channel interference which, in turn, determines overall system performance and the resources required (such as spectrum).

The geometry of the highway plays a role in the propagation characteristics, and the presence of restricting structures like walls, leads to faster variation of signal strength. This may or may not have further implications on performance depending on the data rates and modulation schemes used.

The Rician fading model, although broadly accepted for the class of short-range, or microcellular-type channels, relies on a key parameter, namely K (the ratio of the specular to diffuse component power) which cannot be derived analytically. The specular component can be predicted through the novel multi-ray model (MRM) described in this report, yet its ratio to the diffuse component, i.e., K, as well as the spatial variability of K, require extensive measurements. In the interim, a fairly conservative value of K = 10 was used for preliminary system layout and performance analysis.

Recommendations Undertake an extensive field measurement campaign to determine K in a typical range of highway environments, with representative BS antenna configurations. Upon obtaining the measurement results refine the MRM and incorporate the effects of K, and its possible variations, into the simulation of the physical channel.

9.1.4 Multiple-Access and Modulation

Conclusions Both TDMA and CDMA can be used to meet the communication requirements of ADIS even under pessimistic vehicle traffic and service demand conditions. From the bit error rate (BER) performance analyses of Chapter 5, and the first-cut capacity computations of Chapter 7, TDMA has a small advantage over CDMA (in terms of BER performance for a given bandwidth) when no coding is used. Including a modicum of forward error correction (FEC) in the CDMA system improves the capacity performance to match that of TDMA without incurring any bandwidth penalty. The cost would be a moderate increase in receiver hardware complexity both at the BS and the mobile. Yet, significantly more detailed analysis is required, particularly of the CDMA system, before such a conclusion could be firmed or before throughput/delay comparisons could be made under general IVHS scenarios.

For a TDMA system operating in the high-SNR Rician fading channel of ADIS, noncoherent and differentialy coherent modulation schemes perform better (i.e., have lower BER) than coherent schemes. Coherent schemes, like BPSK, perform better in the low-SNR Gaussian noise channel. Since noncoherent schemes, like FSK and ASK, and differentialy coherent schemes, like DPSK, are easier to implement and lead to simpler hardware with more robust operation, they are the natural candidates for use in a TDMA architecture. DPSK performs somewhat better than FSK and ASK, but the difference is not significant for the application at hand.

Similarly, for a CDMA system architecture, DPSK performs better in the high-SNR Rician environment of ADIS than does coherent BPSK. Again, DPSK with its relative simplicity and robustness is the candidate for implementation with CDMA. Since CDMA performance is driven by multi-user interference, pulse shaping is particularly important. Somewhat predictably, the raised-cosine pulse shape, with its well contained spectrum, leads to the best performance.

A general conclusion, or perhaps caveat, is that performance results for both TDMA and CDMA are quite sensitive to the value of the Rician channel parameter K used in the analysis. An increase in K by a factor of two, from 10 to 13 dB, results in one order

of magnitude lower BER, and significantly higher capacity. An accurate evaluation of K from field measurements is critical to a refined system performance prediction.

Recommendations Use noncoherent or differentialy coherent modulations with TDMA, or differentialy coherent modulation with pulse shaping for CDMA.

Further analyze CDMA to determine its performance more accurately, particularly under non-ideal conditions of power control, code selection, overlapping cells, soft handoff, etc.

Undertake a measurement campaign to determine the value of K in a host of typical ADIS propagation environments.

9.1.5 Communication Simulation

Conclusions Simulation is critically important to modeling the system due to the system's complexity and time varying nature. Unfortunately, commercially available packages provide inadequate support for the conditions of mobility, time-varying channels and dynamic network interactions present in the IVHS or ADIS environment. Channel modeling requirements will be the most demanding of the simulation tool.

Programming in a powerful high-level language like C results in specialized programs that are much faster and less demanding in terms of memory requirements than commercially available packages. The resulting programs also tend to be adaptable and portable. Much refinement of the capability that has been developed is required for realistic simulation of disparate IVHS conditions and transactions. However, because of the complexity and breadth of such a problem, relying solely on generic C programming may not be a practically feasible approach to creating the support tool for the basic and applied research deemed necessary. A marriage of commercial packages with specialized programming extensions for IVHS seems to be the logical approach.

Recommendations Commercial packages should be further investigated to determine the most suitable candidate to serve as a broad framework to provide a basic set of tools and analysis capabilities. The limits of the package, however, should not confine the extent of the simulation development. C programming should be used to augment the capabilities of the selected package and to extend them to IVHS-specific functions (e.g., mobility, user interactions, channel modeling). The package should therefore be easy to expand upon, and should be widely accepted as a standard modeling tool for communication system design applications.

A dedicated workstation of a capability similar to that of the Sun SPARC 10/30 is essential to performing the simulation tasks, and should be made available for Phase II activities. Moreover, efficient modeling and simulation approaches for the channel must be developed.

9.1.6 Delay/Throughput Analysis

Conclusions For the simple AVI application, under some channel simplifying assumptions, simulation matches well the analytically derived results. The analytical effort can aid in finding good modeling approaches to simplify simulation.

Recommendations Continue the analytical effort maintaining a close tie with the simulation work.

9.1.7 Architecture and Layout

Conclusions System performance is limited by interference from adjacent cells which is directly related to far-region propagation characteristics. This, in turn, depends heavily on BS antenna configuration. Both middle-of-the-road and side-of-the-road BS antennas can be used. However, BS dipole antennas need to be equipped with reflectors or arrayed in simple configurations to produce the required field confinement in the far region.

The objective of attaining a one mile cell diameter can be achieved with transmit powers of 100 mW or less. If larger cells are considered advantageous from an infrastructure perspective, higher powers could be used; however the implications of the increased number of simultaneous users on the parameters of the layout (e.g., data rates, frequency reuse, spreading ratio) would be very significant and the layout issues would have to be addressed anew.

Both the 900 and the 1800 MHz bands can be used. The higher frequency band results in somewhat larger cells due to the less demanding dynamic range requirement placed on the vehicle receiver (see Chapter 4). Doubling the frequency increases the range by roughly 50%. From this perspective, the 1800 MHz band **is** preferable.

Both TDMA and CDMA can meet demanding ADIS requirements even under conditions of heavy/congested traffic and with a conservative channel model. For CDMA, however, significantly more analysis is required to completely characterize its performance.

Many candidate layouts and protocols can be applied but their detailed tradeoffs require extensive simulation.

Recommendations Use a frequency band in the range of 1.8 or 2 GHz to achieve larger microcells along the highway than those likely with 900 MHz.

Use a BS antenna configuration with a metallic reflector or equivalent to confine the radiation in the far region of a cell and to limit adjacent cell interference.

For a TDMA architecture, use a 3 frequency plan in an FDM/TDMA set-up (see Figure 7.5) to meet the generic ADIS requirements projected in this report (Chapter 3). For CDMA, perform more detailed analysis to ascertain if a system with no frequency reuse has a permissible amount of adjacent cell interference.

Investigate other architectural options such as overlapping CDMA cells, TDM/TDMA, and time-division duplexing.

9.1.8 Other Conclusions and Recommendations

FM multiplex can be used as a supplement to an ADIS architecture to disseminate non-car-specific information, primarily to low-intelligence vehicular units. The use of RDS-like techniques (like those already implemented by Autotrack in the Los Angeles area) as a suplement to IVHS deserves further attention.

9.2 Future Work

Phase II of this project will focus mainly on analytical refinements and on accomplishing realistic simulations of IVHS taking especially into account all the channel and protocol particularities.

9.2.1 Functional Requirements

The work of the international standardization bodies (ETSI,...) must be closely followed, especially since a standard on Mobile Radio is expected during 1993. Furthermore, since the major IVHS players, as well as the system solutions, will certainly be global, all experiments and tentative solutions must be thoroughly analyzed.

An important aspect that has been somewhat overlooked is the interaction between vehicular traffic and generated radio traffic (i.e., communication requirements). Studies of the above interaction must be conducted; input from Caltrans is expected and necessary. Caltrans should also help establishing the heuristics reflected in Figures 4.50-4.52.

9.2.2 IVHS Channel Modeling

The measurement and understanding of the behavior of the Rician channel parameter K in the IVHS environments is essential. At the same time, refinements of the channel model need to be undertaken, namely going from a Ray-Tracing to a full Geometric Theory of Difraction approach.

This refinement of the model needs to be done in parallel with efforts in order to simplify the implementation of the MRM. For this purpose, intensive statistical analysis of the temporal samples of the fading channel discussed in Chapter 4, Section 4.4 is necessary. In fact, this will be the emphasis of the beginning of Phase II.

9.2.3 Multiple-Access

As discussed in Chapter 5, only upper-bounds on the PER are available at the moment. The upper-bound corresponds to the totally unrealistic (in the IVHS environment) assumption of very fast fading (referring to the bit/chip duration). Analytical work is therefore needed for the computation of PER under realistic IVHS mobile conditions, where channel variations are expected within the duration of the packet, but "none" from one bit/chip to the next.

9.2.4 Simulation

The simulation needs to incorporate the channel model as derived in Chapter 4. Once the MRM will be the most taxing component of the simulation, as soon as sufficient statistical information is available, as per prior discussion in Section 9.2.2, the time-varying characteristics of the channel should be included.

9.2.5 Delay/Throughput Analysis

Intense effort is needed to incorporate time-variance into the network/protocol analysis. Dynamical queueing theory questions will certainly surface.

9.2.6 Architecture and Layout

Consensus is needed in what refers to optimal cell size, allocated bands (2.5 GHz is also likely, at least in Europe) and bandwidths, allowed BS transmitter power, etc., before any "definitive" analysis can take place.

Appendix A

FM Subcarrier and the IVHS Environment

A.1 Introduction

In this report we analyze one particular implementation of a FM Subcarrier system which has been considered for IVHS applications, namely the SCA system, relying mostly on reports from one of the companies involved with SCA (Modulation Sciences, Inc).

Systems similar to SCA exist or are proposed in Europe (RDS, ARI) and Japan (using L-MSK), but not much information is available at this time. During a RACE meeting in Brussels in September 1992, one of the team members, Jorge M.N. Pereira, had the opportunity to collect information on the European systems, which will be the subject of a later report. Information on the Japanese systems is still being sought.

A.2 FM Deregulation

In recent years the FCC allowed for the opening of the FM baseband to 99 kHz, and relaxed the technical and usage rules. Deregulation has removed all restrictions on allowable modulations. This stirred up great interest in new services via SCA (e.g., teleprinter newscasting, computer data transmission, paging).

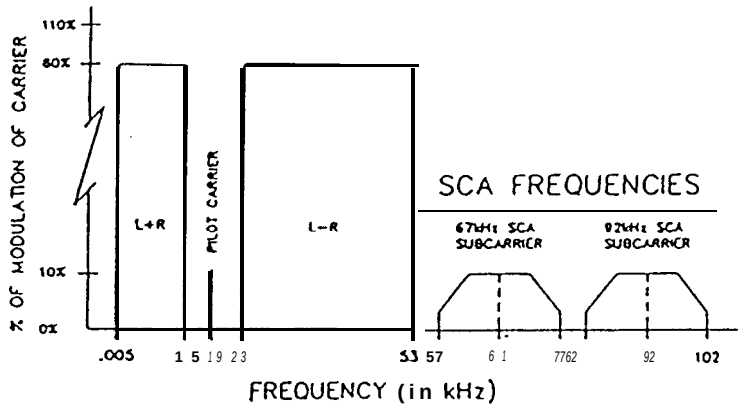

Figure A.l: FM Spectrum

The basic SCA channel audio response is 50 Hz to 5 kHz, with O-20 Hz sometimes available for low speed telemetry applications. By restricting the maximum modulating frequency to 5 kHz one guarantees a bandwidth of 20 kHz for the SCA channel (in fact, as it can be deduced from the figure above, the SCA channel bandwidth is only 14 kHz since the outer 3 kHz fall below the -25 dB threshold established by the FCC – that is why the upper SCA channel could be centered about 92 kHz). The two-SCA channel structure shown above does not necessarily imply that one could not use the whole 53 to 99 kHz to transmit data, although this is an aspect far from being clear at this point.

A.3 Inherent Problems of SCA

The established use of SCA has thus far been in stationary applications. The problems identified in this section limit SCA performance even in the stationary environment. Under mobile conditions, where the propagation conditions are significantly morre severe, more problems and limitations develop as will be discussed later.

The two most important problems inherent to SCA channel operation are crosstalk and the “birdies” effect. Crosstalk is the interference into the SCA channel from the stereo-FM channel, and it determines almost entirely the noise performance of the SCA. It is obviously determinant when operating a Data SCA channel.

The so called "birdies" result from interference caused by the SCA channel into the main stereo-FM channel, and consist of high frequency audio whistles, typically 5-10 kHz, that are frequency modulated by the SCA material. This problem is practically solved by the use of a PLL FM receiver for the case of a standard SCA channel side by side with a main stereo-FM channel. New, unestablished modes of SCA operation, such as Data SCA, the use of odd subchannel frequencies or quadrature-stereo operation, may cause "birdies" in stereo receivers.

A.4 Data SCA

There is at this point no generally accepted technical standards for Data SCA transmission. However, any proposed system must prove non-interference with the main stereo-FM channel, as well as other SCA channels.

Two types of data modulation have been considered, namely Direct and Indirect Data Modulation. In Indirect Data Modulation, also known as Compatible Modulation, the signal that goes into the SCA generator is a sequence of audio tones (AFSK - Audio Frequency Shift Keying). The advantage of this type of modulation is that standard (i.e., no-data) SCA generators can be used unmodified. Thus cheap and easy to use generators are already available. Disadvantages are the slow data rates that can be accommodated (less than 1200 bps), and the relatively expensive demodulator required to turn the audio back into data.

By switching the phase of an audio tone instead of its frequency higher data rates can be achieved, but the cost of the receiver demodulator rises very rapidly with data rate, and, conversely, the tolerance of the system to interference (crosstalk) drops quickly. The advantage of this technique is that it employs the same technology used to send data via the telephone network, thus lots of hardware is around and many people understand it. Usual data rates are below 9.6 kbps.

Direct Data Modulation takes advantage of something available to the SCA user, namely the subcarrier itself. The SCA subcarrier (at 67 or 92 kHz) is available for direct

manipulation by the broadcaster. Instead of varying the frequency of an audio tone that in turn modulates the SCA subcarrier, the frequency of the subcarrier itself is varied. Higher data rates can be achieved with less bandwidth, and the receiver demodulators are cheap too.

One can either use MFSK, varying the frequency of the carrier itself, or MPSK, varying the carrier phase. PSK, however, requires a phase reference. Luckily, in stereo-FM an ideal external phase reference already exists : the 19 kHz pilot. A data rate of up to 56 Kbps can be achieved with MPSK, occupying the entire SCA portion of the FM channel, from 53 to 99 kHz, and requiring a relatively expensive receiver. For instance, Modulation Sciences' Data Sidekick system achieves 4800 bps at a measured BER of 10^{-7} for fixed links under "good" weather conditions.

In fact, the first and foremost problem of SCA, the one that limits the data rate, is multipath. Under fixed conditions, and by using appropriate antennas, one can deal with the multipath and assure a given BER almost always. The biggest problem, even then, remains that of "equalizing" or "zeroing" late/undesirable reflections. Especially in urban environments, the reflection coefficients in the ever present masonry (brick or cinder block walls, cement structures) varies tremendously (as much as 25 dB) depending upon its surface being wet or dry.

A.5 SCA in the IVHS Scenario

By definition, SCA is not suited for two-way communication. One can only envision the use of SCA in very specific broadcast applications of IVHS (e.g., transmitting traffic status information both on the freeway system and on surface streets – a value-added service that may be of interest for some broadcasters). This would require, however, coordination with (or by) the Regional/Local Control Centers and the definition of strict receiver standards to minimize the costs associated with display of information.

Moreover, the most critical performance limitation of SCA is due to multipath. Unfortunately, in the IVHS environments multipath is unavoidable if one wishes to employ

simple (and cheap) receiver antennas (e.g., whip antennas or monopoles).

Under mobile conditions, the ones of interest in the IVHS scenario, it is not possible, without incurring in unacceptable receiver costs, to try to compensate for, or nullify, the multipath effects. Thus, the SCA system must either be designed such that it accounts for the degradation caused by the multipath (e.g., by increasing the SNR) or by explicitly taking into consideration that sometimes (or often) the receiver will not be able to properly receive the information.

A possible operational solution would be to continuously repeat the traffic status information updating it on the run. If it happens that a vehicle is unable to receive for a while due to specific propagation conditions, it would continue to "see" the last successful status report, which would be updated as soon as reliable information would be received. This obviously points to the necessity of a thorough study of the distribution of "good" and "bad" propagation conditions in the real world.

A.6 Conclusions

SCA is by construction a broadcast technology which has severe limitations in the harsh mobile IVHS environment. Moreover, there seems to be unavailable concrete information on deploied systems and their actual performance. SCA may however be able to implement certain broadcast components of IVHS, provided the necessary studies of propagation conditions show that the frequency and extent of the "blind spots" does not make it impractical.

A.7 References

[1] Eric Small, "Data SCA : Some Real World Experiences", Modulation Sciences, Inc.

[2] Eric Small, "Making SCA work in the Real World", Modulation Sciences, Inc.

Appendix B

Glossary

- **AAA** - Automobile Association of America;
- **AACS** - Automobile-Automobile Communication System -JSK's project, Japan;
- **ADEPT** - Automatic Debiting and Electronic Payment for Transport (EEC);
- **ADIS**- Advanced Driver Information System;
- **ADS** - Automatic Debiting Systems;
- **ADVANCE** - a cooperative ($ 35-40 M) project involving the Illinois Department of Transportation, the FHWA, Motorola, and the Illinois Universities Transportation Research Consortium, will provide up-to-the-minute traffic information to 5000 private and commercial vehicles, at the same time gathering traffic information from the vehicles; a combination GPS/dead-reckoning system, in combination with a map displayed on a color CRT, will provide location information; based on a destination entered by the driver and current traffic information, optimum routes will be computed and provided to the driver; any enroute changes of traffic conditions are provided to the driver, and the option to recompute the route will be provided; using the CRT and synthesized voice; the ADVANCE infrastructure is unique in that vehicle probe data is the primary, rather than secondary, source of traffic information (if successful this technique will reduce the need for extensively instrumented roadways, with significant savings in infrastructure costs);

- **Advantage 175** - (design phase near completion) CVO system in the Eastern U.S., will use AVI, AVC, WIM technology as well, with heavy vehicle monitoring performed through a decentralized management network;
- **ALARA** - As Low as Reasonably Achievable;
- **AMPS** - Advanced Moile Telephone System (U.S.);
- **AMTICS** - Advanced Mobile Traffic Information and Communication System - surface streets in-vehicle information system, Japan;
- **Anaheim IVHS Operational Test** - APTS project geared at developing a real-time information system for transit passengers; information on traffic conditions will be provided by the area ATMS;
- **APC** - Average Power Control - usually considered in analyzing non-orthogonal CDMA schemes, tries to compensate for the propagation losses and slow channel fading [1];
- **APTS** - Advanced Public Transportation System - provides for an increased level of service, thereby increasing ridership, and reducing the burden on the congested highway system; it includes AVL and communication systems to enhance fleet management operations, electronic fare media, and new techniques to more effectively use and monitor HOV lanes;
- **ARI** - Autofahrer Rundfunk Information (Radio Information for the Driver);
  - **ARI-2** in U.S.A.;
  - **ARIAM** - ARI on basis of Actual Measurements;
- **ATMS** - Advanced Traffic Management Systems - monitor traffic conditions and provide real-time adjustments to traffic control systems to ensure optimum traffic flow and respond sooner and more effectively to incidents; includes traffic surveillance systems;
- **ATIS** - Advanced Traveler Information System - provide to travelers ATMS data on current traffic and road conditions, vehicle location and navigation information, safety warning messages, and also allow travelers to signal for help when needed;

- **AVCS** - Automatic Vehicle Control Systems - employ advanced sensor and control technologies to assist the driver in responding to the immediate environment on the roadway; AVCS will be developed step by step, seeking first to ehnance the driver's perception of the immediate environment (obstacle detection in vehicle blind spots, collision warning systems, infrared vision enhancement systems); later collision avoidance systems will be developed which take temporary control of vehicle operation; the long term potential of AVCS is to provide fully automated vehicle/highway systems;

- **AVI** - Automatic Vehicle Identification - is used by motor carriers for ETC and other applications requiring the interchange of data with the roadside to reduce the number of required stops enroute;

- **AVL** - Automatic Vehicle Location - enables individual vehicles to be tracked; combined with messaging systems, it is revolutionizing fleet management techniques;

- **Backward Link** - from mobile to cell site/base station;

- **BER** - Bit Error Rate;

- **CACS** - Comprehensive Automobile Traffic Control System - Japan;

- **CADIS** - California Advanced Driver Information System - California's ADIS/ATIS system;

- **Caltrans** - California Department of Transportation;

- Capacity - see Soft Capacity;

- **CARIN** - Car Information and Navigation System - in-vehicle information and navigation system developed by Philips using CD-ROM for data storage;

- **CARMINAT** - project investigating the use of RDS to provide dynamic traffic information to an on-board CARIN unit;

- **CASH** - EEC program to develop CFSs for ADS;

- **CBIN** - Character-Based Identification Number - associated with the Mobile (or Mobile transponder);

- **CCIR** - . . . - International Radio Consultive Committee;
- **CCTV** - Closed Circuit TV;
- **CDMA** - Code Division Multiple Access - is a Spread Spectrum multiple access technique where a number of users, each having a unique spreading sequence, communicates simultaneously over the same frequency band; total interference depends on the spreading factor, the ratio of spread bandwidth to information bandwidth; thus it is interference-limited;
- **CEC** - Commission of the European Community - EEC executive branch;
- **CED** - Common European Demonstrators;
- **CEPT** - *Conférence Européenne des Postes et Telécommunications*;
- **CFS** - Common Functional Specifications (EEC);
- **CHP** - California Highway Patrol;
- **CMS** - Changeable Message Sign;
- **CODIT** - UMTS Code Division Testbed at 2 GHz (EEC);
- **COMIS** - aims at defining, demonstrating and validating applications based on 60 GHz short range links, both vehicle-vehicle and vehicle-roadside (EEC);
- Connecticut Freeways **ATMS** - statewide freeway surveillance and control program (in a preliminary design stage), including an evaluation of roadside mounted radar traffic detectors and CCTV for incident detection/verification;
- **COST** - European Cooperation in the Field of Scientific and Technical Research - EEC program for Cooperation for R&D in Science and Technology;
    - **COST 207** - European Research Project on Digital Land Mobile Radio Communications to develop the harmonized Pan-European digital mobile radio telephone service, currently developing specifications for a selective fading simulator (and examining adaptive baseband equalization techniques);

  * **COST 231** - European Research Project on the evolution of Land Mobile Radio (including Personal) Communications;

- **CRT** - Cathode Ray Tube (???);
- **CSI** - Communication Sciences Institute, at the University of Southern California, Los Angeles;
- CT2 - Cordless Telephone - Second Generation (???);
- **CVO** - Commercial Vehicles Operation - aimed at improving the safety and operational efficiency of commercial vehicles; involves AVI, AVL;
- **DAB** - Digital Audio Broadcasting;
- **DCA** - Dynamic Channel Allocation;
- **DECT** - Digital European Cordless Telephone;
- **DIRECT** - Detroit,MI, ATIS system (in a preliminary design stage), will evaluate various low cost means of providing traffic information to (30) motorists, including Radio Data Systems (transmit data on a subcarrier section of FM broadcast signals), HAR, Automatic HAR, and cellular phone;
- **Diversity - see Macro Diversity;**
- **DoT** - Department of Transportation;
- **DRIVE** - Dedicated Road Infrastructure for Vehicle Safety in Europe;
- **EEC** - European Economic Community;
- **EIA** - Electronic Industries Association;
- **EIRP** - Effective Isotropically Radiated Power;
- **ERCC** - European Radio Communications Committee;
- **ERMES** - European Radio Messaging System - paging;
- **ESPRIT** - European Strategic Programme for R&D in Information Technology;

- **ETC** - Electronic Toll Collection;
- **ETSI** - European Telecommunications Standard Institute;
- **ETTM** - Electronic Toll and Traffic Management - example of ATMS;
- **EUREKA** - European Research Project - Industrial Cooperation Scheme in High Technology;
- **FAA** - Federal Aviation Administration - agency of the DoT;
- **FAME** - Seattle,WA, multi-faceted ATMS program (in implementation) including a demostration of an integrated system for a local freeway which automatically modifies arterial signal control timings in response to freeway conditions;
- **FAST-TRAC** - combination ATMS/ATIS project in MI (in the early negotiation stages); the ATMS is an advanced adaptive traffic control system, with traffic detection provided by video detection systems; route guidance will be provided by an European ATIS system, which uses infrared beacons installed at key intersections; as the vehicle passes by each intersection, an optimum route is computed based on real-time traffic information transmitted by the beacon;
- **FCC** - Federal Communications Commission - independent agency within the Federal Government, responsible for all non-government frequency matters; the Private Radio Bureau is responsible for Land Mobile matters and non-Common-Carrier microwave, both of which will figure in IVHS [2];
- **FDMA** - Frequency Division Multiple Access - noise-limited multiple access technique;
- **FHWA** - Federal Highway Administration;
- **Forward Link** - from cell site/base station to the mobile;
- **FPC** - Fast Power Control - unlike the APC, FPC tries in addition to compensate for the fast channel fading [1]; for an indoor environment see [3]; for an outdoor environment see [4];
- **F(P)LMTS** - Future (Public) Land Mobile Telecommunications Systems;

- **FTA** - Federal Transit Administration;
- **GEO** - Geostationary Orbit;
- **GM** - General Motors, Corp.;
- **GPS** - Global Positioning System;
- **GSM** - ***Group Spécial Mobile*** - CEPT working group for a Pan-European Mobile Telecommunication System;
  - **GSM 900** - transmission in the 900 MHz band;
  - **GSM 1800** - transmission in the 1800 MHz band;
- Guidestar - Minnesota ATMS program (in the early stages) to evaluate multiple IVHS technologies, including traffic information systems for traffic managers and motorists, centralized integration/coordination of traffic signals, and traffic surveillance based on image processing;
- **Handoff** - call transfer procedure between base stations, in such a way as to be transparent to the user;
  - **Soft Handoff** [5] - system feature that a mobile will communicate with two base stations simultaneously during handoff, thus avoiding the "ping-pang" effect of regular "hard" handoff; additionally, the receiver at the mobile can make use of the diversity (e.g. RAKE receiver) to enhance its performance;
  - **Softer Handoff** [5] - channel element capability to communicate with a mobile via more than one sector in case of intra-cell/inter-sector hand-off; to the mobile, similar to soft hand-off, to the base station(s), the signals received from the mobile via two sectors can be diversity-combined to improve SNR ratio performance;
- **HAR** - Highway Advisory Radio;
- **HDLC** - High-Level Data Link Control;
- **HELP-Crescent** - CVO project involving 15 and 110, from British Columbia to Texas; implementation of an integrated heavy-vehicle monitoring system using AVI,

AVC, and WIM technology along a major trucking corridor; 40 equipped roadway locations are involved; to date 1500 trucks have been equipped with transponders;

- **IBC** - Integrated Broadband Communications (EEC);
- **IBCN** - Integrated Broadband Communications Network (EEC);
- **INFORM** - operational Long Island/New York ATMS, integrates surveillance and control of three freeways, cross, and arterial streets; traffic information is provided via CMSs
- **Integrated Freeway Project** - operational Anaheim,CA, ATMS project which addresses congestion in response to numerous area special events through the use of a computerized traffic control system, HAR, CCTV, and CMSs, and electronic coordination with the regional State TIC;
- **IRIDIUM** - Satellite Mobile Communication System for Sparsely Populated Areas;
- **IRTE** - Integrated Road Transport Environment - EEC concept, the goal of DRIVE;
- **ISTEA** - Intermodal Surface Transportation Efficiency Act of 1991 - authorized approximately $660 M over six years to fund IVHS efforts;
- **ITS** - Institute of Transportation Studies, University of California, Berkeley;
- **IVHS** - Intelligent Vehicle Highway Systems - is a major initiative of Government, Industry and Academia to apply advanced technology to the operation of the Nation's surface transportation system, so as to improve mobility and transportation productivity, enhance safety, maximize the use of existing transportation facilities, conserve energy resources, and reduce adverse environmental effects [6]; based upon information transfer between the highway infrastructure and vehicles, and between the vehicles themselves;
- **JDC** - Japan Digital Cellular [7];
- **JSK** - Association of Electronic Technology for Automotive Traffic and Driving - created by MITI, Japan;

- **LANELOCK** - computer vision system (AVCS) developed by the GM Research Labs which uses image processing of lane striping to maintain lateral position on a roadway;

- **LCD** - Liquid Crystal Display;

- **LEO** - Low Earth Orbit;

- **LLNL** - Lawrence Livermore National Laboratory, Stanford, CA;

- **Macro Diversity** - the Mobile is/may be connected to more than one Base Station at the same time;

- **MBS** - Mobile Broadband Systems (EEC) at 60 GHz;

- **Meteor Scatter Communication Network** - uses the ionized trails of meteors entering the atmosphere as "free" naturally occurring satellite channels [8];

- **MITI** - Ministry of International Trade and Industry - Japan;

- **MOBILISE** - EEC program dealing with the Personal Communication Space, i.e., a generalized form of personal mobility encompassing both the fixed and the mobile networks;

- **Mobility Manager Demonstrations** - FTA sponsored APTS projects underway in OR, MD, and VA, include the linkage of various transportation providers to provide an integrated service, traveler information, and electronic fare media technology such as "Smart Cards";

- **MONET** - Mobile Network Project (EEC);

- **Multi-Jurisdictional Live Aerial Video System** - MD/VA ATMS system near completion employing a video communications link from an aircraft down to the traffic operations center of the two counties which share a congested freeway;

- **NADC** - North American Digital Cellular [9];

- **NHK** - Japanese broadcasting organization;

- **No1** - Notice of Inquiry - FCC mechanism that solicits responses from interested parties on an issue with broad applicability;

- **NoPR** - Notice of Proposed Rulling - FCC mechanism that solicits specific comments on pending Allocation issues;

- **NTIA** - National Telecommunications and Information Administration - an agency within the DoC responsible for Government frequency matters;

- **ORA** - Opportunity for Application of Information and Communication Technologies in Rural Areas;

- **PABX** - Private Branch Exchange;

- **PANDORA** - Prototyping a Navigation Database of Road Attributes - EEC's DRIVE project;

- **PATH** - Partners for Advanced Transit and Highways - ongoing AVCS ($ 150 M) research program being conducted by a partnership of California Universities, with government sponsorship, with the goal of advancing safety, improving fuel efficiency, and reducing traffic congestion and air pollution;

- Pathfinder - cooperative ATMS/ATIS ($2.5 M) project between the FHWA, Caltrans, and GM, taking place along a 13 miles stretch of the 110 (Santa Monica Freeway), between Santa Monica and Los Angeles, known as the Santa Monica corridor, which inludes the freeway service roads and five major parallel arterial roads which can be used as alternatives to the freeway; first in-vehicle navigation system project in the United States (1988), tries to assess the benefits of providing real-time traffic congestion information to drivers, enabling them to modify their routes and thus avoid congested areas; additionally it tries to evaluate the utility of using vehicles as traffic probes, whereby vehicles report traffic speeds back to a central traffic monitoring system as an additional source of traffic information; Pathfinder consists of three subsystems : the **vehicle subsystem** hardware is based on the ETAK Travelpilot (a navigational system that displays electronic road maps, stored in CD-ROMs, on a monochrome CRT display), with an RF link that conveys congestion data to the 25 vehicles (presented visually, textually, and aurally); the

central subsystem which performs the function of fusing congestion data from the arterial street computer system, the freeway computer system, the Pathfinder vehicles, and other sources; this congestion data is passed to the **communications subsystem** which **uses** a packet radio system to broadcast congestion data to all vehicles once a minute, which then return information concerning vehicle location, heading, and speed during a preassigned time slot within the minute;

- **PCN** - Personal Communication Network;
- **PCS** - Personal Communication Services;
- **PER** - Packet Error Rate;
- **PLATON** - Advanced Cell Planning Methods and Tools for the Third Generation Mobile Systems;
- **Platoon** - the concept of "platooning" has been developed at PATH for high density automated highway operations, whereby groups of up to 15 vehicles follow each other at very close spacings; techniques to facilitate both longitudinal and lateral control are also being investigated;
- **PROMETHEUS** - Programme for European Traffic with Higher Efficiency and Unprecedent Safety - EEC's EUREKA research project;
- **PLMRS** - Private Land Mobile Radio Services;
- **RACE** - R&D in Advanced Communication Technologies in Europe;
- **RACS** - Road Automobile Communication System - expressway in-vehicle information system, Japan;
- **RDS** - Radio Data System;
    - **RDS-TMC** - RDS-Traffic Message Channel;
- **RTI** - Road Transportation Informatics (???) - European concept;
- **SAP** - ???;

- **Satellite Communications Feasibility Study** - Philadelphia,PA, ATMS study (near completion) to evaluate satellite communications as a means of passing freeway surveillance and control data from the roadside to the local operations center, to include video images;

- **SMART Corridor** - Los Angeles ATMS project (in completion); traffic is monitored via a extensive network of inductive loop detectors; CMSs, HAR, and kiosks are used to pass congestion information **to** drivers;

- **SMART** - Strategy for Mobile Advanced Radio Telecommunications (EEC);

- **Smart Bus Demonstrations** - FTA sponsored APTS projects underway in OR, IL, and MI; include the use of sensors at bus stops which would respond to an "emergency" button on a "smart card" to enhance personal security, bus fleet AVL systems, and traffic signal preemption systems for buses;

- **Smart Card** - "credit card" equiped with a microprocessor;

- **Smart Traveler Demonstrations** - APTS systems underway in WA, CA, TX, and MN; using mobile communications, rapid ridemaching techniques to enhance carpooling are being investigated, as well as several traveler information systems and smart card techniques;

- **SOCRATES** - System for Cellular Radio for traffic Efficiency and Safety - EEC's DRIVE program in the area of Telecommunications;

- **Soft Capacity** - graceful degradation when cell gets overloaded;

- **STAR** - Science & Technology Programme for Less Advanced Regions;

- **TACS** - ???;

- **TARDIS** - Traffic and Roads-Drive Integrated Systems - EEC's DRIVE program in the area of Telecommunications;

- **TDMA** - Time Division Multiple Access - noise-limited multiple access technique;

- **TET** - Transport Exper Team - team of experts appointed by the European standardization bodies;

- **TIBAS** - The Interaction Between Automotive and Supplies Industries (EEC);
- **TIC** - Traffic Information Center;
- **TMS** - Traffic Management System;
- **TRANSCOM** - North New Jersey/New York City Metro area ATMS (in the design stage); will use **1000** commercial vehicles equipped with ETTM transponders as traffic probes, with readers placed at strategic locations to monitor speed;
- **TravTek** - Travel Technology - **is** a public/private ($12 M) partnership involving the City of Orlando, the Florida Department of transportation, GM, and the AAA; it is a combination ATMS/ATIS system, providing traffic congestion information, motorist services, information, tourist information, and route guidance to 100 specially equiped test vehicles; the route guidance reflects real-time congestion information broadcasted from a central TMC; the in-vehicle system provides the driver with up-to-the-minute traffic information and routing (routing to selected destinations is provided on a turn-by-turn basis); it includes a UHF-FM transceiver to exchange information with the TMC, and a GPS receiver to augment the dead-reckoning navigation system;
- **Two-Way Messaging/Positioning System** - private satellite-based CVO systems are used by long-haul truckers; local fleets exchange data via mobile data nets; generally GPS is used to provide positioning; these systems have resulted in dramatic increases in fleet efficiencies;
- **UMTS** - Universal Mobile Communications System (EEC);
- **UPT** - Universal Personal Communications (EEC);
- **Urban Congestion Alleviation Project** - ATMS project in Northern Virginia (near completion) to test the usefulness of a Video Imaging Detection System on a heavily traveled freeway bridge in monitoring traffic flow and detecting incidents;
- **VICS** - Vehicle Information and Communication System - Japanese project with the objective of establishing a consensus on an IVHS architecture;
- **VMS** - Variable Message Signs - Europe's equivalent to CMS;

- **VRC** - Vehicle-to-Roadside Communications – system proposed by Hughes;
- **WIM** - Weight-in-Motion;

B. 1 References

[1] P. Diaz, R. Agusti, "Analysis of a Fast CDMA Power Control Scheme in an Indoor Environment", *42nd IEEE Veh. Tech. Conf.*, May 92

[2] J. Chadwick, V. Patel, "Strategies for Acquiring Radio Frequencies for Intelligent Vehicle Highway Systems (IVHS)", *42nd IEEE Veh. Tech. Conf.*, May 92

[3] K. Yamada, K. Daikoku, H. Usui, "Performance of Portable Radio Telephone using Spread Spectrum", *IEEE Trans. Comm.*, Jul 84

[4] A. Salsami, K.S. Gilhousen, "On the System Design Aspects of Code Division Multiple Access (CDMA) Applied to Digital Cellular and Personal Communications Networks", *41st IEEE Veh. Tech. Conf.*, May 91

[5] K.K. Ho, "Architectural Design of a Code Division Multiple Access Cellular System", *42nd IEEE Veh. Tech. Conf.*, May 92

[6] F.J. Mammano, J.R. Bishop,Jr., "Status of IVHS Technical Developments in the United States", *42nd IEEE Veh. Tech. Conf.*, May 92

[7] Research and Development Center for Radio Systems (RCR) Standard 27, Apr 91

[8] J. Weitzen, J. Larsen, R. Mawrey, "Design of a Meteor Scatter Communication Network for Vehicle Tracking", *42nd IEEE Veh. Tech. Conf.*, May 92

[9] "Dual-Mode Mobile Station/Base Station Compatibility Standard", *EIA/TIA Specification* **IS-54,** Oct 90